# ALTERATIONS IN INTERSTITIAL ACID-BASE HOMEOSTASIS DURING CEREBRAL ISCHAEMIA

BY

DEANNA LESLEY TAYLOR



A thesis submitted to the University of London in fulfilment of the requirements for the degree of Doctor of Philosophy.

Gough-Cooper Dept. of Neurological Surgery
Institute of Neurology
Queen Square
London U.K.

1997

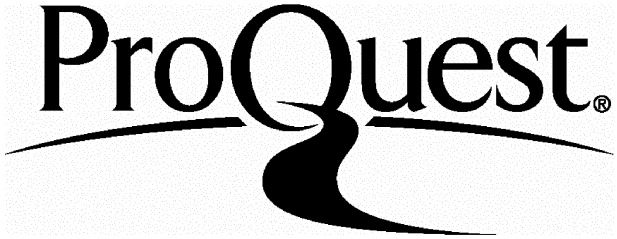

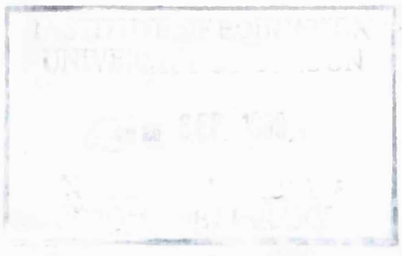

## ABSTRACT

Brain tissue is extremely sensitive to a reduction in blood flow (cerebral ischaemia) and even brief ischaemic episodes can produce irreversible neurological deficit. Experimental studies of cerebral ischaemia have identified several dominant processes which alone or combined underlie ischaemia-induced neuronal damage. Among these, tissue acidosis is a critical factor. This study focused on acid-base changes in the extracellular fluid, the neuronal microenvironment, associated with both ischaemia and spreading depression. The latter phenomenon, which occurs in the region surrounding the ischaemic core associated with focal ischaemia, produces a transient disruption in ionic gradients, and as with ischaemia, leads to failure of residual acid-base homeostasis with subsequent acidification of brain tissue.

By investigation of the changes in extracellular concentrations of carbonate, hydrogen ions and lactate, especially in relation to the occurrence of depolarisation, this study has demonstrated the following:

(i) The transmembrane mechanisms contributing to intracellular acid-base regulation are markedly activated during ischaemia, resulting in a rapid acidification of the extracellular fluid.

(ii) The efficacy of these mechanisms is abolished as the cellular membrane permeability to ions, including $H^+$ and pH-changing anions, suddenly increases with depolarisation.

(iii) Various cells of the central nervous system may have a different acid-base homeostasis, at least with regard to membrane permeability and ionic exchange mechanisms for $HCO_3^-/CO_3^{2-}$.

(iv) Efflux of intracellular lactate is markedly reduced when cell membrane ionic gradients are perturbed, confirming the involvement of a transporter.

(v) Probenecid, used to block lactate transport across the cellular membrane, inhibited $K^+$-induced spreading depression and reduced the amplitude of anoxic depolarisation.

These data strengthen the concept that anoxic depolarisation and spreading depression are critical events in the pathophysiology of cerebral ischaemia and other related insults and therefore, relevant targets for neuroprotective strategies against stroke.

# TABLE OF CONTENTS

# LIST OF FIGURES

CHAPTER 6

# LIST OF TABLES

## ABBREVIATIONS

| | |
|---|---|
| ACSF | Artificial cerebrospinal fluid |
| ADP | Adenosine diphosphate |
| AMP | Adenosine monophosphate |
| ATP | Adenosine triphosphate |
| $[CO_3^{2-}]_e$ | Extracellular carbonate concentration |
| DC potential | Direct current potential |
| ECF | Extracellular fluid |
| EEG | Electroencephalogram |
| EMF | Electromotive force |
| GABA | gamma-amino butyric acid |
| $[H^+]_e$ | Extracellular hydrogen ion concentration |
| $[HCO_3^-]_e$ | Extracellular bicarbonate concentration |
| ISM | Ion-selective microelectrode |
| KCl | Potassium choloride |
| $K^+$-ACSF | Potassium artificial CSF |
| LDH | Lactate dehydrogenase |
| $[lact]_d$ | Dialysate lactate concentration |
| MABP | Mean arterial blood pressure |
| mM | Millimolar ($1 \times 10^{-3}$ Molar) |
| $\mu$M | Micromolar ($1 \times 10^{-6}$ Molar) |
| nM | Nanomolar ($1 \times 10^{-9}$ Molar) |
| mmHg | Millimetres of mercury |
| mV | Millivolts |
| NMDA | *N*-methyl-D-aspartate |
| PCr | phosphocreatine |
| $PCO_2$ | Partial pressure of carbon dioxide |
| $PO_2$ | Partial pressure of oxygen |
| SD | Spreading depression |
| sem | Standard error of the mean |

## ACKNOWLEDGEMENTS

I would like to thank my supervisors, Professor Lindsay Symon and Dr Tiho Obrenovitch, for their support and for giving me the opportunity to do this work. I would also like to express my sincere gratitude to Tiho, not only for his continuous encouragement and critical guidance throughout the duration of this project, but for his friendship and patience.

My thanks go to the people at the Institute of Neurology, past and present, for their assistance and friendship over the years (in alphabetical order): Chris Bashford, Neil Branston, Samantha Darling, Sîan Davies, Sas Djik, Wael El-Deredy, Colin Farman, Masaki Gotoh, Aidan Hardy, Achamma Koshy, She-Yen Lok, Mitsuhito Mase, Sean Maywood, Doug Richards, Yukihiko Ueda, Jutta Urenjak and Elias Zilka.

I also wish to thank Mick Burnham for printing numerous copies of this thesis, a very generous and much appreciated gesture.

Finally, I would like to extend a special thank you to Andrew, and my family and friends, for their continual moral support and numerous attempts to understand exactly what I was doing for my Ph.D.

This thesis is dedicated to my parents, with love.

# CHAPTER 1 INTRODUCTION

## 1.1 General Introduction

Brain tissue is extremely sensitive to a local or global reduction in blood flow (ischaemia) and even brief ischaemic episodes can produce irreversible neurological deficit. Cerebral ischaemia remains one of the most important pathological conditions encountered within neurology and neurosurgery. The principal clinical syndrome caused by cerebral ischaemia is that of stroke, one of the most frequent causes of death and disability in Great Britain, with crucial social implications in an increasingly ageing population. Other syndromes associated with cerebral ischaemia include memory loss affiliated with brain damage following cardiac arrest, as may occur during severe coronary artery occlusion; delayed cerebral damage subsequent to head injury; and spastic paraplegia following birth hypoxia. Brief ischaemic periods are also experienced by pilots of high performance aircraft who are subject to transient loss of consciousness due to gravitational stress-induced failure of blood delivery to the brain (Hetherington et al., 1994). The outcome of cerebral ischaemia depends on both the length and severity of the insult.

Occlusion of major cerebral vessels does not always result in total complete ischaemia, and some residual blood flow may persist within the affected area. Under these circumstances, surrounding a core of densely ischaemic tissue, there is a region with a level of blood flow below that needed to sustain electrical activity (i.e. neuronal function), but above that required to maintain cellular ionic gradients (penumbra). Within the penumbra, repeated transient disruptions of ionic homeostasis and membrane depolarisation have been observed in animal models of stroke (Iijima et al., 1992), and these changes are characteristic of spreading depression, a propagating transient suppression of electrical activity with membrane depolarisation. Although in normal tissue spreading depression is sublethal (Nedergaard and Hansen, 1988), as it produces marked disruption in ionic homeostasis, increased energy demand, acidosis, and neurotransmitter effluxes, it may be deleterious in regions such as the penumbra where residual blood supply can only sustain basal ionic homeostasis.

Experimental studies of cerebral ischaemia have identified several dominant processes which, alone or combined, underlie ischaemia-induced neuronal damage. These include intracellular calcium overload (Siesjö and Bengtsson, 1989), free radical-related damage

which may primarily target vascular tissue (Siesjö et al., 1990), glutamate-receptor mediated neurotoxicity (Obrenovitch and Richards, 1995), and acidosis (Siesjö, 1988b). Acidosis promotes ischaemic brain tissue injury (Siesjö et al., 1993), by itself, and by potentiating other deleterious processes (Siesjö, 1985, 1988b), although extracellular acidosis protects cultured neurons against *N*-methyl-D-aspartate (NMDA)-receptor mediated injury (Tombaugh and Sapolsky, 1993).

This study set out to acquire a better knowledge of the mechanisms underlying brain tissue acidification during ischaemia and spreading depression. Intracellular acidosis has been extensively investigated (Siesjö, 1985) and new insights have recently been provided by nuclear magnetic resonance (NMR) spectroscopy (Brooks and Bachelard, 1992; Ben-Yoseph et al., 1993; Conger et al., 1995). This study focused on extracellular acid-base changes, firstly because the extracellular space is the neuronal microenvironment where neurotransmitters, cell messengers, and drugs are available to receptors; and secondly, because analysis of these changes can provide information on the efficacy of transmembrane mechanisms involved in acid-base regulation under these conditions.

## 1.2 Acid-Base Homeostasis

Acid-base homeostasis is a well conserved physiological process which enables tissues to maintain an environment conducive to vital cell processes. The changes in intra- and extracellular pH ($pH_i$ and $pH_e$, respectively) have been studied in a variety of tissues, including the brain. pH regulation has triggered much interest as pH is an important modulator of metabolic processes, including enzymatic function and protein synthesis (Busa and Nuccitelli, 1984), and because acidosis is a mediator of cell death (Siesjö, 1985, 1988b; Nedergaard et al., 1991). More recently, it has been suggested that pH transients during neuronal activity serve a modulatory role in brain function (Chesler, 1990; Chesler and Kaila, 1992).

### 1.2.1 Brain Acid-Base Regulation Under Basal Conditions

#### 1.2.1.1 Determinants of Brain Acid-Base Homeostasis

The fact that cells behave as open systems which can exchange not only carbon dioxide ($CO_2$) with the surrounding medium, but also protons ($H^+$) and bicarbonate ions ($HCO_3^-$), requires a complex mathematical model to accurately describe cellular acid-base

equilibria (Stewart 1981, Siesjö, 1985). Therefore, before considering the dynamics of pH in the brain, it is useful to consider some formalisms of acid-base physiology and regulation.

The pH of a biological solution is determined by interactions between three variables, which change independently of each other, and which dictate the changes of dependent variables that can not be altered individually (Stewart, 1981). The independent variables are the partial pressure of carbon dioxide ($PCO_2$); the strong ion difference ([SID]), i.e. the difference between the concentration of strong base cations (i.e. $Na^+$, $K^+$, $Ca^{2+}$, $Mg^{2+}$) and strong acid anions (i.e. $Cl^-$, $SO_4^{2-}$, lactate), which is equivalent to buffer base concentration (Siesjö and Messeter, 1971); and the total concentration of weak acid buffers ($[A_{tot}]$). Regulation of pH involves modulation of one or more of these variables, to remove or produce $H^+$ as necessary.

In many biological settings the bicarbonate/carbonic acid system ($HCO_3^-/H_2CO_3$) constitutes the major buffer system, and involves $CO_2$, an end product of oxidative energy metabolism within cells. $CO_2$ diffuses freely across biological membranes and through biological fluids and consequently the $PCO_2$ in different compartments of the brain will always tend towards equilibrium. In biological fluid, $CO_2$ dissolves to form carbonic acid ($H_2CO_3$) which can then dissociate to form $H^+$ and $HCO_3^-$ ions according to the following equation:

$$CO_2 + H_2O \underset{}{\overset{a}{<\!\!-\!\!-\!\!-\!\!-\!\!-\!\!>}} H_2CO_3 \overset{b}{<\!\!-\!\!-\!\!-\!\!-\!\!-\!\!>} \begin{matrix} HCO_3^- \\ + \\ H^+ \end{matrix} <\!\!-\!\!-\!\!-\!\!-\!\!-\!\!> CO_3^{2-} + H^+$$

Equation 1.A

The hydration of $CO_2$ (step **a**) is catalysed by the enzyme carbonic anhydrase which is critical for this reaction to rapidly attain equilibrium, and in the absence of this enzyme, sudden changes in pH would be less rapidly buffered. Inhibition of carbonic anhydrase with acetazolamide amplified interstitial pH transients (Kraig et al., 1983) demonstrating that this enzyme may help to mitigate rapid acid-base shifts. The dissociation constant for carbonic acid (step **b**) is 6.1 which makes it a weak acid at physiological pH (Mitchell et al., 1965). In biological fluids, some of the $H^+$ formed with $HCO_3^-$ is buffered by other bases and $HCO_3^-$ accumulates. As $H^+$ is removed, more $H_2CO_3$ is formed and the concentration of the latter becomes proportional to the amount

of $CO_2$ dissolved (Siesjö, 1985). The $CO_2$ formed by the combination of $HCO_3^-$ and $H^+$ can be removed by the blood. The $HCO_3^-/H_2CO_3$ buffering capacity of the ECF in an open system is significant, and can be defined as 2.3 $[HCO_3^-]$ + 4.6 $[CO_3^{2-}]$ or approximately 50 - 58 mM (Roos and Boron, 1981; Chesler, 1990). In a closed system (e.g. brain tissue during complete ischaemia), the reduction in cerebral blood flow prevents $CO_2$ from leaving the tissue and $PCO_2$ rises, greatly reducing the $HCO_3^-/H_2CO_3$ buffering capacity (Chesler, 1990).

Regulation of pH may also be achieved by alterations in the balance of strong cations and anions ([SID] or [BB]). In most biological fluids there is an excess of strong base cations which is associated with an equal concentration of $OH^-$. The latter is neutralised by the formation and dissociation of carbonic acid, and replaced by the weak base, $HCO_3$. Intracellularly, the [SID], and hence pH, can be altered either by the production of a certain amount of strong acid, e.g. lactic acid which would ionise to lactate and $H^+$, or by the efflux/influx of $H^+$ or $HCO_3^-$ ions. Although the latter fluxes as such would not change [SID] *per se*, which is defined as [strong cations] - [strong anions] (Stewart, 1981), these ions are transported across the membrane in exchange for, or with, a counterion (e.g. $Na^+/H^+$ and/or $HCO_3^-/Cl^-$ exchanges) (Siesjö, 1985).

The remaining method of pH regulation is through weak acid buffers present in biological fluids. These are only partially ionised, and any change in $[H^+]$ will alter that degree of ionisation and will function as a physicochemical buffer. Weak buffers cannot easily move from one tissue compartment to another, and for the purpose of acute pH regulation, $[A_{tot}]$ can be considered virtually constant (Siesjö, 1985). The intracellular fluid (ICF) contains a multitude of such buffers, which comprise free or bound phosphate and protein groups which ionise at physiological pH values (e.g. imidazole groups) (Siesjö and Messeter, 1971; Siesjö, 1985). On the other hand, the ECF of the brain contains negligible concentrations of proteins and organic acids (Fencl, 1986), and therefore, its pH is regulated predominantly by the other two processes.

To summarise, the pH of a given biological fluid is determined by interaction of the three independent variables $PCO_2$, [SID] and $[A_{tot}]$. These completely define $[H^+]$ (i.e. pH) and other dependent variables (Stewart, 1981), which include $H^+$, $OH^-$, $HCO_3^-$, $CO_3^{2-}$, anions of weak acids as well as undissociated weak acids. From an acid-base point of view, the ECF is mimicked by a solution that contains $Na^+$, $Cl^-$ and $HCO_3^-$, equilibrated with $CO_2$. As such, the $pH_e$ can be decreased by either a rise in $PCO_2$ or a reduction in

[SID]. A decrease in [SID] could be due to: (i) the release of a strong acid from cells (e.g. lactic acid); (ii) influx of $H^+$ into cells via $Na^+/H^+$ exchange; or (iii) $HCO_3^-$ efflux from cells via $HCO_3^-/Cl^-$ exchange.

### 1.2 1.2 Source and Sink of $H^+$, Coupled to Brain Energy Metabolism

Within cells, protons are turned over continuously during energy yielding and energy consuming reactions, and as such, the balance between the two determines the intracellular $H^+$ concentration, and consequently $pH_i$. Protons are produced in large quantities in a multitude of metabolic reactions. In aerobic tissue, the major contribution to $H^+$ production is adenosine triphosphate (ATP) hydrolysis (Siesjö, 1985, 1988b). ATP is hydrolysed to produce adenosine diphosphate (ADP) and inorganic phosphate ($P_i$), releasing $H^+$ in an amount that varies with $pH_i$ and intracellular $Mg^{2+}$ concentration (Hochachka and Mommsen, 1983). The respiratory chain is also a major source of $H^+$, and the latter being produced during reduction of flavin and nicotinamide coenzymes, and cytochromes. Since cerebral metabolism primarily involves the oxidation of glucose, glycolysis is widely considered to be an important source of $H^+$. However, the end product of glycolysis is actually lactate, and not lactic acid (i.e. lactate and $H^+$). In fact the lactate dehydrogenase reaction consumes $H^+$ when catalysing lactate formation from pyruvate. Therefore, this process does not generate $H^+$ unless accompanied by hydrolysis of ATP (Krebs et al., 1975).

Net acid production is counter-balanced by a corresponding consumption of $H^+$. The main sink for $H^+$ is oxidative phosphorylation, since $H^+$ ions are removed when ATP is synthesised, and reduced coenzymes and cytochromes are reoxidised (Siesjö, 1978). Formation of ATP from the hydrolysis of phosphocreatine (PCr), catalysed by creatine kinase, is accompanied by the uptake of $H^+$. Since at physiological pH, this reaction favours the synthesis of ATP, any ADP formed will be immediately rephosphorylated by PCr with the consumption of $H^+$. As such, the creatine kinase reaction forms a dynamic $H^+$ buffer system.

Under basal aerobic conditions, the balance between the hydrolysis and resynthesis of ATP maintains net production of $H^+$ at a low value, and consequently there is no major changes in $pH_i$. However, when the rates of ATP synthesis and utilisation become uncoupled, aerobic energy metabolism can produce either an increase or a decrease in $pH_i$.

### 1.2.1.3 Bicarbonate/Carbonate Buffering

Carbonic acid buffer species, $HCO_3^-$ and $CO_3^{2-}$, play a key role in numerous vital processes of animal cells and tissues, and are essential for the normal operation of a wide variety of metabolic and physiological processes. As previously discussed (section 1.2.1.1), the capacity of the ECF to buffer $H^+$ is largely dependent on $HCO_3^-$ and $CO_3^{2-}$. Quantitatively, $HCO_3^-$ is more important than $CO_3^{2-}$ since previous measurements of $CO_3^{2-}$ with ion-selective microelectrodes have shown that its concentration within the brain ECF was around 50 $\mu$M (Chesler et al., 1994), i.e. 200 fold less than the extracellular concentration of $HCO_3^-$ (Siesjö, 1985). Nevertheless, $CO_3^{2-}$ is an important component of the bicarbonate/carbonic acid buffer system, and in equilibrium with $HCO_3^-$ (see Equation 1.A).

In the mammalian brain under physiological conditions, the intra- and extracellular concentrations of $HCO_3^-$ ($[HCO_3^-]_i$ and $[HCO_3^-]_e$, respectively) have been calculated to be approximately 12.5 and 25 mM, respectively (Siesjö, 1985). As a consequence, the ECF has a larger buffer capacity, despite the fact that the ICF also contains non-bicarbonate buffers (Siesjö, 1985). This also implies that the buffer capacity of the ECF becomes very low when $[HCO_3^-]_e$ is exhausted, whereas the ICF retains some capacity to buffer $H^+$. The importance of $HCO_3^-$ in the acid-base regulation of the ECF is emphasised by studies of aquatic species in which $[HCO_3^-]_e$ is approximately 5 mM (Chesler, 1990). Thus, the interstitial buffering power in the brain of aquatic species, is generally four-fold less than that of terrestrial species, and as such, extracellular pH shifts associated with neuronal activity are expected to be larger in aquatic animals. Studies of $pH_e$ transients in the cerebellum of the skate *in vivo* (Rice and Nicholson, 1988) revealed that stimulus-evoked alkaline shifts are 5-10 times greater than comparably-evoked pH transients in the rat cerebellum (Kraig et al., 1983).

$HCO_3^-$ and $CO_3^{2-}$ buffering coupled to membrane-based ion transport systems (Boron, 1985; Chesler, 1990), create a predominant means of modulating $pH_i$ and $pH_e$ (see section 1.2.1.4). Critical reduction in cerebral $HCO_3^-$ levels, as occurs during severe acidosis associated with ischaemia, has been considered to be a potentially important first step toward the destruction of neuronal tissue (Kraig et al., 1986; Kraig and Chesler, 1990).

### 1.2.1.4 Intracellular pH Regulation - Ionic Exchanges at the Cellular Membrane Interface

The fact that the intracellular concentrations of $H^+$ and $HCO_3^-$ ($[H^+]_i$ and $[HCO_3^-]_i$, respectively) are different from those predicted from passive electrochemical distribution across the cellular membrane suggests that the intracellular concentration of these ions is regulated (Siesjö, 1985). Conclusive evidence for $pH_i$ regulation was not obtained until 1971 from studies of hypercapnia (Messeter and Siesjö, 1971; Siesjö and Messeter, 1971). With hypercapnia, the ICF is subjected to an acid load as $CO_2$ diffuses across cell membranes and is hydrated to form carbonic acid. After 15 min of hypercapnia, the average brain $pH_i$ decreased, but after 3 hours, despite sustained hypercapnia, $pH_i$ recovered. As the calculated apparent buffer capacity of the brain was significantly higher than under normal conditions, it was concluded that $pH_i$ was regulated by mechanisms other than physicochemical buffering, and that metabolic consumption of acid played a major role in this process. Decreases in the levels of metabolic acids, especially lactic acid, during hypercapnia (Siesjö and Messeter, 1971; Folbergrová et al., 1972), and increases in metabolic acids, during hypocapnia (Kjallqvist et al., 1969; MacMillan and Siesjö, 1973) supported the regulatory role of consumption and production of metabolic acids. However, physicochemical buffering and the consumption/production of acids only lessened the impact of changes in $PCO_2$ upon $pH_i$, and could not account for restoration of $pH_i$ to normal values (Hakim and Shoubridge, 1989). Subsequent studies on single cells established that the principal mechanism of recovery from an intracellular acid load was transmembrane acid extrusion (Thomas, 1984).

Although net metabolism produces little $H^+$, due to a balance of $H^+$ production and consumption, cells possess and require mechanisms for extruding $H^+$. Under resting conditions, $[H^+]_i$ is close to that of the extracellular fluid ($[H^+]_e$), with $[H^+]_i$ being slightly more acidic (maintained at around 7.0). Microelectrode measurements of $pH_e$ have consistently produced values around 7.3 (Kraig et al., 1983; Mutch and Hansen, 1984; Siesjö et al., 1985a) which means that intra- and extracellular $H^+$ concentrations are about 90 and 50 nM, respectively. As the equilibrium potential for $H^+$ is more positive than the membrane potential, an inward electrochemical gradient exists for $H^+$ (Siesjö, 1985). This implies that acid must be extruded to the surrounding extracellular environment.

Plasma membrane $H^+$ extrusion mechanisms in some combination have been identified in a variety of animal cells including mammalian glia (Kimelberg et al., 1979, 1982; Kimelberg and Bourke, 1982; Mellergård et al., 1993, 1994) and vertebrate neurons (Chesler and Nicholson, 1985; Mellergård et al., 1994). The most important of these may be the plasma membrane $Na^+/H^+$ exchanger which mediates the extrusion of $H^+$ in exchange for $Na^+$. This ion exchange system is driven by the transmembrane $Na^+$ gradient maintained by the $Na^+/K^+$-ATPase pump and the selective permeability to $Na^+$, and is therefore dependent on ATP availability (Thomas, 1977; Roos and Boron, 1981; Thomas, 1984; Chesler and Nicholson, 1985; Chesler, 1986). Although the $Na^+/H^+$ antiport may be virtually quiescent at physiological $[H^+]_i$, it is activated by an increase in $[H^+]_i$ (Aronson, 1985; Grinstein and Rothstein, 1986) and/or when the $H^+$ gradient across the plasmalemna is altered (Jean et al., 1985; Tolkovsky and Richards, 1987). There is overwhelming evidence for the presence of this exchanger in both neuronal and glial cells. For example, $Na^+$-dependent acid extrusion from many types of glial cells was inhibited by amiloride and its derivatives (Kimelberg et al., 1979; Deitmer and Schlue, 1987; Kettenmann and Schlue, 1988). Regulation of $pH_i$ in cultured sympathetic neurons was also largely achieved by an amiloride-sensitive $Na^+/H^+$ exchange (Tolkovsky and Richards, 1987). The presence of a $Na^+/H^+$ exchanger in both neurons and glial cells was confirmed by removal of extracellular $Na^+$ from bathing medium of cultured astrocytes and synaptosomes, which was followed by a reduction in baseline $pH_i$ (Mellergård et al., 1993; Sánchez-Armass et al., 1994). Therefore, the $Na^+/H^+$ exchanger counteracts the intracellular acidification due to passive influx of $H^+$ along its electrochemical gradient and metabolic $H^+$ generation (Grinstein et al., 1985).

In some vertebrate cells the regulation of $pH_i$ also involves $HCO_3^-/Cl^-$ exchange, which translocates $HCO_3^-$ into the cell in exchange for $Cl^-$ (Roos and Boron, 1981; Thomas, 1984). The energy source of this exchanger is not obvious; a "passive" exchanger would translocate $HCO_3^-$ outwards (i.e. acidifying the cell) since the extracellular to intracellular $Cl^-$ gradient (10:1) is usually much larger than that of $HCO_3^-$ (around 2:1). It seems likely that an "active" $HCO_3^-/Cl^-$ exchanger, i.e. one translocating $HCO_3^-$ inwards against it concentration gradient, is coupled to (and driven by) the $Na^+$ gradient, and is therefore ATP-dependent. Evidence has suggested a carrier-mediated exchange of $HCO_3^-$ against $Cl^-$ in glial cells (Kimelberg, 1981; Ahmad and Loescheke, 1983) which is dependent on extracellular $HCO_3^-$ and $Na^+$ and on intracellular $Cl^-$, and inhibited by stilbene derivatives (e.g. 4-acetamido-4'-isothiocyanato-stilbene-2,2'-

disulfonic acid [SITS], and 4,4'-diisothiocyanostilbene-2,2'-disulfonic acid [DIDS]) (Kimelberg et al., 1979; Deitmer and Schlue, 1987; Mellergård et al., 1993). These are characteristics of a $Na^+$-dependent $HCO_3^-/Cl^-$ exchanger, and the following data suggest that it is important for glial pH regulation: (i) the intracellular $Cl^-$ concentration was found to decrease during $pH_i$ regulation following acid loading (Thomas, 1977; Moody, 1981); (ii) during $CO_2$ exposure, depletion of intracellular [$Cl^-$] markedly retarded $pH_i$ regulation (Thomas, 1977); and (iii) application of SITS, which inhibits anion exchange, was found to block or markedly slow down $pH_i$ regulation following HCl injections (Thomas, 1977; Moody, 1981).

Data related to the role of $HCO_3^-$ on $pH_i$ regulation during intracellular acidosis in neurons are conflicting. In rat sympathetic neurons, recovery from acid loading was principally mediated by $Na^+/H^+$ exchange, since SITS or $Cl^-$-free solutions had no effect, but addition of $HCO_3^-$ to the bathing medium accelerated $pH_i$ recovery (Tolkovsky and Richards, 1987). However, Naschen and Drapeau (1988) found no evidence to support the participation of $HCO_3^-$ transport in $pH_i$ regulation. The latter was supported by the finding that recovery of synaptosomal $pH_i$ from an acid load was effective in $HCO_3^-$-free solution (Sánchez-Armass et al., 1994). No evidence was found for the involvement of a $Na^+$-coupled $HCO_3^-/Cl^-$ antiporter in $pH_i$ regulation of rat cortical neurons (Ou-yang et al., 1993). These results suggest that regulation of neuronal $pH_i$ does not involve a $Na^+$-dependent $HCO_3^-/Cl^-$ transporter, but essentially relies on a $Na^+/H^+$ exchanger. In contrast, lamprey neurons appear to extrude acid using both an amiloride-sensitive $Na^+/H^+$ exchanger and a separate $HCO_3^-$-dependent DIDS-sensitive mechanism (Chesler, 1986). Since glial cells use an $HCO_3^-$-dependent mechanism to extrude $H^+$, the overall intracellular pH regulation may be more efficient in these cells than in neurons (Ou-yang et al., 1993).

An alternative, relevant mechanism for the regulation of $pH_i$ may be an electrogenic $Na^+$-$HCO_3^-$ cotransporter. This symporter has been identified in several glial types, including glia of the leech central nervous system (Deitmer and Schlue, 1987, 1989), and some vertebrate glial cells (Astion and Orkand, 1988; Kettenmann and Schlue, 1988; Newman and Astion, 1991), but as yet no direct evidence for such a cotransporter has been found in neurons (Ou-yang et al., 1993). This cotransporter mediates a net inward movement of $HCO_3^-$ driven by the $Na^+$ gradient, the direction of the transport probably being determined both by the extra- and intracellular $HCO_3^-$ concentrations, and by the

membrane potential (Deitmer and Schlue, 1989; Kettenmann and Schlue, 1988; Deitmer, 1991).

An additional, important mechanism for translocation of $H^+$ across membranes is provided by the permeation of organic acids, like lactic acid. Transport of lactate between the intra- and extracellular compartments in the brain may occur via simple diffusion of the undissociated lactic acid molecule through the cell membrane (Roos and Boron, 1981; Smith et al., 1986), or by the facilitated transport of lactate and $H^+$ (Kuhr et al., 1988). Such mechanisms may be important in reducing differences in pH between different compartments when acid is produced within one of them.

#### 1.2.1.5 Lactate Production and Metabolism under Basal Conditions

In mammalian cells there are two pathways that produce energy (i.e. ATP), glycolysis and oxidative phosphorylation. The coupling between the two processes is particularly tight in the brain because glucose is the principal metabolic fuel under aerobic conditions, and oxidation of alternative sources, such as fats or ketone bodies is minimal (Siesjö, 1978). Nervous tissue contains both glucose and glycogen, however, little of either is stored. Since the brain is almost exclusively dependent on oxidative phosphorylation for ATP synthesis (Siesjö, 1978), normal brain function requires a continuous replenishment of both glucose and oxygen from the circulation (Lund-Andersen, 1979).

Glycolysis, the first step in the catabolism of glucose occurs in the cytoplasm and produces 2 moles of pyruvate per mole of glucose. In the presence of oxygen, pyruvate is first oxidised by pyruvate dehydrogenase to acetyl CoA, and then converted to $CO_2$ and water via the combined action of the tricarboxylic acid (TCA) cycle and the respiratory chain, both of which occur in the mitochondria.

Oxidative phosphorylation provides over 95 % of total ATP synthesis (Siesjö, 1978), and as such, regulation of mitochondrial respiration is central to cerebral metabolism and function. Under basal conditions when oxygen is not limiting, oxidative phosphorylation is primarily dependent on the interplay of two parameters: the concentration of ATP, ADP and $P_i$, and the mitochondrial $NADH/NAD^+$ (Erecinska and Silver, 1994). The key regulatory process in glycolysis is the phosphofructokinase reaction, although two other steps, catalysed respectively by hexokinase and pyruvate kinase provide additional controls. All three reactions are regulated by factors other than the concentration of their

substrates (Erecinska and Silver, 1994). In addition to glycolysis and oxidative phosphorylation, which are net energy producing processes, cells possess two other mechanisms that help maintain a constant level of ATP. These are the phosphocreatine/creatine (PCr/Cr) system, which is linked to the adenine nucleotides through a rapid equilibrium in the creatine phosphokinase reaction, and the adenylate kinase reaction.

In whole brain *in vivo* more than 95 % of glucose is metabolised by the TCA cycle and the respiratory chain. However, under basal conditions, despite adequate oxygen tension, a small fraction of pyruvate is converted anaerobically to lactate in a reversible reaction catalysed by lactate dehydrogenase (LDH) (Equation 1.B).

$$\text{Pyruvate} + \text{NADH} + \text{H}^+ \overset{\text{LDH}}{<\text{------}>} \text{Lactate} + \text{NAD}^+$$

Equation 1.B

The equilibrium of the LDH reaction and lactate formation depend on the ratio between pyruvate and lactate, the concentration of $H^+$ (thus $pH_i$) and the concentration of NADH. As such, acidification or an increase in the level of NADH will alter the equilibrium towards lactate production. This non-oxidative metabolism produces less than 1 % of the brains energy under basal conditions (Siesjö, 1978; Fox et al., 1988). In contrast to this, in cultured neurons and glia lactate generation accounts for about 50 % of glucose usage (Hertz et al., 1988). In addition to its essential role in energy production during anaerobic conditions, glycolytic ATP may be required under basal aerobic conditions to maintain some of the vital functions of cortical nerve terminals (Kauppinen and Nicholls, 1986; Kauppinen et al., 1988). Although cerebral formation of lactate is generally considered to reflect glycolysis, whether aerobic or anaerobic, evidence suggests that 1-3% of total lactate may be derived from the pentose phosphate shunt (Ben-Yoseph et al., 1995). This could explain the apparent existence of a pool of brain lactate which is derived neither from glycolysis nor from influx of plasma lactate into brain (Cremer and Heath, 1974).

Cerebral glycogen can also serve as a substrate for energy production. Glycogen is located predominantly in astrocytes (Koizumi, 1974) where it is subject to rapid metabolic turnover (Watanabe and Passonneau, 1973). Astrocytes appear to be the primary site of glycogen catabolism since glycogen phosphorylase has been found almost exclusively in

this cell type (Pfeiffer et al., 1990), although evidence suggests that neurons may also be capable of glycogenolysis as this enzyme was present in synaptoplasm (Knull and Khandelwal, 1982). When glial glycogen is degraded, lactate leaves these cells, suggesting that astrocytes may be a store for lactate rather than glucose (Dringen and Hamprecht, 1993; Dringen et al., 1993). It is suspected that glial cells produce more lactate than neurons due to a higher rate of anaerobic glycolysis (Pauwels et al., 1985).

Lactate may not be strictly an end product of energy metabolism, but rather a secondary energy substrate. Energy production from lactate entails its conversion to pyruvate by LDH, followed by the entry of pyruvate into the TCA cycle (Schurr et al., 1988). Lactate utilisation for energy production has already been suggested (Vicario et al., 1991; Dringen et al., 1993). In support of this, lactate, in the presence of oxygen, restored and maintained synaptic transmission in slices of hippocampus in the absence of glucose (Schurr et al., 1988), and lactate was the main metabolic substrate for cells derived from the neonatal brain (Vicario et al., 1991). Lactate is simultaneously released and absorbed by nervous tissue, and therefore lactate in the ECF may be an intermediate of carbohydrate metabolism shared by many cells (Larrabee, 1992). For example, during metabolic stress glial cells may supply lactate to the neurons in order to maintain their metabolic status and function (Dienel et al., 1995; Larrabee, 1995). Recent studies have suggested that extracellular glutamate and gamma-aminobutyric acid (GABA) can be converted into pyruvate or lactate *in vitro* (Sonnewald et al., 1993; Bachelard et al., 1994). It has also been hypothesised that glutamate and GABA, taken up by astrocytes *in vivo*, to some extent are also converted into lactate (Hassel and Sonnewald, 1995). Therefore, lactate could be envisioned as having a role in the glial-neuronal trafficking of metabolites.

#### 1.2.1.6 Lactate Transport

The transport of lactic acid out of the cell is of fundamental importance to cells, including those in the brain, especially when anaerobic glycolysis becomes a major source of energy (e.g. during ischaemia or spreading depression). As it is lactic acid (i.e. lactate and $H^+$) which is produced by metabolism, it might be expected that lactate would be transported across the plasma membrane with $H^+$. Although efflux of lactic acid in this way could play an important part in the intracellular acid-base regulation of the tissue, the mechanism remains unclear.

Lactate exchanges between intra- and extracellular compartments in the brain have often been assumed to be mediated by simple diffusion of undissociated lactic acid through the cell membrane (Roos and Boron, 1981; Smith et al., 1986; Nedergaard et al., 1989). At low pH or very high concentrations of lactic acid, free diffusion of the undissociated acid may become quantitatively important (Goldman et al., 1989; Poole and Halestrap, 1993). However, since under physiological conditions lactic acid (pKa 3.86) exists almost entirely in its dissociated anionic form (i.e. as lactate and $H^+$), the transport rate of lactic acid is very slow (Poole and Halestrap, 1993). Although some diffusion of lactic acid across the plasma membrane may occur, the findings that lactate release from hippocampal slices was saturable and stereospecific (Assaf et al., 1990), and was inhibited by probenecid, an inhibitor of organic acid transport systems (Yuwiler et al., 1982; Kuhr et al., 1988), rather suggested the involvement of a facilitated transport within the brain.

Since the identification of a stereospecific, saturable transport of lactate and pyruvate across the blood-brain barrier (BBB) (Oldendorf, 1972), carrier-mediated transport of monocarboxylic acids has been described in various other cells including erythrocytes (Halestrap, 1976), tumour cells (Spencer and Lehninger, 1976), mitochondria (Halestrap, 1975), and in the sarcolemmal membrane of the heart (Mann et al., 1985). Although most cells appear to possess monocarboxylate transporters, these exhibit distinct properties with respect to substrate specificity (e.g. lactate, pyruvate, and/or acetate) and sensitivity to pharmacological inhibition (Spencer and Lehninger, 1976; Halestrap et al., 1990). As a result, it has been suggested that there is a family of monocarboxylate transport proteins (Halestrap et al., 1990).

In erythrocytes, lactate transport across the membrane can occur in two ways: (i) via a lactate/$H^+$ cotransporter (Dubinsky and Racker, 1978; Halestrap et al., 1990; Poole and Halestrap, 1993); and (ii) in exchange for another anion such as $Cl^-$ or $HCO_3^-$ (Halestrap, 1976). In brain tissue, a lactate/$H^+$ cotransport system has been found in astrocytes (Lomneth et al., 1990), peripheral nerves (Schneider et al., 1993) and the hippocampus (Assaf et al., 1990). The finding that lactate efflux from both cultured astrocytes and neurons was inhibited by DL-*p*-hydroxyphenyl lactate, a lactate/$H^+$ exchange inhibitor (Walz and Mukerji, 1988b), provided clear evidence for the existence of a lactate/$H^+$ cotransporter within the brain. The involvement of other anions in lactate transport is unlikely since lactate efflux from both cultured astrocytes and neurons, and isolated peripheral nerves, was not affected by the $HCO_3^-/Cl^-$ exchange inhibitor DIDS (Walz and

Mukerji, 1988b; Schneider et al., 1993).

From kinetic studies in erythrocytes, efflux (and influx) of lactate via a lactate/$H^+$ cotransport system can be explained by the model depicted in Fig. 1.2.A (De Bruijne et al., 1983, 1985; Deuticke, 1989). According to this model, an efflux cycle (clockwise) is initiated by the binding of $H^+$ to the internal side of the transporter, followed by the binding of lactate, and formation of a translocation complex. Subsequently the transporter reorientates, transporting $H^+$ and lactate outside. Lactate is released first followed by $H^+$. For a new translocation cycle to start, the transporter must return to its initial conformation in order for the binding sites to be exposed to the inside. This model implies a 1:1 stoichiometry between lactate and $H^+$ across the membrane. Influx of lactate may occur via the reversal of this mechanism (anticlockwise in Fig. 1.2.A).

Lactate removal from intracellular compartments *in vivo* was thought to depend on $Na^+/K^+$ transmembrane gradients because it was only effective when energy supplies maintained membrane integrity and function (Kuhr et al., 1988). In contrast, lactate exchanges between brain slices and their outer medium were apparently dependent neither on ATP nor on extracellular $Na^+$. Lactate release was observed with depleted ATP levels (Assaf et al., 1990; Kauppinen and Williams, 1990) and both intracellular lactate concentration and lactate efflux were not altered by the removal of $Na^+$ from the bathing medium (Pirtillä and Kauppinen, 1992). Similarly, it is now generally accepted that the lactate transport system of the BBB is dependent on neither energy nor $Na^+$ (LaManna et al., 1993).

The monocarboxylate carriers of erythrocytes, ascite cells, hepatocytes and myocytes are all proton-linked (Halestrap et al., 1990), suggesting that transport via these carriers, and those found in brain cells, could depend on the transmembrane proton gradient. Several findings support this hypothesis: (i) lactate efflux from erythrocytes was stimulated when external $[H^+]$ was decreased (Dubinsky and Racker, 1978); (ii) net transport via the erythrocyte monocarboxylate carrier was accelerated as the $[H^+]$ on the opposite side of the membrane to the substrate decreased (Halestrap et al., 1990); (iii) lactate transport across the BBB was strongly modulated by pH and brain uptake of lactate increased when the $[H^+]$ of an intracarotid injected bolus was increased (Oldendorf et al., 1979); and (iv) lactate accumulation in cultured astrocytes was enhanced by an increased inwardly directed proton gradient (Lomneth et al., 1990; Walz and Mukerji, 1990). It is important to note that a change in the transmembrane gradient of protons may, by itself,

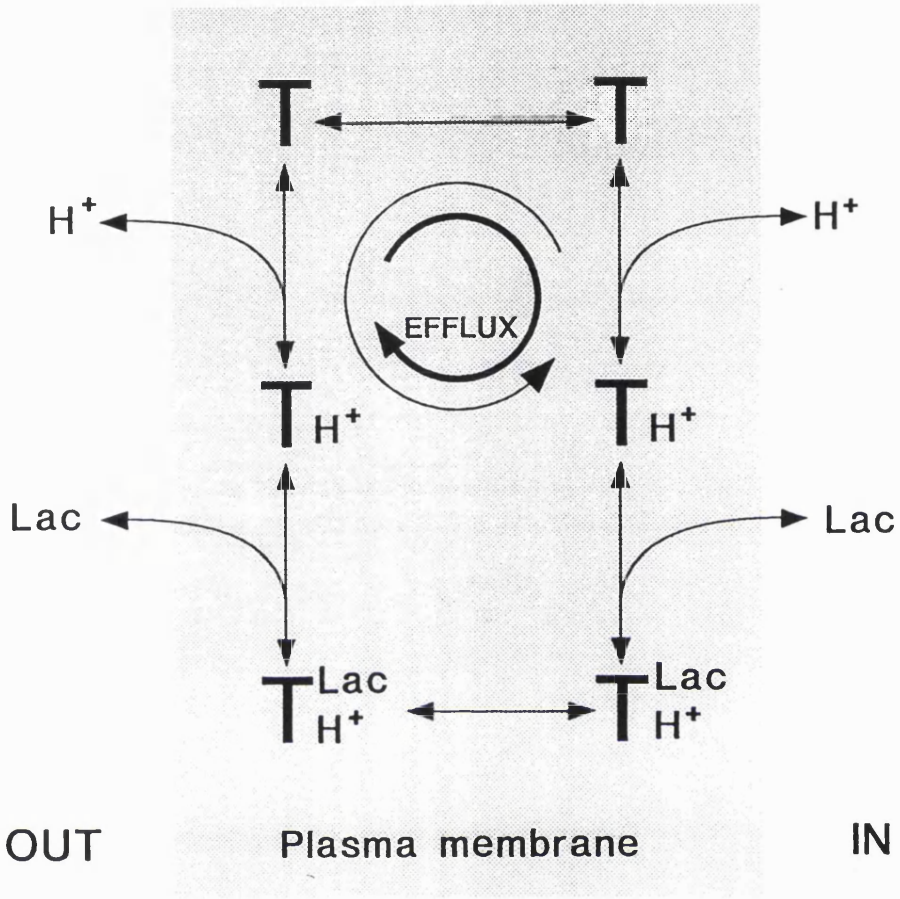


**FIG. 1.2.A** Model of lactate efflux (and influx) via a lactate/$H^+$ cotransport system. An efflux cycle (clockwise) is initiated by the binding of $H^+$, followed by lactate to the internal side of the transporter, and formation of a translocation complex. Reorientation of the transporter moves $H^+$ and lactate to the outside, where lactate is released first followed by $H^+$. For a new efflux cycle to start, the transporter must return to its initial conformation so the binding sites are exposed to the inside. Reversal of this mechanism may result in influx of lactate (anticlockwise).

lead to the reversal of the lactate/$H^+$ cotransport system (Fig. 1.2.A; Spencer and Lehninger, 1976).

As lactate is continuously produced, the lactate/$H^+$ cotransporter may act to regulate the intracellular concentration of lactate, instantly releasing newly formed lactate. This is in line with the finding that in cultured astrocytes the intracellular lactate concentration is maintained at about 23 mM, with any excess lactate being released via the carrier into the extracellular space (Walz and Mukerji, 1988a). Removal of lactate with $H^+$ may play an important role in the intracellular acid-base regulation of brain tissue. However, a lactate/$H^+$ transporter dependent on transmembrane ionic gradients implies that when ionic homeostasis is disrupted, lactate/$H^+$ cotransport could be severely impaired.

#### 1.2.1.7 Contribution of Other Strong Acid/Bases to Acid-Base Homeostasis

High levels of taurine in the neonatal rat brain provide a significant buffering capacity against brain tissue acidosis (Nakada et al., 1991, 1992). Although taurine has been shown to be essential for fetal development (Sturman et al., 1977), the majority of taurine in the brain is thought to be metabolically inert and exists as a free amino acid in the cytosol. Due to high taurine levels, the neonatal brain is significantly more resistant to anoxia than adult brain, and possesses a remarkable capacity to maintain near normal pH in the face of high lactic acid concentrations generated by anaerobic metabolism (Nakada et al., 1991, 1992). Taurine acts as an intracellular buffer (pKa 8.74), and may play a role in the immature brains' higher resistance against anoxia/ischaemia. However postnatally, cerebral levels of taurine rapidly decline.

N-acetyl-aspartate (NAA), the second most abundant amino acid in mature brain, is almost negligible in the fetal brain but increases steadily after birth, complementally related to the decline in taurine (Nakada, 1991). This change from taurine to NAA may reflect a maturational change in acid-base regulation from the fetal to the adult type (Nakada et al., 1992). The fact that NAA is present in large amounts in the brain (Birken and Oldendorf, 1989) and appears to be metabolically inert in the adult brain is compatible with a role in osmoregulation (Taylor et al., 1994a, 1995) and/or acid-base homeostasis (Hoffmann and Simonsen, 1989; Taylor et al., 1994a).

Histidine, an amino acid with a pKa of 6.0, has significant buffering capacity at pH 7.0, i.e. near the pH of intracellular fluids. Other amino acids present in the brain have pKa values too far away from pH 7 to be effective buffers at this pH (Lehninger, 1982).

Ammonia is a volatile brain buffer linked to neurotransmitter and energy metabolism (Ljunggren et al., 1974c; Kraig and Cooper, 1987). However, the extremely small amount of $NH_3$, compared with $HCO_3^-$ present, adds little to the $H^+$ buffering capacity of the brain (Kraig and Cooper, 1987).

## 1.3 Alteration of Brain Acid-Base Homeostasis Subsequent to Imbalance Between Energy Supply and Demand

### 1.3.1 Introduction

There is very tight coupling between brain tissue levels of ATP and ionic gradients in neurons and glial cells. Changes in energy availability result in alterations in ionic homeostasis, and reciprocally, changes in ionic gradients exert pronounced effects not only on cerebral energy levels but also on the rate of energy generation. This study, focused on extracellular acid-base changes during two such events: global ischaemia (terminal and transient) and $K^+$-induced spreading depression (SD). There are fundamental differences between the origin of changes in the energy parameters associated with SD and ischaemia. In SD, increased neuronal activity leads to ionic redistribution and adenine nucleotide breakdown, while the intact energy-producing pathways increase their activity in response to these alterations. In ischaemia, limitation in the substrates of energy metabolism (oxygen and glucose) results in a reduced production of ATP, compromising the energy state of the tissue. Changes in ionic homeostasis in this situation are secondary, and usually occur when the energy-consuming ionic pumps are unable to maintain homeostasis.

### 1.3.2 Global Cerebral Ischaemia: Terminal or Transient

The brain is dependent on continued oxidative metabolism for maintenance of its functional and structural integrity. As the oxygen reserve in the brain is negligible compared to its rate of consumption, the brain requires continuous replenishment of its oxygen content by the circulation. Accordingly, limitation of oxygen supply produces drastic effects on brain cellular function and, if sustained, results in neuronal death. Even ischaemia of minimal severity is known to disrupt cellular energy state, acidify intra- and extracellular fluids and cause loss of ion homeostasis (Siesjö, 1981, 1988a,c). The crucial acid-base events in ischaemia are deterioration of cerebral energy state, stimulation of anaerobic glycolysis with conversion of glucose (and glycogen) to lactic acid, and

impairment of the ion exchanges contributing to intracellular pH regulation.

The changes that occur initially during ischaemia (phase 1) are reversible and no permanent neurological deficit develops as long as the insult is of short duration (Obrenovitch, 1995). However, if ischaemia is severe and sustained then, within a few minutes, dramatic and synchronous ionic redistributions occur across the cellular membrane (Harris and Symon, 1984; Hansen, 1985). These marked ionic shifts, referred to as anoxic depolarisation, signify the beginning of a second phase of ischaemia (phase 2) which may be critical for cell survival (Somjen et al., 1990; Obrenovitch, 1995).

#### 1.3.2.1 Energy Metabolism During Ischaemia

When the cerebral circulation is completely interrupted, the brain is converted into a closed system with an energy production (i.e. ATP generation) limited to the metabolism of substrates present in the brain parenchyma. This leads, within seconds, to shortage of glucose and oxygen, the substrates of oxidative phosphorylation and glycolysis, and thus reduces ATP generation. Although ATP synthesis from oxidative phosphorylation is curtailed, ATP utilisation continues. Hydrolysis of ATP results in increased levels of ADP, $P_i$ and $H^+$, which favours the breakdown of PCr by creatine kinase, and ATP levels are transiently maintained at the expense of PCr (Bachelard et al., 1985; Obrenovitch et al., 1988; Cox et al., 1988). Accordingly, a decrease in PCr/Cr precedes any change in adenine nucleotides (Erecinska and Silver, 1994), and ATP levels are maintained until PCr stores are depleted (Siesjö, 1978; Ekholm et al., 1993). When this occurs, some ATP is made available by the adenylate kinase reaction, in which 2 moles of ADP are converted to 1 mole of ATP and 1 mole of AMP.

The decline in PCr and ATP, and the associated rises in Cr, $P_i$, ADP and AMP, activate glycolysis and glycogenolysis via stimulation of phosphofructokinase and glycogen phosphorylase, respectively (Lowry et al., 1964; Ljunggren et al., 1974c). The pyruvate formed from glycolysis would normally be oxidised to $CO_2$ and water by the mitochondrial enzymes (Siesjö, 1978). However, during ischaemia, falling oxygen tension can no longer maintain oxidative phosphorylation and any pyruvate formed is converted anaerobically to lactate (see Equation 1.B). Stimulation of anaerobic glycolysis with lactate synthesis maintains ATP levels as long as glucose remains available (Erecinska and Silver, 1994).

### 1.3.2.2 Ischaemia-Induced Increase in Intracellular $H^+$ Formation

Deterioration of cerebral energy state, with the ensuing stimulation of anaerobic glycolysis and continued ATP hydrolysis, results in the production of lactate and $H^+$ (i.e. lactic acid), and ultimately in intracellular acidosis. Breakdown of triglycerides and phospholipids to free fatty acids may be an additional source of $H^+$, however, this is quantitatively of minor importance in comparison to anaerobic glycolysis with ATP hydrolysis, in which each mole of glucose is converted to two moles of lactic acid.

Initially, $H^+$ is consumed by the breakdown of PCr via the creatine kinase reaction, but this is short lived since PCr stores are rapidly depleted (Ekholm et al., 1992). Accordingly, when PCr breakdown and oxidative phosphorylation cease (i.e. effective sinks for $H^+$), but ATP hydrolysis continues, $H^+$ rapidly accumulates in the cytosol decreasing $pH_i$ (von Hanwehr et al., 1986; Chopp et al., 1987). Increased brain tissue concentration of $CO_2$ may also contribute to intracellular acidosis (Siesjö, 1985; Smith et al., 1986; von Hanwehr et al., 1986), since cerebral blood flow is severely reduced or ceases during ischaemia, $CO_2$ levels will rise and diffuse freely through all brain tissue compartments.

### 1.3.2.3 Processes Counteracting Intracellular Acidification Before Anoxic Depolarisation

The $H^+$ ions accumulated intracellularly react with $HCO_3^-$ and non-bicarbonate buffers. Although the $HCO_3^-/H_2CO_3$ buffering system in an open system is significant, with the reduction in cerebral blood flow, the $CO_2$ formed is prevented from leaving the tissue, further reducing the intracellular buffering capacity. As intracellular $H^+$ concentration exceeds the buffering capacity within the ischaemic brain cells, active extrusion mechanisms are stimulated, which remove $H^+$ from the intra- to the extracellular space (Kraig et al., 1985; Siesjö, 1985; see section 1.2.1.4).

Increased $[H^+]_i$ stimulates the $Na^+/H^+$ exchanger, which mediates the extrusion of $H^+$ in exchange for $Na^+$ (Grinstein and Rothstien, 1986; Deitmer and Schlue, 1987; Ouyang et al., 1993; Mellergård et al., 1993). Apart from containing a binding site for $H^+$ on the intracellular side, the $Na^+/H^+$ exchanger also has a pH-sensing modulatory site which activates the exchanger when $pH_i$ falls below the "set point" which is usually taken to be around 7.0 (Boron et al., 1979; Grinstein et al., 1983; Jean et al., 1986). As a result, the rate of $H^+$ efflux (and $Na^+$ influx) increases with a decrease in $pH_i$. However,

the rate also depends on $pH_e$, suggesting that $H^+$ competes with $Na^+$ for an external site of the exchanger, or that it decreases the affinity of the external site for $Na^+$ (Jean et al., 1985, 1986).

A number of findings suggest that the $Na^+/H^+$ exchange is stimulated by intracellular acidosis: (i) $pH_i$ regulation following acid transients was completely dependent on extracellular $Na^+$ in cultured rat neurons (Ou-yang et al., 1993) and astrocytes (Mellergård et al., 1993); (ii) recovery from acid loading in both sympathetic neurons and astrocytes was impaired by amiloride, an inhibitor of $Na^+/H^+$ exchange, and its derivatives (Tolkovsky and Richards, 1987; Mellergård et al., 1993); and (iii) harmaline, an inhibitor of $Na^+$-dependent transport, efficiently inhibited neuronal $pH_i$ regulation during acid transients (Ou-yang et al., 1993). Ischaemia-induced increase in $[H^+]_i$ also stimulates the $HCO_3^-/Cl^-$ exchanger, which translocates $HCO_3^-$ inwards in exchange for $Cl^-$ (Roos and Boron, 1981; Thomas, 1984). Both these plasma membrane exchangers are coupled to and driven by the $Na^+$-gradient, and are therefore dependent on ATP availability.

It is unlikely that the passive exchanger recently identified in both neurons and astrocytes (Mellergård et al., 1993; Ou-yang et al., 1993), which allows the release of $HCO_3^-$ in exchange for $Cl^-$ (i.e. a $Na^+$-independent $HCO_3^-/Cl^-$ exchanger), contributes to $pH_i$ regulation during this phase of ischaemia (Mellergård et al., 1993). In contrast to the $Na^+$-dependent $HCO_3^-/Cl^-$ exchanger, it is normally activated at increased $pH_i$ values (Mellergård et al., 1993; Ou-yang et al., 1993) and may actually be inhibited at a low pH (Olsnes et al., 1987; Frelin et al., 1988). Therefore, it is likely that this exchanger functions to translocate $HCO_3^-$ outward and $Cl^-$ inward to accelerate $pH_i$ regulation during alkaline transients.

The electrogenic $Na^+$-$HCO_3^-$ cotransporter evident in vertebrate glial cells (Astion and Orkand, 1988; Kettenmann and Schlue, 1988; Newman and Astion, 1991) may play a role in pH regulation during this phase of ischaemia. This cotransporter mediates a net inward movement of $HCO_3^-$ driven by the $Na^+$ gradient, the direction of the transport probably being determined both by the extra- and intracellular $HCO_3^-$ concentrations, and by the membrane potential (Kettenmann and Schlue, 1988; Deitmer and Schlue, 1989; Deitmer, 1991). Depolarisation-dependent alkalinisation of glial cells, subsequent to stimulation, has been attributed to the electrogenic cotransport of $Na^+$ and $HCO_3^-$ (Chesler and Kraig, 1989; Deitmer and Schlue, 1989; Deitmer and Szatowski, 1990). In support

of this regulatory mechanism, recovery from intracellular acidification was mediated via a $Na^+$-$HCO_3^-$ cotransporter in glial cells of different origin (Deitmer and Schlue, 1987, 1989; Kettenmann and Schlue, 1988; Astion and Orkand, 1988; Astion et al., 1989). In theory, such a mechanism could be activated early during ischaemia by the following events: a decrease in the intracellular $HCO_3^-$ concentration, and an inwardly directed $Na^+$ gradient.

Support for the involvement of other transport systems in the regulation of $pH_i$ during acidosis has been gained from the observation that inhibition of $Na^+/H^+$ exchange with amiloride does not completely abolish $pH_i$ regulation (Mellergård et al., 1993; Ouyang et al., 1993). This could imply that there are different populations of $Na^+/H^+$ antiporters, with varying sensitivity to amiloride, or different subpopulations of cells contain different $Na^+/H^+$ antiporters. Alternatively, it may suggest the involvement of other transport systems, a theory proposed by Wuttke and Walz (1990) who observed a $Na^+$- and $HCO_3^-$-independent regulation of $pH_i$ in cultured mouse astrocytes, and suggested the contribution of a lactate/$H^+$ transport system. Efflux of lactic acid in this way could play an important part in the intracellular acid-base regulation of the tissue during ischaemia when energy supply is inadequate. The effectiveness of this mechanism in $pH_i$ regulation was supported by the finding that lactate/$H^+$ transport, and not $Na^+/H^+$ or $HCO_3^-/Cl^-$ exchange was the dominant process for intracellular $H^+$ removal in isolated hypoxic peripheral nerves (Schneider et al., 1993). Although lactate removal was not a major route for $H^+$ extrusion from cortical brain slices after anoxia (Pirtillä and Kauppinen, 1992), lactate/$H^+$ transport across the cellular membrane may play a part in intracellular [$H^+$] during ischaemia.

As long as transmembrane ionic gradients are preserved, the intracellular buffering capacity together with activation of the $Na^+/H^+$ and $HCO_3^-/Cl^-$ exchanges attempt to maintain intracellular acid-base homeostasis. However, stimulation of these mechanisms implies that $pH_i$ is regulated to the detriment of the ECF, which rapidly acidifies.

#### 1.3.2.4 Ischaemia-Induced Extracellular Acid-Base Changes

It has been known since 1954 that ischaemia is associated with acidification of the extracellular fluid (Thorn and Heitmann, 1954). Since then, the progressive brain tissue acidification resulting from ischaemia has been thoroughly investigated (Siesjö, 1988b). The changes in extracellular pH remained poorly understood, partially due to the

difficulty in directly measuring the interstitial hydrogen ion concentration. However, the development of ion-selective microelectrodes has greatly facilitated the study of brain extracellular ionic composition following cerebral ischaemia (Kraig and Nicholson, 1978; Hansen and Zeuthen, 1981), and subsequent studies have shown that $pH_e$ decreases during ischaemia by approximately 0.6 to 0.9 units (Nemoto and Frinak, 1981; Kraig et al., 1983, 1985, 1986; Mutch and Hansen, 1984).

During ischaemia, stimulation of anaerobic glycolysis produces marked increases in lactate levels in the tissue (Lowry et al., 1964; Folbergrová et al., 1970, 1974; Paschen et al., 1987; Siesjö, 1988b), the amount of lactate accumulated being determined by the preischaemic tissue stores of glucose and glycogen. Under normoglycaemic circumstances, these suffice to raise the tissue lactate contents to 12-15 $\mu mol.g^{-1}$ of brain tissue (Lowry et al., 1964; Ljunggren et al., 1974a,b; Folbergrová et al., 1974). Larger amounts of lactate may, in principle, accumulate during incomplete ischaemia of a density that give extensive energy failure since glycolysis is then maximally stimulated and the residual blood flow delivers additional glucose to the tissue (Siesjö, 1988b). Moderate hyperglycaemia is sufficient to raise tissue lactate levels significantly, and during severe hyperglycaemia, tissue lactate contents may rise up to 30-40 $\mu mol.g^{-1}$ (Nordström and Siesjö, 1978; Welsh et al., 1980). Morphological studies suggest that when the tissue lactate concentration during severe ischaemia exceeds 16 $\mu mol.g^{-1}$, irreversible tissue damage prevails (Plum, 1983; Norenberg et al., 1987).

The degree of reduction of $pH_e$ correlates with the amounts of lactate formed during ischaemia (Siemkowicz and Hansen, 1981). Thus when ischaemic tissue lactate concentrations are altered by preischaemic variations in plasma (and tissue) glucose concentration, the change in $pH_e$ is expected to vary accordingly (Siesjö, 1988b). At first sight, it is expected that the changes in $pH_e$ are directly proportional to the change in lactate, since accumulation of lactate, with a stoichiometrical amount of $H^+$, is the most important single event acidifying the intra- and extracellular fluids (Siesjö et al., 1990). However, $pH_e$ was subsequently found to change in a discontinuous fashion with tissue lactate during complete ischaemia (Kraig et al., 1985, 1986). Between lactate concentrations of 17-20 $\mu mol.g^{-1}$, $pH_e$ did not increase linearly but showed two plateau values. Such results revealed that factors other than $CO_2$ and lactic acid diffusion determined the ischaemia-induced alteration in $pH_e$ and suggested that $H^+$ and/or $HCO_3^-$ exchanges occurred in the tissue lactate range over which ischaemic damage is aggravated

in hyperglycaemic animals (Siesjö, 1981, 1984, 1988b). The same data also revealed a discontinuous relationship between the $PCO_2$ and tissue lactate, which implied that at high tissue glucose concentrations, lactic acid is formed in a compartment (possibly glia) whose $HCO_3^-$ content was close to zero (Kraig et al., 1985, 1986). Subsequently, direct measurement of $pH_i$ supported the theory of $H^+$ compartmentalisation as the ischaemic tissue of grossly hyperglycaemic animals contained compartments with severely low pH values (pH about 5.3) in comparison to that of neuronal and ECF pH (about pH 6.2) (Kraig and Chesler, 1990). However, several lines of evidence conflict with the notion of $H^+$ compartmentation during ischaemia: (i) $^{31}P$ NMR studies failed to detect any heterogeneity in pH during ischaemia in either normo- or hyperglycaemic animals (Boris-Möller et al., 1988); (ii) in normo- or hyperglycaemic animals, with or without hypercapnia, the relationship between lactate and $PCO_2$ was strictly linear (Ekholm et al., 1991; Katsura et al., 1991, 1992); and (iii) cultured astrocytes, loaded with lactic acid, did not "trap" the acid, and the latter rapidly equilibrated between glia, neurons and extracellular fluid (Walz and Mukerji, 1988a, 1990).

Whereas the lactate accumulated during ischaemia is proportional to the degree of acidosis (i.e. $pH_i$ and $pH_e$) (Siemkowicz and Hansen, 1981; Ekholm et al., 1991; Katsura et al., 1991, 1992), this relationship may not exist after transient ischaemia since $pH_i$ may be regulated back to normal, or turn alkaline, when tissue lactate contents are still elevated (Mabe et al., 1983; Siesjö et al., 1985a; Paschen et al., 1987). Although the hypothesis of $H^+$ compartmentalisation during ischaemia remains to be clarified, it exemplifies the complex array of mechanisms that may contribute to acidosis during ischaemia.

Most studies of ischaemia have concentrated on changes in tissue lactate, however, marked increases in extracellular lactate have been observed during ischaemia produced by cardiac arrest (Kuhr et al., 1988), suggesting that lactate formed intracellularly is removed to the ECF (Walz and Mukerji, 1988a). Transport of lactate between the intra- and extracellular compartments in the brain has often been assumed to be mediated by simple diffusion of undissociated lactic acid through the cell membrane (Roos and Boron, 1981; Smith et al., 1986; Nedergaard et al., 1989). However, carrier-mediated lactate transport has been suggested, since increases in extracellular lactate following cardiac arrest and electroconvulsive shock were delayed in contrast to those in tissue lactate, and the increase in extracellular lactate was much smaller than that observed in the tissue

(Kuhr and Korf, 1988; Kuhr et al., 1988). Carrier-mediated lactate transport implies that efflux of lactate out of the cell during ischaemia may cease when the available energy supply is consumed and membrane function is impaired (Kuhr et al., 1988). Since accumulation of lactate during ischaemia has been directly associated with cell dysfunction and death (Rehncrona et al., 1981; Plum, 1983; Norenberg et al., 1987), the regulation of intra- and extracellular lactate levels may play an important role in the overall mechanism by which cell function is restored following gross metabolic insults. Although during sustained ischaemia, lactate cannot serve as a useful substrate due to the insufficient oxygen levels, it may serve to retain substrate for generation of energy, to be used as soon as the ischaemia is relieved. Indeed it has been shown that brain tissue can restore and maintain basic electrical and biochemical functions after ischaemia for a limited time period without supply of glucose (Bock et al., 1993), and that in the presence of oxygen and absence of glucose, lactate can restore and maintain synaptic transmission in slices of hippocampus (Schurr et al., 1988).

The acidification of the brain cell microenvironment before anoxic depolarisation is associated with a gradual increase of extracellular $K^+$ activity (Harris and Symon, 1984; Kraig et al., 1983) reflecting a progressive failure of the ATP-dependent $Na^+/K^+$ pump and/or increase in the cell membrane permeability to $K^+$. Apart from a slight rise in $[Ca^{2+}]_e$, possibly a consequence of increasing extrusion of $Ca^{2+}$ from the cells, subsequent to release of $Ca^{2+}$ from an intracellular store (Obrenovitch et al., 1990b), interstitial activities of $Na^+$ and $Cl^-$ are maintained within the normal range (Harris and Symon, 1984; Hansen, 1985; Hansen and Nedergaard, 1988). The changes that occur initially during ischaemia (i.e. before anoxic depolarisation, phase 1) are reversible. The duration of this phase of ischaemia has been shown to be influenced by pre-ischaemic tissue glucose concentrations (Hansen and Nordström, 1979; Siemkowicz and Hansen, 1981) and metabolic rate (Astrup et al., 1980).

The efficacy of the mechanisms regulating $pH_i$ during ischaemia-induced acidosis requires both maintenance of the overall impermeability of the plasma membranes to ions, and a functioning $Na^+/K^+$-ATPase pump. Progressive loss of $Na^+/K^+$-ATPase pump activity compromises the $Na^+$ gradient, thus impairing mechanisms regulating $pH_i$. With continued ischaemia, anaerobic energy production via glycolysis is not sufficient to keep up with the basal energy demands that are needed to maintain ionic homeostasis. As such ionic gradients collapse resulting in cellular membrane depolarisation.

### 1.3.2.5 Breakdown of Processes Counteracting Intracellular Acidification with Anoxic Depolarisation

Anoxic depolarisation is characterised by a massive release of $K^+$ from cells, influx of $Ca^{2+}$, $Na^+$ and $Cl^-$, and is accompanied by loss of volume regulation with cell volume increasing at the expense of the extracellular space (Kraig and Nicholson, 1978; Hansen and Olsen, 1980; Hansen and Zeuthen, 1981). Disruption of transmembrane ionic gradients implies the collapse of a number of plasmalemnal transport/exchange systems which are driven by these gradients, including those contributing to cellular acid-base homeostasis.

The smooth acidification of the ECF during ischaemia is interrupted by a transient alkalinisation that coincides in time with the DC potential shift and the rapid ionic fluxes during this phase of ischaemia (Kraig et al., 1983; Mutch and Hansen, 1984; Hansen, 1985). Similar alkalotic shifts occur with membrane depolarisation subsequent to spreading depression (Kraig et al., 1983; Mutch and Hansen, 1984) and application of excitatory amino acids (Endres et al., 1986). The origin of the transient fall in $[H^+]_e$ associated with depolarisation has remained undefined (Kraig et al., 1983; Mutch and Hansen, 1984). It has been suggested that this phenomenon is due to the rapid shrinkage of the extracellular space, known to be associated with alterations in ionic distribution subsequent to acute ischaemia (Hansen and Olsen, 1980), resulting in a sudden increase in the $[HCO_3^-]_e$ (Kraig et al., 1983). However, the speed at which this phenomenon occurs and its close association with the breakdown of ionic gradients, suggest that alkalotic transients may reflect a fast redistribution of $H^+$ and $HCO_3^-$ between the intra and extracellular space (Obrenovitch et al. 1990a). This still remains speculation since pH changing anions (i.e. $OH^-$, $HCO_3^-$, $CO_3^{2-}$) have not been measured during ischaemia.

Although tissue levels of lactate continue to increase after terminal ischaemia (Lowry et al., 1964; Folbergrová et al., 1970, 1974; Paschen et al., 1987; Siesjö, 1988b), findings suggest that extracellular lactate decreased several minutes postmortem despite persistent high tissue lactate levels (Kuhr et al., 1988). This implies that lactate removal from intracellular compartments was dependent on transmembrane ionic gradients, as it was only effective when energy supplies maintained membrane integrity and function (Kuhr et al., 1988). Therefore, when ionic homeostasis is disrupted with anoxic depolarisation lactate transport may be impaired and "trapping" lactate intracellularly, aggravating the deleterious effects of ischaemia.

## 1.3.3 Spreading Depression

### 1.3.3.1 Introduction

Spreading depression (SD) was first described by Leáo (1944) as an electrophysiologic phenomenon elicited by a variety of noxious stimuli. It is characterised as a propagating transient suppression of electrical activity associated with cellular depolarisation (Leáo, 1944; Bures et al., 1974). SD spreads like a wave from its site of elicitation at a relatively slow speed (approximately 3 $mm.min^{-1}$ in rat cortex), and is accompanied by marked changes in interstitial ion concentrations (Nicholson and Kraig, 1975; Hansen and Olsen, 1980), blood flow (Gjedde et al., 1981; Lacombe et al., 1992), extracellular space volume (Phillips and Nicholson, 1979; Hansen and Olsen, 1980), tissue oxygen tension (Tsacopoulos and Lehmenkühler, 1977), and tissue metabolites (Quistorff et al., 1979). SD is a reversible process with ionic changes returning to basal levels within a few minutes (Hansen and Zeuthen, 1981; Nicholson and Kraig, 1981). Although repetitive elicitation of SD in normal brain tissue is not associated with irreversible damage (Nedergaard and Hansen, 1988), SD has been implicated in the pathophysiology of a number of neurological conditions such as stroke (Somjen et al., 1990), migraine with aura (Pearce, 1985), epilepsy (Marshall, 1959), and head injury (Mayevsky et al., 1995).

It has been proposed that recurrent SD occurs within the region surrounding the ischaemic core associated with focal ischaemia (i.e the penumbra) (Nedergaard and Astrup, 1986; Iijima et al., 1992). Although SD originate from ischaemic foci outside the infarct, once elicited, they inevitably spread to the rest of the ischaemic hemisphere. SD induces a significant lowering of tissue glucose content (Lauritzen et al., 1990), probably due to ensuing increased activity of ionic pumps (Mutch and Hansen, 1984). Therefore, SD in tissue with reduced blood flow may exhaust local energy stores due to increase demands on energy metabolism. Reduced glucose in the infarct border may render tissue more susceptible to SD elicitation (Bures and Buresová, 1960) and once SD is elicited, retard normalisation of ion perturbations (Kraig and Chesler, 1987; Gidö et al., 1993). SD may contribute to neuronal damage due to the repeated marked disruption in ionic homeostasis, acidosis, enhanced energy demand and neurotransmitter effluxes in regions where residual blood supply can only sustain basal ionic homeostasis. Pharmacological reduction in the number of spontaneous waves of depolarisation reduces tissue damage in the same area (Nedergaard and Astrup, 1986; Gill et al., 1992; Iijima et al., 1992).

Both experimental and clinical evidence also point to cortical SD as the most likely cause of migraine aura (i.e. neurological disturbances associated with the development of a migraine headache) (Lauritzen, 1994): (i) visual auras indicate a wave of intense excitation of the primary visual cortex moving at around 3 $mm.min^{-1}$, i.e. exactly the rate of propagation of cortical SD; (ii) the pattern of changes in brain blood flow during attacks of migraine with aura have been replicated in animal experiments during cortical SD; (iii) hypercapnia aborts migraine attacks and inhibits cortical SD; and (iv) the behavioural changes caused by cortical SD in animals are consistent with the transient neurological deficits recorded during migraine aura, even though rats do not experience hippocampal or cortical SD as aversive.

#### 1.3.3.2 Extracellular Acid-Base Changes During Spreading Depression

Spreading Depression had triggered much interest because it produces disruptions in cellular ionic homeostasis that are similar to those associated with anoxic/ischaemic depolarisation (Kraig and Nicholson, 1978; Tegtmeier, 1993), and can therefore serve as a useful analogy of cerebral dysfunction during ischaemia. With SD, the ionic composition of the brain extracellular space is subject to significant changes. There are rapid fluxes of ions and the concentrations of $Na^+$, $Cl^-$ and $Ca^{2+}$ decrease (Kraig and Nicholson, 1975, 1978; Hansen and Zeuthen, 1981), whilst the $K^+$ concentration undergoes rapid elevation (Hansen, 1977; Nicholson and Kraig 1975; Vyskocil et al., 1972), characterising cell membrane depolarisation. Increased extracellular $K^+$ and intracellular $Na^+$ concentrations stimulate the activity of $Na^+/K^+$-ATPase pump (Walz, 1992), which utilises ATP to transport $Na^+$ back out of the cell and $K^+$ back into the cell, in order to restore the ionic gradients across the cellular membranes. Hydrolysis of ATP is enhanced, with the consequent generation of ADP resulting in a decrease the ATP/ADP ratio (Mies and Paschen, 1984; Lauritzen et al., 1990). The [PCr]/[Cr] falls, accompanied by a rise in $P_i$, as the creatine phosphokinase reaction is linked to ATP hydrolysis. These changes, in turn, stimulate glycolysis and oxidative phosphorylation with a higher cellular oxygen consumption (Erecinska and Silver, 1989). When the cellular oxygen content is reduced to a level insufficient to support oxidative phosphorylation, cellular NADH content rises, leading activation of anaerobic glycolysis, and ultimately results in increased intracellular lactate production (Assaf et al., 1990; Hansen and Quistorff, 1993). Continued hydrolysis of ATP is associated with the enhanced intracellular production, and subsequent accumulation, of $H^+$.

Marked changes in $pH_e$ are associated with SD, indicating that the mechanisms regulating $pH_i$ remove $H^+$ to the extracellular compartment (Kraig et al., 1983; Mutch and Hansen, 1984). Changes in $pH_e$ with SD occurred in a triphasic pattern intimately related to the changes in membrane potential (Kraig et al., 1983; Mutch and Hansen, 1984). The first noticeable change in $pH_e$ is a small acidic shift (Kraig et al., 1983; Mutch and Hansen, 1984) which precedes the rapid negative change in membrane potential which signifies depolarisation. This shift in $pH_e$, which is not as pronounced as that observed with the onset of ischaemia, was enhanced with application of acetazolamide, an inhibitor of carbonic anhydrase activity (Mutch and Hansen, 1984). This suggested that this initial acidification could result from a slight increase in local $CO_2$ tension. Immediately following the acidic shift was a rapid transient alkaline shift, closely associated with cell depolarisation (Mutch and Hansen, 1984). This alkaline shift was followed by a marked acidic shift which persisted, with $pH_e$ returning to basal levels after approximately 8 minutes (Mutch and Hansen, 1984).

Although stimulation of anaerobic glycolysis results in intracellular lactate production, extracellular lactate increases with SD (Scheller et al., 1992) suggesting that SD-induced excess of intracellular lactate may be transferred to the ECF. As observed with ischaemia (Paschen et al., 1987) changes in extracellular lactate occurred in close correlation with those in $pH_e$ (Scheller et al., 1992), with a rapid increase associated with SD-induced extracellular acidosis. Lactate efflux from intracellular compartments may be linked to transmembrane ionic gradients and therefore be only effective when energy supplies maintain membrane integrity and function (Kuhr et al., 1988). If such a dependence exists, then intra-extracellular transport of lactate should be impaired during SD when ionic gradients are markedly perturbed.

Recovery of lactate after SD has been shown to occur within two phases closely correlated with changes in $pH_e$, suggesting that lactate movements across the cellular membrane may occur via active transport (Scheller et al., 1992). This biphasic removal of lactate could also indicate compartmentation of the transport of lactate, i.e. the release of lactate into the ECF or reuptake of lactate from the ECF by the neuronal compartment might be different from that of the glial compartment (Walz and Mukerji, 1990). Although SD-induced changes in $pH_e$ have been extensively investigated (Kraig et al., 1983; Mutch and Hansen, 1984; Scheller et al., 1992), the changes in extracellular lactate have remained largely undefined (Scheller et al., 1992).

### 1.3.4 Acidosis-Related Mechanisms of Tissue Damage

Thorn and Heitmann (1954) had suggested that rising lactic acid levels and lowered pH values enhanced cerebral ischaemic damage, and subsequent studies supported the involvement of lactacidosis in ischaemic brain damage (Salford et al., 1973; Salford and Siesjö, 1974; Siesjö, 1981, 1985, 1988b). It has been demonstrated that preischaemic hyperglycaemia worsens damage due to transient global or forebrain ischaemia probably by enhancing production of lactic acid during ischaemia (Myers and Yamaguchi, 1977; Rehncrona et al., 1981; Kalimo et al., 1981; Pulsinelli et al., 1982; Siesjö, 1988b). The strongest evidence for an association between acidosis and brain damage was the finding that hypoglycaemic coma, a condition that causes extensive energy failure and loss of ionic homeostasis, but no acidosis (Siesjö, 1981, 1988a), gave rise to neuronal necrosis but not to infarction, nor did it cause extensive edema or postischaemic seizures (Auer et al., 1984). This suggested that tissue acidosis was an important factor in the transition from neuronal necrosis to infarction. A strong correlation between both $H^+$ and lactate accumulation, and the extent of ischaemic brain damage strengthened the acidosis hypothesis of ischaemic injury (see Siesjö, 1988b). How acidosis damages nervous tissue remains unclear, as several mechanisms could interact to worsen damage in severely acidotic tissue, and prevent or retard recovery during reoxygenation.

Acidosis may trigger cell swelling via stimulation of the $Na^+/H^+$ and $HCO_3^-/Cl^-$ exchangers, which are involved in cell volume regulation (Siesjö, 1985; Kimelberg et al., 1990a). It is suspected that if acidosis activates the $Na^+/H^+$ exchanger and $H^+$ leaks back via the $HCO_3^-/Cl^-$ antiporter, a vicious circle is created which causes accumulation of $Na^+$ and $Cl^-$, and ultimately osmotic water intake. In support of this mechanism acidosis enhanced cell swelling *in vitro* (Kempski et al., 1988), and pharmacological inhibition of $HCO_3^-/Cl^-$ exchange correlated with the inhibition of brain slice swelling and protection against head injury (Kimelberg et al., 1990b).

Substantial evidence exists that reactive oxygen species contribute to tissue damage following both sustained and transient cerebral ischaemia (Siesjö et al., 1996a,b). A direct coupling between acidosis and enhanced formation of free radicals could trigger or increase free radical damage to membranes, microvessels and mitochondria (Pulsinelli et al., 1985; Rehncrona et al., 1989; Siesjö et al., 1989, 1996a). One likely triggering event for free radical damage is delocalisation of protein-bound iron (Siesjö et al., 1985b: Rehncrona et al., 1989), which catalyses the conversion of poorly reactive species ($^{\bullet}O_2^-$,

$H_2O_2$) into the highly reactive $^{\bullet}OH$ radical, that can damage DNA, proteins and carbohydrates (Halliwell and Gutteridge, 1985). The binding capacity for some iron-binding proteins is highly pH sensitive, as such ischaemia-induced intra- and extracellular acidosis may favour iron release, catalysing the formation of $^{\bullet}OH$.

Acidosis may enhance calcium-related damage since changes in $pH_e$ and $pH_i$ are known to affect cell $Ca^{2+}$ metabolism in a variety of cells, by modulating membrane fluxes of $Ca^{2+}$ across plasma and intracellular membranes, or by modulating its binding to proteins and other macromolecules (Busa and Nuccitelli, 1984). It has been postulated that loss of cellular $Ca^{2+}$ homeostasis with a marked increase in the free intracellular $Ca^{2+}$ concentration leads to neuronal necrosis under such conditions as ischaemia, hypoglycaemia and status epilepticus (Siesjö, 1981, 1988c; Meldrum, 1983). A rise in intracellular $Ca^{2+}$ is believed to cause cell damage by overactivation of destructive lipases and proteases, secondarily affecting protein synthesis and gene expression, to such an extent that membrane dysfunction ensues. There is a complex interplay between loss of cellular $Ca^{2+}$ homeostasis and acidosis. On the one hand, a rise in intracellular $Ca^{2+}$ is apt to cause partially oxygen-deprived mitochondria to take up $Ca^{2+}$, further interfering with ATP production and enhancing acidosis. On the other hand, intracellular acidosis leads to a release of $Ca^{2+}$ from intracellular stores, possibly because $Ca^{2+}$ and $H^+$ compete for the same binding sites on the "buffering" proteins calmodulin and calcibindin and increased $H^+$ levels are likely to displace $Ca^{2+}$, therefore contributing to the rise in intracellular $Ca^{2+}$ (Ou-yang et al., 1994).

Acidosis may also hinder postischaemic metabolic recovery due to inhibition of mitochondrial energy metabolism with reduced ATP formation (Shields et al., 1980). Prompt restitution of mitochondrial function requires that intracellular pH is increased, which occurs by oxidation of accumulated lactate and by accelerated $Na^+/H^+$ exchange. However, both these events are probably inhibited at low pH values (Siesjö et al., 1990). Clearly, severely acidotic tissue is at risk even when circulation is restored due to the prevention of recovery of a normal energy state and restitution of a normal intracellular pH.

Despite the deleterious effects of acidosis outlined above, results obtained *in vitro* have questioned whether acidosis is deleterious to tissue since they have demonstrated a protective effect of acidosis. Lowering the extracellular pH reduced $Ca^{2+}$ currents through NMDA receptor-gated channels in isolated neurons (Tang et al., 1990; Traynelis and

Cull-Candy, 1990; Vyklicky et al., 1990). Enhanced calcium influx through such channels is considered a potential threat to cell viability (Rothman and Olney, 1987; Choi, 1988; Siesjö, 1988c). Consistent with this idea are results showing that a lowering of $pH_e$ *in vitro* reduces $^{45}Ca^{2+}$ accumulation and protects neurons against the detrimental effects of glutamate exposure and anoxia (Giffard et al., 1990a,b; Tombaugh and Sapolsky, 1990), although acidosis did not reduce survival of astrocytes in culture (Norenberg et al., 1987; Goldman et al., 1989; Giffard et al., 1990a). Such results have led some to postulate that so-called excitotoxic damage is attenuated by acidosis.

Although these studies showed a protective effect of acidosis, both neurons and astrocytes were irreversibly damaged by exposure to low pH solutions *in vitro* (Goldman et al., 1989) and *in vivo* exposure to low pH caused coagulation necrosis (Kraig et al., 1987). In addition, both hyperglycaemia and hypercapnia, situations associated with excessive acidosis, exaggerated brain damage *in vivo* (Katsura et al., 1994b; Siesjö et al., 1996b). Therefore, the beneficial effects which acidosis may have by reducing rate of $Ca^{2+}$ influx into cells having high density of NMDA receptors (Kristián et al., 1994) is out weighed by the effects that acidosis *in vivo* on other cellular targets such as endothelial cells or astrocytes. Evidence *in vivo* indicates that acidosis is an aggravating factor in the pathogenesis of ischaemic brain damage suggesting a deleterious synergism between acidosis and ischaemic metabolic sequelae (Katsura et al., 1994b).

## 1.4 Relevance and Aim of This Study

Experimental data strongly support the concept that brain tissue acidification is a common and major factor responsible for neural tissue damage resulting from inadequate oxygen supply to the brain or head trauma (Rosner and Becker, 1984). This investigation was set out to acquire a better knowledge of some of the mechanisms underlying brain tissue acidification during ischaemia and spreading depression, concentrating on the extracellular activities of the variables involved in the regulation of brain tissue acid-base homeostasis.

The capacity of the ECF to buffer $H^+$ is largely dependent of $HCO_3^-$ and $CO_3^{2-}$. Although the extracellular concentration of $HCO_3^-$ is larger than that of $CO_3^{2-}$ (Siesjö, 1985; Chesler et al., 1994), $CO_3^{2-}$ is an important component of the bicarbonate/carbonic acid buffer system which has been previously neglected, and its changes during ischaemia and SD undefined (Siesjö, 1985). Failure of cellular ion homeostasis associated with

anoxic depolarisation is suggested to play a key role in ischaemia-induced neuronal death. The sudden increase in membrane permeability with anoxic depolarisation is associated with a rapid, transient alkalotic shift in $[H^+]_e$. The speed at which this phenomenon occurs and its close association with the breakdown of ionic gradients, suggest that alkalotic transients may reflect a fast redistribution of $H^+$ and $HCO_3^-/CO_3^{2-}$ between the intra and extracellular space (Obrenovitch et al. 1990a). However, this still remains speculation since none of the pH-changing anions (i.e. $OH^-$, $HCO_3^-$, $CO_3^{2-}$) have been measured during ischaemia.

Although lactic acid distribution between the intra- and extracellular space during ischaemia is likely to play an important part in the overall mechanisms leading to brain tissue damage, this aspect has been seldom studied *in vivo* (Kuhr et al., 1988; Assaf et al., 1990). The deleterious effects of stroke and head trauma, which combine lactacidosis and altered membrane function, may be aggravated by a collapse of intracellular acid-base regulation subsequent to "trapping" of intracellular lactate, and increased cellular membrane permeability to $H^+$ and $HCO_3^-$ (Obrenovitch et al., 1990a). Despite this, little is known about lactate changes in the extracellular fluid, i.e. the neuronal microenvironment.

# CHAPTER 2 METHODS USED IN THIS STUDY

## 2.1 Investigation of Changes in Extracellular Fluid Composition

Intracellular acidosis has been extensively investigated (Siesjö, 1985) and nuclear magnetic resonance (NMR) spectroscopy has provided a wealth of information (Brooks and Bachelard, 1992; Ben-Yoseph et al., 1993; Conger et al., 1995). However, application of techniques such as NMR spectroscopy have provided information concerning the chemical changes occurring within the whole brain, representing a mixture of intracellular as well as extracellular contents. The measurement of total ion contents provides little information about the compartmental distribution and dynamic fluxes of the ions of interest.

This study focused on the acid-base changes occurring within the ECF i.e. the neuronal microenvironment. Originally thought to conform to the concept of "la fixité du milieu intérieur" (Bernard, 1878), it is now clear that the ECF is not a static environment, but rather one that undergoes specific dynamic changes (Hansen, 1977; Kraig and Nicholson, 1978; Nicholson, 1980). The ECF constitutes approximately 20 % of the total brain volume and is the site of extensive chemical trafficking between nerve cells, glial cells and blood vessels. It is where various neurotransmitters and drugs are available to receptors, and the compartment through which cell-cell signalling may be exerted by messengers (e.g. nitric oxide)(Garthwaite, 1991). Isolated from the blood by the blood-brain barrier on one side, and from the cytosol by cellular membranes, the extracellular space is a separate entity, with a composition different from that of the two surrounding compartments.

Accurate information on the events occurring in the ECF would certainly contribute to a better understanding of brain function. The need for reliable and continuous *in vivo* analysis of the brain ECF has resulted in the development of a number of different sampling methods, such as cortical cup perfusion (Moroni and Pepeu, 1984), push-pull (Gaddum, 1961), microdialysis (Bito et al., 1966), and both ion-selective (Thomas, 1978; Zeuthen, 1981) and chemical-specific electrodes (Marsden et al., 1984). This study relied on ion-selective microelectrodes and intracerebral microdialysis to provide measurements of the relevant variables of interest in the different brain regions under investigation.

### 2.1.1 Ion-Selective Microelectrodes

Ion-selective microelectrodes (ISM) allow the detection of a number of ions and are a very useful tool in physiological and pathological investigations *in vivo*. This technique requires the implantation of a glass electrode containing an exchange resin selective to the ion of interest. By measuring the difference in the potential generated across the ion-exchange resin to a reference electrode, ion activities can be accurately measured. Like all methods, they have advantages and limitations. The most important advantage of ISM is that they enable direct measurement of ion activity. Due to the rapid response time the results are obtained immediately, and dynamic changes in ion activity can be monitored. It is possible to make continuous recordings over a period of many hours, and to also measure the activities of more than one ion simultaneously. The main limitation of ISM is their potential lack of selectivity, i.e. the interference from other ions encountered under the experimental conditions. Due to their high impedance, ISM can also pick up electrical interference and shielding is required to achieve an appropriate signal to noise ratio. Another difficulty is the intricate construction of ISM to such extent that their fabrication has been likened to an art rather than a science (Thomas, 1978).

### 2.1.2 Intracerebral Microdialysis

Microdialysis is a major research tool and has provided a wealth of information on the metabolism and function of the intact brain. Microdialysis, in principle, is the only technique from those mentioned above which can collect virtually any substance from specific brain regions with a limited amount of tissue trauma. This technique requires implantation of a dialysis fibre, permeable to small-size molecules, through which an artificial medium is perfused. Low-molecular-weight compounds diffuse along their concentration gradient, from the ECF to the perfusate, which is collected and analysed. By changing the perfusion medium, controlled alterations of the ECF composition or the local application of drugs can also be achieved. Microdialysis probes cause minimal tissue damage on implantation which makes them ideal for introduction into various structures of the brain (see Benveniste and Hüttemeier, 1990). They can be easily adapted by either varying the length of the dialysis membrane according to the brain structure under investigation, or by altering the membrane itself.

The main limitation of intracerebral dialysis, when it is associated with high precision liquid chromatography (HPLC) analysis, lies in the large number of brain

dialysate samples which are collected for subsequent off-line analysis. The changes measured with this method are limited by the sampling time and therefore will not reveal dynamic alterations occurring. In this study, intracerebral dialysis was coupled with on-line enzymatic fluorometric analysis, which takes advantage of the selectivity of an enzymatic system. This technique, lactography, is based on microdialysis allowing continuous sampling from the ECF, enzymatic conversion of lactate in the dialysate, and on-line detection of the fluorescent NADH produced. By eliminating the need to collect samples and to isolate the substrate of interest, this combination provides information rapidly with a good time resolution (Kuhr and Korf, 1988; Kuhr et al., 1988). Lactography is a relatively simple and inexpensive technique that can be applied *in vivo* to study metabolism in brain regions in the rat and human (Kuhr and Korf, 1988; During et al., 1994).

### 2.1.3 Electrophysiological Recordings

Extracellular recording of $CO_3^{2-}$, $H^+$ or lactate levels was combined with that of the extracellular direct current (DC) potential and electroencephalogram (EEG). These electrophysiological variables provided information on the severity of ischaemia, and the DC potential allowed precise detection of the occurrence of anoxic or $K^+$-induced depolarisation (Sugaya et al., 1975).

Previously, simultaneous electrophysiological recordings with microdialysis have been made using electrodes attached to the probe or implanted adjacent to it, but such strategies aggravate tissue damage within the region under study. Non-invasive monitoring of the ionic and electrical status of brain tissue has also been accomplished by placing multiparametric recording devices on the cortical surface, however, this cannot provide information on specific structures within the brain. The microdialysis probes used in this study contained a miniature electrode which allowed the monitoring of both EEG and the DC potential precisely at the dialysis sampling site (Obrenovitch et al., 1993). Therefore, the probe was used to monitor electrical activity and membrane polarisation, as well as the neurochemistry. With ISM, the reference barrel was used to measure EEG and the DC potential in the same structure as the variables under investigation.

## 2.2 Animal Models

The number of methods available to produce cerebral ischaemia in animals illustrates the difficulty of simulating stroke in man (Cohen, 1974). Focal ischaemia, produced by permanent occlusion of a major cerebral artery, is considered to mimic stroke in humans (Siesjö, 1992). Focal ischaemia differs from global or forebrain ischaemia in two major respects. Firstly the reduction in cerebral blood flow is usually less severe than that during global or forebrain ischaemia and it is usually more sustained. Secondly, the "stroke lesion" can be considered to consist of a central core of densely ischaemic tissue with surrounding areas of less dense ischaemia (penumbra) (Obrenovitch, 1995). In the rat model of focal ischaemia the penumbra is a narrow, unstable region (Tyson et al., 1984; Bolander et al., 1989) whose location cannot be accurately determined in individual experiments. Furthermore, implantation of a microdialysis probe in the penumbra is likely to alter its fragile state (Obrenovitch, 1995).

Due to these considerations, models of terminal complete (global) and transient forebrain ischaemia were used for this study. Global ischaemia produced by cardiac arrest only allows brief ischaemic periods to be studied. However, a very similar type of ischaemia can be induced by occlusion of major cerebral arteries (Hossmann, 1985). In this study, transient forebrain ischaemia was produced by occlusion of the carotid and vertebral arteries, the four major vessels supplying the brain. This model of 4-vessel occlusion, provides a highly reproducible method for achieving reversible but near-total forebrain ischaemia (Pulsinelli and Bierley, 1979; Blomqvist et al., 1984). Although major forebrain structures such as the cortex and striatum are densely ischaemic, other areas such as the brain stem have near normal flow rates, and as such recovery of circulatory and respiratory functions after ischaemia is facilitated (Pulsinelli et al., 1983).

Although, variation in the severity of cerebral ischaemia produced by the 4-vessel occlusion method has previously been reported (Furlow, 1983), this may be attributed to: (i) incomplete thermo-coagulation of the vertebral arteries; (ii) continued cerebral blood flow arising from the anterior spinal artery and the collateral arteries in the cervical paravertebral muscles (Pulsinelli et al., 1983); and/or (iii) a difference between strains of rats used (Furlow, 1982). In this study, care was taken during surgical preparation to ensure that the carotid and vertebral arteries were completely occluded, and provision was taken so that the neck could be ligated if ischaemia was seen to be incomplete as indicated from the DC potential and EEG recordings. Since studies with Sprague-Dawley rats

subjected to 4-vessel occlusion showed variability in the severity of ischaemia between and within regions of the brain (Furlow, 1982), Wistar rats were used for all ischaemia experiments as these have less collateral blood supply to the brain and are therefore be more susceptible to 4-vessel occlusion (Furlow, 1983).

In this study, the variables of interest were measured in two different regions of the brain, the cerebral cortex and dorsolateral striatum. Extracellular $CO_3^{2-}$, $H^+$ and lactate changes during ischaemia were recorded in the cerebral cortex, since most previous investigations of ischaemia-induced ionic changes which have been performed in this structure (Hansen and Nedergaard, 1988; Obrenovitch et al., 1990b). Lactate changes were also recorded in the rat striatum because ischaemia-induced changes in extracellular lactate have previously been studied in this region (Kuhr and Korf, 1988; Kuhr et al., 1988) and the method of recording DC potential through the microdialysis probe was validated in this brain structure (Obrenovitch et al., 1993, 1995). Simultaneous recording of extracellular $CO_3^{2-}$ and $H^+$ with lactate could not be performed in the striatum as implantation the fine-tipped ISM deep into the brain tissue was not possible. Obtaining data from two brain regions also enabled comparison of the changes occurring within each region during the conditions investigated.

High $K^+$ has long been used to investigate cerebral function *in vitro* and *in vivo* during depolarisation because the gradient of $K^+$ across the cellular membrane is a principle determinant of its resting potential (Spira et al., 1984). In the present study, depolarisation was induced by perfusing ACSF containing a high concentration of $K^+$ through the microdialysis probe. Although the pharmacology of SD *in vivo* is commonly studied in the cerebral cortex, this study remains relevant however, because SD has been observed in the human striatum (Sramka et al., 1977/78) and SD associated with focal ischaemia was recorded in the rat striatum (Wahl et al., 1994).

## 2.3 Drugs

Probenecid [p-(dipropylsulphamoyl) benzoic acid], introduced by Sharpe and Dohme in 1950, is widely used as a uricosuric agent in the treatment of chronic gout, and as an adjunct to enhance blood levels of antibiotics (such as penecillins and cephalosporins). Probenecid is a lipid soluble benzoic acid derivative and a competitive (i.e. transportable) inhibitor of short-chain monocarboxylic acid transport, and has been employed as a classical competitive inhibitor of active transport processes in the brain, kidney and liver. In this study, probenecid in ACSF was perfused through the microdialysis probe to inhibit lactate transport (Kuhr et al., 1988).

# CHAPTER 3 ION-SELECTIVE MICROELECTRODES

## 3.1 Introduction

Ion-selective microelectrodes have largely contributed to a better understanding of many ionic mechanisms in the brain. A variety of ions can now be measured due to the development of highly selective liquid ion-exchange resins. In this study, ion-selective microelectrodes were used to provide direct measurement of extracellular changes in $HCO_3^-/CO_3^{2-}$ and $H^+$ occurring within the cerebral cortex.

The first reliable measurements of "$HCO_3^-$" were performed in skeletal muscle fibres and kidney cells (Khuri et al., 1974, 1976) with a "$HCO_3^-$" exchange resin developed by Wise (1973). Later, this resin was found to be sensitive to $CO_3^{2-}$ and not $HCO_3^-$ as originally reported (Herman and Rechnitz, 1975; Kraig and Cooper, 1987). The ion-exchange resin used in this study (sold as a $HCO_3^-$ exchange resin; World Precision Instruments Inc. Sarasota, FL. U.S.A.) was postulated to be similar in composition as the resin developed by Wise (1973; Kraig and Cooper, 1987).

Initial pH measurements were performed using glass electrodes which were limited practically by their large size and slow response times. It was not until 1981 with the development of a selective ion-exchange resin, that accurate measurements of $H^+$ could be achieved (Ammann et al., 1981). Subsequently, highly selective exchange resins have become commercially available (Kraig et al., 1983; Mutch and Hansen, 1984).

The remainder of this chapter covers the basic principles of ISM, their fabrication, calibration and *in vitro* assessment and their selectivity.

## 3.2 Basic Principles of Ion-Selective Microelectrodes

Ion-selective microelectrodes (ISM) allow the determination of the activity of a given ion in solutions. The active component of an ISM is an ion-selective barrier, in this case a liquid ion-exchange resin, separating an internal reference solution from the sample solution (Fig. 3.2.A). By selectively transferring the ion to be measured from the sample solution to the membrane phase of the ion-selective electrode, a potential difference between the internal reference solution and the sample solution is generated. This potential, the electromotive force (EMF), is measured relative to a

reference electrode to minimise artifacts and provide a stable signal (Fig. 3.2.B). In theory, the EMF is a linear function of the logarithm of the activity of the ion in the test solution and is described by the Nernst equation:

$$EMF = E_o + s.\log a_i \qquad \text{Equation 3.A}$$

where:

EMF = electromotive force (mV).

$E_o$ = reference potential.

$a_i$ = the activity of the ion *i* in the sample solution.

s = the Nernstian slope (mV) defined as:

$$s = 2.303\ RT/F.z_i \qquad \text{Equation 3.B}$$

where:

R = gas constant (8.314 $JK^{-1}mol^{-1}$).

T = absolute temperature (K).

F = Faraday equivalent ($9.6487.10^4$ $Cmol^{-1}$).

$z_i$ = charge (valency) of the ion *i* in the sample solution.

In practice, however, additional contributions to the EMF result from the presence of interfering ions (*j*) in the sample solution. The relationship between the electrode potential and the logarithm of the measuring ion activity in the presence of interfering ions is represented by the extended Nicolsky-Eisenman equation:

$$EMF = E_o + s.\log [a_i + \Sigma K_{ij}^{pot}(a_j)^{zi/zj}] \qquad \text{Equation 3.C}$$

where:

EMF = electromotive force (mV).

$K_{ij}^{pot}$ = selectivity coefficient; a measure of the preference of the ion-exchange resin for the primary ion over the interfering ion.

$z_i$, $z_j$ = charge (valency) of the primary and interfering ions, respectively.

$a_i$, $a_j$ = activities of the primary and interfering ions, respectively.

$E_o$ = reference potential.

The potential $E_o$ is a sum of unavoidable potential differences generated between the filling solutions, ion-exchange resin and metallic leads of the electrode, and the sample solutions, and is defined as:

$$E_o = E^o_i + E_R + E_D \qquad \text{Equation 3.D}$$

where:

$E^o_i$ = constant potential difference including the boundary potential difference between the internal reference solution and the ion-exchange resin.

$E_R$ = potential difference between the metallic leads and the internal reference and reference solutions.

$E_D$ = potential difference between the reference solution and the sample solution.

The sum $E^o_i + E_R$ encompasses, for a given set of conditions, all the contributions that are independent of the sample composition. $E_D$ is sample dependant and will vary with each sample solution. The potential $E^o_i$ cannot be avoided. In an attempt to minimise $E_R$ chlorided silver wires were used as the metallic leads to the amplification system. The influence of $E_D$ was reduced by using 130 mM KCl as the reference solution and by using calibration solutions with a similar ionic content to that of the extracellular fluid.

Using separate ion-selective and reference electrodes (i.e. single-barrelled electrodes; Fig. 3.2.B) *in vivo* suffers from interference due to variable DC potentials across the cerebral cortex, which produce artifactual changes in the signal recorded. This problem can be overcome by bringing the two electrodes together to form a double-barrelled electrode, thus recording both the ion and reference potentials in exactly the same extracellular site (Fig. 3.2.C). To produce triple-barrelled electrodes for studying two different ions, the double-barrelled electrode is modified and another active barrel added (Fig. 3.2.D).

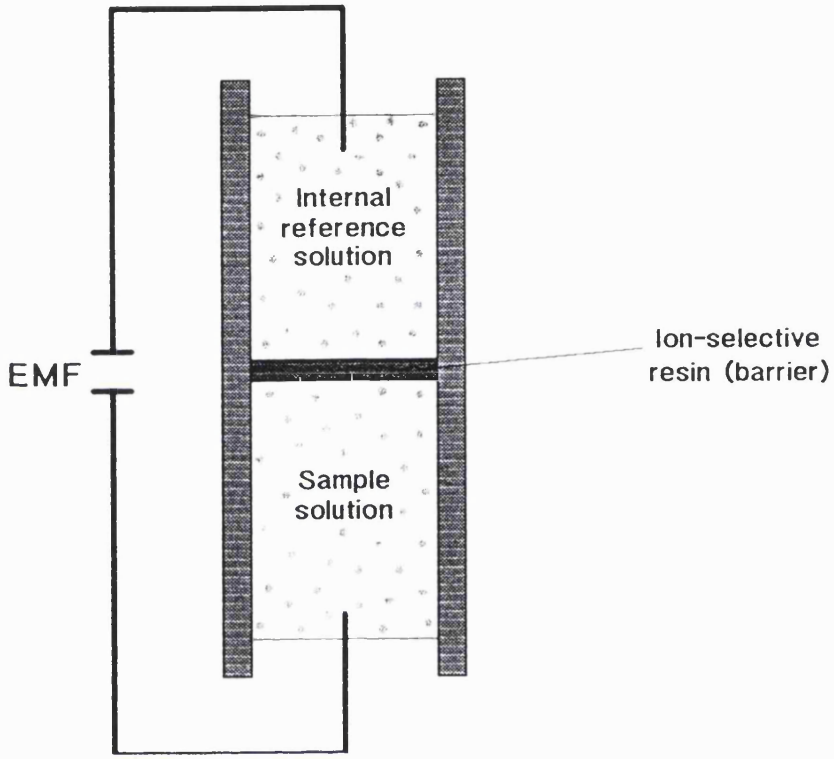


**FIG. 3.2.A** Principle of an ion-selective microelectrode. Transference of the ion to be measured from the sample solution to the membrane phase (i.e. ion-exchange resin) generates a potential difference between the internal reference solution and the sample solution (electromotive force or EMF).

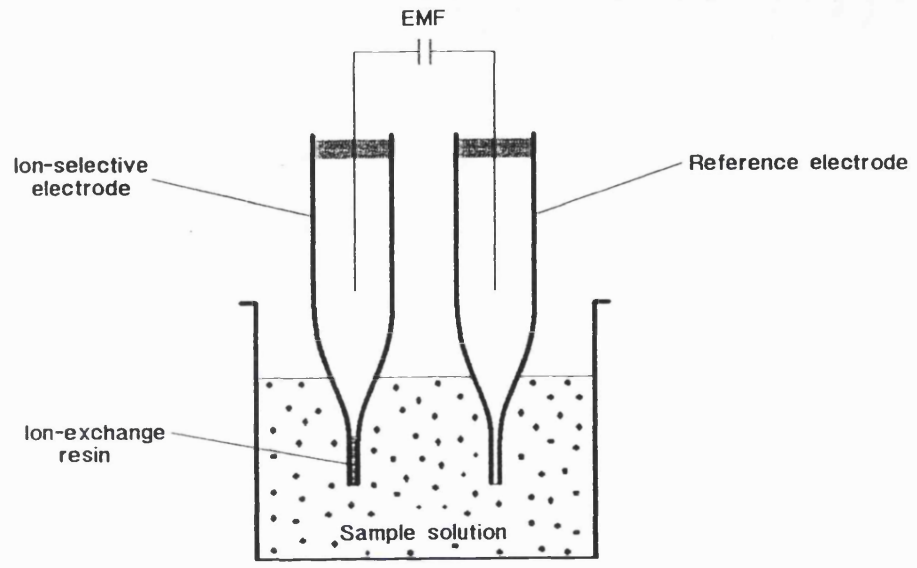


**FIG. 3.2.B** Separate single-barrelled reference and ion-selective microelectrodes for measurement of EMF.

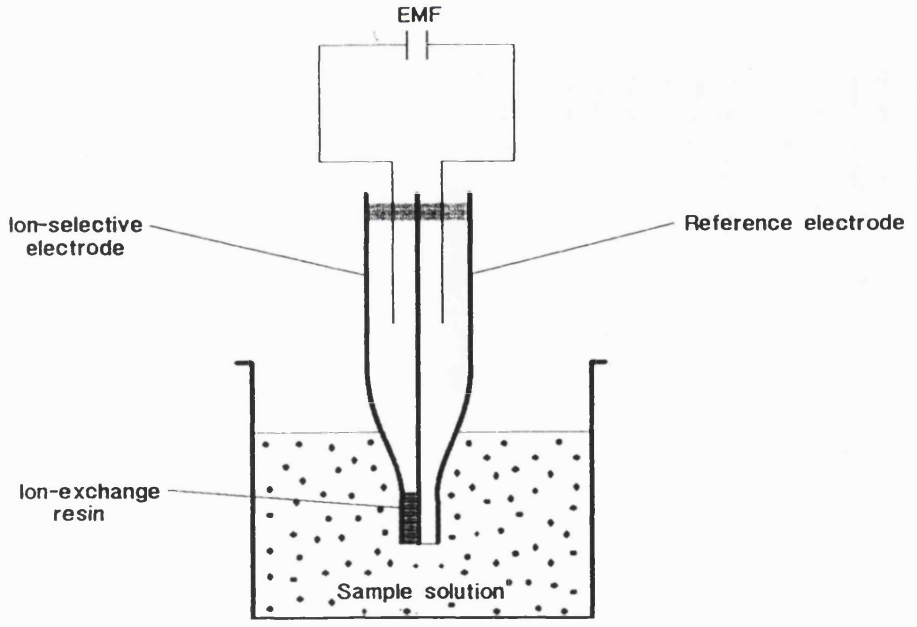


**FIG. 3.2.C** Double-barrelled ion-selective microelectrode records the ion and reference potentials from the site.

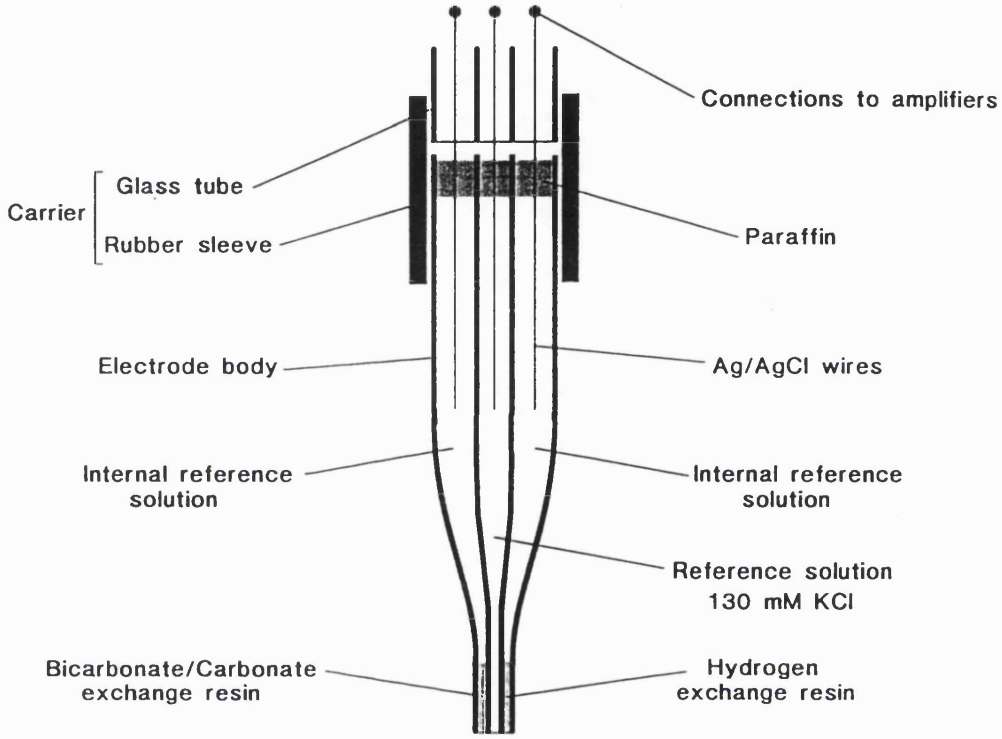


**FIG. 3.2.D** Triple-barrelled ion-selective microelectrodes enabled simultaneous measurement of bicarbonate/carbonate and hydrogen ion concentrations in exactly the same extracellular site.

## 3.3 Fabrication of Ion-Selective Microelectrodes

Preparation of Electrode Blanks: Double- and triple-barrelled microelectrodes were constructed from 15 cm lengths of double-barrelled borosilicate capillaries (2 mm o.d.; TGC200-10; Clark Electromedical Instruments, Reading, U.K.) and tri-lumen theta capillaries (2.7 mm by 3.2 mm o.d.; Glass Company of America, New Jersey, U.S.A.), respectively. After thorough cleaning with acetone, capillaries were pulled using a horizontal electrode puller (BB-CH, Mecanex, Geneve, Switzerland) to produce electrode blanks with a shank length of approximately 20 mm. Heating to 120 °C in an oven for 30-60 minutes removed any residual water. To ensure proper adhesion between the ion-exchange resin and the inner glass surface of the electrode, it was necessary to make the latter hydrophobic. This was achieved by back filling the tips of the active barrels with a 10 % solution of N,N-Dimethyltrimethylsilyamine (Aldrich Chemical Company, Gillingham, Dorset, U.K.) in carbon tetrachloride ($CCl_4$; BDH, Lutterworth, Leicestershire, U.K.). The electrodes were suspended vertically in an oven at 200 °C for 1 hour to evaporate the $CCl_4$ and bake the silane onto the glass. Electrode tips were cut to produce a tip diameter of 10-15 $\mu$m.

Filling of Double-Barrelled Microelectrodes: The silanised and reference barrels were back-filled with the internal reference solution and 130 mM KCl, respectively (Table 3.3.A). The ion-exchange resin was placed in a glass capillary tube and brought in contact with the tip, until the resin had reached a height of 1-2 mm in the silanised barrel (Fig. 3.2.C).

Filling of Triple-Barrelled Microelectrodes: The electrode blanks were held on a stage, and filling capillaries were introduced into each barrel using a micromanipulator (Prior Scientific Instruments Ltd., Cambridge, U.K.). $H^+$-exchange resin was introduced into the very tip of one active barrel to a height of 1-2 mm. Then, the barrel was filled with the respective internal reference solution using a filling capillary, the tip of which was positioned slightly above the ion-exchange resin. The same procedure was used to fill the second active barrel with $HCO_3^-$-exchange resin and the corresponding internal reference solution (Fig. 3.2.D). The resins and internal reference solutions used are shown in Table 3.3.A. The reference barrel was filled with 130 mM KCl. A thin layer of paraffin placed at the top of each barrel prevented evaporation and any current leakage between the barrels. ISM were left to equilibrate

overnight in 130 mM NaCl.

Signal Recording and Display: Signals from triple-barrelled ion-selective microelectrodes were recorded using two separate differential amplifiers, each using the reference barrel as one input. Electrodes were connected to the amplifiers using an electrode carrier system modified from that previously developed in this laboratory (Harris and Symon, 1981). The carrier consisted of a rubber sleeve placed over a short length of triple-barrelled glass tubing. Three lengths of tinned copper wire (1.6 mm diameter; RS Components Ltd, Corby, Northants, U.K.) were connected directly to the amplifier and the glass tubing glued onto the centre wire. The electrode was secured into the rubber sleeve and chlorided silver wires (Ag wire 0.125 mm diameter; Goodfellows Metals Ltd., Cambridge, U.K.) were passed down each barrel and soldered onto the wires from the amplifiers, the central wire providing the electrical connection for the reference barrel. The same arrangement was used for double-barrelled electrodes but recordings were made using just one amplifier. The signal generated across the ion-exchange resin was amplified and displayed on a 10 channel chart recorder (Rikadenki, U.K.).

| PRIMARY ION | ION-EXCHANGE RESIN | INTERNAL REFERENCE SOLUTION (mM) |
|---|---|---|
| carbonate / bicarbonate | WPI IE 310 | 490 KCl<br>10 $KHCO_3$ *<br>10 K-citrate<br>(pH = 4.82) |
| hydrogen | Fluka 92297<br>Cocktail A | 130 NaCl<br>40 $K_2HPO_4$ **<br>(pH = 6.90) |

* Kajino et al. (1982) ** Harris (1985)

**TABLE 3.3.A** Ion-exchange resins and the composition of the corresponding internal reference solutions used in the fabrication of ion-selective microelectrodes.

## 3.4 *In Vitro* Assessment and Calibration of Ion Selective Microelectrodes

*In vitro* calibration allowed the conversion of the values recorded in unknown solutions and *in vivo* to ion activities. As our aim was to monitor ionic changes in the brain extracellular fluid, ISM were calibrated in solutions of varying ion activities that covered the range expected *in vivo*. Microelectrodes were also tested for their response time to sudden changes in ionic concentration, and for their stability.

### 3.4.1 Methods of *In Vitro* Assessment and Calibration

Due to the difficult construction of triple-barrelled electrodes, *in vitro* assessment of ISM was performed using double-barrelled electrodes. The temperature of the calibrating solutions was maintained using a thermostatically controlled heating block (BT3, Grant, Cambridge, U.K.). The pH and $PCO_2$ of the solutions were monitored constantly using a pH meter (Phillips, Cambridge, U.K.) and $PCO_2$ semi-microelectrode (World Precision Instruments Inc., Stevenage, Hertfordshire, U.K.), respectively. These measurements were verified with a blood gas analyser (AVL Medical Instruments Ltd, Staffordshire, U.K.), which also allowed determination of $HCO_3^-$ concentration.

The response time of the ISM was taken as the delay necessary for the response to reach 90 % of the final value, following immersion of the electrode tip into a sample solution. Electrode drift was measured in a solution of constant concentration and temperature over a period of 24 hours. The change in electrode sensitivity was determined by repeating calibration at intervals during 24 hours.

#### 3.4.1.1 Assessment of $HCO_3^-/CO_3^{2-}$ Microelectrodes

Calibration was achieved using two different methods. As the ion-exchange resin was reported to be sensitive to $HCO_3^-$, ISM were initially calibrated in solutions with increasing $HCO_3^-$ concentration, At a later stage, a "$HCO_3^-$" exchange resin was found to measure $CO_3^{2-}$ rather than $HCO_3^-$ (Wietasch and Kraig, 1991). Consequently, a different method was used to ascertain whether the ion-exchange resin used in this study was also sensitive to $CO_3^{2-}$ rather than $HCO_3^-$.

Method 1: Calibration was performed by adding aliquots of $NaHCO_3$ to a known volume of distilled water (37 °C) to vary the $NaHCO_3$ concentration between 0.1 and 35 mM. The solutions were bubbled with air to maintain a stable $PCO_2$ (2-4 mmHg) and pH. As pure solutions of $NaHCO_3$ contain both $HCO_3^-$ and $CO_3^{2-}$ (Fig. 3.4.A, upper graph), ISM responses could be related to changes in either anion. The concentration of $CO_3^{2-}$ in each solution was calculated from the pH and $PCO_2$, according to:

$$[CO_3^{2-}] = K_3 \times K_C \times PCO_2 \ / \ [H^+]^2 \qquad \text{Equation 3.E}$$

where:

$K_3$ = dissociation constant of $HCO_3^-$ ($6.0 \times 10^{-11}$ (Eq/litre)²/mmHg at 37 °C).

$K_C$ = dissociation constant of $H_2CO_3$ ($2.6 \times 10^{-11}$ Eq/litre at 37 °C).

(Stewart, 1981).

Method 2: Electrodes were placed in a solution of 10 mM $NaHCO_3$ (37 °C) bubbled with air which produced a relatively constant $CO_2$ tension of 2-4 mmHg. When the ISM output and pH were stable, bubbling was switched to 10 % $CO_2$ in $N_2$ (approximate $PCO_2$ was 76 mmHg). This change in $CO_2$ tension induced a large decrease in the concentration of $CO_3^{2-}$ but did not alter the $HCO_3^-$ concentration (Fig. 3.4.A, lower graph; Stewart, 1981). When the ISM and pH became stable, bubbling was then turned back to air, which increased the $CO_3^{2-}$ concentration steadily as the solution acidity returned to initial levels. ISM output was recorded and plotted against changes in $CO_3^{2-}$ concentration calculated from Equation 3.E.

Response time was determined using 10 mM $NaHCO_3$. Electrode drift was recorded in 130 mM NaCl.

### 3.4.1.2 Assessment of $H^+$ Microelectrodes

Calibration was performed in solutions of phosphate buffered saline (40 mM potassium dihydrogen phosphate, 130 mM NaCl) with pH adjusted to 5.9, 6.4, 6.9 and 7.4 (274, 116, 100 and 61 nM $[H^+]$, respectively) at 37 °C. Response time was measured between pH solutions 6.4 and 7.4. Electrode stability was recorded over a period of 24 hours in a pH 7.4 solution.

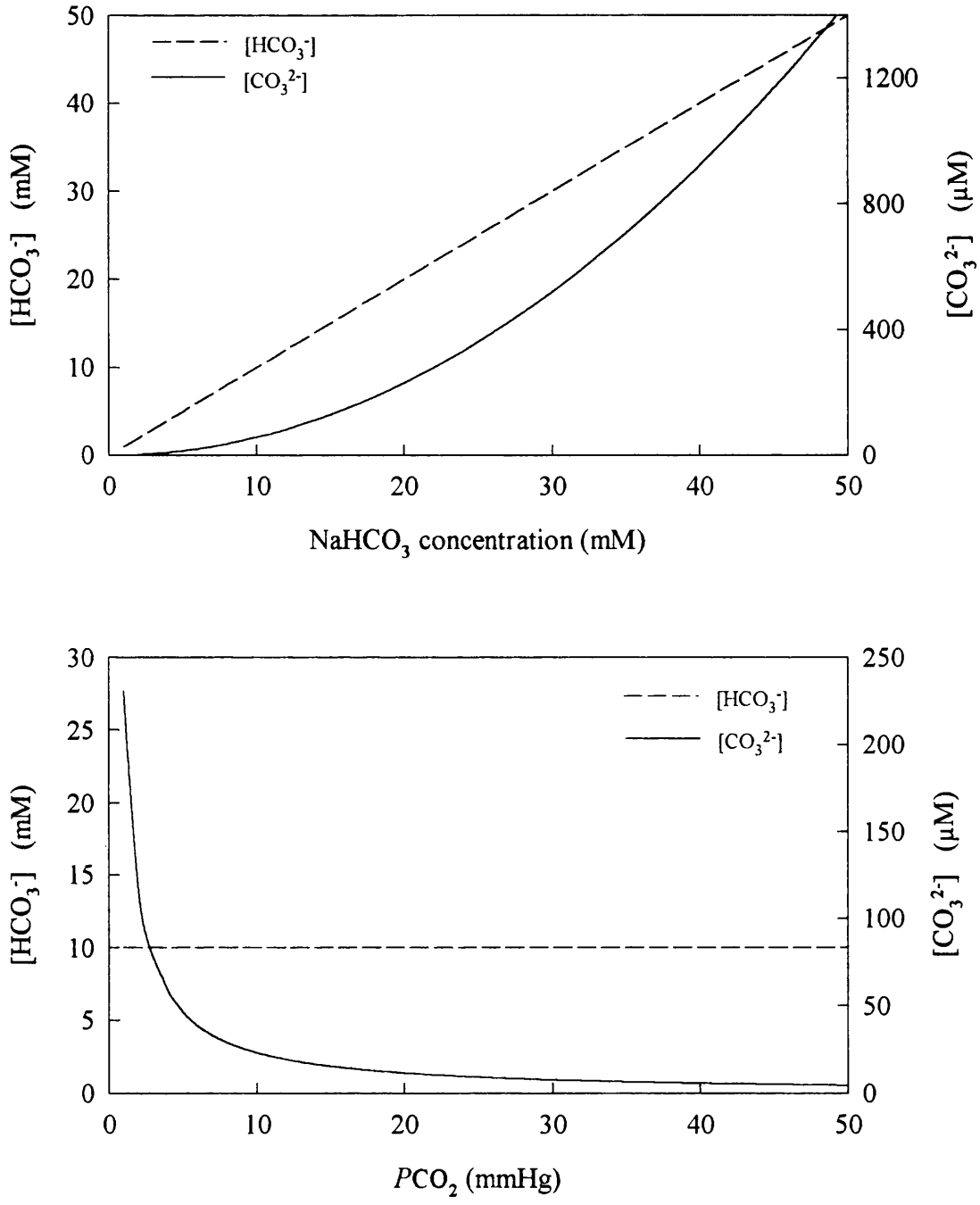


**FIG. 3.4.A** Theoretical changes in $HCO_3^-$ and $CO_3^{2-}$ concentration in the two calibration methods used. In Method 1 (upper graph) increasing the $NaHCO_3$ concentration at a constant $PCO_2$ increases both $HCO_3^-$ and $CO_3^{2-}$ concentration. In Method 2 (lower graph) increasing $PCO_2$ in a solution containing a fixed $NaHCO_3$ concentration induces a marked decrease in $CO_3^{2-}$ concentration without any change in that of $HCO_3^-$.

## 3.4.2 Results/Discussion of *In Vitro* Assessment

### 3.4.2.1 Results for $HCO_3^-/CO_3^{2-}$ Microelectrodes

Microelectrode responses to changes in $HCO_3^-$ concentration ($[HCO_3^-]$) were linear over the range tested (0.1-35 mM). Plotting ISM responses against $\log[HCO_3^-]$ (Fig. 3.4.B, upper graph) showed that the two variables were closely related (correlation coefficient $r = 0.988 \pm 0.004$; $n=11$; $p<0.001$ for each individual electrode). The slope was $39.2 \pm 1.4$ mV per decade change in $[HCO_3^-]$, which is significantly lower than the 59.2 mV predicted by the Nernst equation for ISM measuring a monovalent ion such as $HCO_3^-$ (see Section 3.3). Plotting ISM responses against $\log[CO_3^{2-}]$ (Fig. 3.4.B, lower graph) also showed a close correlation ($r = 0.989 \pm 0.003$; $n=13$; $p<0.001$ for each individual electrode). However, in this case the slope was much closer to that predicted by the Nernst equation for ISM measuring divalent ions such as $CO_3^{2-}$ ($25.4 \pm 0.8$ mV per decade change in $[CO_3^{2-}]$ versus 29.6 mV; see section 3.3). This suggests that the ISM may be sensitive to $CO_3^{2-}$ rather than $HCO_3^-$.

Calibration with the second method revealed that the "$HCO_3^-$" exchange resin was in fact responsive to changes in $CO_3^{2-}$ concentration rather than $HCO_3^-$. When the $NaHCO_3$ solution was bubbled with $CO_2$, $[HCO_3^-]$ remained at 10 mM, but $[CO_3^{2-}]$ decreased by $113 \pm 4.2$ $\mu$M ($n=8$) with a corresponding drop in EMF of $28.5 \pm 2.2$ mV (Fig. 3.4.C).

The response time for 90 % full scale deflection was $2.1 \pm 0.04$ s ($n=19$). ISM drift over 24 hours was $0.23 \pm 0.05$ $mV.h^{-1}$ (equivalent to 0.8 $\mu mol.l^{-1}.h^{-1}$) and there was no change in sensitivity during this period.

### 3.4.2.2 Results for $H^+$ Microelectrodes

Microelectrode response to changes in $\log[H^+]$ were linear ($r = 0.989 \pm 0.004$; $n= 12$; $p<0.001$ for each individual electrodes) with a slope of $66.8 \pm 2.2$ $mV.pH^{-1}$ (Fig. 3.4.D), which is higher than that expected from the Nernst equation. The reason for this is unknown but is similar to values found in the literature (e.g. Mutch and Hansen, 1984; Harris, 1985).

Electrodes had a response time of $2.7 \pm 0.04$ s ($n=12$), which increased to approximately 5 s over a period of 24 hours. They exhibited an average drift of 0.13

$\pm$ 0.004 $mV.h^{-1}$ (equivalent to 0.002 pH $unit.h^{-1}$), with no change in sensitivity.

Although both $CO_3^{2-}$ and $H^+$ ISM had a lifetime of several days, they were always used on the day following construction.

FOOTNOTE:

Although ISM only record free ions (i.e. activity), most papers dealing with ISM measurements express results as concentrations. Concentration terms the total amount of ions present in the solution including those bound to other molecules. This implies that the activity of an ion in a solution is less than its total concentration, although in pure solutions activity is almost synonymous with concentration. Calculation of activity, which depends on several parameters including the activity coefficient and total ionic strength (Section 3.5.2), is complex due to the difficulty and inaccuracy in determining activity coefficients in mixed solutions. Therefore, as in previous ISM studies, values in this study are also expressed as concentrations.

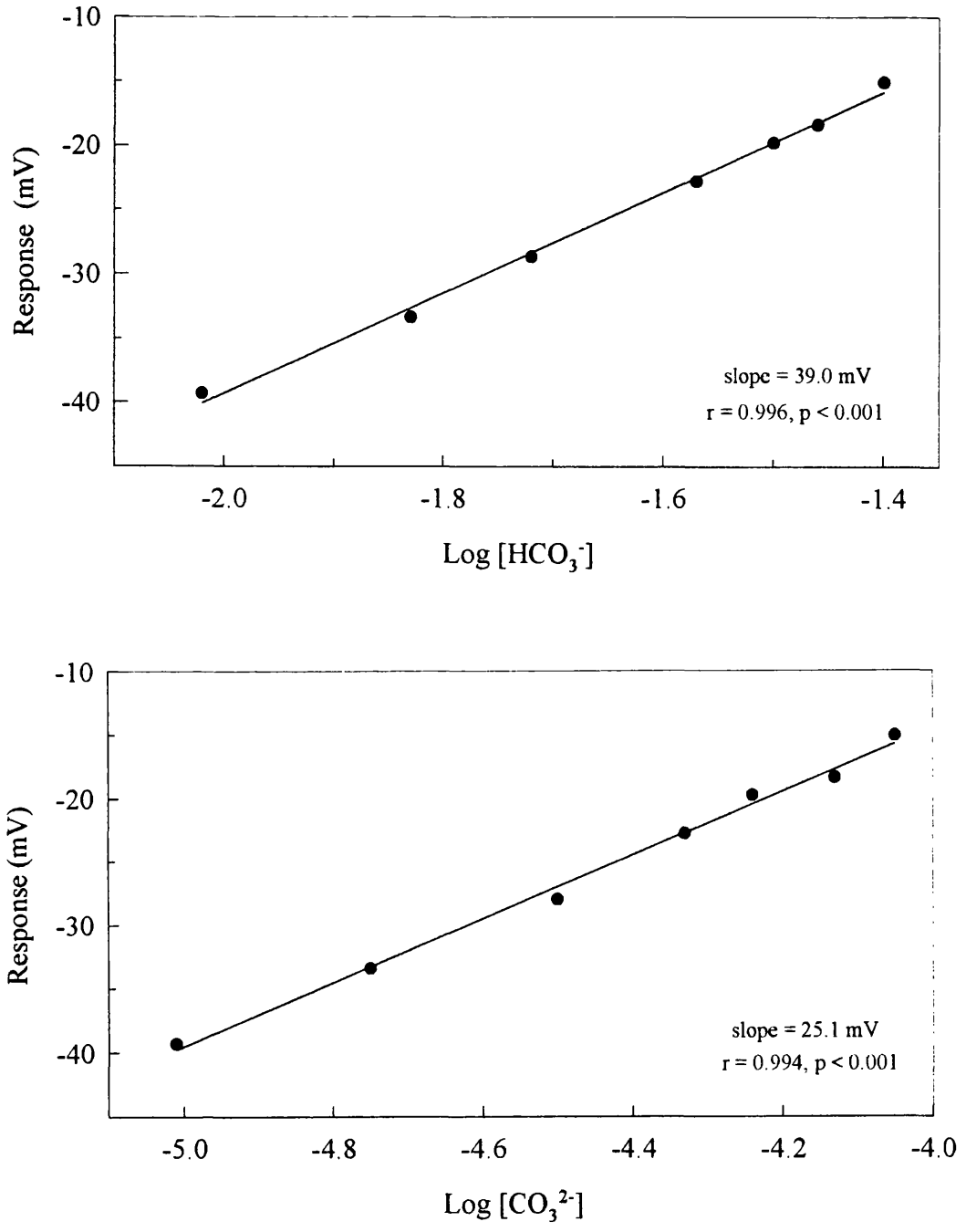


**FIG. 3.4.B** Changes in $HCO_3^-/CO_3^{2-}$ microelectrode response plotted against log[$HCO_3^-$] (upper graph) and log[$CO_3^{2-}$] (lower graph). Data are from a single calibration.

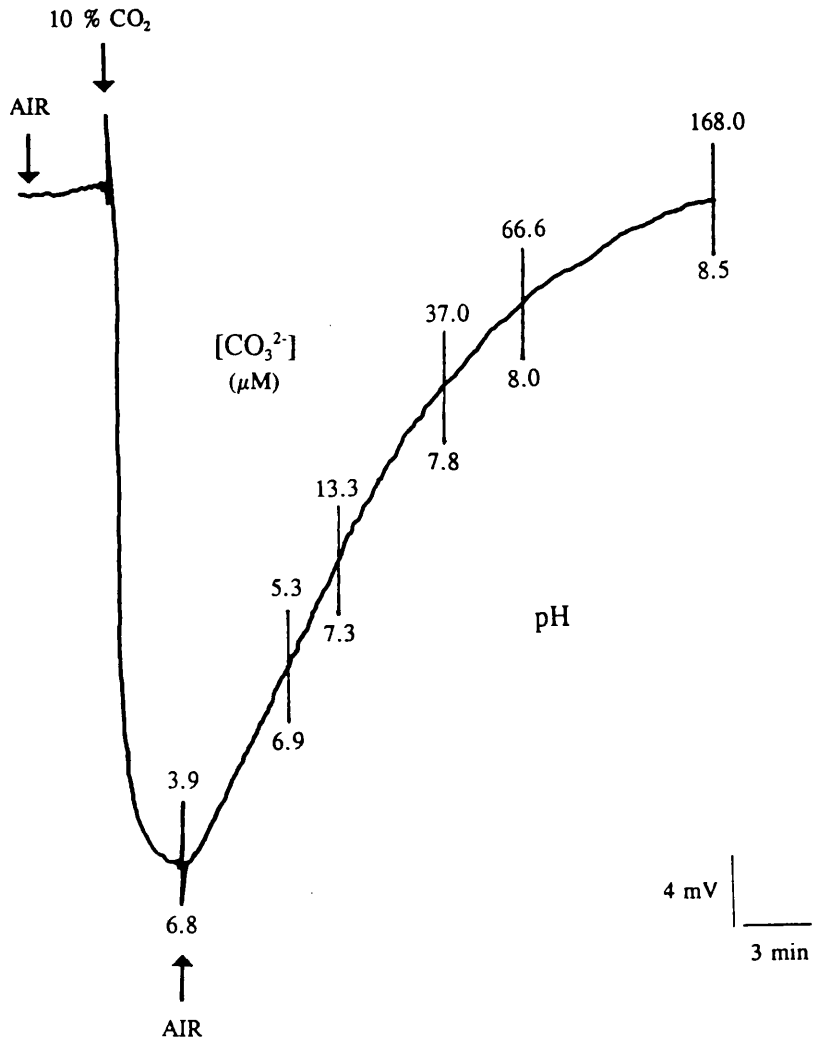


**FIG. 3.4.C** $HCO_3^-/CO_3^{2-}$ microelectrode response to changing $PCO_2$ in a solution of $NaHCO_3$ (10 mM). Bubbling $CO_2$ through the solution provoked a large decrease in $[CO_3^{2-}]$ and a corresponding drop in microelectrode response suggesting that the ion-exchange resin was responsive to changes in $CO_3^{2-}$ rather than $HCO_3^-$.

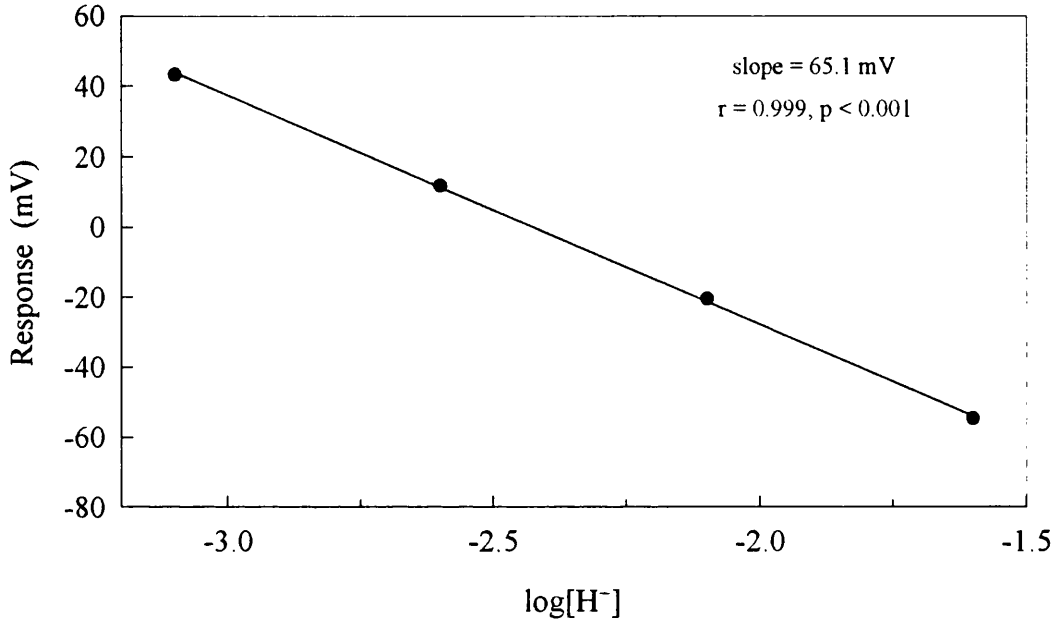


**FIG. 3.4.D** Changes in $H^+$ microelectrode response to changes in $\log[H^+]$. Data are from a single calibration.

## 3.5 Ion-Selective Microelectrode Selectivity

### 3.5.1 Introduction

Good selectivity of the ISM for the primary ion is essential for accurate monitoring of changes in its activity. This requires testing whether other ions present in the extracellular fluid are interfering with the electrode response, especially ions whose concentration may be markedly altered under some experimental or pathological conditions. This section describes the conventional methods available to ascertain ISM selectivity and justifies the practical approach chosen in this study.

### 3.5.2 Conventional Methods for Evaluation of Selectivity

The selectivity coefficient ($K_{ij}^{pot}$) allows quantification of the contribution to ISM output of the interfering ion (*j*) relative to the primary ion (*i*). For an ion-exchange resin perfectly selective to i, $K_{ij}^{pot}$ would be zero. Values for $K_{ij}^{pot}$ are dependant on the method used and the experimental conditions under which the measurements are made. Selectivity coefficients can be determined experimentally using several techniques.

Single Solution Method: Electrode EMF values for the primary and interfering ions are determined separately in pure solutions of a single concentration of each ion. $K_{ij}^{pot}$ is calculated using a rearrangement of the Nicolsky-Eisenman equation:

$$K_{ij}^{pot} = 10^{(Ej-Ei)/s} \cdot a_i / (a_j)^{zi/zj} \qquad \text{Equation 3.F}$$

where:

$K_{ij}^{pot}$ = selectivity coefficient.

$E_i$ , $E_j$ = EMF values for pure solutions of primary and interfering ions, respectively.

$z_i$, $z_j$ = charge (valency) of the primary and interfering ions, respectively.

$a_i$, $a_j$ = activities of primary and interfering ions, respectively.

s = Nernstian slope (see Section 3.2 for definition).

Fixed Interference Method: Electrode response is recorded in solutions containing varying concentrations of the primary ion and a fixed background concentration of a single interfering ion. The value of $K_{ij}^{pot}$ is calculated from the equation:

$$K_{ij}^{pot} = a_i^{DL} / (a_j)^{zi/zj} \qquad \text{Equation 3.G}$$

where:

$a_i^{DL}$ = detection limit, determined from plotting electrode response against primary ion concentration.

(see Equation 3.F for other definitions).

This method corresponds more closely to experimental conditions (i.e. determination of $K_{ij}^{pot}$ values with a fixed background of the interfering ion at concentrations expected *in vivo*).

Mixed Solution Method: Electrode EMF is measured in solutions containing known concentrations of both the primary and an interfering ion. The selectivity coefficient, $K_{ij}^{pot}$, is calculated from:

$$K_{ij}^{pot} = [10^{(E-Eo)/s} - a_i] / (a_j)^{zi / zj} \qquad \text{Equation 3.H}$$

where:

$E_o$ = reference potential (see section 3.2)

E = electromotive force (EMF)

(see Equation 3.F for other definitions).

The methods discussed above for determining ISM selectivity were primarily devised for *in vitro* assessment of electrode performance and the values of $K_{ij}^{pot}$ depend on the experimental method chosen. In addition, determination of $K_{ij}^{pot}$ from these methods, requires calculation of the activities of the primary and interfering ions which is difficult. The activity of an ion in a given solution is calculated from its concentration and activity coefficient (Robinson and Stokes, 1965). The activity coefficient of an ion depends on several parameters such as ionic radii, total ionic strength, free energy of a solution, temperature and charge interactions. This makes their calculation very complex and may introduce errors into the determination of $K_{ij}^{pot}$. In practice, it is of greater value to assess the observed effects of interfering

ions on ISM response (Tsien and Rink, 1980).

### 3.5.3 Practical Evaluation of Selectivity Used in This Study

The selectivity of both ISM was evaluated using an approach similar to the fixed interference method. Electrodes response to increasing concentrations of the primary ion was measured in solutions containing fixed background concentrations of the principle ions suspected to change markedly during ischaemia and SD. The concentration range of interfering ions used to assess selectivity was greater than that presumed to occur *in vivo*. Using this method it was not necessary to know the activities of the ions involved, and as mixed solutions were used the response of ISM was more likely to be comparable to that *in vivo*.

#### 3.5.3.1 Evaluation of $CO_3^{2-}$ Microelectrodes

Selectivity of $CO_3^{2-}$ electrodes to chloride, bicarbonate, phosphate, lactate and glutamate was examined using two methods, based on those previously described for *in vitro* ISM calibration (Section 3.4.1). The first method, in which $NaHCO_3$ was added to a solution of the interfering ion, assessed the influence of all ions except $HCO_3^-$ as its concentration changed with each addition of $NaHCO_3$. The second method enabled the effect on ISM response of all ions, including $HCO_3^-$, to be assessed. The results from both methods were compared.

Method 1: The $CO_3^{2-}$ concentration was altered by adding aliquots of $NaHCO_3$ to a solution containing a fixed low or high concentration of the sodium salt of an interfering ion (Table 3.5.A). All solutions were bubbled with air to maintain $PCO_2$ at a low level (2-4 mmHg) and a stable pH.

Method 2: This approach was based on Method 2 previously discussed in Section 3.4.1. The ISM were placed in a solution of 10 mM $NaHCO_3$ with a fixed concentration of the sodium salt of an interfering ion. The solution was bubbled with air and when pH and ISM output had stabilised, bubbling was switched to 10 % $CO_2$ in $N_2$. This induced a large decrease in $CO_3^{2-}$ concentration and ISM output. When the latter was stable, bubbling was changed back to air and frequent measurements of pH, $PCO_2$ and ISM output were taken as the solution returned to initial levels. To determine the effect of $HCO_3^-$ on electrode response, the concentration of the $NaHCO_3$

solution was varied. The solutions used are shown in Table 3.5.B.

For both methods, the concentration of $CO_3^{2-}$ in each solution was calculated using Equation 3.E. ISM responses in the presence of low and high concentrations of each interfering ion were plotted against $CO_3^{2-}$ concentration, the response slopes compared, and an average change in EMF determined.

### 3.5.3.2 Evaluation of $H^+$ Microelectrodes

Electrode responses in a solution containing a high concentration of an interfering ion was compared to a control solution. The composition of the solutions used is detailed in Table 3.5.C. The pH of all solutions was adjusted to 7.4. The effects of sodium, potassium, calcium, magnesium, bicarbonate and phosphate were tested.

| SOLUTION CODE | INTERFERING ION STUDIED | INTERFERING ION SALT (mM) |
|---|---|---|
| B1 | chloride | 130 NaCl |
| B2 | | 65 NaCl |
| B3 | phosphate | 0 $NaH_2PO_4$ |
| B4 | | 10 $NaH_2PO_4$ |
| B5 | lactate | 0 Na-lactate |
| B6 | | 20 Na-lactate |
| B7 | glutamate | 0 Na-glutamate |
| B8 | | 1 Na-glutamate |

**TABLE 3.5.A** Solutions used to assess the influence of interfering ions on $CO_3^{2-}$ microelectrode response in Method 1.

| SOLUTION CODE | INTERFERING ION STUDIED | $NaHCO_3$ SOLUTION (mM) | INTERFERING ION SALT (mM) |
|---|---|---|---|
| C1 | chloride | 10 | 130 NaCl |
| C2 | | 10 | 65 NaCl |
| C3 | bicarbonate | 10 | - |
| C4 | | 30 | - |
| C5 | phosphate | 10 | 0 $NaH_2PO_4$ |
| C6 | | 10 | 10 $NaH_2PO_4$ |
| C7 | lactate | 10 | 0 Na-lactate |
| C8 | | 10 | 20 Na-lactate |
| C9 | glutamate | 10 | 0 Na-glutamate |
| C10 | | 10 | 1 Na-glutamate |

**TABLE 3.5.B** Solutions used to assess the influence of interfering ions on $CO_3^{2-}$ microelectrode response in Method 2.

| SOLUTION CODE | INTERFERING ION STUDIED | NaCl SOLUTION (mM) | INTERFERING ION SALT (mM) | pH |
|---|---|---|---|---|
| H1 | "control" | 130 | - | 7.38 |
| H2 | sodium / potassium | 75 | 50 KCl | 7.41 |
| H3 | calcium | 130 | 1 $CaCl_2$ | 7.39 |
| H4 | magnesium | 130 | 25 $MgCl_2$ | 7.42 |
| H5 | bicarbonate | 130 | 30 $NaHCO_3$ | 7.37 |
| H6 | phosphate | 130 | 45 $NaH_2PO_4$ | 7.39 |

**TABLE 3.5.C** Solutions used to assess the influence of interfering ions on $H^+$ microelectrode response. All solutions contained 10 mM *N*-2-hydroxyethylpiperazine-*N'*-2-ethanesulfonic acid (Hepes) and the pH was adjusted using HCl.

### 3.5.4 Results of Evaluation of Selectivity

#### 3.5.4.1 Results for $CO_3^{2-}$ Microelectrodes

The influence of interfering ions on ISM response found using both methods is detailed in Tables 3.5.D and 3.5.E. Representative examples of $CO_3^{2-}$ electrode response to alterations in the concentration of chloride, obtained from the two methods described, are shown in Fig. 3.5.A. The mean change in EMF over the range of 65-130 mM chloride was 1.72 $\pm$ 0.24 mV and 2.14 $\pm$ 0.5 mV (n=5) for Methods 1 and 2, respectively. The presence of chloride did not alter the slope of response to $CO_3^{2-}$ (Figs. 3.5.A and 3.4.D). Other ions tested did not alter ISM output.

#### 3.5.4.2 Results for $H^+$ Microelectrodes

There was no change in electrode EMF associated with alterations in the concentration of any of the interfering ions tested (Table 3.5.F).

| SOLUTION CODES | INTERFERING ION STUDIED | CHANGE IN EMF (mV) (mean ± sem: n = 5) |
|---|---|---|
| B1-B2 | chloride | 1.7 ± 0.24 |
| B3-B4 | phosphate | 1.0 ± 0.20 |
| B5-B6 | lactate | 1.1 ± 0.06 |
| B7-B8 | glutamate | 0.8 ± 0.11 |

**TABLE 3.5.D** Change in $CO_3^{2-}$ microelectrode response (EMF) in the presence of interfering ions in Method 1.

| SOLUTION CODES | INTERFERING ION STUDIED | CHANGE IN EMF (mV) (mean ± sem: n = 5) |
|---|---|---|
| C1-C2 | chloride | 2.1 ± 0.50 |
| C3-C4 | bicarbonate | 1.9 ± 0.32 |
| C5-C6 | phosphate | 1.7 ± 0.46 |
| C7-C8 | lactate | 0.6 ± 0.06 |
| C9-C10 | glutamate | 0.41 ± 0.07 |

**TABLE 3.5.E** Change in $CO_3^{2-}$ microelectrode response (EMF) in the presence of interfering ions in Method 2.

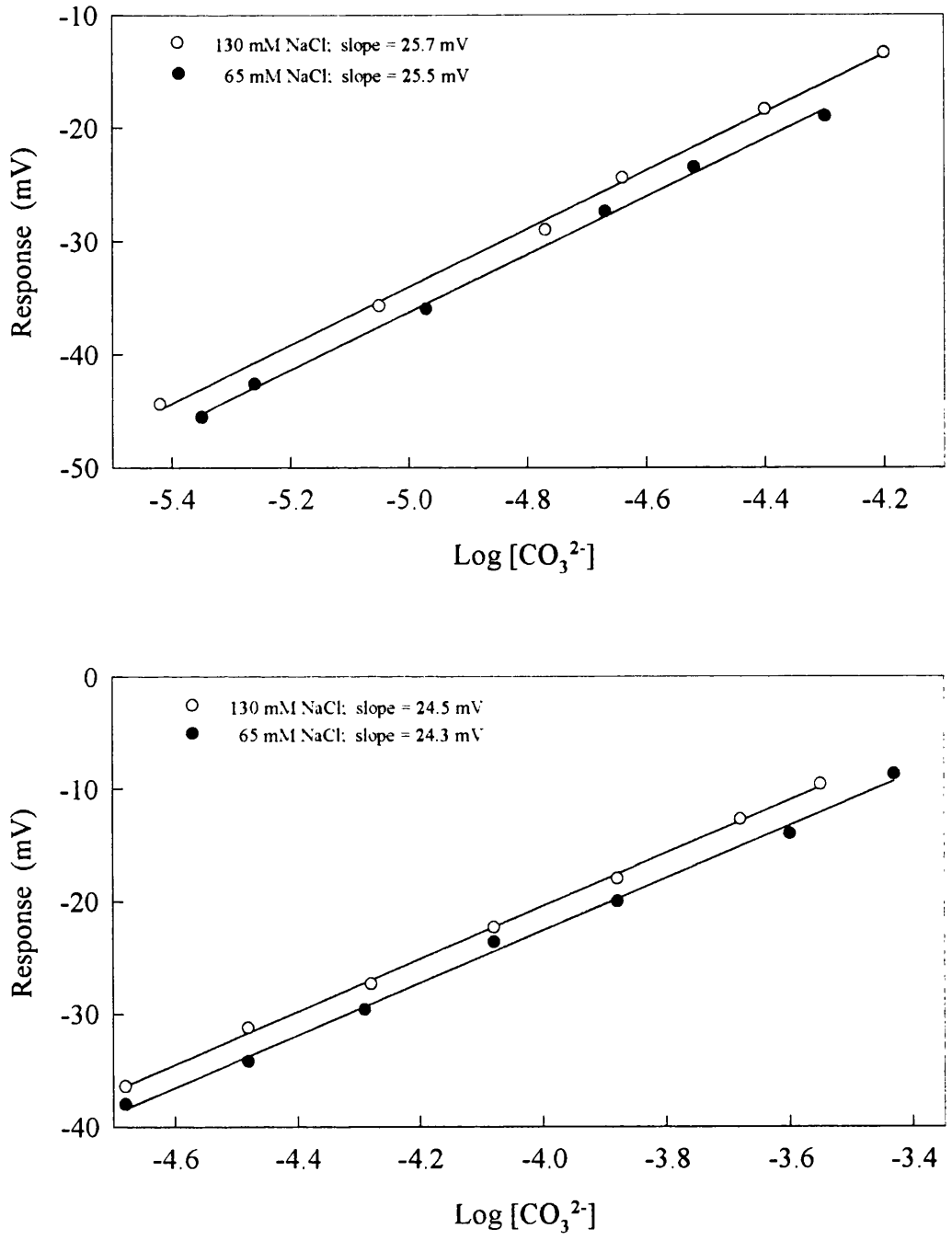


**FIG. 3.5.A** Changes in $CO_3^{2-}$ microelectrode response to alterations in chloride concentration using Method 1 (upper graph) and Method 2 (lower graph). The correlation of electrode response to changes in $CO_3^{2-}$ concentration was not altered by changing the chloride concentration from 130 to 65 mM ($r=0.998$ and 0.998, $p<0.001$ for Method 1; $r=0.999$ and 0.997, $p<0.001$ for Method 2). Data in each graph are from single representative calibrations.

| SOLUTION CODES | INTERFERING ION STUDIED | CHANGE IN EMF (mV) (mean ± sem: n = 6) |
|---|---|---|
| H1-H2 | sodium / potassium | 0.8 ± 0.30 |
| H1-H3 | calcium | 1.0 ± 0.28 |
| H1-H4 | magnesium | 1.25 ± 0.35 |
| H1-H5 | bicarbonate | 0.85 ± 0.29 |
| H1-H6 | phosphate | -0.25 ± 0.07 |

**TABLE 3.5.F** Change in $H^+$ microelectrode response (EMF) in the presence of interfering ions.

### 3.5.5 Discussion of Evaluation of Selectivity

There are discrepancies in the selectivity coefficients reported for the $CO_3^{2-}$ exchange resin initially developed by Wise (1973; Khuri et al., 1974; Herman and Rechnitz, 1975; Wietasch and Kraig, 1991). This variability probably results from the composition of the electrode internal reference solution and the method chosen to calculate $K_{ij}^{pot}$. As the resin used in this study, suspected to be analogous to that developed by Wise (1973), may have a lower selectivity than freshly prepared resin (Kraig and Cooper, 1987; Wietasch and Kraig, 1991), it was purchased and used immediately after manufacture. The $H^+$ exchange resin was almost perfectly selective, a feature previously reported for other commercially available $H^+$ exchange resins (e.g. Mutch and Hansen, 1984; Harris, 1985).

The minimal influence of interfering ions on electrode response indicate that both types of ISM were able to accurately record changes of the primary ion within the concentration range encountered *in vivo*. On this basis, the effects of other ions on the ISM measurements made during *in vivo* experiments were considered to be negligible.

## 3.6 Discussion/Conclusion

Ideal ISM for making extracellular measurements should have the following characteristics: small tip diameter to cause minimal tissue damage on implantation; a good selectivity for the ion under investigation; minimal drift throughout the recording time; and rapid response time. Are these requirements fulfilled in this study?

Implantation of ISM into the brain is invasive but the small tip diameter does not appear to alter the physiology and biochemistry of the surrounding tissue (Hansen et al., 1977) or disrupt the BBB (Heuser et al., 1975; Hansen et al., 1977). The ISM are not perfectly selective, but assessment *in vitro* suggested that any influence from interfering ions will be negligible for *in vivo* measurements. Recordings made *in vitro* and *in vivo* remained stable and were not affected by significant drift. The response time was rapid and adequate to record the sudden transient ion changes *in vivo*. In conclusion, the ISM used in this study could provide accurate measurement of extracellular ionic changes in the cerebral cortex during the physiological or experimental conditions under investigation.

# CHAPTER 4 INTRACEREBRAL MICRODIALYSIS

## 4.1 Introduction

Microdialysis is a versatile sampling method which can provide information on changes in low molecular weight species in the brain extracellular fluid. Described as early as 1966 by Bito et al., the method has undergone several technical modifications. Intracerebral microdialysis was employed in this study for the *in vivo* determination of extracellular lactate activity. On-line fluorometric analysis detection, specific to lactic acid, was coupled directly to the microdialysis probe implanted into the rat brain to allow continuous measurement of lactate changes.

This chapter covers the basic principles of microdialysis, the construction of microdialysis probes, probe recovery, and recording of dialysate lactate.

## 4.2 Basic Principles of Microdialysis

Microdialysis is based on the diffusion of substances between two compartments separated by a semi-permeable membrane. The membrane is continuously flushed on one side with a solution generally devoid of the substances of interest, whereas the other side faces the interstitial fluid. A concentration gradient is created causing diffusion of substances from the interstitial space through the dialysis membrane and *vice versa* (Fig. 4.2.A). A dialysis membrane connected with in- and outlet tubes, allowing fluid to enter and leave the dialysis membrane, respectively, is referred to as a microdialysis probe. Continuous perfusion of fluid through the membrane carries substances to the sampling site for further analysis. By using membranes with different pore sizes it is possible to remove certain compounds selectively whilst retaining others.

## 4.3 Preparation for Intracerebral Microdialysis

### 4.3.1 Construction of Microdialysis Probes

Concentric microdialysis probes were constructed from 15 mm lengths of 24 grade stainless steel tubing (Cooper's Needle Works, Birmingham, U.K.). Two lengths of fused silica tubing (0.19 mm o.d., 0.075 mm i.d.; SGE Ltd., Milton Keynes, U.K.) measuring 30 and 15 mm were inserted into the probe body to form the inlet and outlet tubes, respectively. The exposed 5 mm of both tubes was sleeved with polythene tubing (0.61

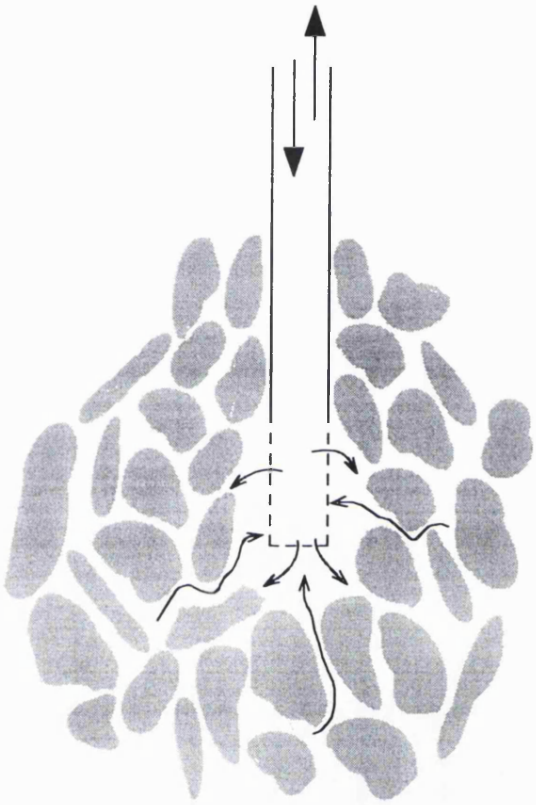

**FIG. 4.2.A** Continuous perfusion of fluid through the microdialysis probe into the tissue creates a concentration gradient causing diffusion of substances from the interstitial fluid through the dialysis membrane and *vice versa* (arrows).

mm o.d., 0.28 mm i.d.; Portex Ltd., Hythe, U.K.; Fig. 4.3.A).

The exposed end of the inlet tube was trimmed to a length of 4.5 mm, and Cuprophan dialysis fibre (0.216 mm o.d., 0.2 mm i.d.; GFE 9, 10 KDa; Gambro Ltd., Sidcup, U.K.) was passed over the tubing into the probe body. The dialysis fibre was cut so it was 0.5 mm longer than the inlet tube. Epoxy resin (554-850, RS Components Ltd., Corby, Northants, U.K.) was used to seal the tip of the fibre, the joint between dialysis membrane and steel body, and the assembly at the head of the probe (Fig. 4.3.A).

In order to assess the severity of ischaemia or occurrence of depolarisation precisely at the microdialysis sampling site, probes incorporated a recording electrode for measurement of EEG and DC potential. These electrodes were prepared by soldering 8 mm lengths of silver wire (0.125 mm diameter; Goodfellows Metals Ltd., Cambridge, U.K.) to 8 mm gold pin contacts (476-817, RS Components Ltd., Corby, Northants, U.K.). The wires were chlorided as the anode, in 0.1 mM hydrochloric acid, using a potential rising at 10 $mV.s^{-1}$ to 610 mV, this potential was then held for 60 seconds. After washing off excess acid, and drying, the pin electrode was inserted alongside the inlet tube, as shown in Fig. 4.3.A, with the connector bent at an angle of 90 $^{\circ}$ to the probe body.

### 4.3.2 Perfusion

It is generally acknowledged that the ionic composition of the perfusion medium should match that of the ECF under physiological conditions (Obrenovitch et al., 1995). However, it has been suggested that the perfusion of normal artificial cerebrospinal fluid (ACSF) may influence the experimental or pathological conditions under study by buffering critical changes in the ECF composition (Obrenovitch et al., 1995). In this study perfusion mediums were unbuffered, since this may influence the extracellular acid-base homeostasis, but precisely adjusted to pH 7.3 with diluted NaOH or HCl.

Unless otherwise stated, microdialysis probes were perfused with control ACSF (composition in mM: NaCl 125, KCl 2.5, $MgCl_2$ 1.18, $CaCl_2$ 1.26; pH 7.3) at a flow rate of 0.5 $\mu l.min^{-1}$ using a high precision syringe pump (CMA/100, Biotech, Luton, U.K.) with a 250 $\mu l$ syringe (Hamilton Co., Reno, NE, USA). A liquid switch (Carnegie Medicin CMA/110, Biotech, Luton, U.K.) enabled switching of the perfusing solution from normal ACSF to ACSF with altered ionic composition or in which probenecid was dissolved.

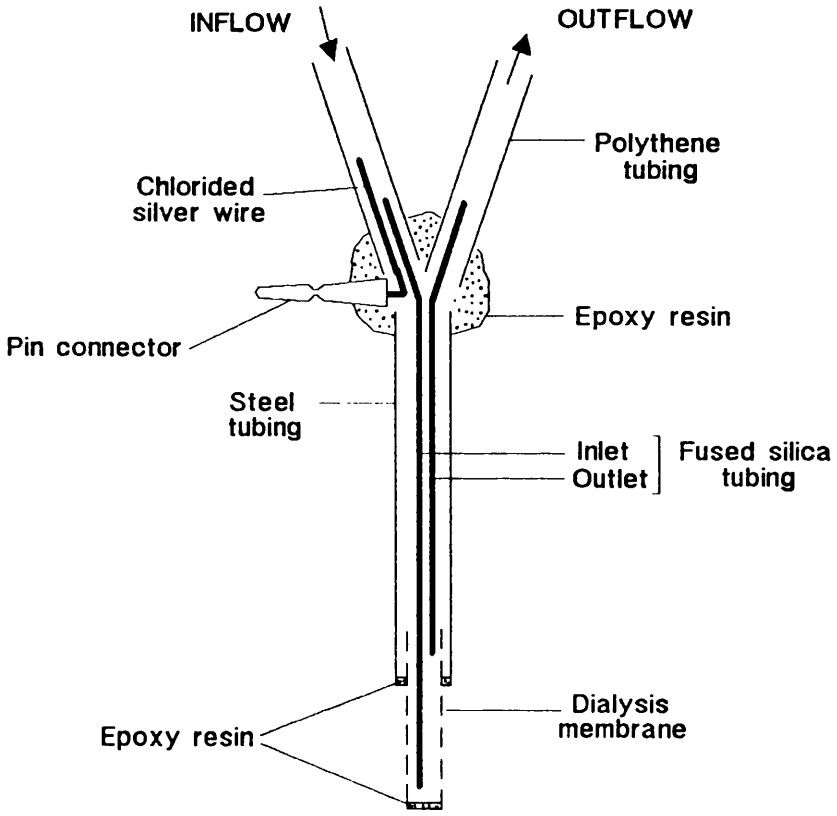


**FIG. 4.3.A** Concentric microdialysis probes incorporated a chlorided silver electrode in the inlet tubing to enable dual recording of changes in extracellular lactate concentration and DC potential at the same tissue site.

## 4.4 Probe Recovery

The solution emerging from an implanted probe is a dialysate of the interstitial fluid and the substance concentrations measured are not true brain interstitial substrate concentrations. The concentration of substance in the dialysate is dependant on the recovery of the probe. Recovery for a given microdialysis probe is increased at lower perfusion rates and is directly proportional to the size of the dialysis membrane area (Benveniste and Hüttemeier, 1990). Recovery, determined from *in vitro* calibration, is defined as the ratio between the concentration of a substance in the outflow solution and the concentration of the same substance in the solution outside the probe (Ungerstedt et al., 1982; Zetterström et al., 1982):

$$\text{Recovery}_{in\ vitro} = C_{out} / C_i \qquad \text{Equation 4.A}$$

where:

$C_{out}$ = concentration of substance in the outflow solution.

$C_i$ = concentration of substance in the solution surrounding the probe.

Dialysate concentrations can then be converted to brain interstitial concentrations from:

$$C' = C'_{out} / \text{Recovery}_{in\ vitro} \qquad \text{Equation 4.B}$$

where:

$C'$ = substance concentration in brain interstitial space.

$C'_{out}$ = concentration of substance in the dialysate.

Diffusion of substances in a tissue is impeded by cell membranes, which give rise to tortuosity, a prolongation of the diffusion pathway (see Fig. 4.2.A.). Therefore, mass transport into the microdialysis probe will be different *in vivo* compared with that *in vitro*. As such, recovery of endogenous compounds *in vivo* cannot be compared to that *in vitro* (Parsons and Justice, 1992; Kehr, 1993), as brain interstitial concentrations calculated with the above method would be inaccurate.

The ideal experimental situation for measurement of *in vivo* recovery would be to measure an extracellular marker which does not exchange with the intracellular compartment (Nicholson and Rice, 1986; Benveniste et al., 1989). Recovery of extracellular lactate can be determined using the "internal reference technique" (Scheller

and Kolb, 1991), where labelled lactate is added to the perfusate and its relative loss measured. However, as lactate can become a major energy source in brain tissue under certain circumstances (Schurr et al., 1988; Bock et al., 1989), calculation of extracellular lactate concentration with this method would be inappropriate, as this method requires the radiolabelled tracer to be inert. In this study, dialysate lactate values obtained were not corrected for recovery and are given as dialysate concentration.

## 4.5 Biochemical Measurement of Lactate in Brain Dialysate

In most experiments the outlet tube of the implanted microdialysis probe was connected to a reaction loop where the dialysate was mixed with an enzymatic reagent, for the on-line assay of lactate (Fig. 4.5.A). Lactate concentration in standard solutions and brain dialysate ($[lact]_d$) was determined by on-line fluorometric detection of NADH resulting from the reaction of lactate and $NAD^+$ catalysed by lactate dehydrogenase (LDH) (see Equation 1.B; Kuhr and Korf, 1988; Obrenovitch et al., 1990c). The enzymatic reagent contained 5.4 $U.ml^{-1}$ LDH (L-Lactate:NAD oxidoreductase, EC 1.1.1.27, isolated from rabbit muscle; 500 $U.mg^{-1}$ specific activity; Boehringer Mannhein U.K. Ltd, East Sussex, U.K.), 45.25 mM $NAD^+$ and 0.29 % v/v hydrazine in Tris buffer (100 mM; pH 8.7). A peristaltic pump (Minipulse 3, Gilson France, Villiers Le Bel, France; 20 $\mu l.min^{-1}$ flow rate) mixed the reagent with standard solutions, or the brain dialysate as it emerged from the implanted microdialysis probe (Fig. 4.5.A). After flowing through polyethylene tubing (530 mm length, 0.4 mm i.d., Portex Ltd, Hythe, U.K.) to allow the enzymatic reaction to occur (reaction time = 3.3 min), NADH was detected fluorometrically (Merck-Hitachi F-1050, Merck-BDH, Leicestershire, U.K.), using a 4 $\mu l$ flow cell, with excitation and emission wavelengths of 340 and 450 nm, respectively. The signal generated from the fluorometer was amplified and displayed on a 10 channel chart recorder (Rikadenki, U.K.). There was a delay of approximately 5 minutes between the changes occurring in the brain tissue and the corresponding change in lactate measured.

Calibration was achieved using standard solutions of lactate (0, 0.5, 1.0, 2.0, 3.5, and 5.0 mM; L-Lactic acid, Fluka Chemicals Ltd, Dorset, U.K.) in ACSF.

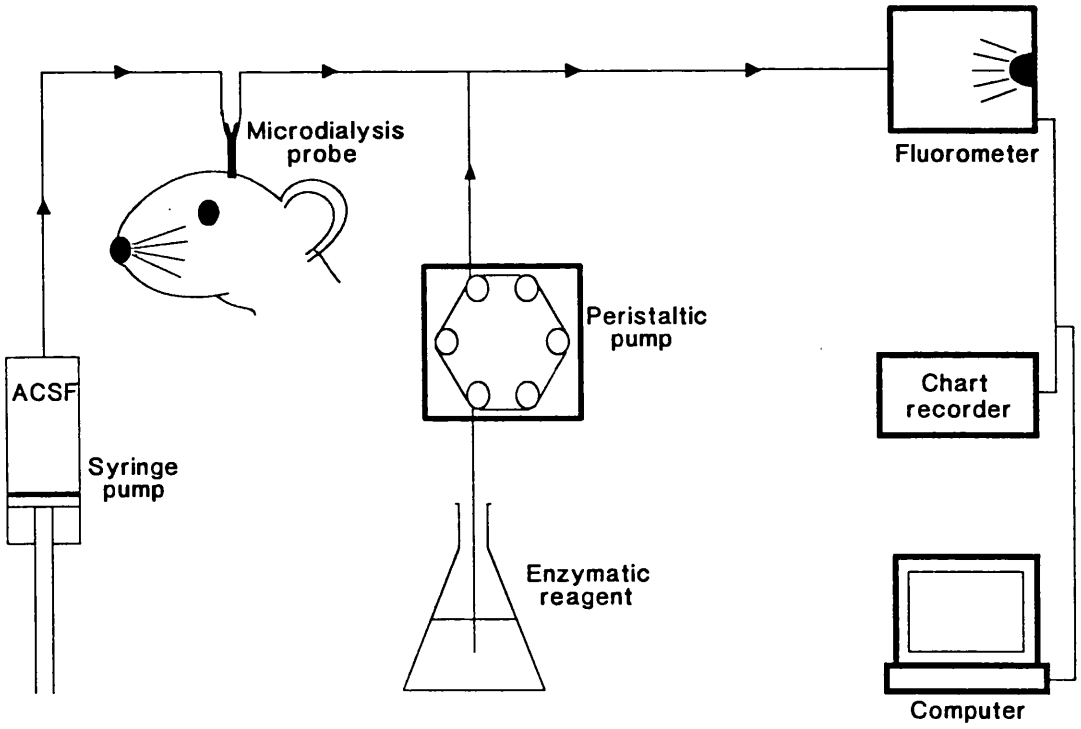


**FIG. 4.5.A** Schematic representation of intracerebral dialysis combined with on-line enzyme-fluorometric flow analysis of cerebral extracellular lactate. A syringe pump perfused the implanted microdialysis probe with ACSF. The emerging dialysate was mixed with the enzymatic reagent, and the NADH generated was fluorometrically detected.

## 4.6 Recording of Dialysate pH

Changes in dialysate pH were investigated in experiments using a miniature pH electrode (MEPH1, World Precision Instruments Inc., Stevenage, Hertfordshire, U.K.) whose tip was introduced directly into the outlet of the implanted microdialysis probe. A reference electrode (Type E255; 0.8 mm o.d.; Clark Electromedical Instruments, Reading, U.K.) inserted into a glass capillary was positioned right below the tip of the outlet tube. The drift of the pH recording system did not allow reliable absolute pH measurements to be obtained, but changes in dialysate pH could be readily monitored.

FOOTNOTE:

Extracellular space volume and tortuosity influence the diffusion of molecules within the brain parenchyma, as well as that from the ECF to the medium perfused through a microdialysis probe (see Section 4.4; Kehr, 1993). Both ischaemia and spreading depression are associated with cell depolarisation which induces cellular swelling to the detriment of the extracellular space which shrinks (Kraig and Nicholson, 1978; Hansen and Olsen, 1980; Hansen and Zeuthen, 1981). It is possible that the changes in dialysate lactate following depolarisation may be influenced by a decrease in microdialysis probe recovery (Nicholson and Phillips, 1981; Scheller and Kolb, 1991) resulting from shrinkage of the extracellular space and changes in brain tissue tortuosity (Nicholson and Rice, 1986). As in this study lactate values are expressed as dialysate concentrations (i.e. not corrected for probe recovery) and that the changes in tortuosity have not been determined during ischaemia (Benveniste and Hüttemeier, 1990), it is not possible to deduce the contribution, if any, of cell swelling on the observed lactate changes.

# CHAPTER 5 EXPERIMENTAL PROCEDURES AND PROTOCOLS

## 5.1 Introduction

The experimental approaches used in this study allowed the combination of extracellular recording of $CO_3^{2-}$, $H^+$ or lactate levels, with that of the DC potential and EEG at the same tissue site. The electrophysiological variables provided information on the severity of ischaemia to which the region under study was subjected, and the initiation and propagation of spreading depression. The DC potential, an index of the average cellular polarisation of the region under study (Sugaya et al., 1975), was especially useful for detection of depolarisation.

## 5.2 Surgical Procedures

### 5.2.1 Anaesthesia

General anaesthesia is a drug-induced state, producing a controllable and reversible loss of consciousness and an absence of motor response to noxious stimuli. Depths of anaesthesia appropriate for the conduct of surgical and experimental procedures can be achieved with a wide variety of drugs, either alone, or in combinations (Flecknell, 1987). In this study, anaesthesia was produced with halothane, a potent inhalation anaesthetic which allows rapid induction and recovery (1-3 min). Like many anaesthetic agents, halothane causes depression of the cardiovascular system and moderate hypotension at surgical levels of anaesthesia as a result of a reduction in cardiac output and peripheral vasodilation. The electrical activity of the brain shows progressive replacement of fast, low-voltage activity by slow waves of greater amplitude as halothane anaesthesia is deepened (Marshall and Longnecker, 1996). Dilation of cerebral vessels may occur causing an increase in cerebral blood flow. There is no indication that halothane interferes with energy metabolism in the brain unless excessive doses are used (Marshall and Longnecker, 1996). The undesirable effects of halothane are not severe in comparison to the profound effects of other drugs, such as barbiturates and ketamine, and therefore halothane was considered to be a good agent for induction and maintenance of anaesthesia in the rat.

Halothane was administered in a 1:1 mixture of oxygen and nitrous oxide. The latter on its own has some anaesthetic potency and causes minimal cardiovascular and

respiratory system depression which may reduce the overall degree of depression of blood pressure or respiration at a particular depth of anaesthesia. In order to minimise a possible interference of halothane anaesthesia with the processes under investigation, once the surgical procedure had been completed, the depth of anaesthesia was carefully controlled by monitoring EEG and mean arterial blood pressure (MABP).

In most experiments, especially those that required minimal surgery, animals were allowed to breath spontaneously with close monitoring of their physiological variables. A tendency towards hypoventilation was observed in halothane anaesthetised rats breathing spontaneously, but this was unlikely to have altered the changes under study and their interpretation (Kraig and Cooper, 1987). In some experiments, animals were artificially ventilated. This allowed the precise control of the duration of inspiration and expiration, the volume of gas delivered to the lungs, and of blood gas parameters. As spontaneous respiratory movements may interfere with ventilation, artificially ventilated animals were relaxed with tubocurarine, a competitive blocking agent at the neuromuscular junction (Flecknell, 1987). Since administration of tubocurarine prevented all movements in response to pain, changes in mean arterial blood pressure, heart rate and EEG were constantly monitored to ensure anaesthesia adequacy.

### 5.2.2 Surgical Preparation

The initial preparation of animals was the same for all experiments. The different surgical procedures that were performed before implantation of an ISM and/or a microdialysis probe depended on the condition under investigation and the variables being measured.

#### 5.2.2.1 Common Surgical Preparation

Experiments were performed on adult male Sprague-Dawley or Wistar rats (Bantin and Kingman, Grimston, U.K.) with food and water freely available. All animal procedures used were in strict accordance with the Home Office guidelines and specifically licensed under the Animals (Scientific Procedures) Act, 1986. Premedication with atropine sulphate (15-30 $\mu g.kg^{-1}$ i.m.) reduced bronchial and salivary secretions which may partially occlude the airways. Atropine also increases heart rate and protects the heart from vagal inhibition which can occur during endotracheal intubation or surgical procedures (Flecknell, 1987). Anaesthesia was induced and maintained with halothane (2

% and 1.0-1.5 %, respectively) in $O_2/N_2O$ (1:1). A femoral artery was cannulated for continuous monitoring of MABP and determination of arterial blood gases, pH and glycaemia. A femoral vein was cannulated for drug administration. Body temperature was maintained at 37.5-38 °C throughout the experiments using a homeothermic pad.

#### 5.2.2.2 Surgery for Artificial Ventilation

The animal was placed on it's back and the neck extended. The skin above the trachea was incised, the underlying muscles separated, and the trachea exposed and isolated. A small incision was made across the trachea between two of the rings of cartilage and a specially prepared tube inserted and secured with 2 ligatures. In animals being prepared for ischaemia, a thread was placed dorsal to the trachea and the two ends secured loosely around the rat's neck to form a tourniquet if required. The animal was then relaxed with tubocurarine (1 $mg.kg^{-1}$ i.v., repeated every hour) and ventilated mechanically (75 $cycles.min^{-1}$; Rodent Ventilator, Harvard Apparatus Co. Edenbridge, U.K.) with an appropriate stroke volume to maintain normocapnia.

#### 5.2.2.3 Surgery for Transient Forebrain Ischaemia

Ischaemia was produced by occlusion of the four major cerebral vessels (Pulsinelli and Brierley, 1979). After a tracheotomy, the common carotid arteries were isolated and encircled with inflatable vascular occluders (Type OC2A, In Vivo Metric, Healdsburg, CA. U.S.A.). The tubing from the occluders was brought out of the wound and connected to a compressed air cylinder to allow remote induction of ischaemia. After closing the wound, animals were placed in the prone position with the head secured in a stereotactic frame. A dorsal cervical incision was made and the cervical muscles divided down to the first cervical vertebra. A monopolar electrode was passed down through the alar foramen on one side, and an intermittent current was applied to electrocoagulate the underlying vertebral artery (Pulsinelli and Buchan, 1988). This was repeated for the other side, and the wound closed. The skull was then exposed in preparation for a craniectomy, the position of which was determined by the region of the brain under investigation. Once surgical procedures were completed the concentration of halothane in the breathing mixture was reduced to 0.8-1.2 %.

#### 5.2.2.4 Ion-Selective Microelectrode Implantation

Pre-experimental *in vitro* calibrations were carried out as described in Section 3.4. A 1-2 mm craniectomy was performed 3 mm posterior to the bregma and 1.5 mm left to the sagittal suture (Paxinos and Watson, 1986). The dura was incised to avoid damage to the electrode tip upon implantation. The amplifier holding the electrode was secured to the stereotactic frame, and the electrode was positioned and lowered until its tip touched the brain surface. The electrode was implanted 1 mm deep into the cortex. The exposed cortical surface was prevented from drying out by covering it with warm paraffin oil. In these experiments, animals were kept in the stereotactic frame throughout.

At the end of the experiment before the ISM was withdrawn, the brain surface was washed repeatedly to remove the paraffin as this can enter the barrels rendering the electrode inactive. A post-experimental calibration *in vitro* was performed to ensure the ISM had not been altered with implantation. If there was a marked difference in the pre- and post-calibrations the experiment was excluded.

#### 5.2.2.5 Microdialysis Probe Implantation

For recordings in the dorsolateral striatum, a 2-3 mm craniectomy was performed 0.7 mm anterior to the bregma and 3 mm left to the sagittal suture (Paxinos and Watson, 1986). The dura was incised to avoid damage to the dialysis membrane on implantation. Probes (4 mm in length) were tested with a syringe containing normal ACSF to ensure there were no leaks or abnormal resistance to flow, and then secured into the electrode holder of the stereotactic frame. The probe was lowered until it touched the brain surface, and was then inserted 7 mm deep into the brain. In some experiments a 2 mm probe was implanted laterally into the cortex, 1.6 mm under the upper brain surface. In these cases, the craniectomy was performed 3 mm posterior to the bregma and 5.6 mm lateral to the sagittal suture. The implanted probe was secured to the skull with surgical bone cement (Surgical Simplex P, Howemedica Ltd, London, U.K.).

With experiments involving microdialysis alone, when the bone cement was dry, the animal was removed from the stereotactic frame and laid on the homeothermic pad. This provided greater flexibility when setting up the equipment around the animal. The implanted probe was perfused with ACSF (see Section 4.3.2) and the outlet tube was connected to the reaction loop (see Section 4.5).

## 5.3 Electrophysiological Recordings

The DC potential and EEG were derived from the potential between the electrode built into the probe or the reference barrel of the ISM (depending on the method used), and a Ag/AgCl reference electrode placed on the conjunctiva or under the scalp, using a drop of electrode gel in the latter case (Neptic, Sandev Ltd., Harlow, U.K.). The Ag/AgCl reference was made of a pellet of Ag-AgCl (Type E255; 0.8 mm o.d.; Clark Electromedical Instruments, Reading, U.K.) placed in a glass tube (1.5 mm i.d.) closed at one end with porous glass and filled with physiological saline. The Ag/AgCl electrodes were selected because of their low offset potential minimises baseline drift. The potential between the wire within the probe and the reference was first amplified with a high impedance input pre-amplifier (Neurolog System, Digitimer Ltd, Welwyn Garden City, U.K.). The AC component in the 1-30 Hz window, amplified 6000-8000 times, provided EEG, and the DC component, the DC potential. The antenna effect of the tubing between the syringes and the microdialysis probe was eliminated by grounding the metal needle of the syringes with wires incorporating 0.01 $\mu$F capacitors.

## 5.4 Drugs

Probenecid [*p*-(dipropylsulphamoyl) benzoic acid] was purchased from Sigma Chemicals (Poole, U.K.). Probenecid -ACSF and -$K^+$-ACSF were prepared from a 200 mM probenecid stock solution. Probenecid was first dissolved in 250 mM NaOH, and the pH of this solution was adjusted to 7.4 with HCl. All the drug solutions were prepared on the day of the experiment.

## 5.5 Data Acquisition

A dedicated application programme allowed all parameters to be continuously acquired, displayed and stored. Linear spectra of consecutive EEG data sections (4 sec) were computed using the Fast Fourier Transformation. For each 4 second epoch, the average amplitude of the EEG linear spectrum within the 6 - 21 Hz frequency window was computed and displayed as an index of electrical activity. Extracellular DC potential, ISM output and MABP values were also digitised and converted to absolute values from prior calibration. Lactate data were stored and converted to millimolar concentrations during data analysis from post-experimental calibration.

## 5.6 Statistical Analysis of Data

Statistical analysis was performed by using Student's unpaired or paired *t*-test. The use of Student's *t*-test for repeated measurements may increase the likelihood of finding a significant difference in the absence of a real difference. However, in the experiments in this study, only data at selected time points (i.e. determined by independent criteria, and not equidistant in time) were compared to basal levels and, therefore, the use of Student's *t*-test was considered to be appropriate (see Matthews et al., 1990). All data are expressed as mean ± standard error of the mean (sem).

## 5.7 Experimental Protocols

A delay of at least 2 hours was allowed after implantation of the recording device before the control period was started. It was verified that the modifications of the perfusion fluid employed in this study ($K^+$- and probenecid-ACSF) did not alter the enzymatic analysis of lactate during either *in vivo* monitoring or post-experimental calibrations.

### 5.7.1 Transient Forebrain Ischaemia

Changes in Dialysate Lactate in the Striatum: Experiments were performed on 11 Wistar rats (weight, 300 ± 6 g). Animals were artificially ventilated to maintain $PCO_2$ within the range 30-40 mmHg. A control period of 60 min (normal ACSF) was followed by 20-min ischaemia. After 80 min reperfusion, cardiac arrest was induced by 1 ml bolus air i.v.. Variables were monitored for 30 minutes post-mortem.

Changes in Dialysate Lactate and Carbonate Concentration in the Cerebral Cortex: A total of 12 experiments were performed on Wistar rats (weight, 340 ± 16 g). All animals were artificially ventilated to maintain normocapnia (i.e. $PCO_2$ between 30-40 mmHg). In half of these experiments (n=6) cortical lactate and carbonate were monitored simultaneously. In these cases the ISM were implanted as previously described (coordinates: 3 mm posterior to the bregma and 1.5 mm left of the sagittal suture; see Section 5.2.2.4) but at a depth of 0.5 mm. This allowed lateral implantation of the microdialysis probe to record the variables under investigation in the same region. As lateral probe implantation was difficult, in the remaining experiments (n=6), carbonate activity was measured alone, and the ISM were implanted to a depth of 1 mm.

After a 60-min control period, transient ischaemia was produced by four vessel for 20 min, followed by 80-min reperfusion. Cardiac arrest was induced by 1 ml bolus air i.v. after which variables were recorded for 30 min.

### 5.7.2 Terminal Complete Ischaemia (Cardiac Arrest)

Extracellular Carbonate and Hydrogen Ion Changes in the Cerebral Cortex: Experiments were performed on a total of 20 Sprague-Dawley rats (weight, 362 ± 12 g). In 10 of these $[CO_3^{2-}]_e$ and $[H^+]_e$ were measured simultaneously, and in the remaining experiments $[CO_3^{2-}]_e$ was measured alone. Animals were artificially ventilated to maintain normocapnia. After a 60-min control period, cardiac arrest was induced by i.v. injection of 1 ml bolus air. Variables were monitored for 30 min post-mortem.

### 5.7.3 Spreading Depression Initiation With Needle Prick

Before cardiac arrest in some of the above experiments, a single spreading depression (SD) was initiated to verify that the ISM was functional. This was done by a needle prick through a small craniectomy 8 mm frontal to the implanted ISM.

### 5.7.4 Lactate Changes with High Extracellular $K^+$ and Spreading Depression Initiation

Recurrent SD was elicited by switching the perfusion medium periodically from normal ACSF to ACSF containing high $K^+$. Experiments were performed on 12 male Sprague-Dawley rats (weight, 330 ± 6 g). All animals were breathing spontaneously. After a 60-min control period, the perfusing fluid was switched from normal ACSF to an iso-osmotic medium with increased $K^+$ (composition in mM: KCl 100, NaCl 27.5, $CaCl_2$ 1.26, $MgCl_2$ 1.18) for 20 min, before a recovery period of 40 min (normal ACSF). A second $K^+$-challenge of the same duration was produced followed by 40-min recovery period.

### 5.7.5 Inhibition of Lactate Transport by Probenecid in the Striatum

#### 5.7.5.1 Concentration-Dependent Effect of Probenecid

Dialysate Lactate in the Striatum: The effect of increasing concentrations of probenecid on striatal lactate was investigated in experiments on 8 Sprague-Dawley rats (weight, 319 ± 13 g) which were allowed to breath spontaneously. After 60-min control period

(normal ACSF), the perfusate was switched for successive 20 min periods to ACSF containing either 1, 2, and 5 mM (n=4), or 5, 10 and 20 mM (n=4) probenecid.

Dialysate pH: The effect of probenecid on dialysate pH was also studied in two groups of parallel experiments (n=4 in each group; weight, 356 ± 10 g, n=8) in which 1, 2 and 5 mM probenecid and 5, 10 and 20 mM probenecid, were applied sequentially following the above protocol.

### 5.7.5.2 Recovery from Probenecid Application

Dialysate Lactate in the Striatum: One pilot experiment was performed on a Sprague-Dawley rat. After a 60-min control period, the perfusate was switched to 5 mM probenecid-ACSF for 20 min followed by 50-min recovery (normal ACSF). Then 20 mM probenecid was perfusion through the probe for 20 min with a further 50-min recovery (normal ACSF).

### 5.7.5.3 Effect of Probenecid on and Lactate Changes with High Extracellular $K^+$ and Spreading Depression Initiation

The changes in striatal $[lact]_d$ associated with high extracellular $K^+$ and SD initiation were measured with and without the application of probenecid.

A total of 27 experiments were performed on Sprague-Dawley rats (weight, 339 ± 7 g) breathing spontaneously. All experiments followed the same protocol. After 60-min control period, the perfusing fluid was switched from normal ACSF to an iso-osmotic medium containing increased $K^+$ for 20 min, followed by 40 min of recovery (normal ACSF). Then, ACSF containing probenecid was perfused through the probe for 50 min before initiation of a second $K^+$-challenge (20 min, $K^+$-ACSF containing probenecid) with a further recovery period of 40 min (ACSF with probenecid).

In the first group of 5 experiments 100 mM $K^+$-ACSF (composition in mM: KCl 100, NaCl 27.5, $CaCl_2$ 1.26, $MgCl_2$ 1.18) was perfused. However, these experiments (and previous experiments in Section 5.7.4) showed that 100 mM $K^+$-ACSF was not always high enough to evoke recurrent SD under the experimental conditions used in this study (corroborated by Szerb, 1991; Herreras and Somjen 1993; Saito et al., 1993). Therefore, further groups of experiments were performed with ACSF, composition as stated above, but containing increasing $K^+$ concentrations [125 mM (6 experiments), 140 mM (4 experiments) and 160 mM (5 experiments)] in conjunction with 5 mM probenecid.

In the last group of experiments (n=7) only $K^+$-ACSF containing the highest $K^+$ concentration was used (i.e. 160 mM $K^+$) with 20 mM probenecid.

These animal groups allowed the investigation of the effects of i) varying [$K^+$] with and without 5 mM probenecid and ii) changing the probenecid concentration at a constant [$K^+$], on DC potential and $[lact]_d$.

### 5.7.5.4 Effect of Probenecid on Lactate Changes During Terminal Complete Ischaemia (Cardiac Arrest)

Experiments were performed on Sprague-Dawley rats (weight, 340 ± 5 g). In 12 control animals, normal ACSF was perfused before and after cardiac arrest which was produced by a rapid i.v. injection of 1 ml of air. In order to examine the effect of probenecid on complete ischaemia-induced lactate efflux, either 5 mM (n=5) or 20 mM (n=7) probenecid-ACSF was perfused for 50 minutes before cardiac arrest. All parameters were recorded for 30-40 min postmortem.

### 5.7.5.5 Effect of Probenecid on Lactate Changes During Transient Forebrain Ischaemia

From the previous studies of $[lact]_d$ changes during terminal complete ischaemia (cardiac arrest, Section 5.6.5.4), it was observed that 5 mM probenecid did not produce a total inhibition of lactate efflux. Therefore, this series of experiments focused on the effects of 20 mM probenecid on $[lact]_d$ changes associated with transient forebrain ischaemia. However, one experiment was carried out with 5 mM probenecid to confirm the previous observation.

Experiments were performed on 11 Wistar rats (weight, 315 ± 8 g). All animals were artificially ventilated and the $P_{CO_2}$ was maintained within the region of 30-40 mmHg. After a 60-min control period the perfusion medium was switched from normal ACSF to ACSF containing either 5 mM (n=1) or 20 mM (n=10) probenecid. After 50 min, forebrain ischaemia was initiated (20 min), followed by 80-min reperfusion/recovery.

# CHAPTER 6 EXPERIMENTAL RESULTS

## 6.1 Transient Forebrain Ischaemia

### 6.1.1 Changes in Dialysate Lactate in the Striatum

Systemic Variables

Arterial blood gases, pH, and concentrations of glucose and bicarbonate were as follows: $P_{CO_2}$, 40.0 ± 1.6 mmHg; $P_{O_2}$, 178 ± 13 mmHg; pH, 7.46 ± 0.04; glucose, 7.1 ± 0.4 mM; bicarbonate, 25.8 ± 1.3 mM (n=11).

Mean arterial blood pressure remained steady throughout the control period at 93 ± 7 mmHg (n=10). In all experiments, ischaemia produced an immediate rise to 132 ± 6 mmHg. In half of the experiments (n=5) this increase persisted except for a small decline, and MABP still remained higher than pre-ischaemic levels throughout the rest of the ischaemic period (131 ± 4 mmHg; Fig. 6.1.A). With the start of reperfusion, there was a sudden transient decrease in MABP to a level comparable to that before ischaemia (102 ± 6 mmHg). In the remaining 5 experiments, MABP stayed high for the first five minutes of ischaemia (at 131 ± 6 mmHg), from where it decreased to 90 ± 14 mmHg (Fig. 6.1.B), and remained at this low level until the end of ischaemia. There was no sudden drop in MABP early during recirculation as observed in the other experiments. In all cases, blood pressure increased progressively during reperfusion, reaching a stable level of 108 ± 7 mmHg within 20 min (n=10).

DC Potential and EEG

Whenever anoxic depolarisation was delayed, this phenomenon was closely associated with MABP (Fig. 6.1.B). In these cases, depolarisation was preceded by a small gradual increase or hyperpolarisation (2.53 ± 0.38 mV, n=5; Fig. 6.1.B). In the other cases, depolarisation occurred within the first minutes of ischaemia (Fig. 6.1.A). The average amplitude of anoxic depolarisation in all cases was 18.1 ± 1.1 mV (n=10). In all experiments, reperfusion was accompanied by an increase in the DC potential indicating repolarisation (18.0 ± 4.5 mV; n=10). In a single experiment, anoxic depolarisation was not observed and the DC potential remained stable throughout the ischaemic period (Fig. 6.1.C).

Forebrain ischaemia produced a rapid reduction in EEG amplitude, and some degree of recovery was evident during reperfusion. In experiments where depolarisation had occurred immediately with the onset of ischaemia, EEG was 26.6 ± 4.2 % of the control after 80-min reperfusion (n=5; Fig. 6.1.A). In the other cases, when depolarisation occurred several minutes after the onset of ischaemia, EEG recovery was significantly higher, reaching 86 ± 16 % of the control (n=5; $p<0.05$; Fig. 6.1.B). In the case when no depolarisation was observed, there was only a partial reduction in EEG during ischaemia and it returned to the control level shortly after reperfusion (Fig. 6.1.C).

Terminal complete ischaemia (cardiac arrest) systematically produced anoxic depolarisation (negative shift of 16.0 ± 2.6 mV) within 2 minutes.

Dialysate Lactate

Changes in striatal $[lact]_d$ during forebrain ischaemia clearly showed 3 different patterns depending on how the DC potential was altered during the insult. With immediate depolarisation there was an initial transient increase in $[lact]_d$, but it decreased to a level close to the pre-ischaemic level until reperfusion (Fig. 6.1.A). With delayed depolarisation the initial increase in $[lact]_d$ was followed by only a slight decrease (Fig. 6.1.B). When depolarisation was absent, the increase in $[lact]_d$ persisted throughout the ischaemic insult (Fig. 6.1.C). However, these differences in $[lact]_d$ changes did not reach statistical significance with n=11, and the results for $[lact]_d$ described below are averages for all experiments, irrespective of these different patterns of changes.

The dialysate concentration of lactate remained relatively stable during the control period at 0.99 ± 0.14 mM (n=11). The onset of ischaemia was accompanied by an immediate and rapid increase in $[lact]_d$ to 3.46 ± 0.38 mM ($p<0.01$; comparison to pre-ischaemic level) an increase of 2.5 ± 0.3 mM at 0.67 ± 0.13 $mmol.l^{-1}.min^{-1}$ (Fig. 6.1.A, 6.1.B and 6.1.C). From this point $[lact]_d$ decreased to 1.9 ± 0.2 mM (at a rate slower than its initial increase (0.28 ± 0.07 $mmol.l^{-1}.min^{-1}$, $p<0.01$), where it remained until reperfusion. With repolarisation there was a marked and rapid increase in $[lact]_d$ to 3.8 ± 0.38 mM (at a rate of 0.34 ± 0.06 $mmol.l^{-1}.min^{-1}$). Then $[lact]_d$ decreased steadily reaching a plateau level of 1.6 ± 0.3 mM after 80 min of reperfusion ($p<0.01$; comparison to pre-ischaemic level).

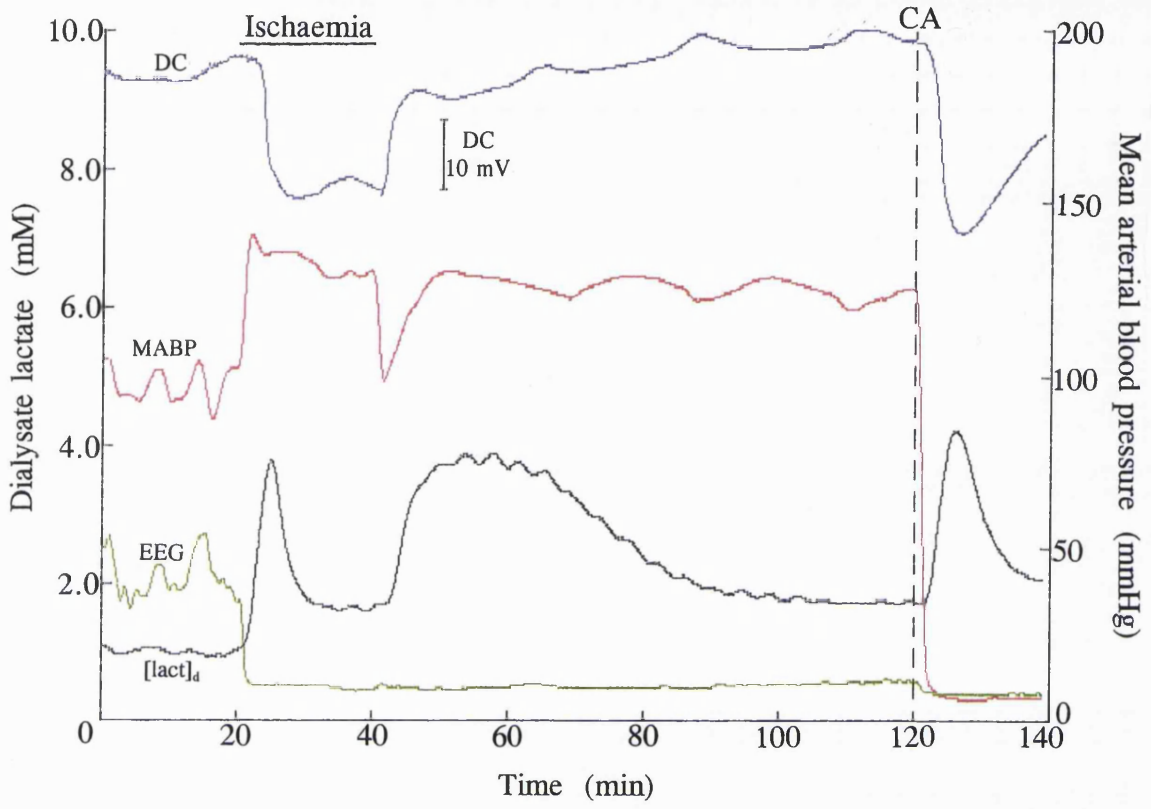


**FIG. 6.1.A** Changes in dialysate lactate ($[lact]_d$), DC potential, MABP and EEG in the striatum during transient forebrain ischaemia (top horizontal line) and reperfusion. These data are from a single, representative experiment. Ischaemia immediately provoked a rapid and marked increase in $[lact]_d$, but this change was reversed subsequent to anoxic depolarisation. Reperfusion produced a second sustained increase in $[lact]_d$, followed by a gradual decrease to near basal levels. Cardiac arrest (dashed line) also produced a pronounced rise in $[lact]_d$.

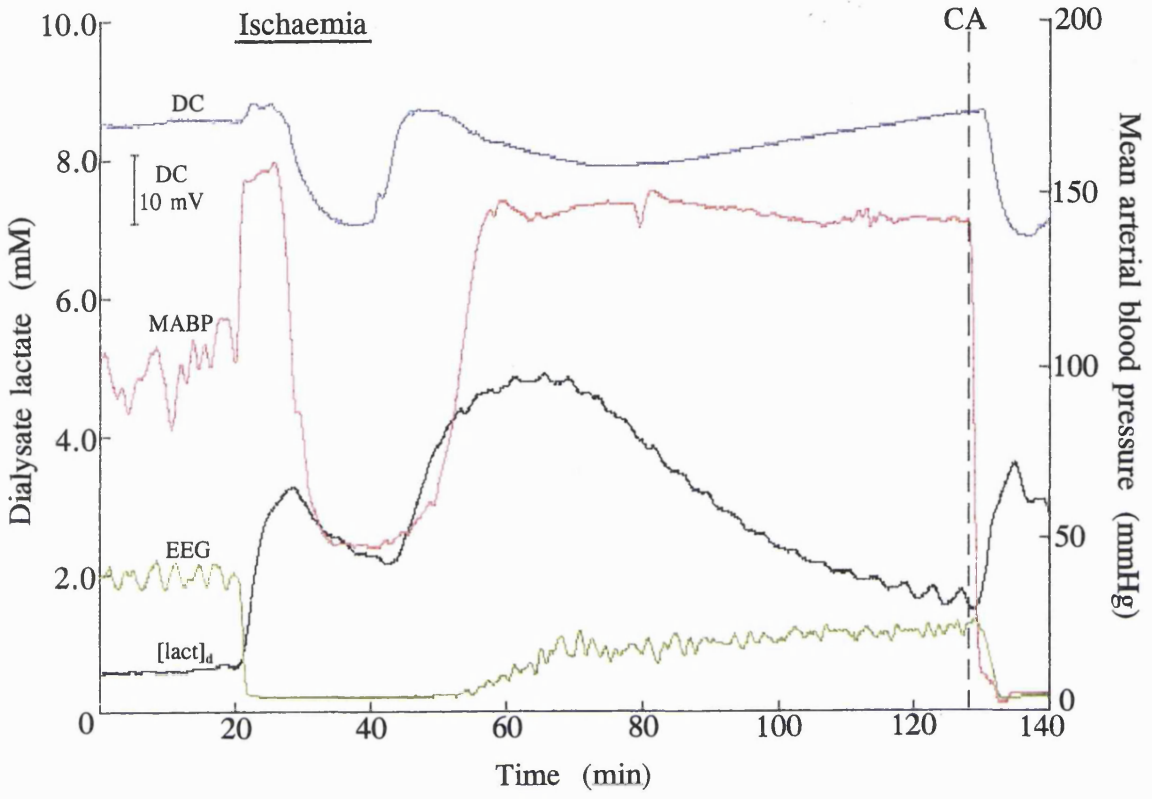


**FIG. 6.1.B** Changes in dialysate lactate ($[lact]_d$), DC potential, MABP and EEG in the striatum during transient forebrain ischaemia (top horizontal line) and reperfusion. These data are from a single representative experiment in which depolarisation was delayed and associated with a drop in MABP. $[lact]_d$ increased with the onset of ischaemia but only decreased slightly with depolarisation. Reperfusion produced a further increase in $[lact]_d$.

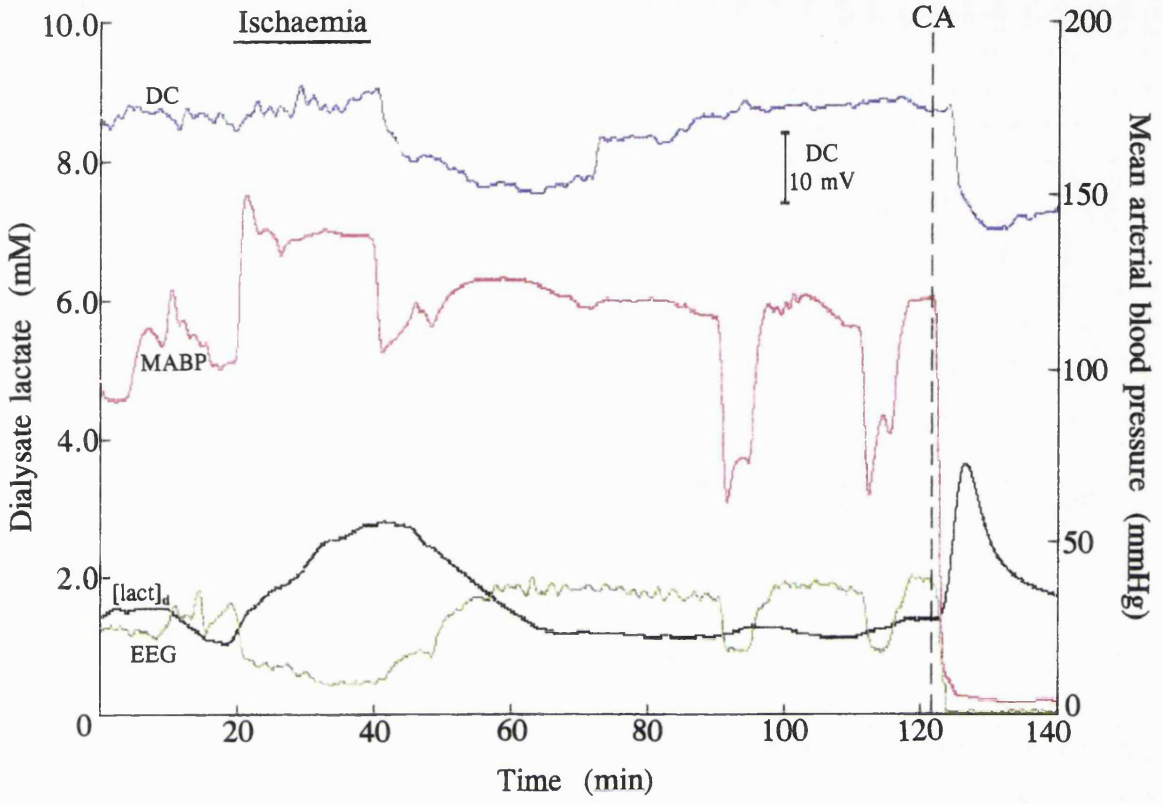


**FIG. 6.1.C** Changes in dialysate lactate ($[lact]_d$), DC potential, MABP and EEG in the striatum during transient forebrain ischaemia (top horizontal line) and reperfusion. These data are from a single experiment in which depolarisation did not occur during ischaemia and $[lact]_d$ increased progressively reaching a plateau, before decreasing after reperfusion. During recovery transient falls in MABP were accompanied by decreases in EEG and slight rises in $[lact]_d$. As in other experiments, cardiac arrest (dashed line) evoked a large increase in $[lact]_d$.

Cardiac arrest evoked an immediate increase in $[lact]_d$ to 3.99 $\pm$ 0.31 mM (an increase of 2.4 $\pm$ 0.2 mM, at a rate comparable to that observed with the onset of transient forebrain ischaemia 0.77 $\pm$ 0.07 $mmol.l^{-1}.min^{-1}$). Then $[lact]_d$ decreased during the 30-min recording post-mortem to 1.78 $\pm$ 0.2 (rate 0.33 $\pm$ 0.03 $mmol.l^{-1}.min^{-1}$, $p<0.001$; compared to rate of increase), a level higher than the basal lactate concentration ($p<0.01$).

---

**Transient Forebrain Ischaemia**

**Major Findings**

- Ischaemia-induced changes in $[lact]_d$ and those of the DC potential (i.e. depolarisation and repolarisation) were closely related:
  - Anoxic depolarisation was associated with a sudden cessation in lactate efflux.
  - Repolarisation was accompanied by a secondary increase of lactate.

---

### 6.1.2 Changes in Dialysate Lactate and Carbonate Concentration in the Cerebral Cortex

Systemic Variables

Arterial blood gases, pH and concentrations of glucose and bicarbonate were as follows: $PCO_2$, 38.4 ± 1.9 mmHg; $PO_2$, 176 ± 21 mmHg; pH, 7.4 ± 0.01; glucose, 7.4 ± 1.1 mM; bicarbonate, 24.9 ± 0.6 mM (n=12).

Mean arterial blood pressure increased from a control level of 70 ± 3 mmHg to 108 ± 8 mmHg immediately with the onset of forebrain ischaemia (Fig. 6.1.D and 6.1.E). Then, in all experiments this increase persisted except for a small drop, but MABP was maintained at pre-ischaemic levels or higher during the rest of the ischaemic period. With reperfusion there was a sudden decrease, and after 80 min MABP had stabilised at a level close to the pre-ischaemic level (59 ± 8 mmHg).

DC Potential and EEG

In the cerebral cortex, four vessel occlusion consistently produced a rapid, marked negative shift in the DC potential of 21.6 ± 2.5 mV, indicating the occurrence of anoxic depolarisation. It is worth noting that the amplitude of depolarisation measured in these experiments with ISM was not significantly different from that measured in the striatum with a microdialysis electrode (21.6 ± 2.5 and 18.1 ± 1.1 mV, respectively). With reperfusion and the associated decrease in MABP, repolarisation (a positive shift of 26.9 ± 1.5 mV) was preceded by a small drop (4.5 ± 2.5 mV) in the DC potential. As in the striatum, cardiac arrest produced an early anoxic depolarisation (negative shift in the DC potential, 23.4 ± 1.4 mV).

Occlusion of the carotid arteries consistently reduced the EEG to noise levels, except in a few cases where significant activity persisted during the ischaemic episode, despite a rapid and pronounced anoxic depolarisation (Fig. 6.1.D). This residual EEG probably reflected electrical activity from posterior regions remote from the recording site and spared from the ischaemic insult. The rapid decrease in EEG and marked anoxic depolarisation in the cortex confirmed that four-vessel occlusion produced near-complete forebrain ischaemia in Wistar rats (Blomqvist et al., 1984; Pulsinelli and Buchan, 1988). After 80-min reperfusion EEG had recovered to 62.1 ± 9.9 % of the original control value, significantly higher than that observed in the striatum after 80-min reperfusion (26.6 ± 4.2 %, $p<0.01$).

Dialysate Lactate

During the control period cortical dialysate lactate ($[lact]_d$) was 0.39 ± 0.07 mM (n=6; Fig. 6.1.D). With the onset of forebrain ischaemia, there was a rapid increase in $[lact]_d$ to 1.29 ± 0.13 mM, at 0.23 ± 0.07 $mmol.l^{-1}.min^{-1}$ (an increase of 0.93 ± 0.17 mM, $p<0.01$). From here $[lact]_d$ slowly decreased reaching 1.0 ± 0.18 mM (at a rate of 0.04 ± 0.009 $mmol.l^{-1}.min^{-1}$, $p<0.05$; comparison to rate of increase). Reperfusion produced a further marked increase in $[lact]_d$ to 1.36 ± 0.09 (at a rate of 0.06 ± 0.01 $mmol.l^{-1}.min^{-1}$), followed by a steady decrease at 0.05 ± 0.007 $mmol.l^{-1}.min^{-1}$ reaching a plateau level of 0.39 ± 0.06 mM after 50-min reperfusion.

With cardiac arrest, $[lact]_d$ increased to 1.19 ± 0.05 mM, an increase of 0.8 ± 0.07 (at a rate comparable to that observed with the onset of transient forebrain ischaemia 0.36 ± 0.09 $mmol.l^{-1}.min^{-1}$). During 30-min post-mortem $[lact]_d$ decreased (at 0.065 ± 0.02 $mmol.l^{-1}.min^{-1}$) to 0.7 ± 0.02 mM which was higher than basal level ($p<0.05$).

Extracellular Carbonate Changes: Simultaneous Measurement with Lactate

During the control period $[CO_3^{2-}]_e$ remained stable at 50.1 ± 5.8 μM (n=6; Fig. 6.1.D). With the onset of ischaemia, but before anoxic depolarisation, there was an immediate decrease in $[CO_3^{2-}]_e$ at 11.7 ± 3.2 $\mu mol.l^{-1}.min^{-1}$ to 37.1 ± 5.2 μM (a decrease of 16.3 ± 3.7 μM, $p<0.01$). Subsequently, there was a sudden transient increase in $[CO_3^{2-}]_e$, (at 60.9 ± 4.3 $\mu mol.l^{-1}.min^{-1}$, mean amplitude = 12.0 ± 3.3 μM) superimposed on the steady $[CO_3^{2-}]_e$ decrease, which was closely associated with the fast negative shift in the DC potential that characterised anoxic depolarisation. Then $[CO_3^{2-}]_e$ decreased to 22.2 ± 3.0 μM and remained at this level for the rest of the ischaemic period. With reperfusion, a further drop in $[CO_3^{2-}]_e$ of 5.0 ± 1.5 μM, preceded a slow increase (at 1.4 ± 0.4 $\mu mol.l^{-1}.min^{-1}$). After 80-min reperfusion, $CO_3^{2-}$ had reached a concentration similar to that observed before ischaemia (57.0 ± 6.5 μM).

With cardiac arrest, $[CO_3^{2-}]_e$ dropped immediately to 36.7 ± 5.5 μM ($p<0.01$), a decrease of 14.5 ± 3.8 μM (Fig. 6.1.D). With the negative shift in the DC potential, there was a sudden transient increase in $[CO_3^{2-}]_e$ (mean amplitude = 6.6 ± 2.2 μM) superimposed on the steady $[CO_3^{2-}]_e$ decrease. Extracellular $[CO_3^{2-}]$ finally decreased to 21.7 ± 3.5 μM.

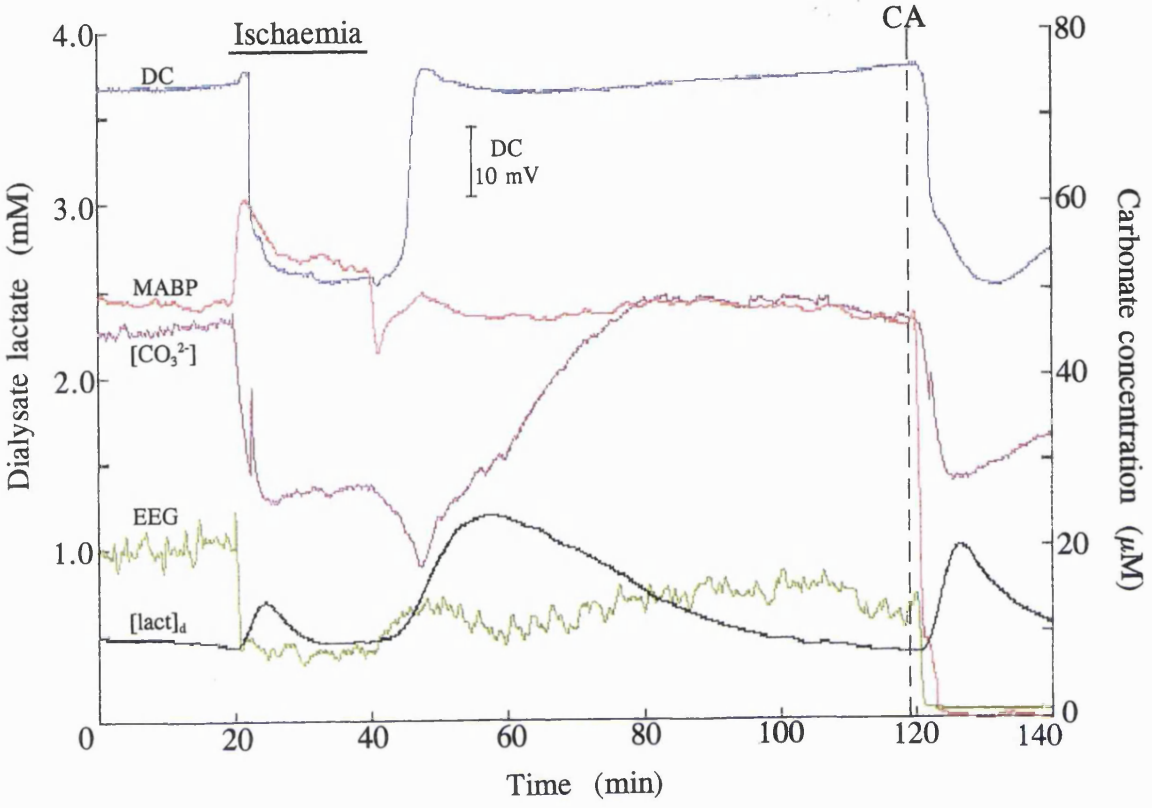


**FIG. 6.1.D** Representative changes in dialysate lactate ($[lact]_d$), carbonate ($[CO_3^{2-}]_e$), DC potential, MABP and EEG in the cerebral cortex during transient forebrain ischaemia (top horizontal line) and reperfusion. The $[CO_3^{2-}]_e$ trace shows 3 relevant features: (i) immediate decrease of $[CO_3^{2-}]_e$ from the onset of ischaemia; (ii) transient increase associated with anoxic depolarisation, and superimposed upon the steady decrease in $[CO_3^{2-}]_e$; and (iii) a further drop in $[CO_3^{2-}]_e$, closely associated with repolarisation, preceding its gradual normalisation. A similar pattern of changes was observed with depolarisation produced by cardiac arrest (dashed line).

Extracellular Carbonate: No Simultaneous Measurement of Lactate

There was no difference in the systemic variables between these animals and the series of experiments above. Of the six experiments in which $[CO_3^{2-}]_e$ was measured alone, three revealed changes comparable to those described above, i.e. a shift in $[CO_3^{2-}]_e$ with the negative shift in the DC potential during transient forebrain ischaemia and terminal ischaemia produced by cardiac arrest.

In the other three experiments however, there was no transient increase in $[CO_3^{2-}]_e$ associated with the negative shift in the DC potential during either transient ischaemia, terminal ischaemia (cardiac arrest), or both (Fig. 6.1.E). In these cases, extracellular $[CO_3^{2-}]$ decreased with the onset of transient forebrain ischaemia and remained low for the rest of the insult (Fig. 6.1.E). With reperfusion, the further decrease in $[CO_3^{2-}]_e$ observed in the experiments with simultaneous measurement of $[lact]_d$ was absent, and $[CO_3^{2-}]_e$ started to increase as repolarisation occurred, and stabilised after 80-min reperfusion. Although this pattern was only seen in a few cases, it could not be attributed to ISM disfunction as a post-calibration was performed and all data shown are from electrodes that had close pre- and post-experimental calibrations. Blockage of the electrode tip during the experiment could be possible, but unlikely, as in some experiments, both patterns of changes were observed i.e. no shift in $[CO_3^{2-}]$ was observed during transient ischaemia but was evident with terminal ischaemia (cardiac arrest). In order to verify if this pattern was due to the severity of the ischaemic insult, another series of experiments were performed to measure $[CO_3^{2-}]_e$, simultaneously with $[H^+]_e$ in some cases, during terminal ischaemia (cardiac arrest) alone, as the severity of this insult is not variable.

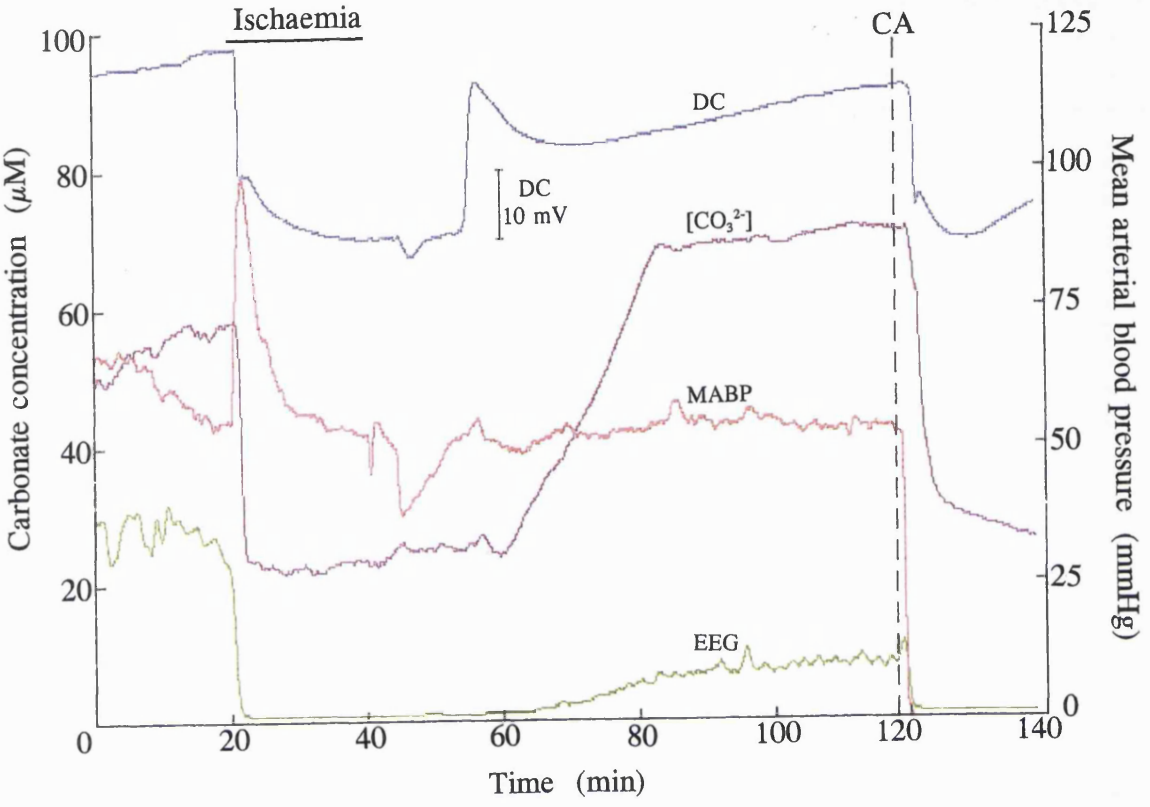


**FIG. 6.1.E** Changes in $[CO_3^{2-}]_e$, DC potential, MABP and EEG in the cerebral cortex during transient forebrain ischaemia (top horizontal line) and reperfusion. These data are from a single representative experiment in which there was no transient shift in $[CO_3^{2-}]_e$ associated with anoxic depolarisation with either transient forebrain ischaemia or cardiac arrest (dashed line).

## Transient Forebrain Ischaemia

### Major Findings

- These data obtained in the cortex confirmed that changes in cellular membrane potential have pronounced effects on lactate efflux.
- Measurement of extracellular $CO_3^{2-}$ revealed 3 distinctive features:
  - an immediate decrease of $[CO_3^{2-}]_e$ from the onset of ischaemia.
  - a sudden transient increase in $[CO_3^{2-}]_e$, superimposed upon its steady decrease, was synchronous with anoxic depolarisation.
  - a further drop in $[CO_3^{2-}]_e$, closely associated with repolarisation, preceding its progressive normalisation during reperfusion.
- In a few cases the transient increase in $[CO_3^{2-}]_e$ associated with depolarisation was not present.

## 6.2 Terminal Complete Ischaemia (Cardiac Arrest)

### 6.2.1 Extracellular Carbonate Changes in the Cerebral Cortex

Systemic Variables

Arterial blood gases, pH, and the concentrations of glucose and bicarbonate were as follows: $PCO_2$, 40 ± 2 mmHg; $PO_2$, 195 ± 16 mmHg; pH, 7.4 ± 0.02; glucose, 6.9 ± 0.3 mM; bicarbonate, 24.0 ± 0.7 mM (n=20). MABP was stable throughout the control period at 75 ± 3 mmHg.

Extracellular Carbonate Concentration

In most experiments (n=15), $[CO_3^{2-}]_e$ started to decrease immediately after the onset of ischaemia from a control value of 53.7 ± 2.4 μM to 38.9 ± 2.6 μM ($p<0.001$; at a rate of 23.0 ± 7.7 $\mu mol.l^{-1}.min^{-1}$), a decrease of 16.9 ± 2.0 μM (Fig. 6.2.A). Subsequently, there was a sudden transient increase in $[CO_3^{2-}]_e$, (at 77.2 ± 5.1 $\mu mol.l^{-1}.min^{-1}$; mean amplitude = 6.4 ± 1.2 μM) superimposed on the steady $[CO_3^{2-}]_e$ decrease, and closely associated with the fast negative shift in the DC potential (23.0 ± 0.9 mV) characterising anoxic depolarisation. Extracellular $[CO_3^{2-}]$ then decreased to 30.9 ± 2.7 μM at a rate comparable to that of the initial decrease (28.7 ± 6.5 $\mu mol.l^{-1}.min^{-1}$).

There was no correlation found between the amplitude of the increase in $[CO_3^{2-}]$ and that of the drop in the DC potential. However, there was a close relationship between the amplitude of the transient increase in $[CO_3^{2-}]$ and the magnitude of the decrease in extracellular $[CO_3^{2-}]$ concentration from ischaemia onset ($r = 0.823$, $p<0.001$; Fig. 6.2.B).

As with transient forebrain ischaemia, in several of these experiments the sudden increase in $[CO_3^{2-}]_e$ associated with the negative shift in the DC potential (membrane depolarisation) was absent and there was only a brief reduction in the steady rate of decrease, seen as a small plateau (arrow, Fig. 6.2.C). In these cases, the pre-ischaemic concentration of $CO_3^{2-}$ was significantly lower in comparison to the group of experiments referred to above (32.8 ± 3.2 μM, n=5; $p<0.001$). With cardiac arrest there was a small and transient increase in $[CO_3^{2-}]_e$ (2.9 ± 0.6 μM) before $[CO_3^{2-}]_e$ decreased by 16.6 ± 2.3 μM, a similar decrease to that observed in the experiments already described, where a plateau was observed.

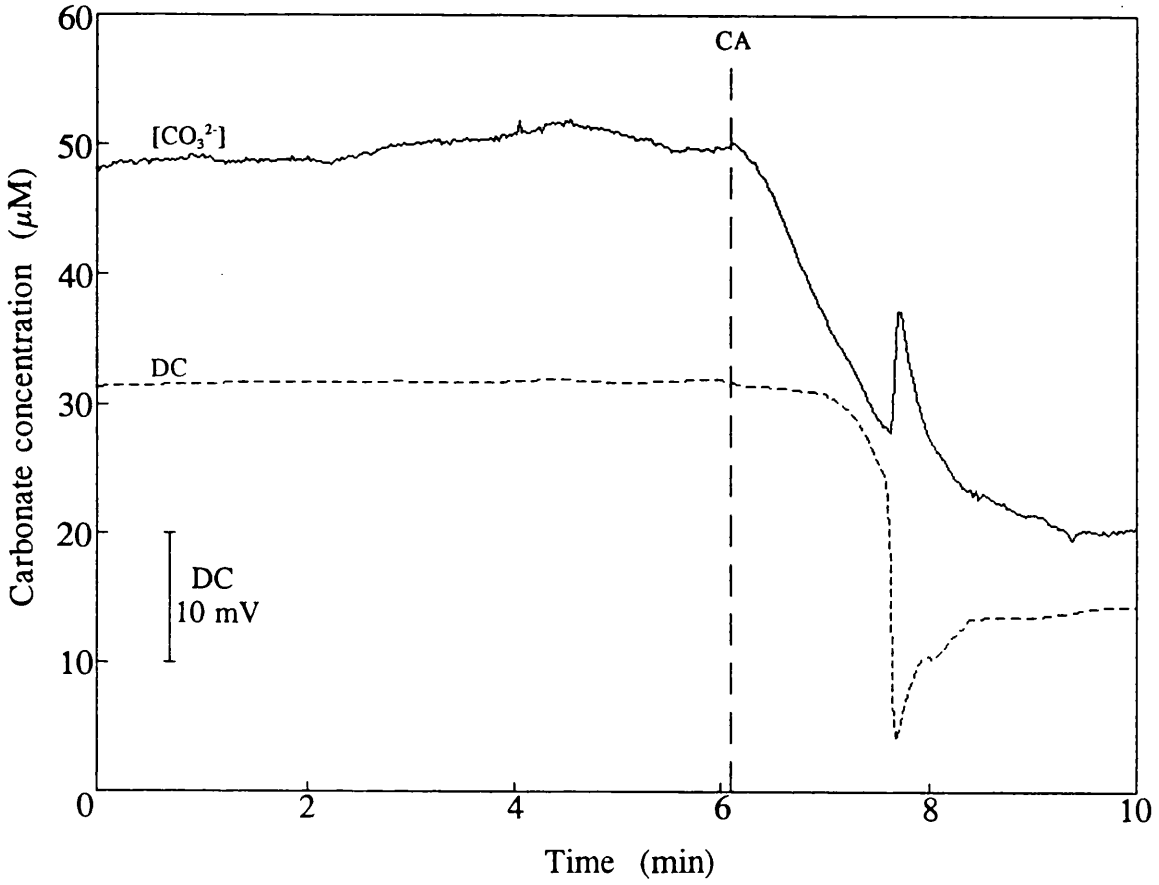


**FIG. 6.2.A** Changes in $[CO_3^{2-}]_e$ and DC potential in the cerebral cortex associated with terminal complete ischaemia produced by cardiac arrest (dashed line). These data, from a single representative experiment, show that $[CO_3^{2-}]_e$ was stable during the 60-min control period (only last part is shown). Cardiac arrest induced an immediate decrease in $[CO_3^{2-}]_e$. With the fast negative shift in the DC potential (anoxic depolarisation) there was a rapid transient increase in $[CO_3^{2-}]_e$ superimposed on its steady decrease.

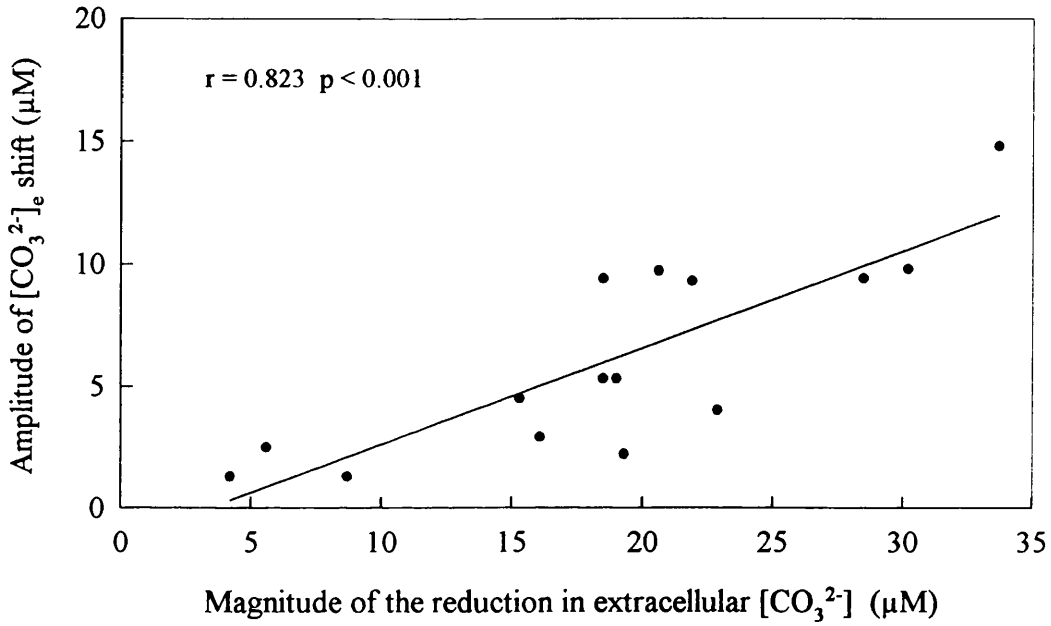


**FIG. 6.2.B** Correlation between the amplitude of the transient increase in $[CO_3^{2-}]_e$ associated with anoxic depolarisation, and the magnitude of the reduction in extracellular $[CO_3^{2-}]$ (i.e. control level minus the level reached before the transient shift occurred; see Fig. 6.2.A).

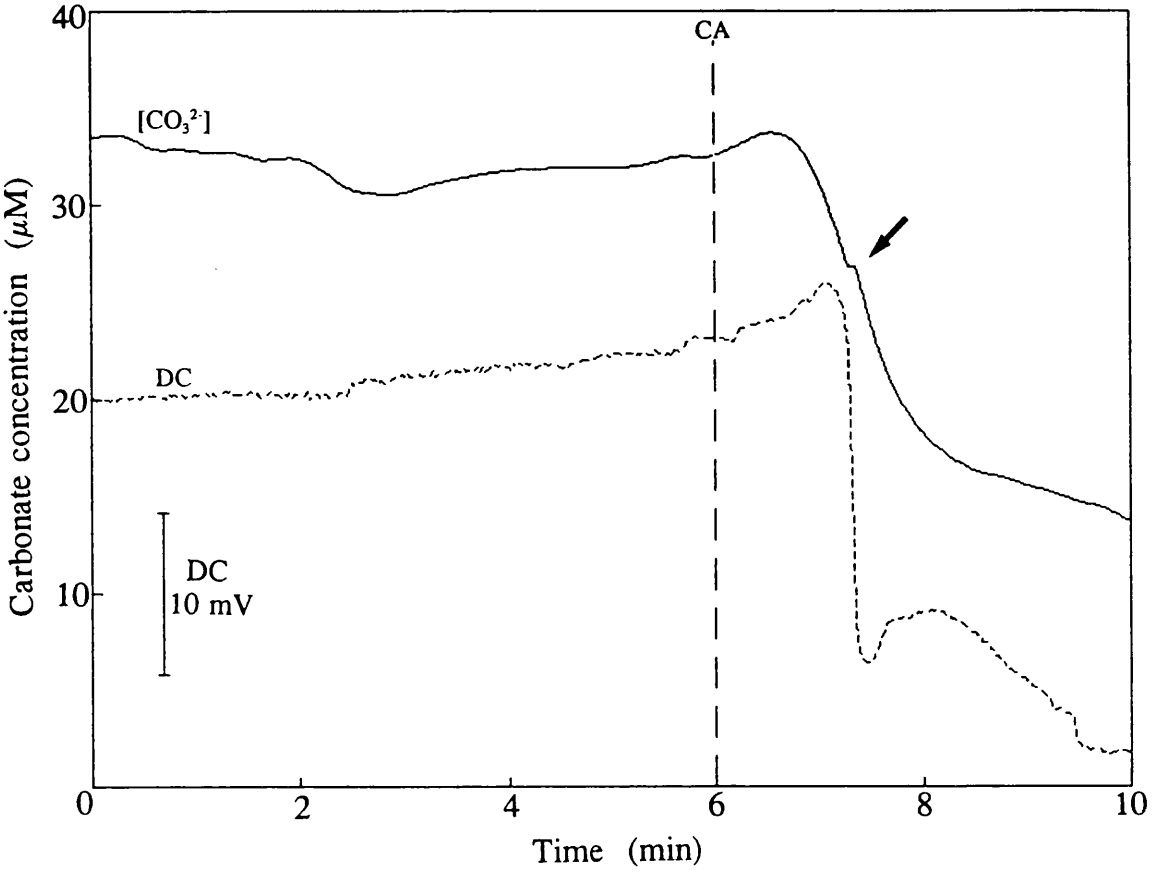


**FIG. 6.2.C** Changes in $[CO_3^{2-}]_e$ and DC potential in the cerebral cortex associated with terminal complete ischaemia produced by cardiac arrest (dashed line). These data are from a single representative experiment in which there was no shift in $[CO_3^{2-}]_e$ associated with anoxic depolarisation. The ischaemia-induced steady decrease in $[CO_3^{2-}]_e$ was preceded by a transient increase, and instead of the sudden shift in $[CO_3^{2-}]_e$, there was momentary reduction in the steady rate of decrease, seen as a small plateau (arrow).

### 6.2.2 Extracellular Hydrogen Ion Changes in the Cerebral Cortex

The concentration of $H^+$ remained stable throughout the 60-min control period (61.1 ± 11.4 nM n=10) (Fig. 6.2.D). Cardiac arrest evoked an immediate sustained increase in $[H^+]_e$ to 223 ± 21 nM, with a sudden transient decrease (mean amplitude = 41.9 ± 5.4 nM) associated with anoxic depolarisation. Extracellular $[H^+]$ finally increased to 264 ± 20 nM.

Further analysis revealed a clear correlation between the magnitude of the transient fall in $[H^+]_e$ and the extracellular $H^+$ concentration at the time at which this occurred ($r=0.918$, $p<0.01$; Fig. 6.2.E, upper graph). There was a similar relationship between the transient increase in $[CO_3^{2-}]_e$ and the extracellular $H^+$ concentration ($r=0.946$, $p<0.01$; Fig. 6.2.E, lower graph). No correlation was found between the amplitude of the transient drop in $[H^+]_e$ and that of the negative shift in the DC potential.

Simultaneous measurements of $[H^+]_e$ and $[CO_3^{2-}]_e$, showed that the rapid transient increase in $[CO_3^{2-}]_e$ (or the plateau in cases where the shift in $[CO_3^{2-}]_e$ was absent), anoxic depolarisation and the alkalotic shift in $[H^+]_e$ were three closely associated events (Fig. 6.2.F). However, analysis of the changes in $[H^+]_e$ revealed no relationship between the different pattern of changes in $[CO_3^{2-}]_e$, and the basal $H^+$ concentration or the amplitude of the alkalotic shift in $[H^+]_e$ observed with depolarisation.

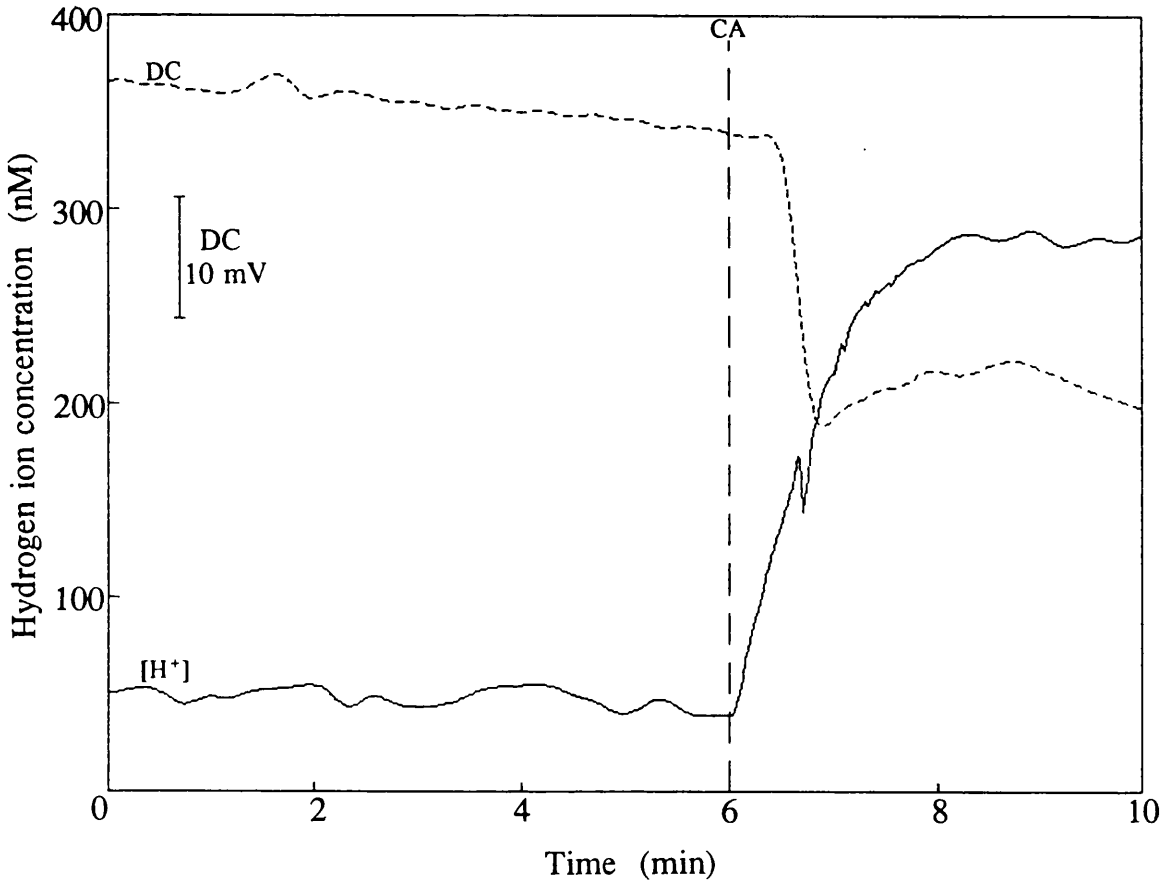


**FIG. 6.2.D** Changes in $[H^+]_e$ and DC potential associated with terminal complete ischaemia produced by cardiac arrest (dashed line). These data, from a single representative experiment, show that ischaemia provoked an immediate increase in $[H^+]_e$, onto which was superimposed a sudden transient decrease closely associated with depolarisation.

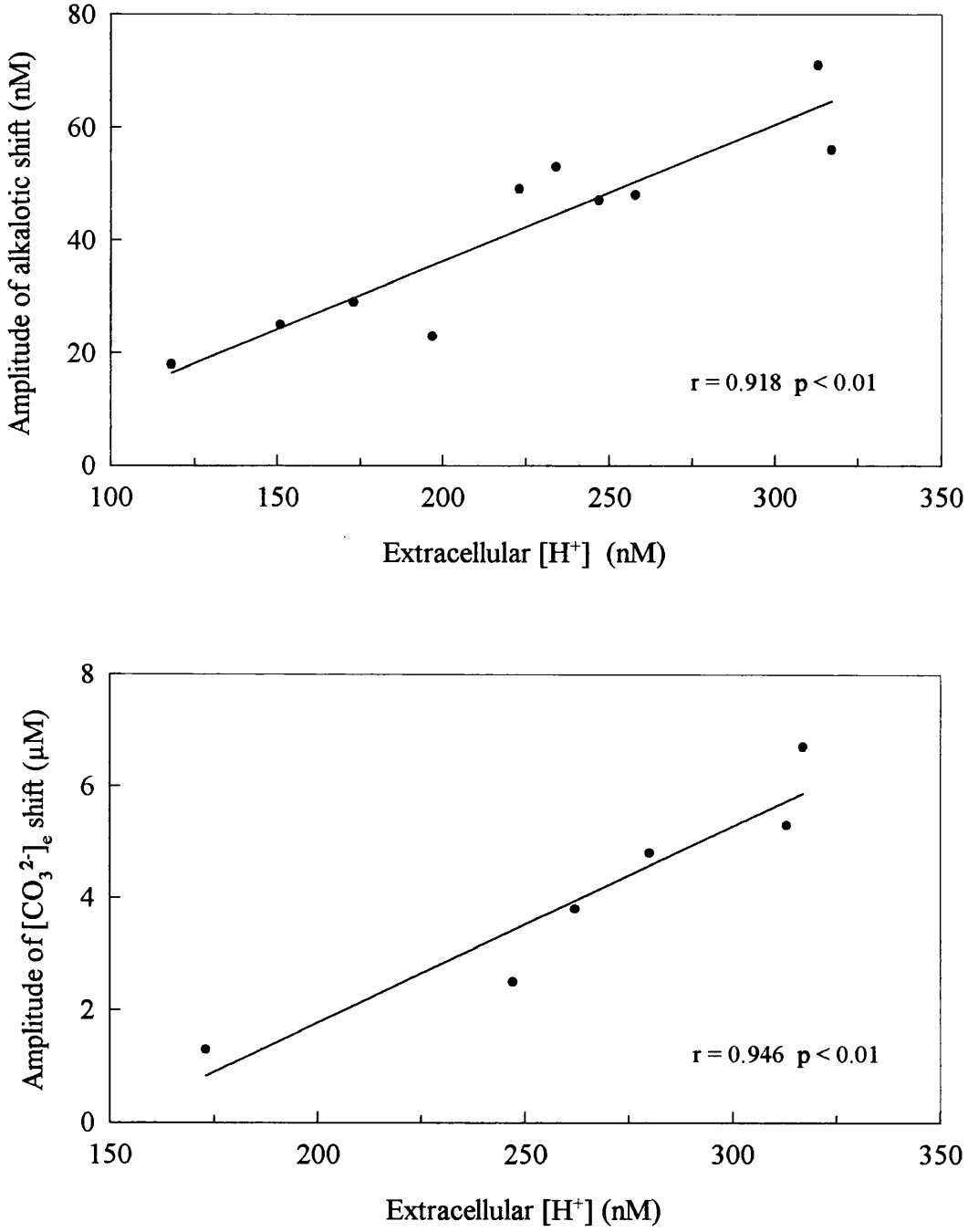


**FIG. 6.2.E** Correlation between both the amplitude of the transient fall in $[H^+]_e$ (upper graph, n=10) and the amplitude of the transient increase in $[CO_3^{2-}]_e$ (lower graph; n=6) with the extracellular $H^+$ concentration at the time these shifts occurred. Data shown in lower graph are from microelectrode recordings where $[H^+]_e$ and $[CO_3^{2-}]_e$ were measured simultaneously during cardiac arrest.

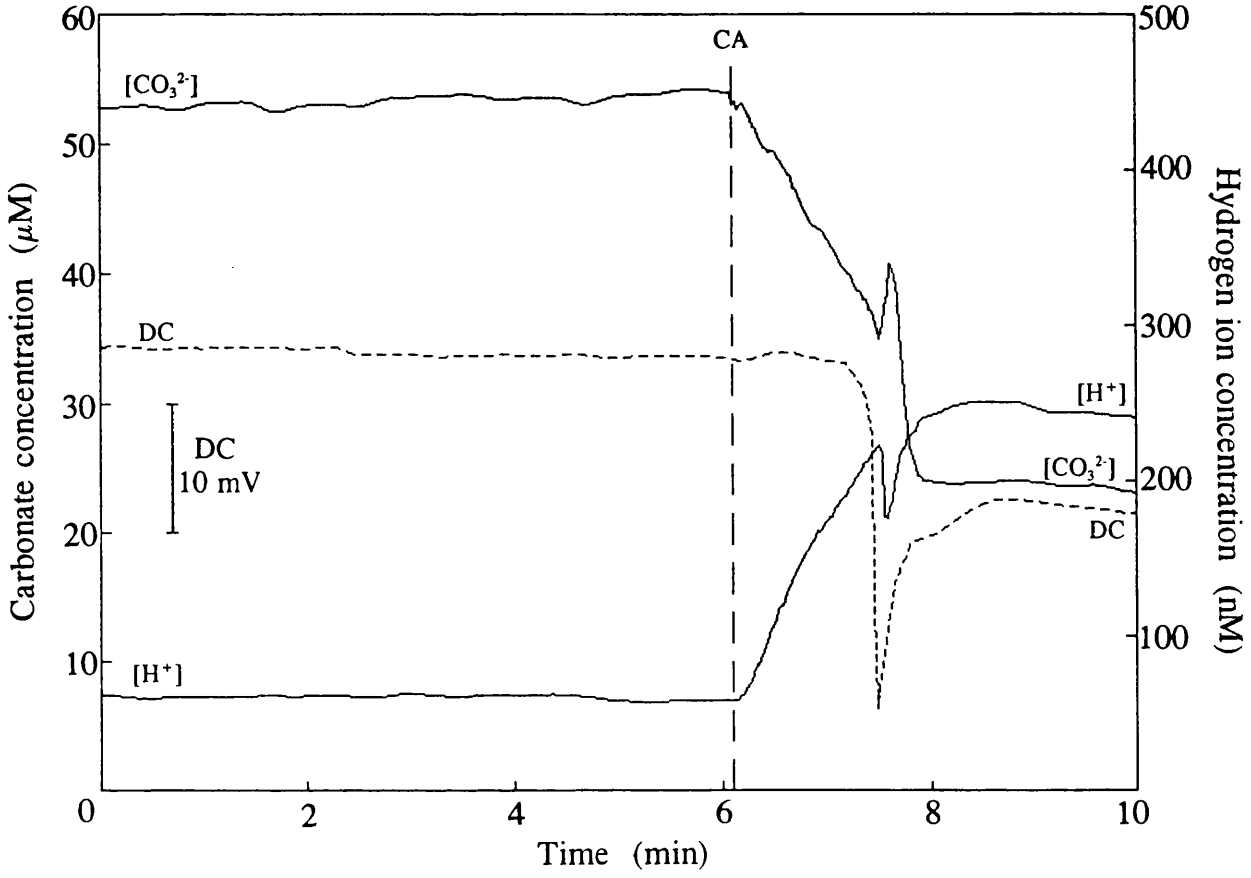


**FIG. 6.2.F** Simultaneous measurement of $[H^+]_e$ and $[CO_3^{2-}]_e$ changes associated with terminal complete ischaemia produced by cardiac arrest (dashed line). These data from a single representative experiment reveal that the alkalotic shift in $[H^+]_e$ and the sudden increase in $[CO_3^{2-}]_e$ were closely associated with anoxic depolarisation.

## Terminal Complete Ischaemia (Cardiac Arrest)

### Major Findings

- Two distinct patterns of changes in extracellular $CO_3^{2-}$ were associated with anoxic depolarisation:
  - in most cases depolarisation was associated with a transient increase in $[CO_3^{2-}]_e$, superimposed onto its steady decrease.
  - In several experiments the transient shift in $[CO_3^{2-}]_e$ was absent and the steady decrease was preceded by a small increase.
- Depolarisation was also associated with an alkalotic shift in $[H^+]_e$.
- The amplitude of the transient shifts in $[CO_3^{2-}]_e$ and $[H^+]_e$ were closely correlated with the extracellular $H^+$ concentration at the time they occurred, and there was a close relationship between the shift in $[CO_3^{2-}]_e$ and the magnitude of its initial decrease.

## 6.3 Spreading Depression Initiation with Needle Prick

Following the needle prick there was a slight increase in the DC potential (hyperpolarisation; Fig. 6.3.A). Approximately 3 minutes after the needle stab, there was a transient decrease in the DC potential indicating depolarisation. There was a slight decrease in $[CO_3^{2-}]_e$ before a sudden rapid increase associated with depolarisation. At this point there was also a sudden decrease in $[H^+]_e$ superimposed on its steady increase. With repolarisation, $[CO_3^{2-}]_e$ increased and $[H^+]_e$ decreased back to a similar level as the control.

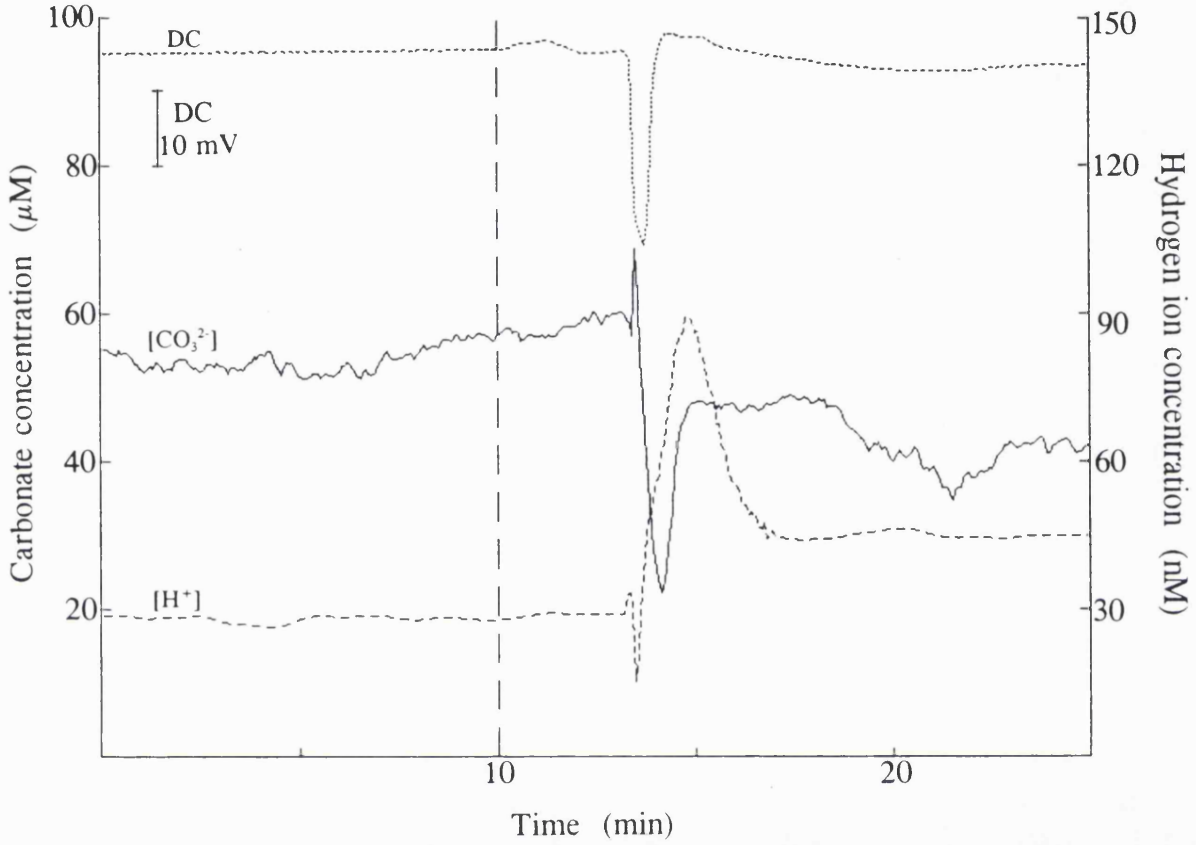


**FIG. 6.3.A** Changes in cortical $[H^+]_e$, $[CO_3^{2-}]_e$ and DC potential associated with a single wave of spreading depression elicited with a needle prick (dashed line). The transient depolarisation was closely associated with a sudden rapid increase in $[CO_3^{2-}]_e$, and a sudden decrease in $[H^+]_e$.

## 6.4 Lactate Changes with High Extracellular $K^+$ and Spreading Depression Initiation in the Striatum

### Systemic Variables

Arterial blood gases, pH and glucose concentration were as follows: $P_{CO_2}$, 63 ± 2 mmHg; $P_{O_2}$, 154 ± 6 mmHg; pH, 7.30 ± 0.01; glucose, 7.8 ± 0.3 mM; bicarbonate, 29.6 ± 0.9 mM (n = 12). MABP was stable throughout the experiment at 86.4 ± 1.6 mmHg.

### Effects of $K^+$ on the DC Potential

High $K^+$ evoked a large and sustained negative shift of the DC potential (mean amplitude 15.4 ± 0.8 mV) onto which were superimposed transient peaks of further depolarisation. The amplitude of the peaks was similar (mean amplitude 9.9 ± 0.9 mV). The number of peaks varied between experiments (between 1 and 6) but there was no significant difference in the number of peaks between the two challenges within experiments, nor in the SD cumulative peak area (Fig. 6.4.A) suggesting no difference in the intensity of SD elicitation (22.6 ± 4.7, 18.7 ± 4.0 mV min, respectively; $p>0.1$). When normal ACSF was perfused, the DC potential returned to a level comparable to that of the control period within 20 minutes (mean amplitude of change 16.5 ± 1.0 mV).

### Effects of $K^+$ on Dialysate Lactate

The dialysate concentration of lactate remained relatively stable throughout the 60-min control period (0.56 ± 0.06 mM). $[lact]_d$ was apparently markedly influenced by change in DC potential, with different patterns of activity depending on the number of depolarisations and the time at which these occurred during the challenge.

The large sustained negative shift in the DC potential was associated with a small decrease in $[lact]_d$ (Fig. 6.4.B). However, when a transient depolarisation occurred shortly after the shift in the DC potential, this decrease in $[lact]_d$ was masked by a transient increase (Fig. 6.4.C) associated with the repolarisation phase of the peak. Whenever a single transient depolarisation peak occurred at the end of the high $K^+$-stimulus, an enhanced increase of $[lact]_d$ was observed as the DC potential was returning to its control level. The rate of the increase in $[lact]_d$ after the $K^+$ challenge was much faster than its rate of decrease (0.2 ± 0.03, 0.07 ± 0.01 $mmol.l^{-1}.min^{-1}$, respectively; $p<0.001$).

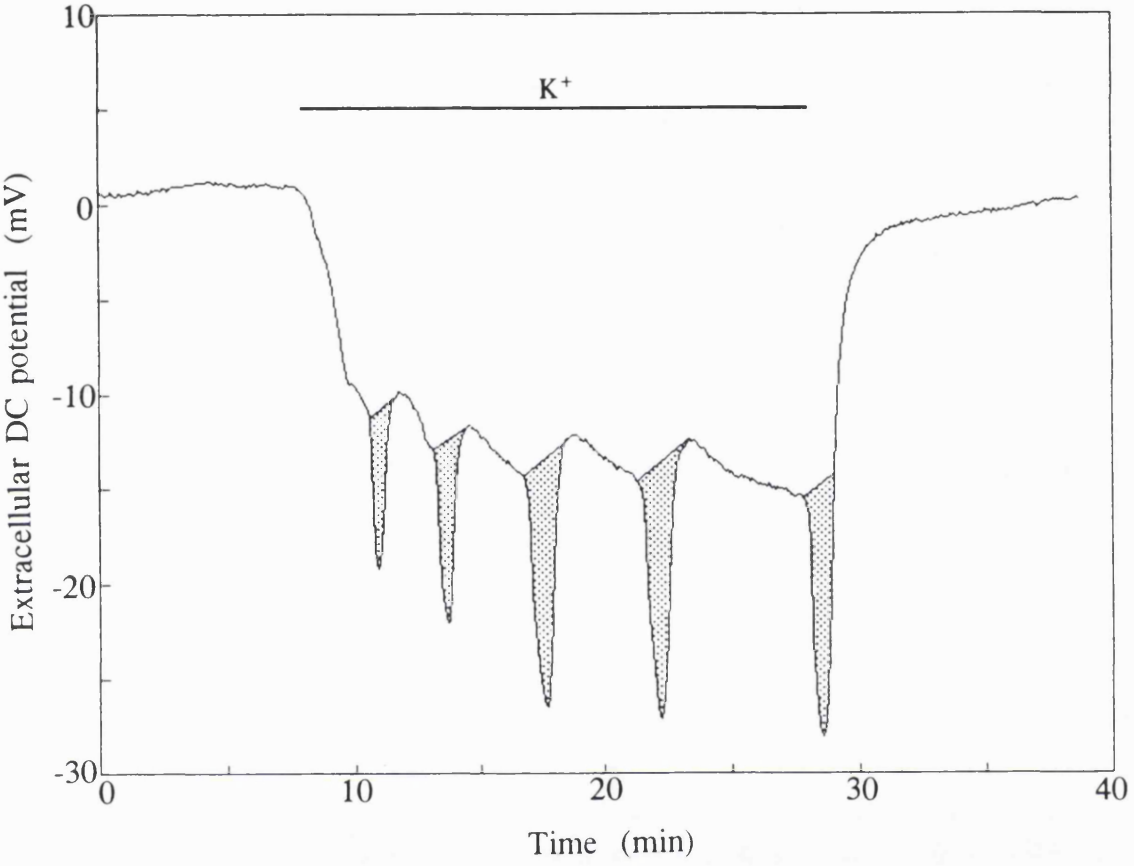


**FIG. 6.4.A** Representative recurrent SD produced in the rat striatum by intracerebral perfusion of 100 mM $K^+$-ACSF for 20 min. The sustained negative shift in the DC potential corresponds to persistent local depolarisation produced by the applied $K^+$. Each further transient peak of depolarisation indicates a wave of SD. The hatched area illustrates how the magnitude of SD elicitation was quantified by integration for each 20-min stimulus. In this case, the corresponding value for the cumulative area of SD peaks was 41.2 mV min.

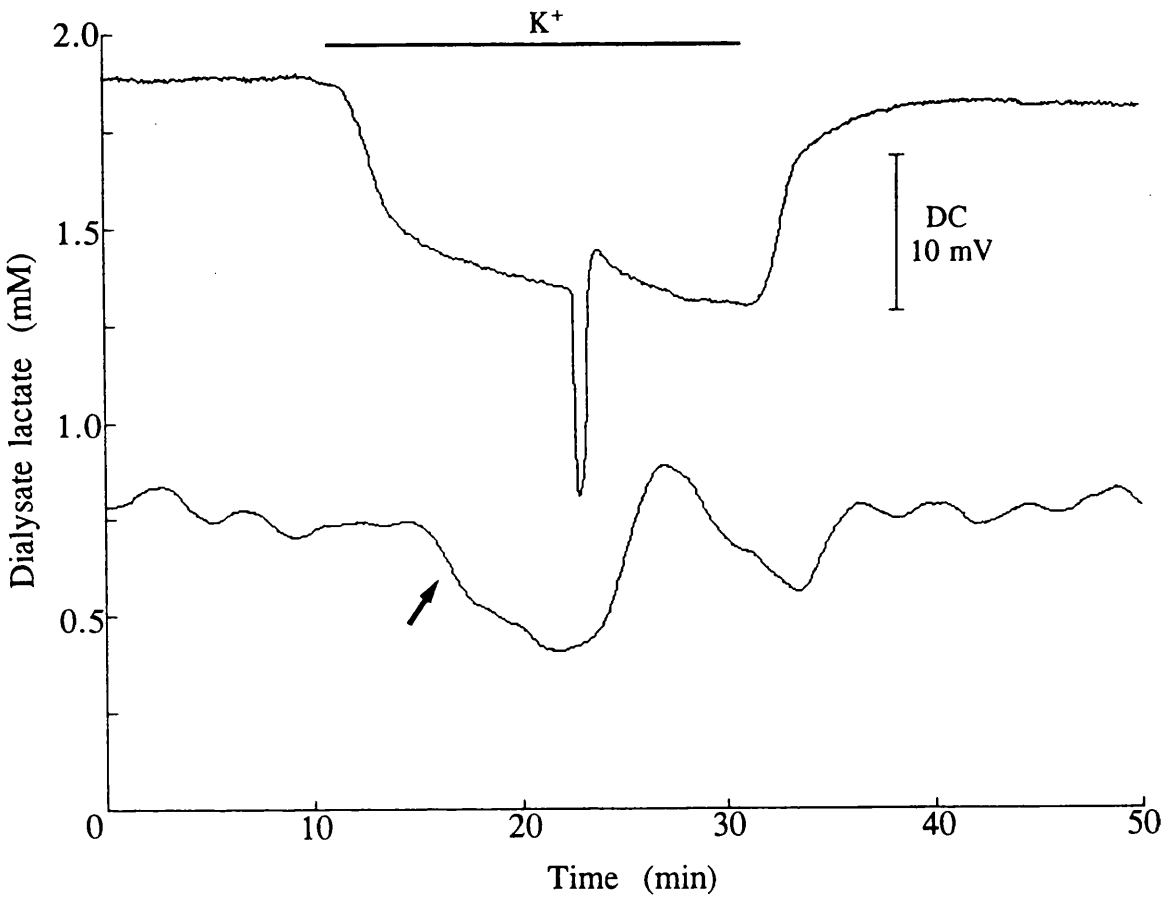


**FIG. 6.4.B** Changes in dialysate lactate ($[lact]_d$; lower trace) and DC potential (upper trace) during a 20-min $K^+$-stimulus in a single representative experiment, where the initial negative shift in the DC potential was associated with a decrease in $[lact]_d$ (arrow). After a single depolarisation there was an increase in $[lact]_d$. The horizontal line at the top of the figure ($K^+$) indicates the period of high $K^+$-stimulation.

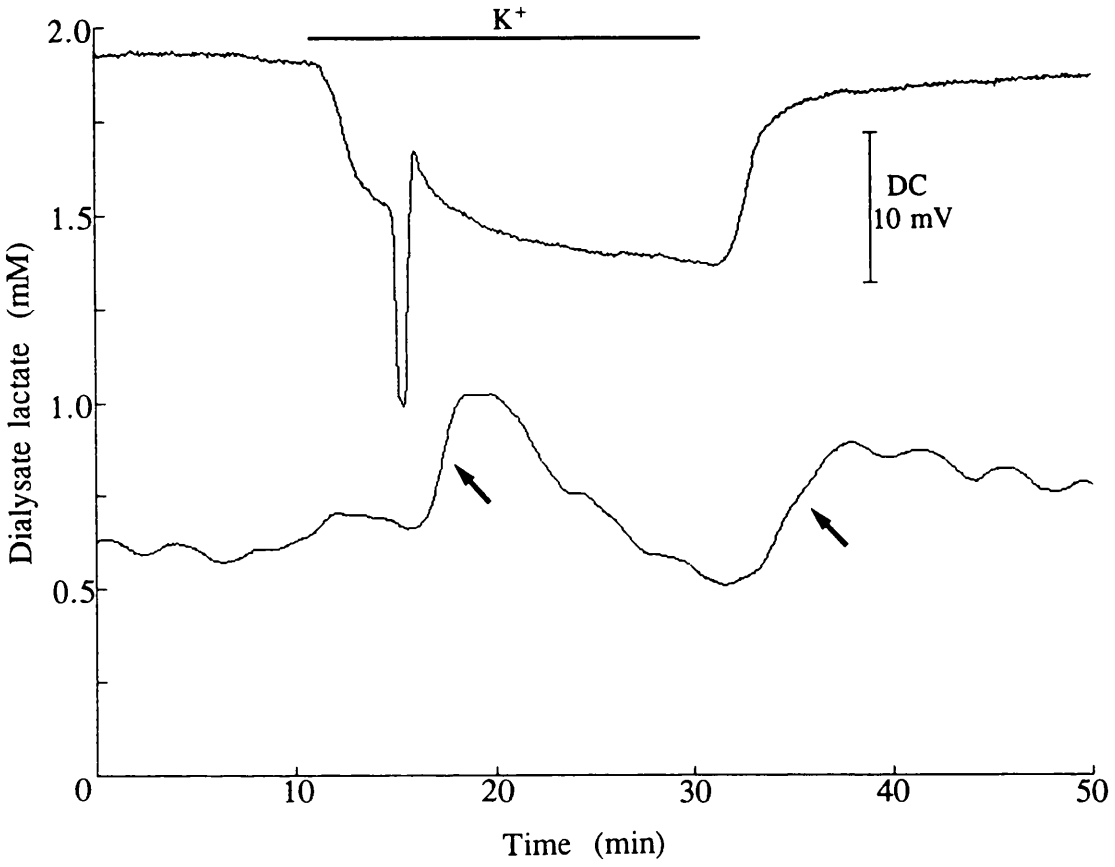


**FIG. 6.4.C** Changes in dialysate lactate ($[lact]_d$; lower trace) and DC potential (upper trace) during a 20-min $K^+$-stimulus in a single representative experiment, where a single depolarisation occurred early in the challenge. An increase in $[lact]_d$ was observed after the transient depolarisation and with repolarisation after the high $K^+$-stimulus (arrows). The horizontal line at the top of the figure ($K^+$) indicates the period of high $K^+$-stimulation.

Multiple depolarisations during a $K^+$-stimulus produced a sustained increase in $[lact]_d$ starting with the initial decrease in the DC potential (Fig. 6.4.D). In these cases, small $[lact]_d$ increases were detected after each transient depolarisation. During recovery, as repolarisation occurred, a large increase in $[lact]_d$ was consistently observed, lasting for 15 min before returning to near baseline level.

Mean changes of $[lact]_d$ for the twelve experiments are summarised in Fig. 6.4.E. The level of $[lact]_d$ before $K^+$-ACSF perfusion (B) was higher for the second challenge than the first (0.68 $\pm$ 0.08 and 0.69 $\pm$ 0.09 mM, respectively, $p<0.05$), but there was no difference between the $[lact]_d$ level during the 20-min $K^+$-stimuli (K). The magnitude of the $[lact]_d$ increase during the DC potential recovery after the first challenge was always higher than that of the second (1.1 $\pm$ 0.2, 1.0 $\pm$ 0.15 mM, respectively; $p<0.01$).

Cardiac arrest produced an immediate and rapid rise in $[lact]_d$ to 1.9 $\pm$ 0.2 mM, an increase of 1.2 $\pm$ 0.2 mM, at a rate of 0.39 $\pm$ 0.04 $mmol.l^{-1}.min^{-1}$), from where it decreased after anoxic depolarisation and throughout the 30-min recording post-mortem (Fig. 6.4.D).

---

## $K^+$-Induced Spreading Depression

### Major Findings

- Regardless of the number of transient depolarisations, $[lact]_d$ increased during periods of repolarisation (i.e. after each depolarisation, and at the end of the $K^+$-stimulus).

---

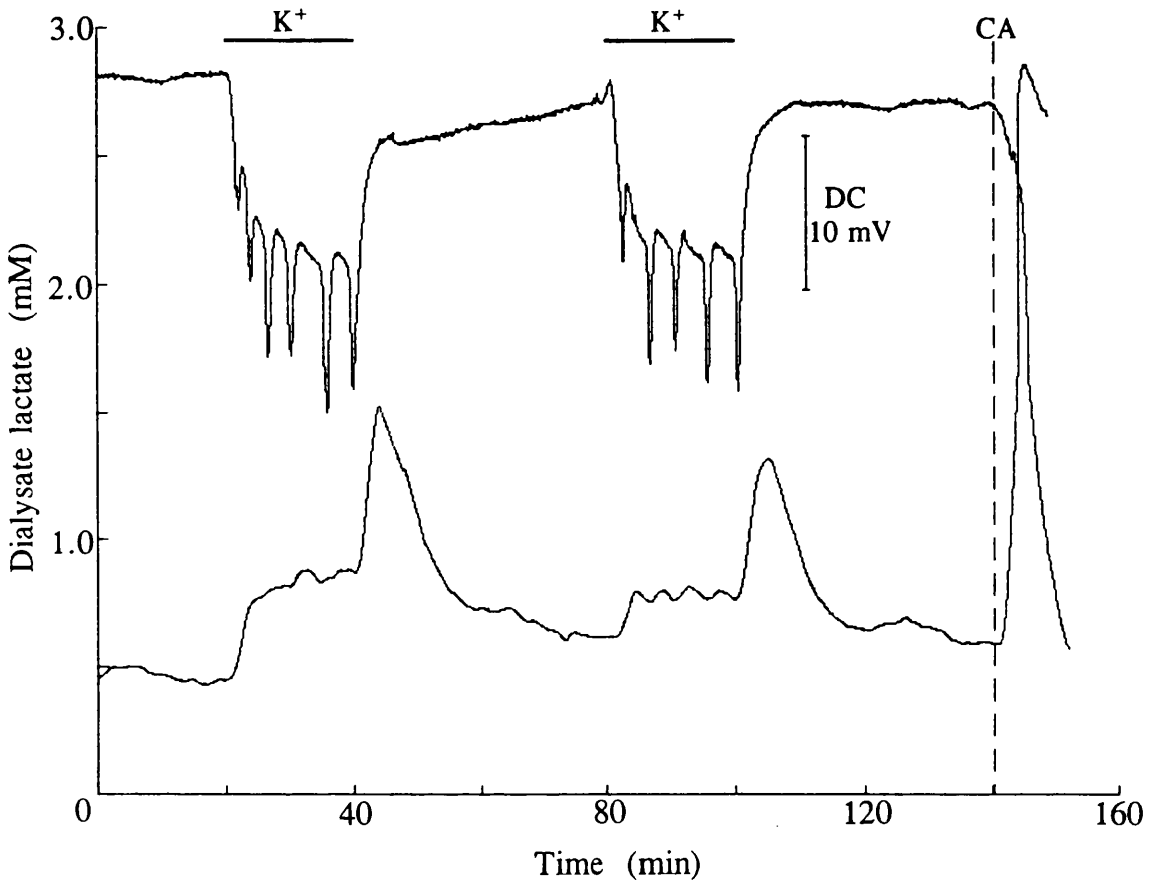


**FIG. 6.4.D** Changes in dialysate lactate ($[lact]_d$; lower trace) and DC potential (upper trace) during two successive 20-min $K^+$-stimuli which were associated with multiple depolarisations. These data, from a single representative experiment show that $[lact]_d$ mainly increased **after** each transient depolarisation. Repolarisation produced a marked increase in $[lact]_d$. With cardiac arrest (dashed line) $[lact]_d$ rose immediately, reaching a peak at which it stabilised, and only decreased slightly thereafter. The horizontal lines at the top of the figure ($K^+$) indicate periods of high $K^+$-stimulation.

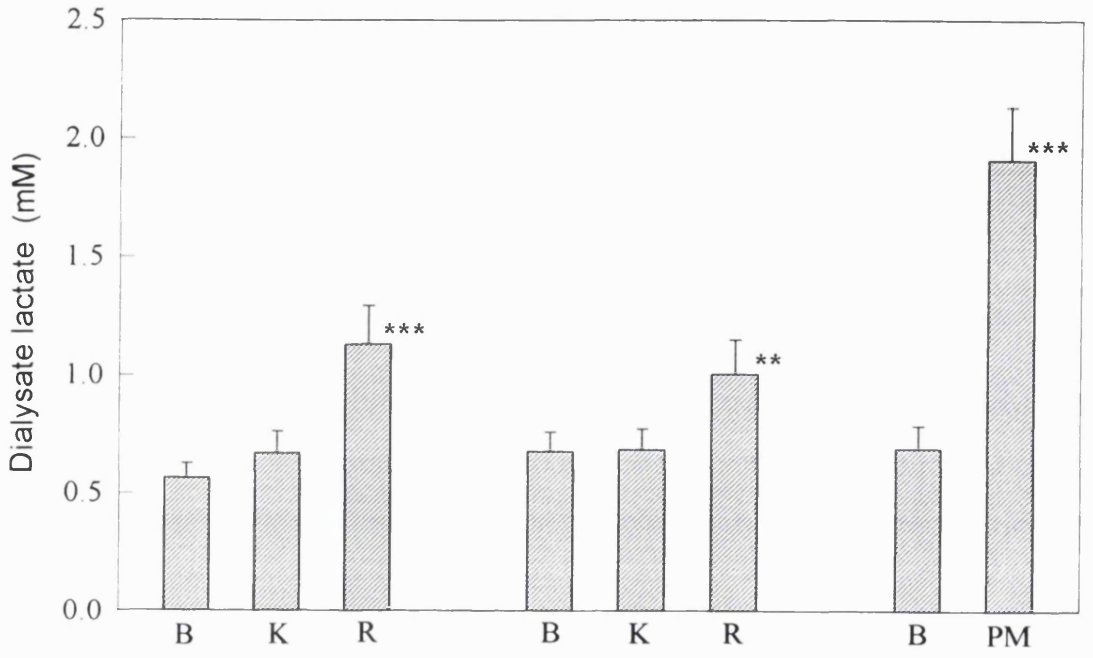


**FIG. 6.4.E** Average changes in dialysate lactate ($[lact]_d$) with application of high $K^+$-ACSF for 20 min. **B** - average concentration during 5 min before a stimulus and cardiac arrest; **K** - mean $[lact]_d$ during the 20 min stimulus, calculated from 3 values taken at 5, 12 and 19 min; **R** - level reached after perfusate was switched back to normal ACSF (i.e recovery). There was no difference between **B** and **K** for either of the two stimuli, but there was a significant difference between **K** and **R** for each challenge. The increase during the postmortem period (**PM**) was significantly higher than the preceding resting level. Values are mean $\pm$ sem, n = 12; ** $p<0.01$, *** $p<0.001$; comparison to preceding $[lact]_d$ level.

## 6.5 Inhibition of Lactate Transport with Probenecid in the Striatum

### 6.5.1 Concentration-Dependent Effect of Probenecid

Systemic Variables

Arterial blood gases, pH, and concentrations of glucose and bicarbonate were as follows: $PCO_2$, 54.9 ± 5.3 mmHg; $PO_2$, 199 ± 9 mmHg; pH, 7.34 ± 0.02; glucose, 8.3 ± 0.7 mM; bicarbonate, 28.3 ± 2.1 mM (n=8). MABP was stable throughout the experiments at 84 ± 2 mmHg.

DC Potential

Application of 1, 2 and 5 mM probenecid-ACSF through the microdialysis probe did not provoke any significant changes in the DC potential, but 10 and 20 mM probenecid-ACSF reduced the DC potential by 1.7 ± 0.1 and 2.3 ± 0.1 mV, respectively.

Dialysate Lactate

The average dialysate concentration of lactate ($[lact]_d$) during the control period was 0.38 ± 0.05 mM for all experiments (n=8). Sequential perfusion of probenecid concentration-dependently increased the basal level of dialysate lactate (Fig. 6.5.A, 6.5.B, 6.5.C and Table 6.5.A). The overall increases in $[lact]_d$ were less pronounced at higher concentrations of probenecid (Figs. 6.5.B and 6.5.C), and switching from 10 to 20 mM probenecid produced an initial decrease in $[lact]_d$ (Fig. 6.5.C).

Dialysate [lact] was higher when the concentration of probenecid-ACSF was increased in steps from 0 to 5 mM (i.e. 1, 2 and 5 mM probenecid) than with direct perfusion of 5 mM probenecid (1.5 ± 0.09; 1.07 ± 0.03, respectively; $p<0.01$), although application of 5 mM probenecid in each series increased $[lact]_d$ by the same amount (0.7 ± 0.07 and 0.77 ± 0.09 mM, respectively).

With the lower doses of probenecid (1, 2 and 5 mM) the initial rate of increase in $[lact]_d$ was greater as the probenecid concentration was increased (0.009 ± 0.002, 0.017 ± 0.001 and 0.05 ± 0.005 $mmol.l^{-1}.min^{-1}$, respectively; $p<0.01$). However, the rate of $[lact]_d$ increase was slower with 10 and 20 mM probenecid (0.012 ± 0.002 and 0.024 ± 0.006 $mmol.l^{-1}.min^{-1}$, respectively).

There was no significant difference in the time taken to reach 90 % of the final dialysate lactate concentration between probenecid concentrations tested. This level was reached approximately 15 minutes after the beginning of drug application.

Dialysate pH

In these experiments arterial blood gases, pH and concentrations of glucose and bicarbonate were as follows: $PCO_2$, 53.5 ± 2.6 mmHg; $PO_2$, 190 ± 14 mmHg; pH, 7.38 ± 0.01; glucose, 8.0 ± 0.5 mM; bicarbonate, 30.4 ± 1.4 mM (n=8). MABP remained stable at 84.0 ± 2.7 mmHg during the experiments. There was no difference between these values and those found for the parallel experiments in which $[lact]_d$ was measured.

Recording of changes in dialysate pH showed that the effects of probenecid on extracellular lactate were not associated with acidification of striatal dialysate. Only switching from 10 to 20 mM probenecid showed a tendency to reduce dialysate pH (decrease of 0.22 ± 0.09 pH unit; $p<0.01$).

---

## Effect of Probenecid

### Major Findings

- Probenecid concentration-dependently increased the dialysate concentration of lactate without associated extracellular acidosis.

---

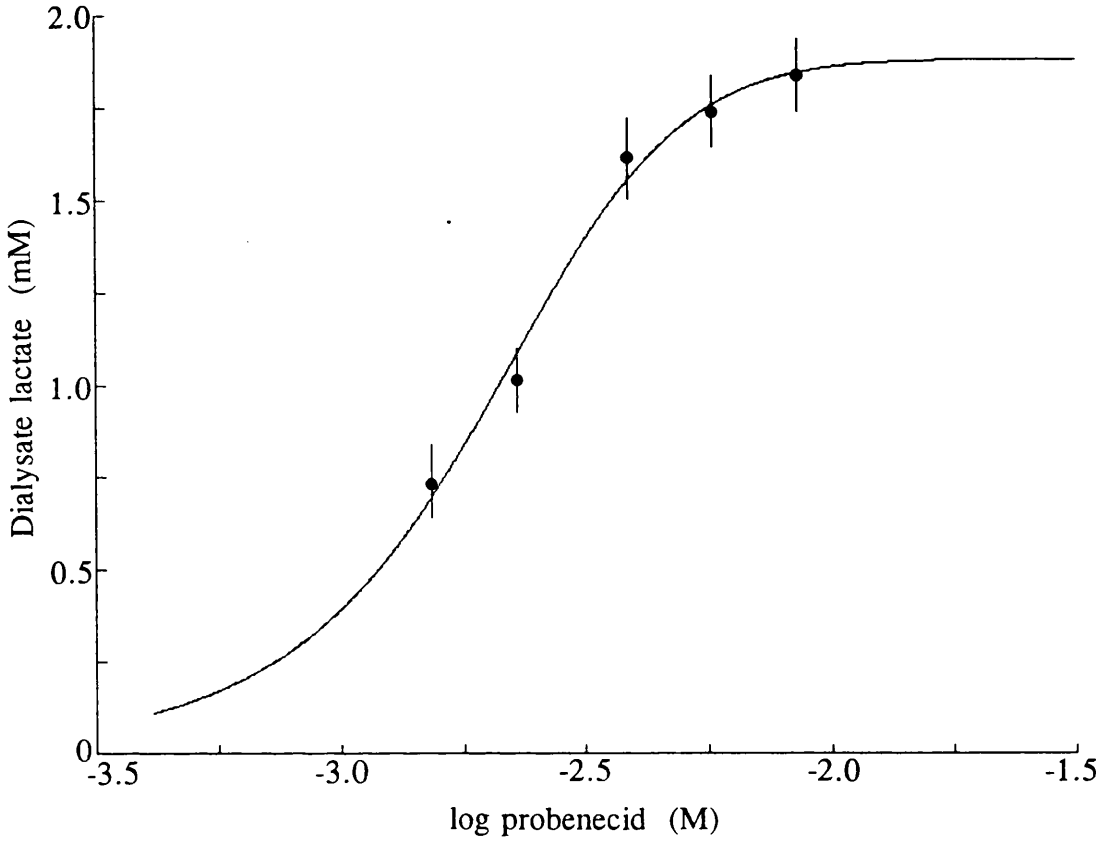


**FIG. 6.5.A** Logarithm concentration-response curve for probenecid. Values for each probenecid concentration are mean ± sem of the experiments from both series (i.e. 1, 2, 5, and 5, 10, 20 mM probenecid-ACSF; n=8). Logarithm concentration-response relationships were fitted by the Gauss-Newton method (ASYST, Keithley, Reading, U.K.) to the function:

$$y = \frac{R_{max}}{1 + (\log \text{"}EC_{50}\text{"}/\log x)^n}$$

where: x is the dialysate concentration of probenecid producing responses amplitude y; $R_{max}$ is the maximal increase in dialysate lactate (equal to 1.51 mM); "$EC_{50}$" is the estimated $EC_{50}$ (i.e. probenecid concentration in the ACSF producing half-maximal response, equal to 2 mM); and n is the slope parameter.

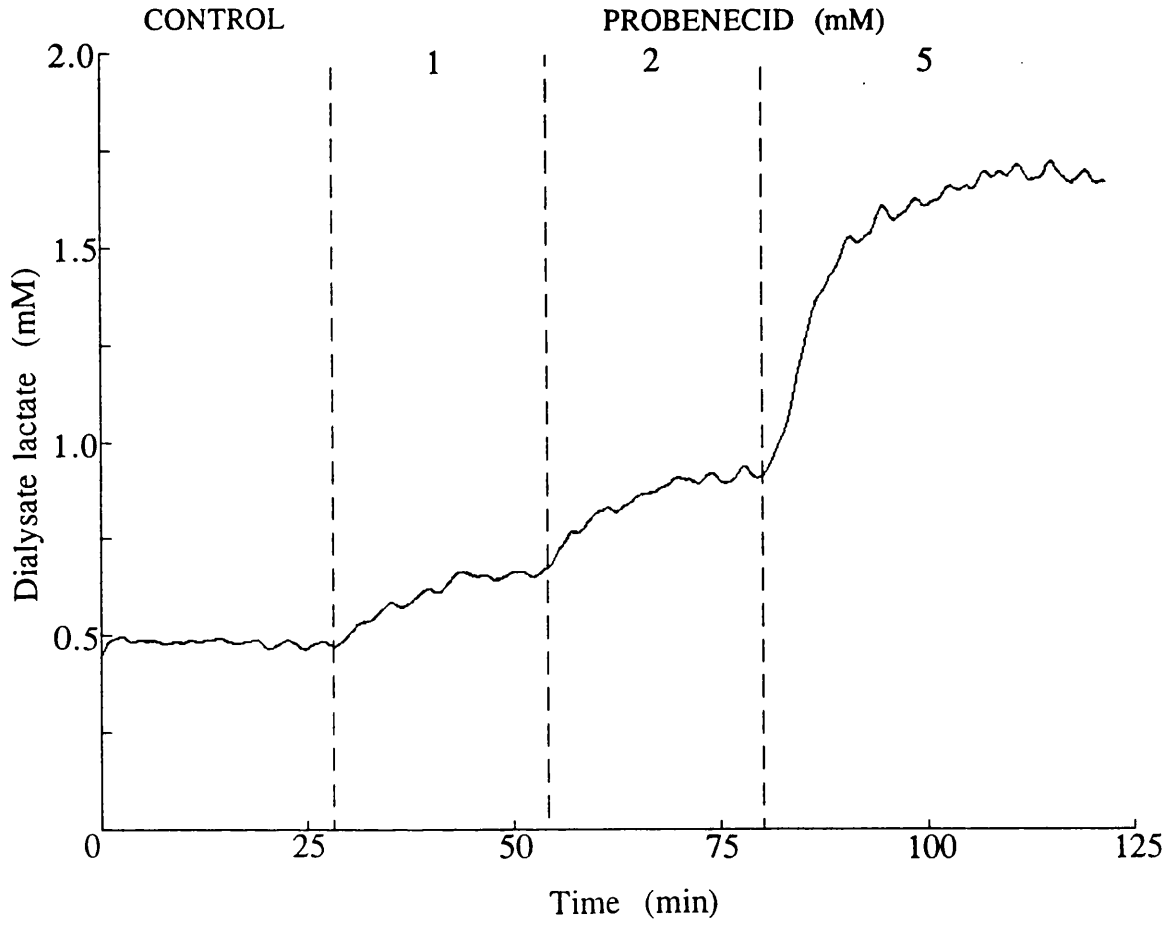


**FIG. 6.5.B** Representative changes in $[lact]_d$ associated with the sequential perfusion of probenecid-ACSF (1, 2 and 5 mM). Probenecid concentration-dependently increased the basal level of $[lact]_d$. Dashed lines indicate periods of perfusion of each concentration of probenecid-ACSF.

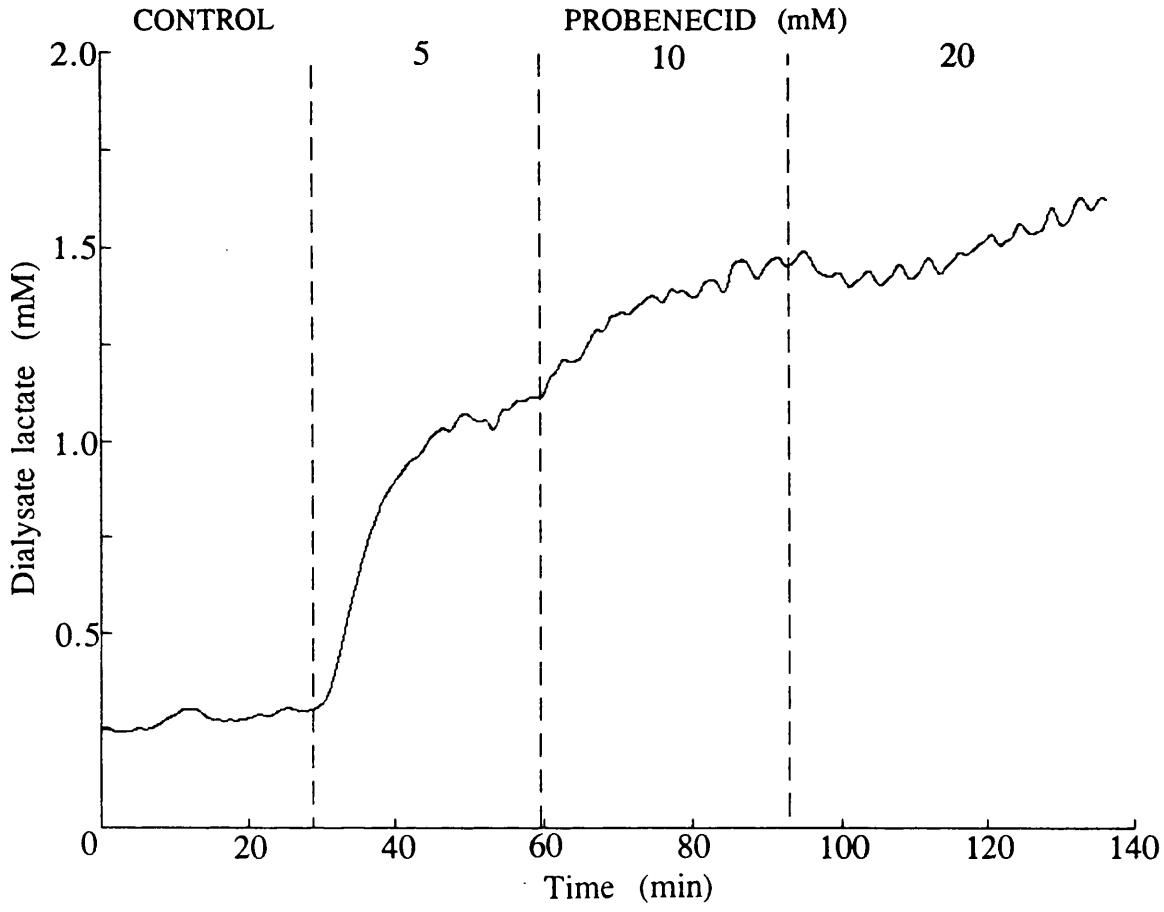


**FIG. 6.5.C** Representative changes in $[lact]_d$ associated with the sequential perfusion of probenecid-ACSF (5 , 10 and 20 mM). Perfusion of 5 mM probenecid markedly increased $[lact]_d$, but with subsequent perfusion of 10 and 20 mM probenecid the overall increases were less significant. Dashed lines indicate periods of perfusion of each concentration of probenecid-ACSF.

| | PROBENECID | | |
|---|---|---|---|
| **CONTROL** | **1 mM** | **2 mM** | **5 mM** |
| 0.45 ± 0.09 | 0.59 ± 0.08 | 0.81 ± 0.08 | 1.5 ± 0.09 |

| | PROBENECID | | |
|---|---|---|---|
| **CONTROL** | **5 mM** | **10 mM** | **20 mM** |
| 0.31 ± 0.04 | 1.07 ± 0.03 | 1.39 ± 0.08 | 1.47 ± 0.11 |

**TABLE 6.5.A** Average changes in $[lact]_d$ with sequential probenecid perfusion in the two series of experiments (1, 2 and 5 mM, and 5, 10 and 20 mM probenecid-ACSF). Values are mM ± sem (n=4 in each series).

### 6.5.2 Recovery from Probenecid Application

Dialysate Lactate in the Striatum

Perfusion of 5 mM probenecid-ACSF produced a marked increase in $[lact]_d$. With the perfusion of normal ACSF, $[lact]_d$ decreased steadily and after approximately 25 min returned to the basal level (Fig. 6.5.D). Subsequent perfusion of 20 mM probenecid-ACSF produced a larger increase in $[lact]_d$, from where it gradually decreased returning to basal level with perfusion of normal ACSF.

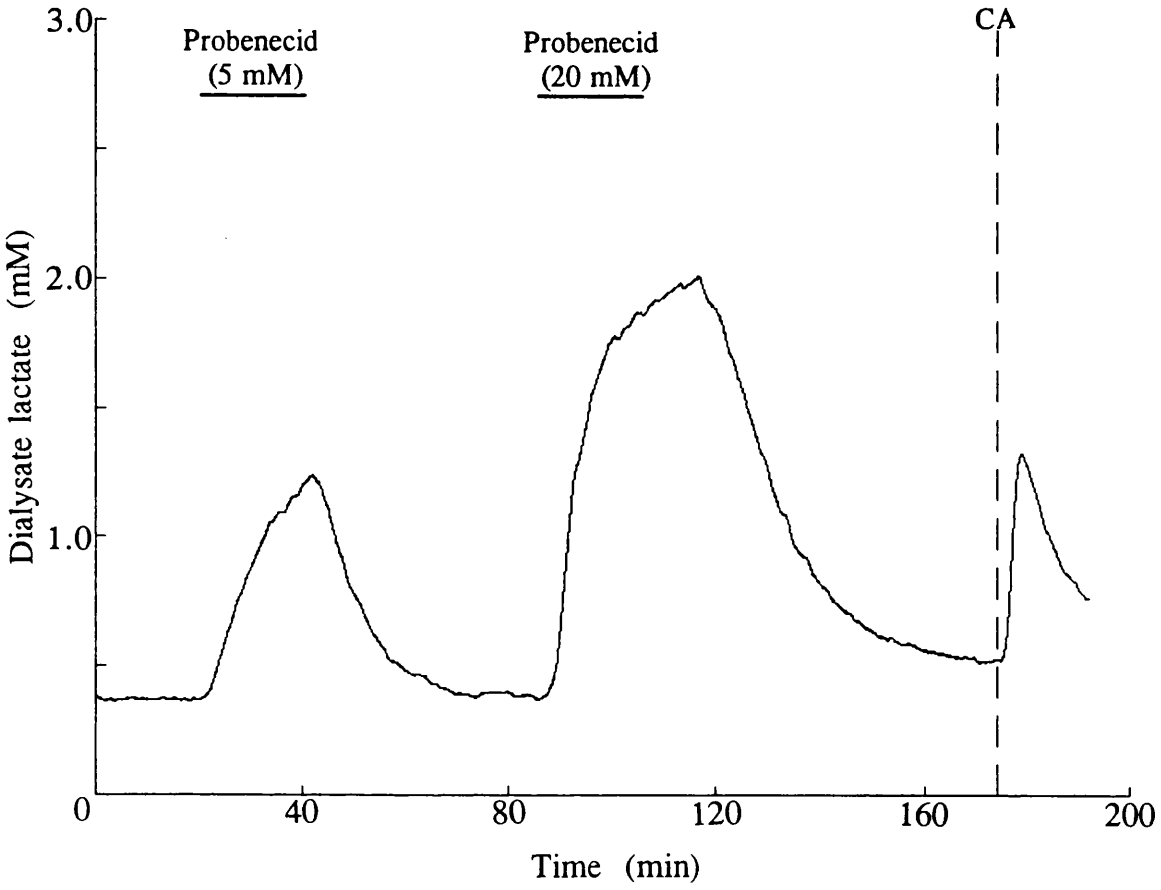


**FIG. 6.5.D** Changes in $[lact]_d$ with successive 20-min perfusions of probenecid-ACSF (5 and 20 mM) from a single representative experiment. The horizontal lines at the top of the figure indicate periods of probenecid-ACSF perfusion. Dashed line (CA) indicates cardiac arrest.

### 6.5.3 Effect of Probenecid on Lactate Changes with High Extracellular $K^+$ and Spreading Depression Initiation

Systemic Variables

In this series, blood gases, pH, glucose and bicarbonate concentrations were as follows: $P_{CO_2}$, 50 ± 2 mmHg; $P_{O_2}$, 212 ± 24 mmHg; pH, 7.36 ± 0.006; glucose, 8.1 ± 0.4 mM; bicarbonate, 27.1 ± 0.9 mM (n=27). MABP was stable throughout the experiments at 88 ± 2 mmHg.

Effects of $K^+$ on the DC Potential

Application of high $K^+$ consistently produced a sustained negative shift of the DC potential (Fig. 6.5.E). The amplitude of this shift gradually increased with the concentration of $K^+$ applied, although there was no significant difference between 100 and 125 mM $K^+$ (mean amplitude 16.2 ± 0.6 and 18.4 ± 1.1 mV respectively, $p>0.05$).

Superimposed onto the sustained negative shift were peaks of further depolarisation (Fig. 6.5.E), each peak corresponding to the elicitation of a wave of SD (Obrenovitch et al., 1993). The number of peaks elicited increased with the $K^+$ concentration (Fig. 6.5.F), without any significant change in amplitude (mean amplitude 9.6 ± 0.4 mV, n=24). Measurement of the SD cumulative peak areas (Fig. 6.5.G) confirmed a more intense elicitation of SD with increasing $K^+$. When normal ACSF was reperfused, the DC potential returned to a level comparable to that of the control within 20 min (Fig. 6.5.E).

Effects of $K^+$ on Dialysate Lactate

Changes in $[lact]_d$ were markedly influenced by those in DC potential (Fig. 6.5.A; see Section 6.4). When a transient depolarisation occurred during the first $K^+$-stimulus, there was a transient increase in $[lact]_d$ (Fig. 6.5.H; see Fig. 6.4.B). Multiple depolarisations, seen more frequently with 125, 140 and 160 mM $K^+$-ACSF, produced a sustained increase in $[lact]_d$ starting with the initial decrease in the DC potential (Fig. 6.5.E). This increase in $[lact]_d$ was not altered with varying $K^+$ concentration (mean increase 0.18 ± 0.02, n=15).

During recovery, as repolarisation occurred, a large increase in $[lact]_d$ was consistently observed, lasting for approximately 15 min, before returning to basal level (Fig. 6.5.E). The magnitude of the $[lact]_d$ increase during the DC potential recovery was

independent of the $K^+$ concentration applied (0.36 ± 0.02 mM, n=15). The rate of increase in $[lact]_d$ after the $K^+$-stimulus was much faster than its rate of decrease (0.2 ± 0.01, 0.06 ± 0.02 $mmol.l^{-1}.min^{-1}$, respectively; $p<0.001$; n=15).

Effects of Probenecid on $K^+$-Induced SD Changes in Dialysate Lactate and the DC Potential

As in the previous series, probenecid, 5 and 20 mM in the perfusion medium produced a marked, progressive increase in $[lact]_d$, which reached plateau levels of 1.18 ± 0.06 and 1.55 ± 0.1 mM, respectively. The DC potential was not affected by the perfusion of 5 mM probenecid-ACSF, but with application of 20 mM there was a decrease of 3.9 ± 0.5 mV.

High $K^+$-ACSF with probenecid evoked the characteristic sustained negative shift in the DC potential, but the amplitude of this shift did not increase with $K^+$ concentrations, as observed with the first challenge without probenecid. In the presence of 5 mM probenecid, instead of an increase, high $K^+$ produced a reduction of $[lact]_d$ levels to 0.78 ± 0.07 mM ($p<0.001$; comparison to the level preceding the second $K^+$ challenge). With 20 mM probenecid, as with the lower dose of probenecid, application of $K^+$ reduced $[lact]_d$ (to 1.14 ± 0.09 mM; $p<0.0001$). The decrease in $[lact]_d$ was not affected by changes in $K^+$ in concentration and was higher with 20 mM probenecid than with the lower dose (0.45 ± 0.02, 0.4 ± 0.04, respectively; $p<0.01$). During the challenge, $[lact]_d$ remained stable until repolarisation occurred, at which point it increased to a level similar to that before the challenge (Fig. 6.5.E).

The number of peaks of depolarisation was reduced with 5 mM probenecid at all $K^+$ concentrations (Fig. 6.5.F), as was the cumulative area of SD peaks (Fig. 6.5.G). Probenecid at 20 mM completely abolished SD elicitation. When a spike of depolarisation occurred in the presence of 5 mM probenecid, there was no corresponding increase in $[lact]_d$ of the type observed after depolarisation during the control stimulus (Fig. 6.5.H). The large increase in $[lact]_d$ consistently observed with repolarisation after the control stimulus was absent in the presence of probenecid.

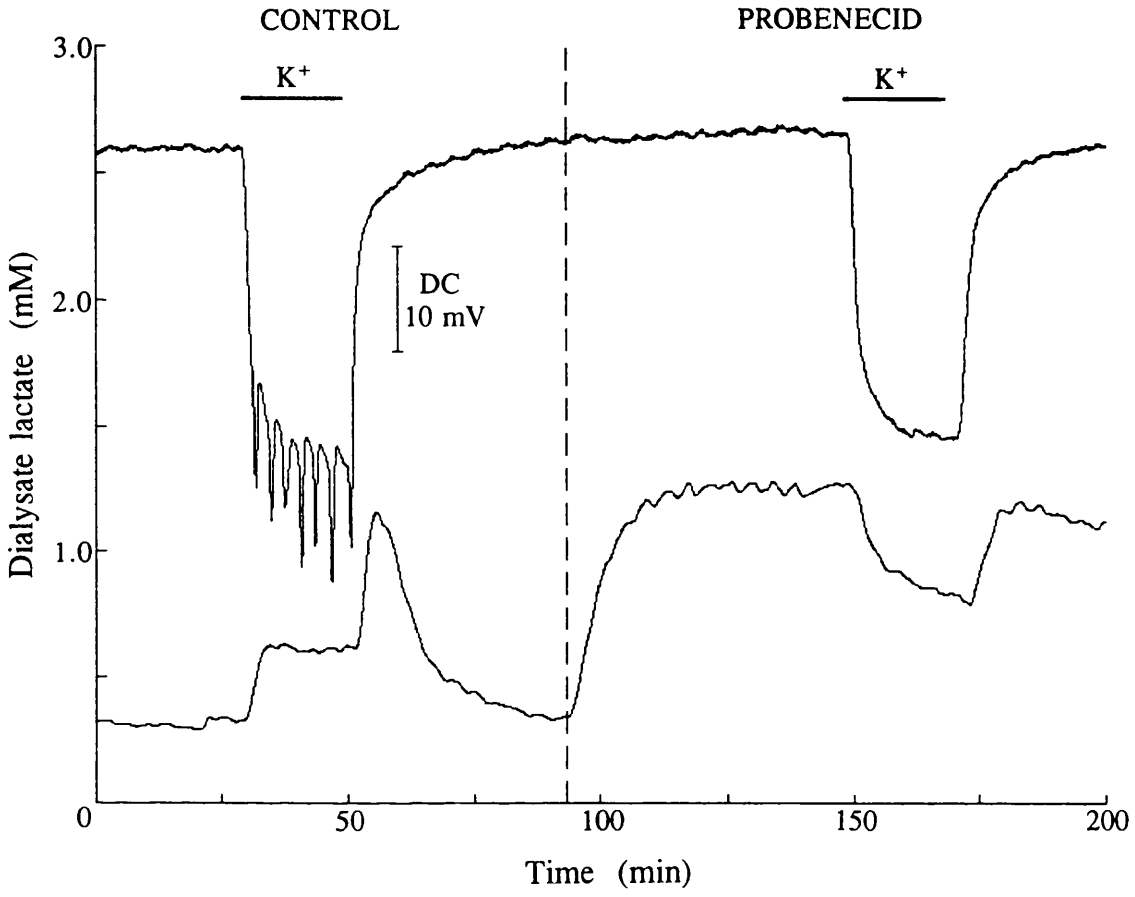


**FIG. 6.5.E** Representative changes in $[lact]_d$ (lower trace) and DC potential (upper trace) with the application of high $K^+$-ACSF (160 mM) for 20 min, with and without 5 mM probenecid. Probenecid was applied 50 min before the second $K^+$-stimulus (dashed line). The horizontal lines at the top of the figure ($K^+$) indicate periods of high $K^+$ stimulation. In the first challenge multiple depolarisations produced a sustained increase in $[lact]_d$, with a further increase with repolarisation. In the presence of probenecid, instead of an increase, high $K^+$-ACSF produced a reduction in $[lact]_d$. With repolarisation, $[lact]_d$ increased to a level similar to that preceding the challenge.

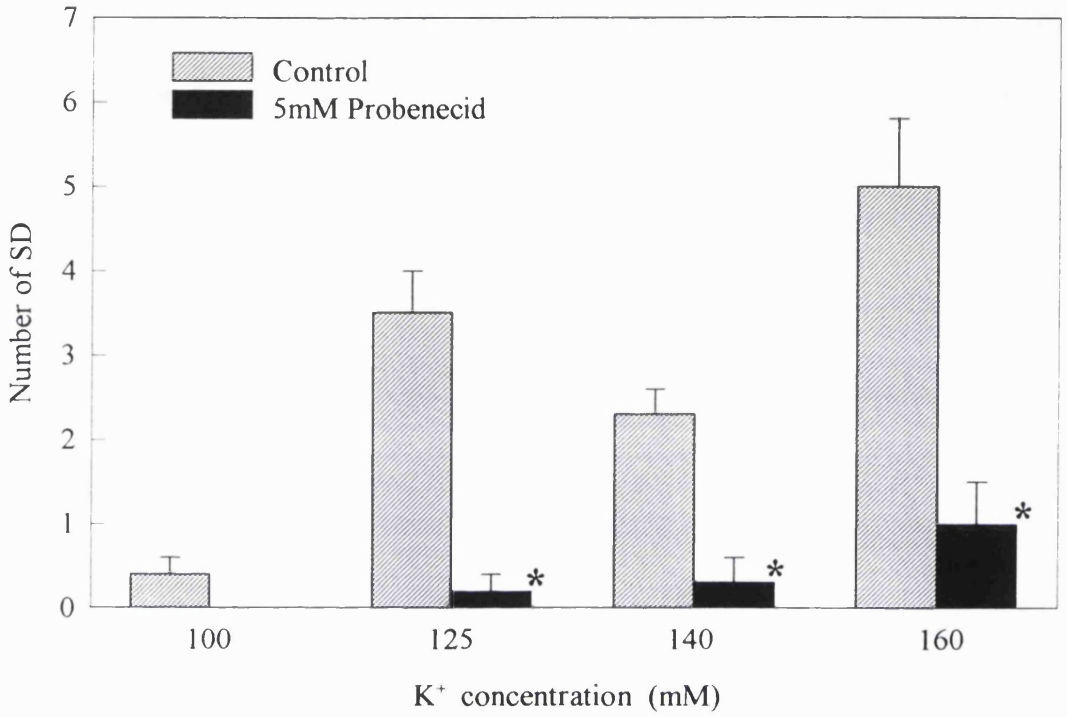


**FIG. 6.5.F** Average number of peaks of depolarisation (SD) with increasing concentrations of $K^+$-ACSF (hatched columns) and the inhibition by 5 mM probenecid (solid columns). Columns represent mean $\pm$ sem. * $p < 0.05$ comparison to control level of same $K^+$ concentration.

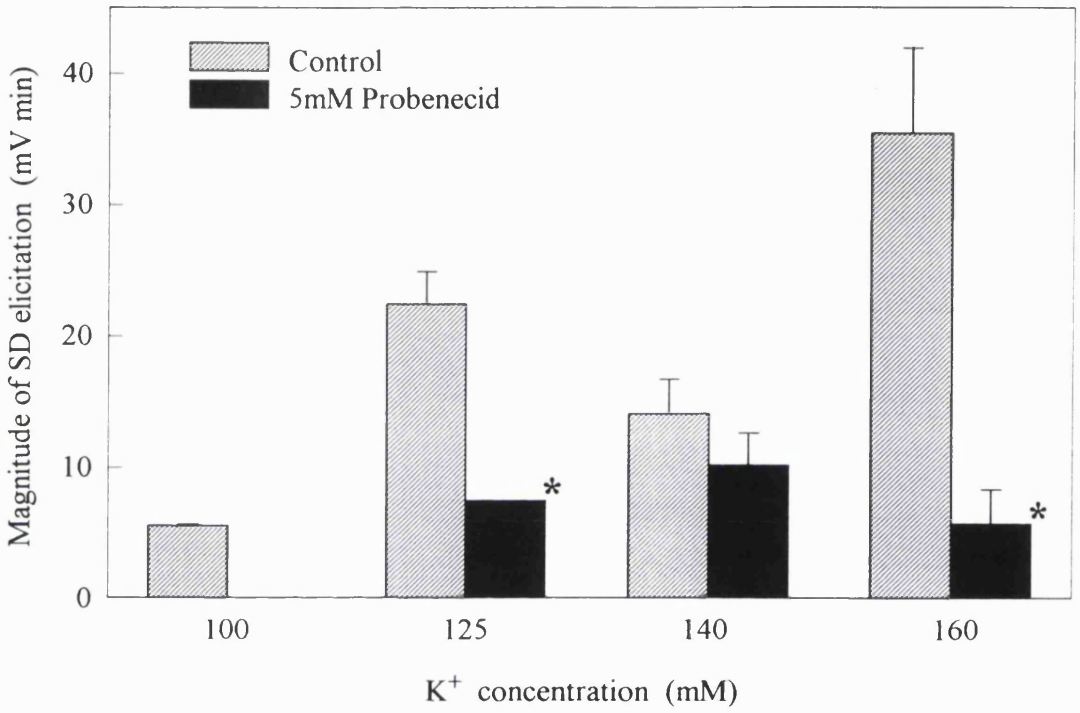


**FIG. 6.5.G** Comparison of the magnitude of SD elicitation (derived from the measurement of cumulative peak area; see Fig. 6.4.A) between control (hatched columns) and 5 mM probenecid (solid columns). Columns represent mean ± sem, * $p < 0.05$ comparison to control level of same $K^+$ concentration.

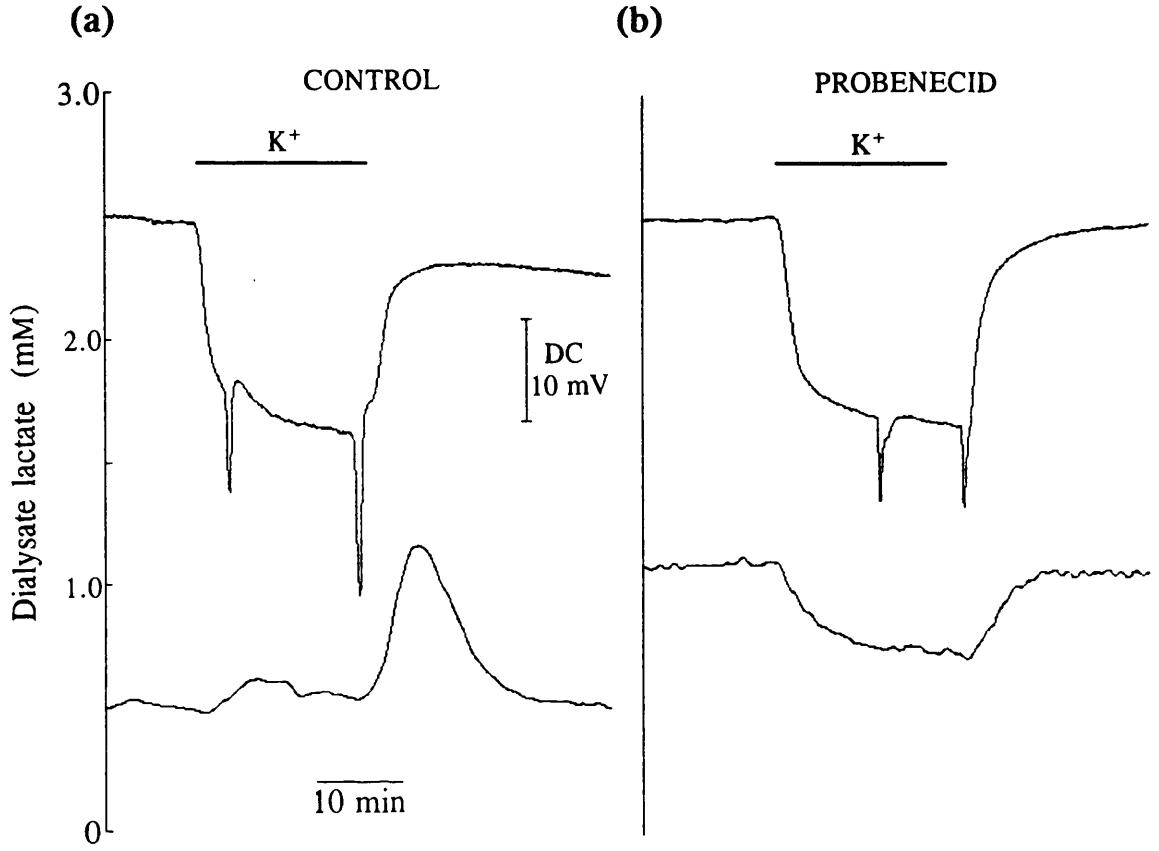


**FIG. 6.5.H** Changes in $[lact]_d$ (lower trace) and the DC potential (upper trace) when the application of high $K^+$-ACSF (160 mM) for 20 min evoked two peaks of SD during the stimulus. **(a)** control challenge (normal $K^+$-ACSF), **(b)** 5 mM probenecid $K^+$-ACSF. These data are from a single, representative experiment. Probenecid markedly altered the pattern of changes in $[lact]_d$ associated with high $K^+$. When spikes of depolarisation occurred in the presence of probenecid there was no corresponding increase in $[lact]_d$ as observed after depolarisation during the control stimulus.

Mean changes in $[lact]_d$ with application of high $K^+$ with 5 and 20 mM probenecid are summarised in Fig. 6.5.1. In the absence of probenecid, there were significant $[lact]_d$ increase both during and after the $K^+$-stimulus. With both concentrations of probenecid-ACSF, instead of an increase, high $K^+$ produced a decrease in $[lact]_d$ during the $K^+$-stimulus (K). The marked $[lact]_d$ increase associated with repolarisation was absent with probenecid, and $[lact]_d$ returned to a level (R) similar to that preceding the $K^+$-stimulus (B). Post-mortem changes showed a small increase in $[lact]_d$ with 5 mM probenecid which was absent with 20 mM.

---

## $K^+$-Induced Spreading Depression

### Major Findings

- Probenecid markedly reduced both the number of SD elicited and their magnitude.
- Probenecid significantly altered the pattern of $[lact]_d$ changes associated with high $K^+$:
  - there were no increases in $[lact]_d$ during periods of repolarisation (i.e. after each depolarisation or after the $K^+$-stimulus).

---

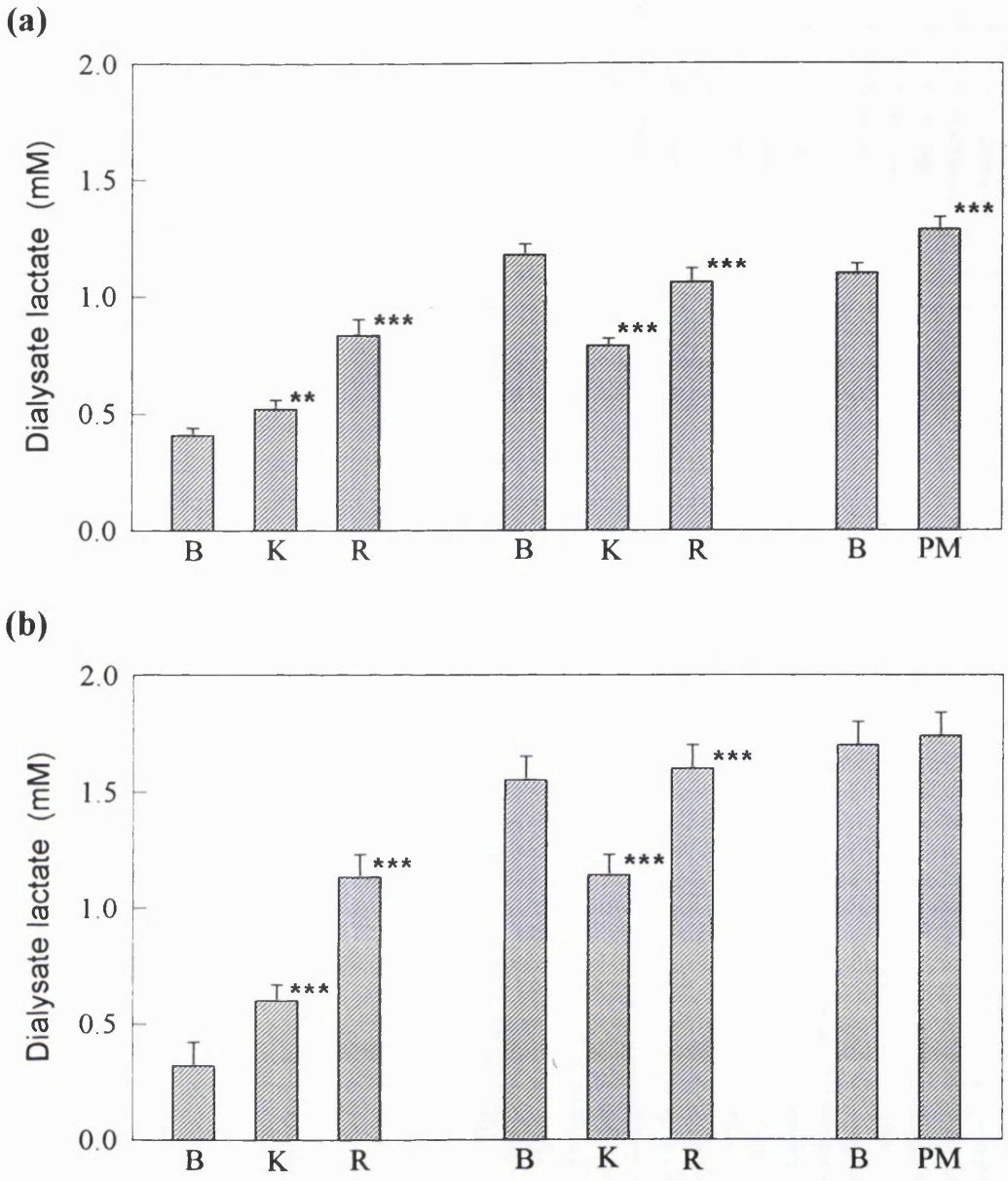


**FIG. 6.5.I** Average changes in $[lact]_d$ with the application of high $K^+$-ACSF for 20 min, with and without either **(a)** 5 mM probenecid (n=20), or **(b)** 20 mM probenecid (n=7). Since the different $[K^+]$ used to trigger SD did not alter $[lact]_d$, all experiments with 5 mM probenecid were averaged. **B** - mean $[lact]_d$ during 5 min before a stimulus and cardiac arrest; **K** - mean $[lact]_d$ during a 20 min $K^+$-stimulus, calculated from values taken at 5, 12 and 19 min; **R** - level reached after perfusate was switched back to normal ACSF; **PM** - post-mortem period. Both concentrations of probenecid produced similar changes in $[lact]_d$ associated with high $K^+$-ACSF, except in the presence of 20 mM probenecid the increase in $[lact]_d$ observed post-mortem with 5 mM was absent. Values are mean $\pm$ sem; ** $p<0.01$, *** $p<0.001$; comparison to preceding $[lact]_d$ level.

### 6.5.4 Effect of Probenecid on Lactate Changes During Terminal Complete Ischaemia (Cardiac Arrest)

Systemic Variables

Arterial blood gases, pH and concentrations of glucose and bicarbonate were as follows: $PCO_2$, 55.8 ± 2.4 mmHg; $PO_2$, 165 ± 6 mmHg; pH, 7.33 ± 0.01; glucose, 7.9 ± 0.3 mM; bicarbonate, 28.5 ± 0.8 mM (n=23). MABP was stable during the experiments at 84 ± 2 mmHg.

Dialysate Lactate

In this series, $[lact]_d$ remained stable throughout the control period with normal ACSF, and the basal lactate level was 0.61 ± 0.07 mM. As in the previous series, probenecid, 5 and 20 mM, increased basal $[lact]_d$ in a concentration-dependent manner (to 1.02 ± 0.04 mM and 1.7 ± 0.1 mM, respectively). With normal ACSF, terminal complete ischaemia produced an immediate and rapid increase in $[lact]_d$ to 2.05 ± 0.2 mM (an increase of 1.3 ± 0.2 mM, n=12; Fig. 6.5.J). This change was significantly reduced by 5 mM probenecid ($p<0.05$; comparison to pre-ischaemic level) where $[lact]_d$ increased by 0.2 ± 0.04 mM ($p<0.01$; compared to increase with normal ACSF, n=5). With 20 mM probenecid the ischaemia-induced increase of $[lact]_d$ was abolished. The rate of $[lact]_d$ increase with ischaemia was faster with normal ACSF than with 5 mM probenecid-ACSF (0.36 ± 0.03, 0.15 ± 0.01 $mmol.l^{-1}.min^{-1}$ respectively; $p<0.001$, n=7). After 30 min post-mortem, the level of $[lact]_d$ with normal ACSF had decreased, but remained higher than the pre-ischaemic level. With probenecid (5 and 20 mM) $[lact]_d$ decreased rapidly reaching a level that was significantly lower than the pre-ischaemic concentration.

---

**Terminal Complete Ischaemia (Cardiac Arrest)**

**Major Findings**

- Probenecid inhibited the efflux of lactate associated with terminal complete ischaemia.

---

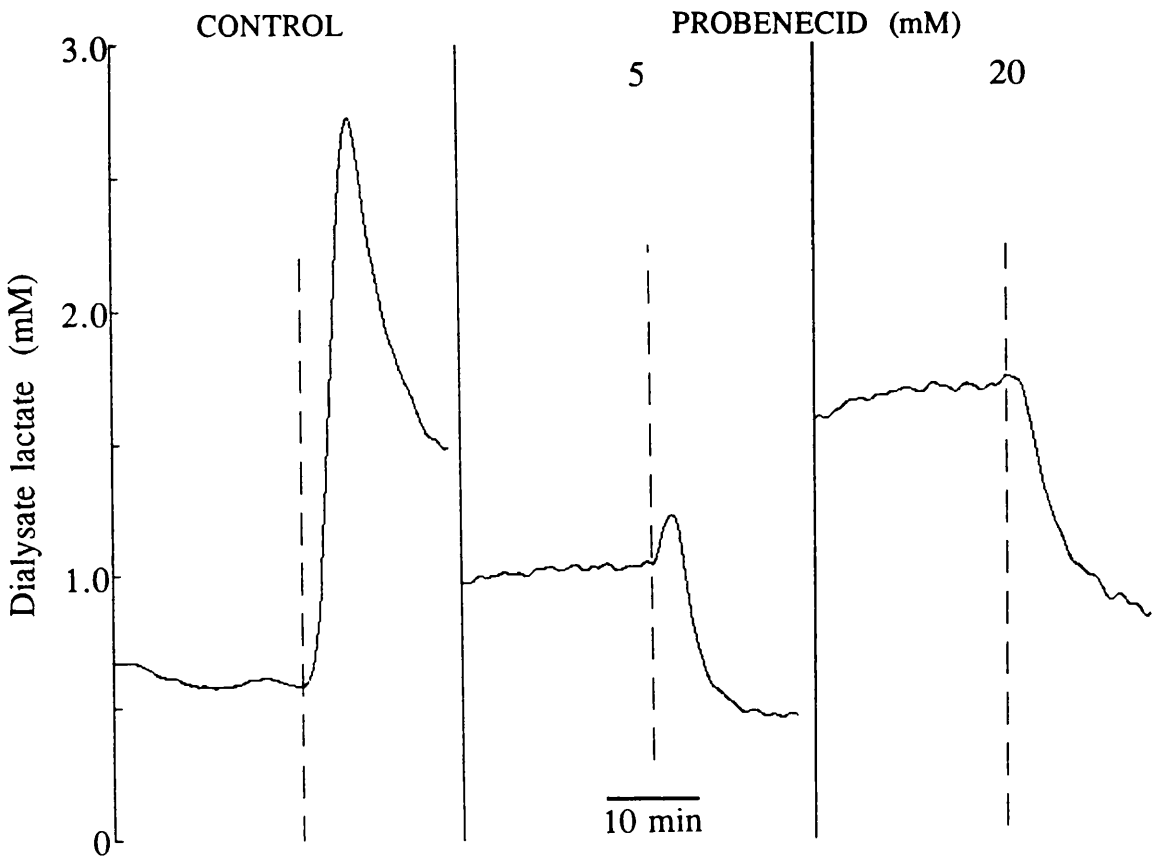


**FIG. 6.5.J** Representative changes in $[lact]_d$ during terminal ischaemia produced by cardiac arrest (dashed lines) under control conditions (normal ACSF) and in the presence of 5 and 20 mM probenecid-ACSF.

### 6.5.5 Effect of Probenecid on Lactate Changes During Transient Forebrain Ischaemia

Systemic Variables

Arterial blood gases, pH, and concentrations of glucose and bicarbonate were as follows: $P_{CO_2}$, 36.7 ± 2.7 mmHg; $P_{O_2}$, 201 ± 12 mmHg; pH, 7.41 ± 0.02; glucose, 5.7 ± 0.4 mM; bicarbonate, 22.5 ± 2.0 mM (n=11).

MABP remained stable throughout the control period at 102 ± 3 mmHg (n=10). Forebrain ischaemia produced a rapid increase in MABP to 136 ± 5 mmHg ($p<0.001$; comparison to pre-ischaemic level). In some experiments (n=4) this increase persisted except for a small decline, but MABP still remained higher than pre-ischaemic levels throughout the rest of the ischaemic period (Fig. 6.5.K). With the start of reperfusion, there was a sudden transient decrease in MABP to a level comparable to that before ischaemia (116 ± 5 mmHg). In the remaining 5 experiments, MABP stayed high for the first five minutes of ischaemia, from where it decreased to 62.8 ± 11.4 mmHg (Fig. 6.5.L) and remained at this low level until the end of ischaemia. With reperfusion there was a slow progressive recovery of MABP. In all cases, after 80-min reperfusion MABP reached a stable level of 113 ± 5 mmHg (n=10).

DC Potential and EEG

Application of probenecid-ACSF (20 mM) induced a decrease in the DC potential of 5.2 ± 0.7 mV ($p<0.001$), followed by partial normalisation whilst probenecid was still being applied. Anoxic depolarisation occurred within the first minutes of forebrain ischaemia. The amplitude of this depolarisation was greatly reduced in comparison to experiments in which normal ACSF was perfused throughout ischaemia (Section 6.1.1; 12.4 ± 1.75 and 18.1 ± 1.1 mV, respectively; $p<0.01$). With reperfusion, in cases where MABP remained elevated during the ischaemic insult, repolarisation occurred within 2 minutes and was preceded by a sudden transient decrease in the DC potential. (Fig. 6.5.K). In the other cases, where MABP recovery was slow, repolarisation was delayed (Fig. 6.5.L). Terminal complete ischaemia produced anoxic depolarisation (negative shift in the DC potential of 19.9 ± 1.1) within 2 minutes.

Application of probenecid did not alter the EEG. With forebrain ischaemia EEG amplitude was significantly reduced. During reperfusion, EEG recovery occurred but after 80 min it had only reached 32.4 ± 3.2 % of the control value. The presence of

probenecid in the perfusate did not seem to alter the extent of EEG recovery after 80-min reperfusion (32.4 ± 3.2 and 26.6 ± 4.2 %; with 20 mM probenecid-ACSF and normal ACSF, respectively).

Dialysate Lactate

Pre-ischaemic $[lact]_d$ was 0.6 ± 0.09 (n=10). With perfusion of 20 mM probenecid, there was an initial rapid increase to 1.91 ± 0.09 and, after 50 min, $[lact]_d$ reached a plateau level of 2.08 ± 0.1 (Figs. 6.5.K and 6.5.L). In these conditions, forebrain ischaemia produced a rapid decrease in $[lact]_d$ to 1.13 ± 0.07 mM ($p<0.001$; compared to level preceding ischaemia) at 0.14 ± 0.008 $mmol.l^{-1}.min^{-1}$. This low level persisted until reperfusion, when $[lact]_d$ increased to a level higher than that before ischaemia (2.47 ± 0.08 mM, $p<0.001$), at a rate slower than its decrease (0.092 ± 0.01 $mmol.l^{-1}.min^{-1}$, $p<0.01$). Then $[lact]_d$ steadily decreased and after 60 min had returned to a level comparable to the level before ischaemia (Fig. 6.5.K). In cases where repolarisation after ischaemia was delayed, $[lact]_d$ recovery was slower (Fig. 6.5.L). At the end of 80-min reperfusion $[lact]_d$ was 1.95 ± 0.11 mM.

Cardiac arrest produced a small increase in $[lact]_d$ of 0.11 ± 0.02 ($p<0.001$) at 0.038 ± 0.005 $mmol.l^{-1}.min^{-1}$, from where it decreased at a rate faster than the increase (0.58 ± 0.005 $mmol.l^{-1}.min^{-1}$, $p<0.01$). It is interesting to note that in other experiments cardiac arrest, following the perfusion of 20 mM probenecid-ACSF, was not associated with an increase in $[lact]_d$.

Reducing the probenecid concentration to 5 mM revealed a similar pattern of changes in $[lact]_d$ during forebrain ischaemia (Fig. 6.5.M). However, with the onset of ischaemia a rise in $[lact]_d$ preceded its decrease, and the $[lact]_d$ increase with reperfusion was more pronounced. Cardiac arrest produced a larger rise in $[lact]_d$ than that observed with 20 mM probenecid.

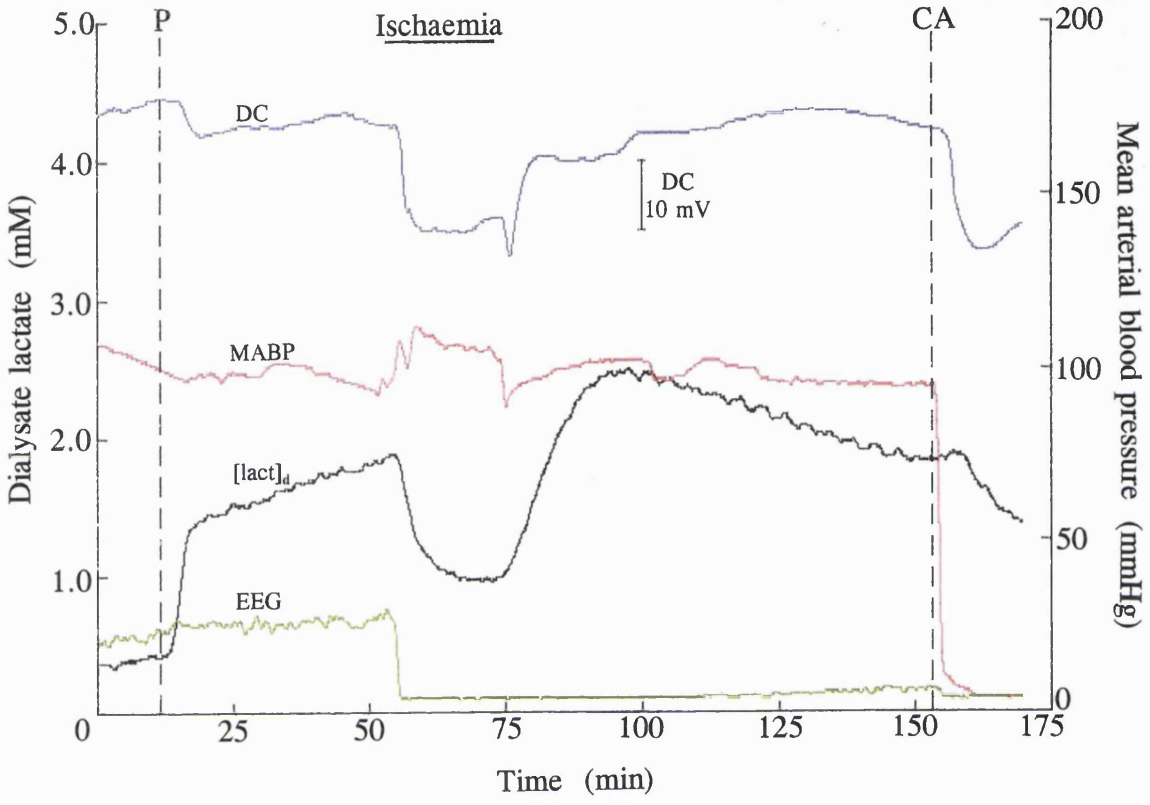


**FIG. 6.5.K** Effects of 20 mM probenecid on $[lact]_d$, DC potential, MABP and EEG in the striatum during transient forebrain ischaemia (top horizontal line) and reperfusion. Probenecid (dashed line P indicates start of drug perfusion) markedly increased basal levels of $[lact]_d$, but totally inhibited the initial increase which preceded anoxic depolarisation in experiments without probenecid perfusion (see Fig. 6.1.A). In contrast, $[lact]_d$ decreased from the onset of ischaemia and remained at a low level throughout the insult. Reperfusion was associated with an increase in $[lact]_d$, which after 80 min, reached a similar level to that observed immediately before ischaemia. Cardiac arrest (dashed line CA) produced a small increase in $[lact]_d$.

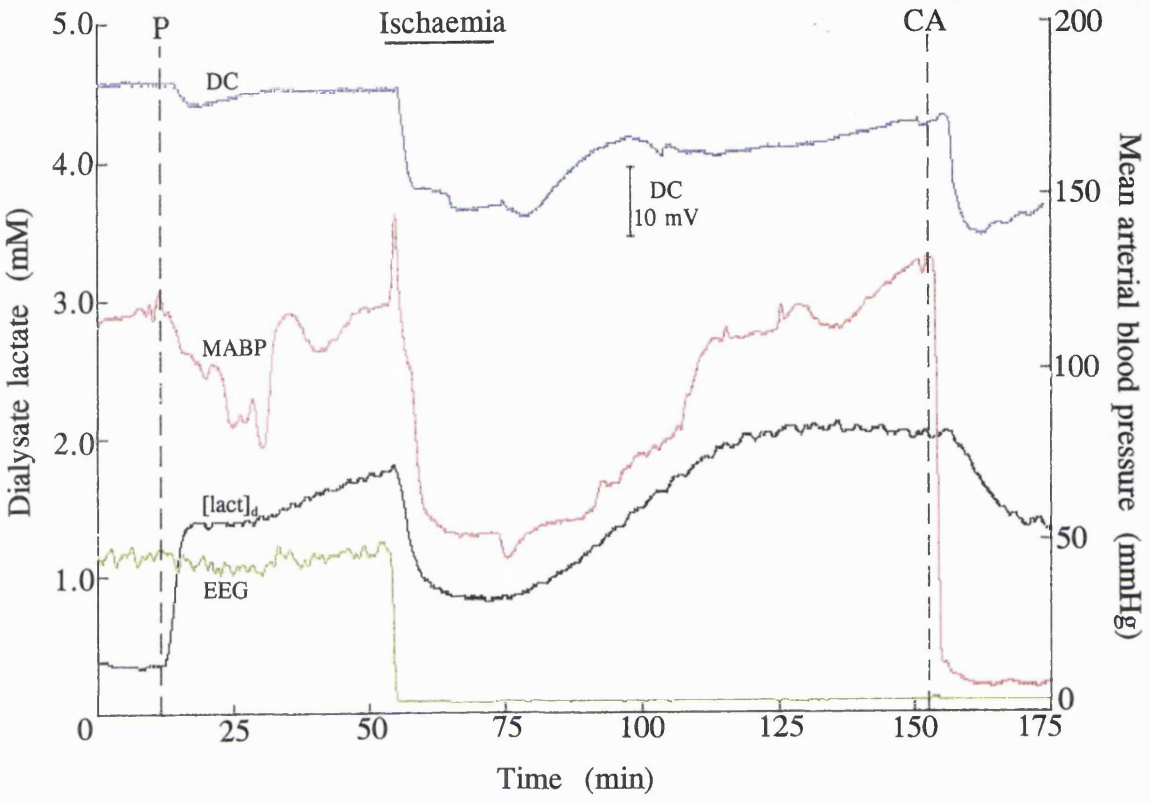


**FIG. 6.5.L** Effects of 20 mM probenecid on $[lact]_d$, DC potential, MABP and EEG in the striatum during transient forebrain ischaemia (top horizontal line) and reperfusion when repolarisation did not occur with the start of reperfusion but was delayed. In this case the return of $[lact]_d$ to pre-ischaemic levels was gradual. Dashed vertical lines P and CA indicate the start of probenecid-ACSF perfusion and cardiac arrest, respectively.

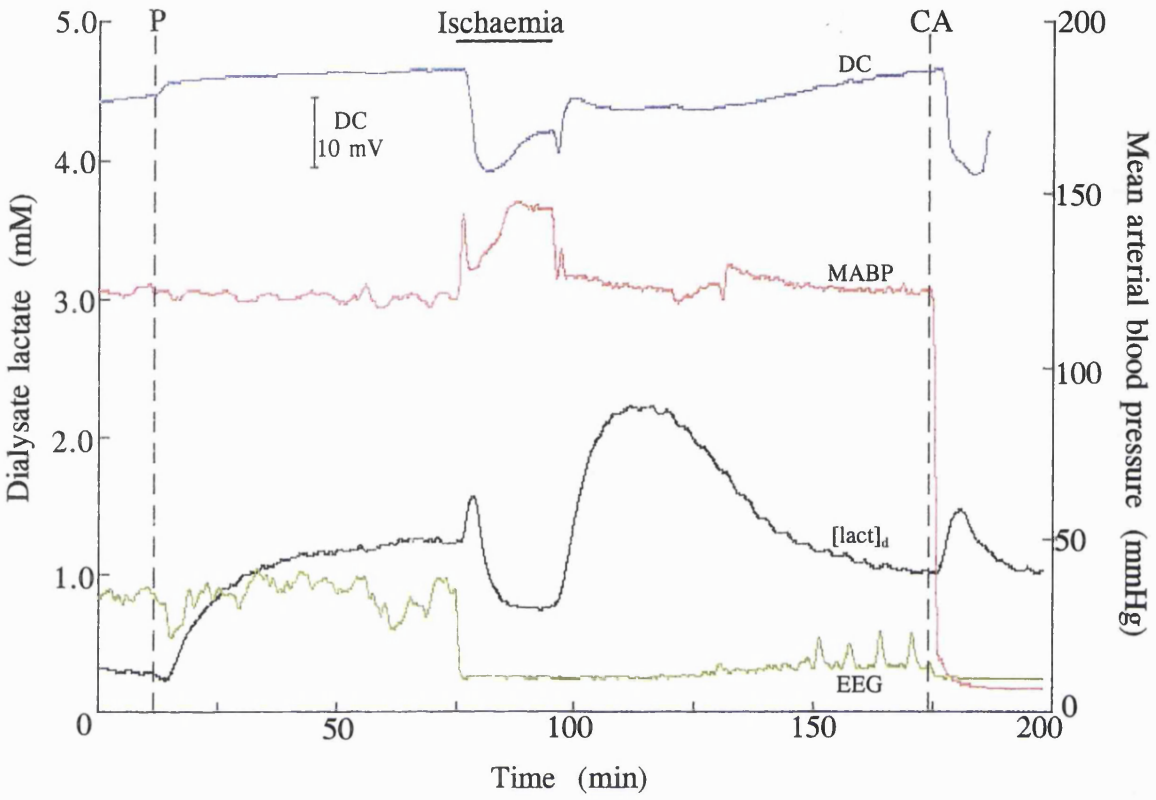


**FIG. 6.5.M** Effects of 5 mM probenecid on $[lact]_d$, DC potential, MABP and EEG in the striatum during transient forebrain ischaemia (top horizontal line) and reperfusion. The pattern of changes in $[lact]_d$ with 5 mM probenecid were similar to those with 20 mM, but the decrease in $[lact]_d$ with the onset of ischaemia was preceded by a small increase. A similar increase was also observed with cardiac arrest. Dashed vertical lines P and CA indicate start of probenecid-ACSF perfusion and cardiac arrest, respectively.

## Transient Forebrain Ischaemia

### Major Findings

- Probenecid significantly altered the pattern of $[lact]_d$ changes associated with transient forebrain ischaemia:
  - the rise in $[lact]_d$ with the onset of ischaemia was absent.
  - with reperfusion there was no marked increase in $[lact]_d$ in comparison to the pre-ischaemic level.

# CHAPTER 7 DISCUSSION

## 7.1 Basal Conditions

In all series of experiments, averages of arterial blood gases, pH, concentration of bicarbonate and glycaemia were within the range expected for normoxic/normocapnic and normoglycaemic animals (Kraig et al., 1987; Flecknell, 1987). Spontaneously ventilated animals were slightly hypercapnic probably due to depression of respiration caused by halothane anaesthesia (Flecknell, 1987). All variables were not altered significantly by the surgical preparation for 4-vessel occlusion.

Ion-selective microelectrode measurements of $pH_e$ in different regions of the cortex have consistently given values between 7.2 and 7.4 (i.e. $[H^+]_e$ in the range 75-60 nM)(Kraig et al., 1983; Mutch and Hansen, 1984; Kraig et al., 1985; Siesjö et al., 1985a; Obrenovitch et al., 1990a). The $[H^+]_e$ measured in this study was within the above range (61.1 nM, i.e. pH 7.4). The extracellular concentration of $[CO_3^{2-}]$ under basal conditions in this study is close to that approximated for interstitial fluid by theoretical calculations (45 $\mu$M; Stewart, 1981). One previous study of hippocampal brain slices *in vitro* found $[CO_3^{2-}]_e$ to be around 50 $\mu$M (Chesler et al., 1994), which is also in line with the values obtained in this study.

The basal concentrations of lactate remained relatively stable throughout the control period, suggesting that the implantation of the microdialysis probe did not produce long-lasting alterations of this variable. Dialysate levels of lactate obtained in this study were much higher than those previously reported (Kuhr and Korf, 1988; Scheller et al., 1992). This was probably due to the lower microdialysis perfusion flow rate that was used to minimise drainage of the tissue surrounding the implanted probe (Benveniste and Hüttemeier, 1990). The stable dialysate lactate levels also supports the finding that lactate is continuously produced intracellularly and released into the extracellular fluid so that intracellular lactate concentration is maintained at a steady level (Walz and Mukerji, 1988a).

## 7.2 Effect of High Extracellular $K^+$ and Spreading Depression

### 7.2.1 Effects of $K^+$ on the DC Potential

The DC potential reflects the average membrane potential of all cell populations surrounding the probe, including both neurons and glia (Caspers et al., 1984). Steep negative shifts in the DC potential, indicating depolarisation, reflect a marked efflux of intracellular $K^+$, and movement of $Na^+$, $Ca^{2+}$ and $Cl^-$ into the cell due an increase in the permeability of cell membranes to ions (Nicholson and Kraig, 1981).

The $K^+$-induced sustained negative shift indicates a direct influence of the perfusion medium on the extracellular ionic composition of the tissue surrounding the microdialysis probe. Perfusion of higher $K^+$-ACSF concentrations through the probe increased this initial shift, suggesting a more intense and sustained depolarisation of the cell populations immediately adjacent to the surface of the dialysis membrane. The peaks of further negativation superimposed on the sustained negative shift in the DC potential correspond to SD initiation (Obrenovitch et al., 1993), and may reflect the depolarisation of cells that are either further away from the probe or are more resistant to high $K^+$-induced depolarisation. Increasing $K^+$-ACSF concentrations increased both the frequency and intensity of these depolarisations. There is some evidence to suggest that the transient peaks of depolarisation reflect alterations in the membrane potential of both glial cells and neurons (Higahisda et al., 1974).

### 7.2.2 Changes in Dialysate Lactate Associated with High $K^+$-ACSF

#### 7.2.2.1 Relationship Between Dialysate Lactate and the DC Potential

$K^+$-induced changes in $[lact]_d$ were closely related to those of the DC potential. The initial sustained depolarisation was accompanied by a decrease in $[lact]_d$, which was apparent whenever the first transient peak of further depolarisation occurred towards the middle or the end of the $K^+$-stimulus. This decline in $[lact]_d$ presumably reflects a drop in the extracellular lactate level, superimposed to persistent microdialysis drainage of the region under study (Benveniste and Hüttemeier, 1990). It is also possible that the magnitude of this decrease may be amplified by a decrease in microdialysis recovery (Nicholson and Phillips, 1981; Scheller and Kolb, 1991), due to the shrinkage of the extracellular space known to occur during depolarisation (Hansen and Olsen, 1980).

Within each SD, the positive shift in the DC potential indicating cell repolarisation was associated with a rise in $[lact]_d$. This phenomenon was observed irrespective of whether the SD was isolated or part of a repetitive pattern. Another consistent feature was a marked and rapid increase in $[lact]_d$ after the $K^+$-stimulus. Taken together, these data strongly suggest that extracellular lactate levels mostly increased during periods of repolarisation.

#### 7.2.2.2 Lactate Production During Spreading Depression

Anaerobic glycolysis is stimulated by the ionic changes associated with SD and exposure to high $K^+$, as indicated by increased lactate levels in both tissue and the extracellular space (Mutch and Hansen, 1984; Scheller et al., 1992; Taylor et al., 1994b). These ionic changes initiate a cascade of events leading to lactate production: (i) increased extracellular $K^+$ and intracellular $Na^+$ concentrations stimulate the activity of $Na^+/K^+$-ATPase (Walz, 1992), which uses ATP to transport $Na^+$ back out of the cell and $K^+$ back into the cell, in order to restore their gradient across the cellular membrane; (ii) hydrolysis of ATP is enhanced, increasing the energy demand of the tissue; (iii) these changes, in turn, stimulate glycolysis via phosphofructokinase activation, and enhance oxidative phosphorylation, with a higher cellular oxygen consumption (Erecinska and Silver, 1989); and (iv) when the cellular oxygen content is reduced to a level insufficient to support oxidative phosphorylation, anaerobic glycolysis is stimulated, ultimately increasing intracellular lactate production (Assaf et al., 1990; Hansen and Quistorff, 1993).

Findings suggest that changes occurring prior to depolarisation (i.e. before the marked transmembrane ionic shifts) result in an early increase in tissue energy demand with subsequent stimulation of anaerobic glycolysis. Levels of ATP decreased early with SD suggesting activation of ionic pumps before depolarisation (Mies and Paschen, 1984). The progressive increase in extracellular $K^+$ before depolarisation (Kraig and Nicholson, 1978) may stimulate $K^+$ uptake by glial cells which counteract increases in extracellular $K^+$, through a process known as spatial buffering. Uptake of $K^+$ into glial cells occurs via a $Na^+/K^+$-ATPase carrier, which is stimulated by both high external $K^+$ and intracellular $Na^+$, in conjunction with a NaCl/KCl cotransporter, which transports $K^+$ and $Na^+$ inwards (Walz and Mukerji, 1988c). Activation of glial $Na^+/K^+$-ATPase carriers for $K^+$ uptake and consequent removal of intracellularly accumulated $Na^+$ from the cell, may

account for the early decline in ATP levels and an increase in energy demand before the marked ionic changes associated with depolarisation occur.

Other findings suggest that energy demand is increased by changes occurring early with SD which may stimulate anaerobic glycolysis: (i) a decrease in the ATP/ADP ratio as well as an increase in the lactate/pyruvate ratio preceded the SD wave in the rat cortex (Quistorff et al, 1979); (ii) the marked ionic shifts characterising depolarisation were preceded by an increase in glucose consumption (Gjedde et al., 1981) and a decrease in oxygen tension (Lacombe et al., 1992); and (iii) a transient burst of "spontaneous" neuronal activity was observed before the rise in extracellular $K^+$ and occurrence of SD (Somjen et al., 1992).

After depolarisation, restoration of ionic homeostasis increases energy demand to such an extent that the mitochondria are required to function at a rate well in excess of the available oxygen supply, even though this phase of SD is associated with a pronounced increase in blood flow (Gjedde et al., 1981; Kocher, 1990; Lacombe et al., 1992). Each marked ionic shift that occurs during the phase of cellular depolarisation is associated with further decreases in ATP concentration (Mies and Paschen, 1984). Additional metabolic stress may result from $Ca^{2+}$ influx (Kraig and Nicholson, 1978), which affects the ATP-dependent $Ca^{2+}$ pump in cell membranes. Increased intracellular $Ca^{2+}$ is also sequestered by mitochondria at the expense of oxidative phosphorylation (Carvalho, 1982), and as $Ca^{2+}$ uptake by mitochondria *in vitro* interferes with ATP synthesis (Hillered et al., 1983), depletion of ATP levels is amplified by augmented consumption and restriction of ATP synthesis. However, ATP levels are not depleted during SD (Kocher, 1990) suggesting that stimulation of anaerobic metabolism maintains tissue energy requirements (Gjedde et al., 1981; Csiba et al., 1985).

It is likely that activation of anaerobic glycolysis and subsequent intracellular lactate accumulation occurred early and throughout the $K^+$-stimuli in these experiments. However, increases in extracellular lactate were mainly associated with periods of repolarisation. Therefore, these data suggest that, when transmembrane ionic gradients were disrupted (i.e. during depolarisation), the production of lactate was reduced and/or inhibited, or lactate transport out of some cells was impaired.

7.2.2.3 Possible Origins of Observed Lactate Changes During Spreading Depression

The absence of increases in extracellular lactate during depolarisation revealed in these experiments could reflect impairment of glycolysis through pH-induced changes in glycolytic enzyme activity. Intracellular pH declines during SD (Csiba et al., 1985; Gault et al., 1994), with increased ATP hydrolysis due to activation of the $Na^+/K^+$-ATPase and an increase in tissue $PCO_2$ (Lauritzen et al., 1982) contributing to this acidosis (Siesjö, 1985). Even when persistent energy demands continue to stimulate glycolysis, glucose phosphorylation may be inhibited by reduced $pH_i$ (Newman et al., 1991). During the passage of SD, the increased extracellular $K^+$ activates glycolysis, but a lowered $pH_i$ could prevent substrate from entering the glycolytic pathway, producing a temporary "metabolic debt". As such, during repolarisation, when ionic gradients are re-established, initiation of $pH_i$ restoration would remove the inhibition of glucose phosphorylation, resulting in a burst of glycolytic flux and an increase in lactate production.

Some regulatory enzymes in the energy-producing pathway exhibit a pH-dependence. The most important of those in the brain is phosphofructokinase, the key rate-controlling enzyme of glycolysis (Passonneau and Lowry, 1962) which is potently inhibited by acidosis (Trivedi and Danforth, 1966). However, the extent of phosphofructokinase inhibition by $H^+$ is very sensitive to changes in adenine nucleotides and in particular ATP, with the highest sensitivity to pH in the ATP-inhibited state (Trivedi and Danforth, 1966; Dobson et al., 1986). Moreover, AMP is able to reverse the blocking effect of ATP at low pH (Trivedi and Danforth, 1966). Thus, under conditions of increased ATP hydrolysis, when ATP concentration falls, and the levels of ADP and AMP rise, phosphofructokinase is not only stimulated by an increase in the concentrations of its activators (ADP, AMP and $P_i$) and a concomitant fall in the level of its inhibitor (ATP), but through the relief of the inhibition by $H^+$. Experimental evidence of large increases in lactate production during ischaemia, when $pH_i$ is markedly reduced, supports the suggestion that other stimulators of enzyme activity must overcome the inhibitory effect of increased $[H^+]$ (Siesjö, 1978).

The activity of phosphofructokinase is enhanced by increased pH (Erecinska and Silver, 1994). During SD glial cells become alkaline (Chesler and Kraig, 1989) which in turn could augment the rate of anaerobic glycolysis and lactate production from these cells. The finding that local cerebral glucose utilisation was increased in alkalotic brain (Van Nimmen et al., 1986) supports this hypothesis. Intracellular acidosis may in fact

enhance ATP production from anaerobic glycolysis, through the inhibitory effect of $H^+$ on mitochondrial respiratory chain (Rouslin, 1991; Erecinska et al., 1993). This is highlighted by the finding that although a fall in $pH_i$ reduced mitochondrial respiration (Hillered et al., 1985), lactate production in synaptosomes and C6 glioma cells, under these conditions, was enhanced (Erecinska et al., 1993). Reduced pH may also favour lactate production from pyruvate, since pyruvate binding to the lactate dehydrogenase enzyme complex requires the latter to be protonated. Therefore, it is unlikely that pH-induced impairment of glycolysis contributed to the changes in extracellular lactate observed in this study.

Excessive intracellular $Na^+$ loading (i.e. intensive electrical stimulation, anoxic depolarisation or treatment with veratridine) may also inhibit anaerobic glycolysis. Tetrodotoxin (TTX), at concentrations which block the generation of action potentials and the associated influx of $Na^+$, enhanced the rate of anaerobic glycolysis of brain cortex slices from rats and guinea pigs by approximately 300 % (Shankar and Quastel, 1972). A similar effect was observed with low concentrations of local anaesthetics. Protoveratrine, which induces $Na^+$ influx, diminished the glycolytic stimulation brought about by TTX in $Ca^{2+}$-free medium (Shankar and Quastel, 1972). These observations suggest that the influx of $Na^+$ and efflux of $K^+$ under these conditions blocked anaerobic metabolism, possibly at the level of pyruvate kinase. This enzyme, a regulatory step in glycolysis converting phosphoenolpyruvate to pyruvate with the formation of ATP, is activated by $K^+$ and inhibited by $Na^+$ (Takagaki, 1968; Rose and Rose, 1969). Inhibition of anaerobic metabolism by $Na^+$ was recently confirmed in synaptosomes (Gleitz et al., 1993). Veratridine application at the onset of anoxia concentration-dependently reduced anaerobic ATP synthesis. This effect was linked to $Na^+$-influx as it was blocked by TTX. However, TTX application did not alter the lactate generation in cultured synaptosomes or C6 glioma cells (Erecinska et al., 1993). The inhibitory effect of intracellular $Na^+$ loading implies that anaerobic metabolism, the major source of ATP when oxygen tension is reduced, is abolished, however, ATP levels were not depleted during SD (Kocher, 1990). Restoration of the ionic gradients with $Na^+$ efflux after SD would result in an increase in lactate production. The changes in lactate observed in this study are consistent with this hypothesis.

Alternatively, the changes observed could also reflect altered efflux of lactate from cells during depolarisation. Lactate exchanges across the plasma membrane are generally

considered to occur by passive diffusion of undissociated lactic acid (Nedergaard et al., 1989), or via a lactate/$H^+$ cotransporter (Lomneth et al., 1990; Assaf et al., 1990; Schneider et al., 1993; see Section 1.2.1.6). The energy dependency of lactate transport from brain cells remains unclear. On one hand, lactate exchanges between brain slices and the outer medium were neither dependent on ATP (Kauppinen and Williams, 1990; Assaf et al., 1990) nor on $Na^+$ (Pirtillä and Kauppinen, 1992). In contrast, findings suggest that lactate removal from intracellular compartments may involve a transporter that is either directly or indirectly coupled to energy-dependent transmembrane gradients and hence membrane function: (i) cardiac arrest, in these experiments, provoked a rapid increase in extracellular lactate, which decreased after terminal anoxic depolarisation although tissue lactate levels continue to increase even when stores of glycogen and glucose were depleted (Lowry et al., 1964); and (ii) increases in ECF lactate during complete ischaemia and after electroconvulsive shock were delayed in comparison to those of tissue lactate (Kuhr et al., 1988).

Various data have suggested that, as in other tissues, lactate transport via a lactate/$H^+$ cotransporter is dependent on the transmembrane proton gradient (Halestrap et al., 1990; Lomneth et al., 1990; Walz and Mukerji, 1990). Initially with SD, there is an acidic shift in $[H^+]_e$ (see Section 6.3) which may suggest activation of the $Na^+/H^+$ and/or $HCO_3^-/Cl^-$ exchange systems resulting in efflux of intracellular $H^+$. These exchangers are dependent on and driven by the transmembrane $Na^+$ gradient maintained by the $Na^+/K^+$-ATPase pump (see Section 1.2.1.4). However, with depolarisation, transmembrane ionic gradients are disrupted, the occurrence of an alkalotic shift in $[H^+]_e$ at this time (see Section 6.3) implies that the proton gradient is transiently disrupted. The changes in lactate associated with SD observed in this study (i.e. lactate decreased during transient depolarisation, increasing markedly only during the subsequent repolarisation phase) may reflect a trapping of intracellular lactate due to altered proton gradient. With $K^+$-induced depolarisation (and anoxic depolarisation) disruption of the $H^+$ gradient may render the lactate/$H^+$ cotransporter ineffective, and prevent the efflux of intracellularly accumulated lactate. With repolarisation, ionic gradients are re-established, and lactate efflux from the cell restored as the proton gradient recovers.

### 7.2.2.4 Changes in Lactate After Spreading Depression

During the slow recovery from SD, lasting between 5 and 20 minutes, the redox state of the tissue gradually recovers from lactate acidosis and returns to basal levels (Haselgrove et al., 1990). Removal of extracellular lactate after the $K^+$-stimulus was significantly slower than its initial efflux. It is unlikely that clearance via the vascular system was a significant contributor to lactate removal, despite the transient hyperaemia subsequent to SD and high $K^+$-stimuli (Lauritzen, 1987), since monocarboxylic acid transport across the BBB is negligible in the adult rat (Cremer et al., 1979; Kuhr et al., 1988), and only a small percentage of lactate produced during hypoxia was removed from the brain via the venous blood supply (Zimmer and Lang, 1975). Increasing blood levels of lactate did not increase lactate levels in the ECF (Kuhr et al., 1988). The $K_m$ value for lactate transport across the BBB (1.9 mM) is lower than other membranes (e.g. $K_m$ for tumour cells is 20 mM; Spencer and Lehninger, 1976), which reflects a high affinity for lactate. The low $K_m$ of BBB approximates normal plasma level of lactic acid. As a consequence, elevations in plasma lactate above the normal concentration are not readily transferred to the brain (Pardridge and Olendorf, 1977). Thus, the high affinity of BBB lactate transport could protect the brain from increased circulating concentrations of lactic acid, for example during exercise when high levels of lactate accumulate in the blood. However, the high affinity could also provide a basis for the selective vulnerability of the CNS to anoxia or conditions that cause high brain levels of lactate. Slow efflux of lactate into blood may be the result of saturation of the BBB monocarboxylic acid transport. As there is clear evidence that lactate can become a major energy source in brain tissue under certain circumstances (Schurr et al., 1988; Bock et al., 1989), removal of ECF lactate probably occurred through re-entry into the cells, and recycling to pyruvate with normalised oxygen demand (Zimmer and Lang, 1975; Kuhr et al., 1988).

Recovery of extracellular lactate levels in the cortex after SD was found to be biphasic, suggesting a difference in lactate production and/or transmembrane exchange between neurons and glia (Walz and Mukerji, 1990; Scheller et al., 1992). However, this biphasic recovery was not observed in the striatum after SD in this study. Although both astrocytes and neurons have apparently identical transport mechanisms for lactate (Walz and Mukerji, 1988b), it has been shown that glial cells in culture have a higher rate of anaerobic glycolysis than neurons and produce more lactate (Pauwels et al., 1985; Walz and Mukerji, 1988a,b, 1990).

In summary, although the $K^+$-induced decrease in extracellular lactate observed in this study may not be due to the effects of a reduced pH on glycolysis, it is possible that this change could reflect an inhibition of glycolysis by $Na^+$, an altered efflux of lactate, or a combination of both. Further studies of the effects of high $K^+$ and SD initiation on extracellular lactate were performed in the presence of probenecid, an inhibitor of monocarboxylic acid transport, in an attempt to evaluate the contribution/significance of lactate transport under these conditions.

## 7.3 Global Cerebral Ischaemia: Terminal and Transient

### 7.3.1 Introduction

The changes that occur initially with the onset of ischaemia (phase 1) are reversible, and no permanent neurological deficit develops as long as the insult is of short duration. However, if ischaemia is severe and sustained, then within a few minutes, dramatic and synchronous ionic redistributions occur across the cellular membrane (Harris and Symon, 1984; Hansen, 1985). These marked shifts, referred to as anoxic depolarisation, signify the beginning of a second phase (phase 2), which is critical for cell survival. For the sake of clarity, the alteration of acid-base homeostasis during the two phases of ischaemia, and during reperfusion, are discussed separately.

### 7.3.2 Alteration of Acid-Base Homeostasis Before Anoxic Depolarisation (Phase 1)

#### 7.3.2.1 Energy Metabolism

Suppression of spontaneous electrical activity (EEG), together with that of evoked potentials, are the first functional changes associated with the onset of ischaemia (Branston et al., 1974). In some experiments, this functional loss was associated with a slight positive shift in the DC potential, possibly originating from hyperpolarisation of neurons due to an increased $K^+$ conductance. The relevance of this phenomenon may be to reduce depolarisation-induced $Ca^{2+}$ loading of cells and attenuate stimulus-coupled transmitter release from presynaptic terminals (Duchen, 1990; Duchen et al., 1990). The initial increase in $K^+$ conductance may originate from the opening of $Ca^{2+}$-dependent $K^+$ channels subsequent to an increase in intracellular free $Ca^{2+}$ and/or the opening of ATP-sensitive $K^+$ channels (Obrenovitch et al., 1990b).

Ischaemia leads to inadequate supplies of glucose and oxygen, the substrates of oxidative phosphorylation and glycolysis, and thus reduces ATP generation. Although ATP synthesis from oxidative phosphorylation ceases, ATP utilisation does not. Initially the breakdown of phosphocreatine via the creatine kinase reaction maintains ATP levels at about 95 % of control. As such the fall in PCr precedes that in ATP during limitation in ATP synthesis in ischaemia (Lowry et al., 1964; Ljunggren et al., 1974c; Cox et al., 1988). However, within 30 seconds of ischaemia onset, Pcr stores are depleted (Ekholm et al., 1992). The decline in PCr and ATP, and the associated rise in Cr, inorganic phosphate, ADP and AMP, activate glycogenolysis and glycolysis via stimulation of glycogen phosphorylase and phosphofructokinase, respectively (Lowry et al., 1964; Ljunggren et al., 1974c).

Since inadequate oxygen supply cannot maintain oxidative phosphorylation, and oxidation of pyruvate is retarded, the latter is anaerobically converted to lactate (Erecinska and Silver, 1994). During this phase of ischaemia (i.e. before anoxic depolarisation occurs), anaerobic glycolysis maintained ATP levels at about 90 % of control values as long as glucose was available (Ekholm et al., 1992).

#### 7.3.2.2 Extracellular Acid-Base Changes

The deterioration of cerebral energy state with the ensuing stimulation of anaerobic glycolysis and continued hydrolysis of ATP, results in the production of lactic acid (i.e. lactate and $H^+$), and ultimately leads to intracellular acidification. Brain cells must rely on regulatory mechanisms to maintain intracellular acid-base homeostasis (Siesjö, 1988b).

Although ischaemia-induced acidosis is initiated intracellularly, extracellular levels of $H^+$ ($[H^+]_e$) increased immediately after the onset of ischaemia. This was closely associated with a decrease in $[CO_3^{2-}]_e$ indicating that progressive reduction of the $H^+$ buffering capacity of the ECF is an early event in ischaemia. These initial changes in extracellular $H^+$ and $CO_3^{2-}$ may be partly due to increased brain tissue concentration of $CO_2$ (Siesjö, 1985; Smith et al., 1986; von Hanwehr et al., 1986). Increased intracellular $H^+$ is buffered by $HCO_3^-$ to form $CO_2$ which would normally be removed to the circulation. This is no longer possible when cerebral blood flow is severely reduced or ceases during ischaemia. As the $HCO_3^-/H_2CO_3$ buffer system is greatly reduced in these conditions, providing only 10 % of its normal capacity, other acid-base mechanisms are required to maintain $pH_i$. Acetazolamide, an inhibitor of carbonic anhydrase, increased

the initial acidic shift with ischaemia onset (Mutch and Hansen, 1984) supporting the proposal that local rise in $CO_2$ tension contributes to increased acidosis. However, acidification of the extracellular environment may also reflect a marked activation of the plasmalemnal $Na^+/H^+$ and $HCO_3^-/Cl^-$ exchangers, which regulate $pH_i$.

Various studies suggest that ischaemia-induced acidosis stimulates the $Na^+/H^+$ exchanger which mediates the extrusion of $H^+$ in exchange for $Na^+$ (Tolkovsky and Richards, 1987; Mellergård et al., 1993; Ou-yang et al., 1993). The increase in $[H^+]_i$ also stimulates the $HCO_3^-/Cl^-$ exchanger, which translocates $HCO_3^-$ inwards in exchange for $Cl^-$ (Roos and Boron, 1981; Thomas, 1984). Although the stoichiometry and exact model of the underlying ion exchange of this exchanger is unknown, kinetic studies have suggested that net acid extrusion occurs via the influx of $NaCO_3$ in exchange for internal $Cl^-$ (Boron, 1985; Boron and Knakal, 1989). The apparent $K_m$ of the transport was 80 $\mu$M (Boron, 1985). Influx of $CO_3^{2-}$ via this exchanger may contribute to the observed decrease in $[CO_3^{2-}]_e$ and associated rise in $[H^+]_e$.

The electrogenic $Na^+$-$HCO_3^-$ cotransporter evident in vertebrate glial cells (Astion and Orkand, 1988; Kettenmann and Schlue, 1988; Newman and Astion, 1991) may contribute to the changes in $[CO_3^{2-}]_e$ observed during the initial phase of ischaemia. This cotransporter mediates a net inward movement of $HCO_3^-$ driven by the $Na^+$ gradient, the direction of the transport probably being determined both by the extra- and intracellular $HCO_3^-$ concentrations, and by the membrane potential (Kettenmann and Schlue, 1988; Deitmer and Schlue, 1989; Deitmer, 1991). However, recent studies of this transport system suggest that $CO_3^{2-}$, rather than $HCO_3^-$, may be the transported species, since inhibition of carbonic anhydrase activity enhanced depolarisation-induced acid secretion from gliotic hippocampal slices (i.e. tissue with a dense proliferation of glial cells and absence of neuronal cells)(Grichtchenko and Chesler, 1994). This is supported by the finding that in the basolateral membrane vesicles, electrogenic $Na^+$-$HCO_3^-$ cotransport actually involved the transport of $CO_3^{2-}$ (Soleimani and Aronson, 1989). In theory, such a mechanism could be activated during ischaemia by decreased intracellular $HCO_3^-/CO_3^{2-}$ concentration, and inwardly directed $Na^+$ gradient.

As glial cells use an $HCO_3^-$-dependent mechanism to extrude $H^+$, mechanisms regulating acid transients are more efficient in these cells than in neurons (Ou-yang et al., 1993). This together with the high permeability of the glial cell membrane to $HCO_3^-$ (Kraig et al., 1986), suggests that glia may actively buffer transient changes in the

neuronal microenvironment acid-base balance by releasing $HCO_3^-/CO_3^{2-}$ (Katsura et al., 1994a) at the expense of their internal pH (Astion et al., 1987).

### 7.3.2.3 Extracellular Lactate Changes

Although lactate is produced intracellularly subsequent to stimulation of anaerobic metabolism (Siesjö, 1985; Smith et al., 1986; Obrenovitch et al., 1988; Conger et al., 1995), extracellular levels of lactate increased rapidly after the onset of ischaemia, indicating that removal of lactate from the intra- to extracellular space is effective early in ischaemia (Nilsson et al., 1990; Scheller and Kolb, 1991; Taylor et al., 1996). As lactate is transported across the plasma membrane with $H^+$ (i.e. lactic acid; see Section 1.2.1.6), this could play a role in $pH_i$ regulation. The effectiveness of such a mechanism in nervous tissue is supported by the finding that lactate/$H^+$ cotransport, and not $Na^+/H^+$ or $HCO_3^-/Cl^-$ exchange, was the dominant process responsible for interstitial acidification in isolated hypoxic peripheral nerves (Schneider et al., 1993). Although lactate removal was not a major route for $H^+$ extrusion from cortical brain slices during anoxia (Pirtillä and Kauppinen, 1992), it is likely that lactate/$H^+$ cotransport across the cellular membrane plays a part in the brain regulation of intracellular $[H^+]$, and contributes to the rapid acidification of the extracellular space when oxygen supply becomes deficient. This is supported by the following: (i) superfusion of rat cerebellum with fluoride, a glycolysis inhibitor, restored $pH_e$ to normal despite elevated $[K^+]_e$ (Kraig et al., 1983), suggesting that lactic acid production accounted for the interstitial acid shift, since lactate is produced after the glycolytic step inhibited by fluoride; (ii) stimulus-evoked acid shifts were inhibited by solutions in which glucose was omitted or replaced by pyruvate (Spuler et al., 1987).

The efficacy of the mechanisms regulating $pH_i$ during ischaemia-induced acidosis requires both maintenance of the plasma membranes overall impermeability to ions, and a functional $Na^+/K^+$-ATPase pump. Therefore, the early, progressive reduction in extracellular $CO_3^{2-}$ and the associated rise in $H^+$ support the concept that transmembrane ionic exchanges contributing to intracellular $H^+$ regulation are functional and activated in the initial stage of the ischaemia insult, with intracellular $[H^+]$ being kept close to normal levels (Ekholm et al., 1992) to the detriment of the extracellular $[H^+]$ which acidifies (Obrenovitch et al., 1990a). Removal of intracellular lactate/$H^+$ may also contribute to this acidification. However, with sustained ischaemia, a subsequent marked drop in ATP

levels (Ekholm et al., 1992) implies that anaerobic energy production via glycolysis is not sufficient to keep up with the basal energy demands that are needed to maintain ionic homeostasis. Consequently, the ionic gradients cannot be upheld, leading to cellular membrane depolarisation.

### 7.3.3 Collapse of Acid-Base Homeostasis with Anoxic Depolarisation (Phase 2)

#### 7.3.3.1 Extracellular Acid-Base Changes

Anoxic depolarisation is due to a marked, sudden increase in the permeability of the cellular membrane to ions. The large negativation of the DC potential signalling this event reflects marked changes in the extracellular ionic composition, which approaches that of the intracellular compartment subsequent to efflux of $K^+$ and influxes of $Na^+$, $Cl^-$ and $Ca^{2+}$ (Harris and Symon, 1984; Hansen, 1985; Hansen and Nedergaard, 1988; Obrenovitch et al., 1990a). Disruption of transmembrane ionic gradients implies the collapse of a number of plasmalemnal transport/exchange systems which are driven by these gradients, including those contributing to cellular acid-base homeostasis.

Direct measurement of $[CO_3^{2-}]_e$ consistently revealed a sudden transient increase, superimposed upon the steady $[CO_3^{2-}]_e$ decrease, and intimately related to cell membrane depolarisation (Fig. 6.2.A). This rapid change, which occurred at a greater rate than other decreases/increases in measured $[CO_3^{2-}]_e$, was associated with sudden decrease in $[H^+]_e$, i.e. an alkalotic shift which has been previously characterised (Kraig et al., 1983; Harris and Symon, 1984; Mutch and Hansen, 1984; Obrenovitch et al., 1990a,b).

One possibility is that the shifts in $[H^+]_e$ and $[CO_3^{2-}]_e$ with anoxic depolarisation do not reflect a real change in their interstitial activities, but are only artifacts produced by sudden changes in the ionic composition of the medium surrounding the microelectrode tip. However, the following contradict this hypothesis: (i) *in vitro* evaluation of the selectivity of the ISM showed that changes in interfering ions, similar to those that are known to occur during anoxic depolarisation, had a negligible effect on the output of the ISM. Even if the marked change in $[Cl^-]_e$ with depolarisation altered ISM response in this study (observed in other $CO_3^{2-}$-ISM studies; Wietasch and Kraig, 1991; Chesler et al., 1994), it would have resulted in under estimation of the $[CO_3^{2-}]_e$ shift since the deflection caused by $Cl^-$ from high to low levels was in the opposite direction to the $[CO_3^{2-}]_e$ shift; (ii) there was no correlation between the amplitude of the transient shifts in $[H^+]_e$ and $[CO_3^{2-}]_e$, and that of the drop in the DC potential which is closely related to ionic changes

in the extracellular space (Kraig and Nicholson, 1978); and (iii) transient decreases in $[H^+]_e$ have also been shown to occur after local stimulation of the cerebral cortex surface (Kraig et al., 1983), an event which does not produce ionic shifts as massive as those associated with anoxic depolarisation.

As initially proposed by Kraig et al. (1983), the transient fall in $[H^+]_e$ may be the consequence of a sudden increase in the bicarbonate activity within the ECF, resulting from a rapid reduction of the extracellular compartment combined with a selective impermeability of the cellular membrane to $HCO_3^-$. It is true that both SD and ischaemia-induced depolarisation markedly alter the ionic distribution which results in cell swelling to the detriment of the extracellular space, which shrinks (Hansen and Zeuthen, 1981; Nicholson and Kraig, 1981). However it is unlikely that an increase in $[HCO_3^-]_e$ occurred in this way as it has been demonstrated that changes in ionic distribution subsequent to SD and anoxic depolarisation are due to the opening of non-specific channels with pore diameters of approximately 6.6 Å (Phillips and Nicholson, 1979), which is larger than the apparent ionic diameters of $HCO_3^-$ and $CO_3^{2-}$ (approximately 4.0 Å; Bormann et al., 1987). Furthermore, GABA- and/or glycine-gated anion channels have been shown to be significantly permeable to $HCO_3^-$ when activated (Bormann et al., 1987; Kaila and Voipio, 1987; Kaila et al., 1989).

On the contrary, the transient shifts in $[H^+]_e$ and $[CO_3^{2-}]_e$ with anoxic depolarisation support the theory that there is a rapid redistribution of $H^+$ and pH-changing anions between the intra- and extracellular compartments due to increased membrane permeability to ions and, therefore, a collapse of active ion exchange mechanisms contributing to residual intracellular acid-base regulation in ischaemia (Obrenovitch et al., 1990a). Analysis of the changes in $[H^+]_e$ and $[CO_3^{2-}]_e$ revealed that the amplitude of the transient drop in $[H^+]_e$ and increase in $[CO_3^{2-}]_e$ correlated with the level of extracellular acidosis at the time they occurred. Although alkalotic shifts in $[H^+]_e$ have been previously characterised, in most studies this relationship remained unnoticed due to the use of pH (i.e. log of the inverse of $[H^+]$) to express proton activities (Obrenovitch et al., 1990a). The pH notion obscures qualitative aspects of the chemical relationships that are involved in acid-base behaviour and distorts the quantitative significance of $[H^+]$ (Stewart, 1981; Obrenovitch et al., 1990a).

The relationship between the magnitude of alkalotic shift and the tissue acidosis at that time may reflect activation of the processes regulating $[H^+]_e$ by tissue acidosis. This

is supported by the finding that the cell membrane permeability to $H^+$ markedly increases in depolarised voltage-clamped snail neurons (Thomas and Meech, 1982) to such extent that $[H^+]_i$ becomes similarly determined by $[H^+]_e$ and the potential across the cell membrane. Furthermore, recordings of extracellular and astroglial $[H^+]$ in rat neocortex showed that acidification of the extracellular space was associated with a decrease in astroglial $[H^+]$ shortly after the onset of ischaemia (Kraig and Petito, 1989). However, the above speculative mechanism is contradicted by data obtained with drugs that inhibit $Na^+/H^+$ or $HCO_3^-/Cl^-$ antiports. Mutch and Hansen (1984) observed that pretreatment with amiloride or DIDS increased the magnitude of the alkaline shifts of $[H^+]_e$ evoked by SD or anoxic depolarisation. According to the mechanism proposed above, inhibition of $Na^+/H^+$ or $HCO_3^-/Cl^-$ exchangers should rather decrease these transients.

Another explanation is that the correlation between the magnitude of the transient fall in $[H^+]_e$ and the level of extracellular acidosis may reflect alteration of the extracellular buffering capacity during ischaemia. The latter is directly related to extracellular $HCO_3^-$ and $CO_3^{2-}$ (Siesjö, 1985). As the increase in $[H^+]_e$ from the onset of ischaemia is accompanied by a decrease in $[CO_3^{2-}]_e$, the extracellular $H^+$ buffering capacity becomes diminished, and a given acid-base perturbation would produce a larger change in $[H^+]_e$. Such an acid-base alteration could be caused either by an influx of $H^+$ through unspecific cation channels (e.g. those gated by glutamate receptors), or by an efflux of $HCO_3^-$ and $CO_3^{2-}$ through GABA-activated $Cl^-$ channels (Bormann et al., 1987). Another possible route for the rapid transfer of $H^+$ across the membrane is through slowly-inactivating voltage-gated $Na^+$ channels. Although permeation of $H^+$ through these channels could contribute significantly (Hille, 1991), this is unlikely since the amplitude of the alkalotic shift in $pH_e$ with anoxic depolarisation, as with the abrupt drop in $[Na^+]_e$, was not altered by TTX (Xie et al., 1994).

The transient nature of this alkalosis would then follow from the fact that, once the cellular membranes have depolarised, the electrochemical gradients from passive flux of $H^+$ or $HCO_3^-/CO_3^{2-}$ reverse. Experimental support for this hypothesis has been reported (Obrenovitch et al., 1990a). This latter mechanism is compatible with the data of Mutch and Hansen (1984), i.e an increased alkalotic shift with depolarisation after administration of DIDS. These authors proposed that, during the alkaline transient, increased $[HCO_3^-]_e$ and decreased $[Cl^-]_e$ stimulate the $HCO_3^-/Cl^-$ exchanger which attempts to maintain a set $[HCO_3^-]_e/[HCO_3^-]_i$ - $[Cl^-]_e/[Cl^-]_i$ ratio, resulting in $HCO_3^-$ uptake in exchange for $Cl^-$,

which attenuates the magnitude of the alkaline shift. Inhibition of this mechanism by DIDS results in an enhanced alkaline shift. Active neurons release $HCO_3^-$ which is removed by glial cells as $CO_2$ (Mutch and Hansen, 1984). Interfering with this pathway would cause accumulation of $HCO_3^-$ in ECS, therefore increasing alkalotic shift.

Therefore, it is likely that the transient extracellular alkalosis (i.e a drop in $[H^+]_e$ with a rise in $[CO_3^{2-}]_e$) may result from a rapid redistribution of $H^+$ and/or $CO_3^{2-}/HCO_3^-$ between the intra- and extracellular compartments subsequent to the opening of ionic channels and increased membrane permeability with anoxic depolarisation. A discontinuity in the ischemia-induced increase in tissue $pCO_2$ with a steeper rise synchronous with anoxic depolarisation supports the notion of a sudden transmembrane redistribution of $H^+$ and $HCO_3^-$ (Obrenovitch et al., 1990a). The pattern of changes in $[H^+]_e$ and $[CO_3^{2-}]_e$ observed when a single wave of spreading depression was initiated with a needle prick were similar to those observed during forebrain ischaemia, but were of a lower magnitude. This suggests that the changes in acid-base regulation occurring in these two events are similar (Mutch and Hansen, 1984).

It is noteworthy that, in several experiments, the characteristic transient $[CO_3^{2-}]_e$ shift associated with anoxic depolarisation was not present. In these cases, the $[CO_3^{2-}]_e$ before ischaemia was significantly lower, and a slight rise in $[CO_3^{2-}]_e$ preceded its steady decrease shortly after the onset of ischaemia (Fig. 6.2.C). Extensive *in vitro* testing showed that this distinct pattern of $[CO_3^{2-}]_e$ changes was neither due to a poor time response of the ion-selective microelectrode nor to a lack of its selectivity. A consistent electrode tip diameter of 10-15 $\mu$m ensured that recordings were extracellular, i.e. that the electrode would not penetrate the cellular components of the cortex. This peculiar pattern of $[CO_3^{2-}]_e$ changes was also not due to a difference in ischaemia severity, since similar results were observed with terminal complete ischaemia produced by cardiac arrest (Fig. 6.2.C). On the basis of this observation, it is possible that these two distinct patterns of changes in $[CO_3^{2-}]_e$ may reflect events taking place in different cellular environments, resulting from a slight different implantation depth of the ion-selective microelectrode within the laminated cellular arrangement of the mammalian cerebral cortex (Donoghue and Wise, 1982). These findings imply that various cells within the cerebral cortex may have a different acid-base homeostasis, at least with regards to membrane permeability and ionic exchange mechanisms for $CO_3^{2-}$ and/or $HCO_3^-$.

In support of this, in experiments where microelectrodes were implanted at a depth of 0.5 mm (for simultaneous measurement of $[CO_3^{2-}]_e$ and cortical dialysate lactate), in contrast to 1 mm in all other microelectrode experiments, this pattern of changes was not observed and a shift in $[CO_3^{2-}]_e$ was consistently associated with anoxic depolarisation.

Studies of the rat somatosensory cortex have shown that the laminae of the cortex contain different cellular components, for example, neurons are more abundant in all cortical layers except in layers I and VI (60 and 1600 $\mu$m from the brain surface, respectively) where glial cells exceed neurons (Bass et al., 1971). Although the thickness and, as such the depth of the laminae, may alter slightly across the cortex, implantation of the $CO_3^{2-}$-selective microelectrode at depths of 0.5 and 1.0 mm into the cortex, would result in the electrode tip being in layers III, and IV or V, respectively (Paxinos and Watson, 1986), i.e. laminae containing primarily neurons. However, an exaggerated implantation of the electrode to a slightly greater depth (for example at 1.2 mm) could result in the electrode tip entering layer VI (Paxinos and Watson, 1986), i.e. laminae with more glial cells. This could imply that the different pattern of changes (i.e. no shift in $[CO_3^{2-}]_e$ with anoxic depolarisation) may be due to recording from a different laminae of the cortex than originally intended, one which has been found to have a greater density of glial cells than neurons (Bass et al., 1971).

It is interesting that in cases where no shift in $[CO_3^{2-}]_e$ was apparent, the steady decrease was always preceded by an increase in $[CO_3^{2-}]_e$, a phenomenon that was never observed in cases where there was a $[CO_3^{2-}]_e$ shift with depolarisation. This increase, which may reflect an efflux of $CO_3^{2-}$ into the extracellular space, was associated with membrane hyperpolarisation, which could imply the activation of an electrogenic process. The electrogenic $Na^+$-$HCO_3^-$ cotransporter found in glial cells could be reversed when the membrane potential becomes hyperpolarised, resulting in efflux of $CO_3^{2-}$. Glial cells may actively buffer transient changes in $pH_e$ by releasing $HCO_3^-/CO_3^{2-}$ at the expense of their own pH homeostasis (Astion et al., 1987; Katsura et al., 1994a). Regulation of $pH_e$ may help sustain neuronal pH homeostasis since $pH_i$ regulation may only occur if $pH_e$ is maintained close to normal values, because $H^+$ extrusion is inhibited by reduction of $pH_e$ (Roos and Boron, 1981; Katsura et al., 1994a).

The absence of a transient increase extracellular $CO_3^{2-}$ with anoxic depolarisation in these cases, after an initial efflux of $CO_3^{2-}$, could reflect intracellular depletion of $CO_3^{2-}$ in the cells surrounding the electrode tip. Under ischaemic conditions, glial cells have

been found to become severely acidified (approximately pH 4.5 to 5.5) which has been attributed to the loss of internal $HCO_3^-$ stores from these cells (Kraig and Chesler, 1990). In cells with reduced or depleted intracellular $CO_3^{2-}/HCO_3^-$ levels, with anoxic depolarisation and opening of ionic channels, there would be no outward flux of $CO_3^{2-}$, and therefore the transient increase in $[CO_3^{2-}]_e$ would be absent.

### 7.3.3.2 Extracellular Lactate Changes

Efflux of lactate via a transporter dependent on functional plasma membrane implies inactivation of this efflux with anoxic depolarisation, since the latter event reflects the collapse of transmembrane ionic gradients. The sudden switch from increase to decrease in extracellular lactate which occurred with anoxic depolarisation (Fig. 6.1.A) agrees with this hypothesis. This rapid change in the time course of changes in dialysate lactate cannot be exclusively attributed to glucose shortage (Lowry et al., 1964). The decrease in extracellular lactate observed at this point presumably reflected cessation of lactate transport, superimposed to persistent microdialysis drainage of the region under study (Benveniste and Hüttemeier, 1990). The drop in extracellular lactate could also partly reflect a reduction in the rate of lactate production, subsequent to glucose shortage and inhibition of anaerobic glycolysis by the influx of $Na^+$ and efflux of $K^+$ occurring with anoxic depolarisation (see Section 7.2.2). The magnitude of the decrease in lactate with anoxic depolarisation may be amplified by a decrease in microdialysis recovery (Nicholson and Phillips, 1981; Scheller and Kolb, 1991) resulting from the shrinkage of the extracellular space known to be associated with this ischaemic event (Kraig and Nicholson, 1978; Hansen and Olsen, 1980; Hansen and Zeuthen, 1981).

Changes in dialysate lactate during transient forebrain ischaemia were clearly dependent on the alteration in the DC potential during the insult. In cases where depolarisation was delayed, striatal lactate continued to increase until depolarisation occurred, which was associated with a slight decrease (Fig. 6.1.B) before recirculation. When ischaemia was not severe enough to cause anoxic depolarisation (i.e. incomplete ischaemia), the increase in lactate persisted throughout the ischaemic insult (Fig. 6.1.C). This suggested that in the absence of depolarisation, lactate continued to be produced intracellularly and its transport into the extracellular space remained functional.

7.3.3.3 Implications of These Phenomena

The alkalotic shift in $[H^+]_e$ implies than an acid shift of $[H^+]_i$ occurs simultaneously with each transient alkalotic shift of $[H^+]_e$, and that intracellular biochemical processes are suddenly exposed to a more severe acidosis that will be sustained until energy becomes available again to restore ionic gradients. Measurement of the simultaneous changes of $[H^+]_i$ and $[H^+]_e$ in and around spinal cord motorneurons during application of excitatory amino acids, revealed an acidic transient of $[H^+]_i$ associated with the alkalotic $[H^+]_e$ transient occurring with depolarisation (Endres et al., 1986). It is possible that such a change in $pH_i$ may be associated with anoxic depolarisation, which would be a potential threat to the survival of depolarised neurons, along with other well established damaging events known to occur following breakdown of ionic gradients, in particular: net movement of $Na^+$ and $Ca^{2+}$ into the cells leading to a toxic intracellular accumulation of these ions (Goldberg et al., 1986), dramatic release of neurotransmitters resulting in deleteriously high extracellular levels of these substances (Obrenovitch and Richards, 1995), and osmotic swelling of the intracellular compartment at the expense of the extracellular space (Hansen and Zeuthen, 1981).

Lactate efflux is markedly reduced when anoxic depolarisation occurs which implies that lactate removal from intracellular compartments may be impaired when energy supplies to the brain can no longer maintain membrane integrity and function. Collapse of intracellular acid-base regulation subsequent to "trapping" of intracellular lactate and increased cellular membrane permeability to $H^+$ and pH-changing anions is likely to aggravate the deleterious effects of ischaemia.

Whatever the residual efficacy of ion exchangers to control intracellular acidosis after anoxic depolarisation, their actions are abolished. Depolarisation is maintained and the transmembrane ionic gradients remain disrupted. During this period $pH_e$ reaches a steady state, as do extracellular $CO_3^{2-}$ and lactate. No further $H^+$ or lactate is produced since the brain is a closed system. Disruption of the ionic gradients implies that intra- and extracellular compartments may become close to each other. Lactate cannot be used as a alternative fuel source as no oxygen is available. This state persists until reperfusion.

## 7.3.4 Post-Ischaemic Recovery of Acid-Base Homeostasis

### 7.3.4.1 Extracellular Acid-Base Changes

Within the first two minutes of recirculation oxidative phosphorylation is partially resumed and ATP is resynthesised (Ekholm et al., 1993). Since brain lactate content was not reduced at this point (Ekholm et al., 1993), it is likely that the substrate for oxidative phosphorylation is exogenous glucose. Although ATP synthesis is resumed, PCr levels are not normalised at this time, due to the persisting intracellular acidosis which shifts the creatine kinase equilibrium in the direction of PCr hydrolysis (Siesjö et al., 1972).

Recirculation was accompanied by repolarisation, which is associated with a rapid recovery of $[K^+]_e$ reflecting resumption of $Na^+$ and $K^+$ transport when ATP becomes available (Ekholm et al., 1993). Only partial recovery of tissue energy state is required to fuel $Na^+/K^+$-ATPase, since resumption of $Na^+$ and $K^+$ transport occurred at tissue ATP concentration of only 30-50 % of pre-ischaemic levels (Ekholm et al., 1993), i.e. at a concentration which leads to massive downhill fluxes of ions (anoxic depolarisation) with onset of ischaemia.

Cellular repolarisation was associated with a slight drop in $[CO_3^{2-}]_e$ (Figs. 6.1.D and 6.1.E). Transient increases in $[H^+]_e$ have also been observed with repolarisation after ischaemia (Nemoto and Frinak, 1981; Kraig et al., 1983, 1987; Obrenovitch et al., 1990a). The transient increase in $[H^+]_e$ and decrease in $[CO_3^{2-}]_e$ with repolarisation may reflect restoration of normal membrane ionic permeability and active recovery of $[H^+]_i$ regulation subsequent to that of the inward $Na^+$ gradient, resulting in a very effective extrusion of $H^+$ and/or influx of pH-changing anions. Enhanced ATP hydrolysis due to the ionic pumps actively restoring the transmembrane ionic gradients, which are re-established within 2-5 min of recirculation (Siemkowicz and Hansen, 1981; Silver and Erecinska, 1992), may also contribute to the increased production of $H^+$.

This increase and decrease in extracellular $H^+$ and $CO_3^{2-}$ with repolarisation, respectively, indicate a transient worsening of extracellular acidosis with repolarisation. With the restoration of cerebral blood flow, hyperaemic washout of accumulated $CO_2$, during the first 5 min of reperfusion (von Hanwehr et al., 1986), may be a contribute to the recovery of acid-base homeostasis (Kraig et al., 1986; Katsura et al., 1992).

Despite the marked acidosis during ischaemia, $pH_i$ normalises after approximately 15 min of recirculation (Mabe et al., 1983; LaManna et al., 1995). This normalisation

is not due to oxidation of lactate, since its concentration was only moderately reduced at this time (Mabe et al., 1983), but probably reflects enhancement of $Na^+/H^+$ exchange leading to a rapid extrusion of $H^+$ from cells. Therefore, recovery of $pH_i$ after transient cerebral ischaemia will be affected by the degree of ATP recovery, i.e. an accelerated recovery of $pH_i$ at greater ATP levels (Saito et al., 1992). Restoration of $pH_i$ was associated with a subsequent transient alkalosis preceding the final return of $pH_i$ to normal (Mabe et al., 1983; Siesjö et al., 1985a; von Hanwehr et al., 1986; Paschen et al., 1987). Oxidation of lactate, with the removal of a stoichiometrical amount of $H^+$, could contribute to the alkalosis at a time when $Na^+/H^+$ exchange has brought $pH_i$ back to resting levels.

#### 7.3.4.2 Extracellular Lactate Changes

The rapid increase in the extracellular concentration of lactate with recirculation, synchronous with repolarisation (Figs. 6.1.A and 6.1.B), supports the concept that lactate formation and/or its transport out of brain cells may be inhibited by anoxic depolarisation. The finding that this increase is slower than that observed with the onset of ischaemia may reflect the dependence of lactate efflux on restoration of ionic gradients. In support of this, when no depolarisation occurred during the ischaemic insult, there was no further increase in lactate with repolarisation, suggesting that lactate was not trapped intracellularly.

Resumption of $H^+$ gradient would facilitate the efflux of lactate which was trapped when the cells were depolarised and the transmembrane ionic gradients disrupted. Even though recirculation supplies further glucose to the tissue, impaired mitochondrial metabolism may cause additional lactate to accumulate (Hillered et al., 1985; Sutherland et al., 1990). Findings suggest that there is also a further decrease in $pH_i$ (Chopp et al., 1987) which implies that lactate is produced during recirculation. Enhanced lactic acidosis does not adversely affect early postischaemic recovery of mitochondrial function (Hillered et al., 1985).

The sustained increase in lactate during reperfusion also confirmed that normalisation of brain tissue acid-base homeostasis is progressive, much slower than the recovery of transmembrane gradients of $Na^+$, $K^+$, and $Ca^{2+}$ (Obrenovitch et al., 1990b). The return of extracellular lactate to pre-ischaemic levels, reached after about 1 hour of reperfusion, is unlikely to result mainly from clearance via the vascular system, as monocarboxylic

acid transport across the BBB is negligible in the adult rat (Cremer et al., 1979; Kuhr et al., 1988; see Section 7.2.2). Therefore, it is likely that clearance of extracellular lactate probably occurred through re-entry into the cells, and recycling to pyruvate with normalised oxygen demand (Zimmer and Lang, 1975; Kuhr et al., 1988). Several findings support this: (i) brain tissue can restore and maintain basic electrical and biochemical functions after ischaemia for a limited time period without supply of glucose (Bock et al., 1993); (ii) tissue glucose levels did not reach preischaemic values until lactate stores were normalised, probably due to a partial replacement of glucose by lactate in the early reperfusion period (Bock et al., 1993); (iii) there was no period of high lactate production immediately following hypoxia in brain slices (Kauppinen and Williams, 1990), suggesting that the slow return of lactate to normal levels *in vivo* was not a consequence of continued lactate production, but a delayed removal of lactate by oxidation; (iv) inhibition of glycolysis with iodoacetate neither impeded normalisation of ion homeostasis, nor impaired reappearance of EEG after ischaemia in perfused rat brain (Bock et al., 1993).

The delay in lactate oxidation after reoxygenation may be pH dependent. Substrate binding to lactate dehydrogenase requires interaction with an amino acid residue (histidine-195), the charge of which is altered by changes in pH. Although pyruvate binding requires this group to be protonated, lactate binding and oxidation require it to be unprotonated. Thus if pH is low and the group is protonated, lactate oxidation must be blocked (or slowed) kinetically. Therefore, lactate oxidation is probably not accelerated until ATP production is resumed and the $Na^+$ gradient is restored to allow $H^+$ extrusion by $Na^+/H^+$ exchange (see Siesjö et al., 1990). However, since this exchanger operates very slowly at low extracellular pH values, the extrusion of $H^+$ is also slow until extracellular pH has increased.

During reperfusion, tissue glucose accumulates reaching concentrations above those observed before ischaemia (Duffy et al., 1972; Ljunggren et al., 1974a,b; Hillered et al., 1985; Bock et al., 1993). During the postischaemic period, mitochondria are supplied with pyruvate coming from two sources, the accumulated lactate, and resumed aerobic glycolysis. Since the latter may be impaired early in reperfusion as long as the cytosolic pH and ATP levels are low (Duckrow et al., 1981; Tanaka et al., 1986), it is likely that most of the pyruvate for oxidative metabolism comes from the lactate stores rather than glucose. Recovery of glycolysis occurred by 60 min of reperfusion (Sutherland et al.,

1990) as indicated by normal levels of tissue glucose (Bock et al., 1993).

Lactate accumulation during cerebral ischaemia was originally considered detrimental to postischaemic recovery, but it is now considered that the lactate anion itself is relatively benign (Siesjö, 1988a). Moreover, the use of lactate as a metabolic fuel in the brain *in vitro* and *in vivo* (Schurr et al. 1988; Bock et al., 1993), suggests that lactate may serve as an alternative energy source for brain cells during the early postischaemic period when cerebral blood flow is often reduced (Pulsinelli et al., 1982). Therefore, lactate is not strictly an end product of energy metabolism, but rather a secondary energy substrate, which under certain circumstances (i.e. after ischaemia) may become the principal energy source. Lactate in the ECF constitutes a pool of intermediates of carbohydrate metabolism (Larrabee, 1992) that could be used by cells, especially those that may require more energy to regain homeostasis after ischaemia (i.e. neurons) (Dienel et al., 1995; Larrabee, 1995).

In contrast to the rapid repolarisation, EEG recovery was gradual and incomplete after 80 min of recirculation. The slow recovery of EEG suggests that disturbed electrical transmission persists, since ionic gradients are rapidly reestablished (Ekholm et al., 1993). EEG recovery after ischaemia was greater in the cortex than in the striatum suggesting that the striatum may be more vulnerable than the cortex in this model of ischaemia, at least with regards to early functional recovery (Smith et al., 1984; Ginsberg et al., 1985). In support of this, EEG recovery win the striatum as improved when depolarisation was delayed.

## 7.4 Probenecid Inhibition of Lactate Transport in the Striatum

### 7.4.1. Lactate Transport and the Effect of Probenecid

Intracerebral application of probenecid, an inhibitor of monocarboxylic acid transport, concentration-dependently increased the basal level of extracellular lactate. The differential increases in lactate were less marked with the higher concentrations of probenecid (i.e. between 10 and 20 mM), indicating that this effect was saturable. Probenecid-induced increases in the brain extracellular levels of other substances have also been observed, including kynurenic acid (Moroni et al., 1988; Russi et al., 1992; Miller et al., 1992), and the monoamine metabolites 5-hydroxyindoleacetic acid and homovanillic acid (Korf and Van Praag, 1971; Van der Poel et al., 1977).

The probenecid-induced increase in extracellular lactate was unlikely to reflect a direct influence on the brain tissue production of lactate since the drug, at concentrations that blocked lactate efflux from the CSF, had no effect on cerebral content of ATP, ADP, AMP, PCr or Cr (MacMillan, 1987). Intravenous administration of probenecid also had no effect on blood flow in the striatum (La Manna et al., 1993).

Although the removal of extracellular lactate across the BBB is relatively low (e.g. two orders of magnitude less efficient than its transport across the cellular membrane; Cremer et al., 1979; Kuhr et al., 1988), the effect of probenecid on BBB transport could still play a role in the probenecid-induced increase of extracellular lactate, as this drug inhibits BBB transport (Pardridge and Oldendorf, 1977; Yulwiler et al., 1982). However, intraperitoneal administration of probenecid sufficient enough to block transport from the CSF (MacMillan, 1987) failed to increase extracellular lactate within the striatum (Kuhr et al., 1988). This may suggest that the transport of lactate across the BBB did not contribute significantly to the probenecid-induced increase of extracellular lactate observed in this study. Alternatively, the extracellular concentration of probenecid obtained with microdialysis application and systemic administration may not be the same due to different compartmentation of the drug. Different gradients of probenecid across the cellular membrane and BBB may produce different effects as this drug is a competitive (i.e. transportable) inhibitor of anion transport in the CNS. With systemic administration probenecid distributes rapidly and is likely to inhibit, bidirectionally, probenecid-sensitive transports of the BBB and cellular membranes. In contrast, with sustained application of probenecid to the ECS by microdialysis, the concentration of the drug is kept higher

extracellularly than intracellularly and in the plasma and, therefore, this mode of drug application may exert a greater effect on cellular transport.

Although probenecid inhibits the cellular transport of lactate, microdialysis application induced a large increase in extracellular lactate. Increases in extracellular lactate associated with local administration of probenecid have been observed previously and analysis of the cellular lactate transport system suggested that the kinetic parameters of the transporter were changed in the presence of high extracellular probenecid (Kuhr et al., 1988). The important kinetic parameters relating to normal physiological function of the transporter are the affinity for the substrate ($K_m$) and the maximum velocity ($V_{max}$) for net efflux. Application of probenecid decreased the transport affinity (as indicated by an increased in $K_m$) without a change in $V_{max}$, which is typical of competitive inhibition. Therefore, as detailed below, high extracellular concentrations of this competitive inhibitor may increase the steady-state concentration of lactate through heteroexchange.

Heteroexchange of probenecid with lactate probably implies (Fig. 7.4.A): lactate binding to the intracellular site, followed by its translocation and release; probenecid binding to the external site and translocation into the cell; and release of probenecid in exchange with another molecule of lactate. The findings of this study are consistent with this mechanism, (i) probenecid concentration-dependently increased extracellular lactate and the rate of lactate efflux; (ii) lactate release evoked by probenecid was saturable as there was no significant difference in extracellular lactate when probenecid was increased from 10 to 20 mM; and (iii) the recovery of lactate after transient application of probenecid showed that these effects were reversible.

Heteroexchange has been shown to occur with other transport systems: (i) infusion of glutamate into the neostriatum elevated neostriatal ascorbate release (Cammack et al., 1991; Grünewald, 1993); (ii) hippocampal glutamate-induced ascorbate release was dose-dependently inhibited by co-administration of the glutamate reuptake blocker homocysteic acid (Cammack et al., 1991); and (iii) L-*trans*-pyrrolidine-2,4-dicarboxylate (L-*trans*-PDC), a competitive inhibitor of glutamate transport, enhanced glutamate release in hippocampal slices (Issacson and Nicoll, 1993) and dose-dependently stimulated the release of exogenous applied D-[$^3$H] aspartate from cerebellar granule cells (Griffiths et al., 1994). It is worth noting that, similarly to probenecid, kinetic characterisation of D-aspartate uptake in cultured cerebellar granule cells and astrocytes in the presence of L-*trans*-PDC, showed an increase in the $K_m$ value without a corresponding alteration in

$V_{max}$, with an increased efflux of D-aspartate (Griffiths et al., 1994).

A contribution of passive diffusion to the probenecid-induced increase in lactate cannot be ruled out. Despite the relatively small contribution of passive diffusion to intracellular lactate removal under resting conditions, inhibition of cellular lactate efflux which is the major route of intracellular lactate removal, could increase intracellular lactate, and therefore the gradient for lactate removal to the outside via passive diffusion (i.e. a probenecid-insensitive process). Previous data of LaManna et al. (1993) and Schneider et al. (1993) with saturated or blocked carrier-mediated lactate transport supported this hypothesis.

Although high concentrations of probenecid can be toxic to brain tissue (Assaf et al., 1990), the changes observed in this study are not toxic effects. Transient perfusion of probenecid through the microdialysis probe did not appear to have long-lasting effects on dialysate lactate or on the DC potential, both variables returning to control levels after probenecid application.

One interesting observation is that although the extracellular level of lactate increased, there was no significant decrease in dialysate pH. This apparent discrepancy can be explained as follows: (i) the $H^+$ cotransported with lactate into the extracellular space was buffered; (ii) $H^+$ may be released more slowly on the outside than lactate, i.e. lactate upon translocation from the inside, is released on the outside and probenecid binds before the $H^+$ is released from the transporter; or (iii) the order of binding may not be strictly as depicted in Fig.7.4.A.

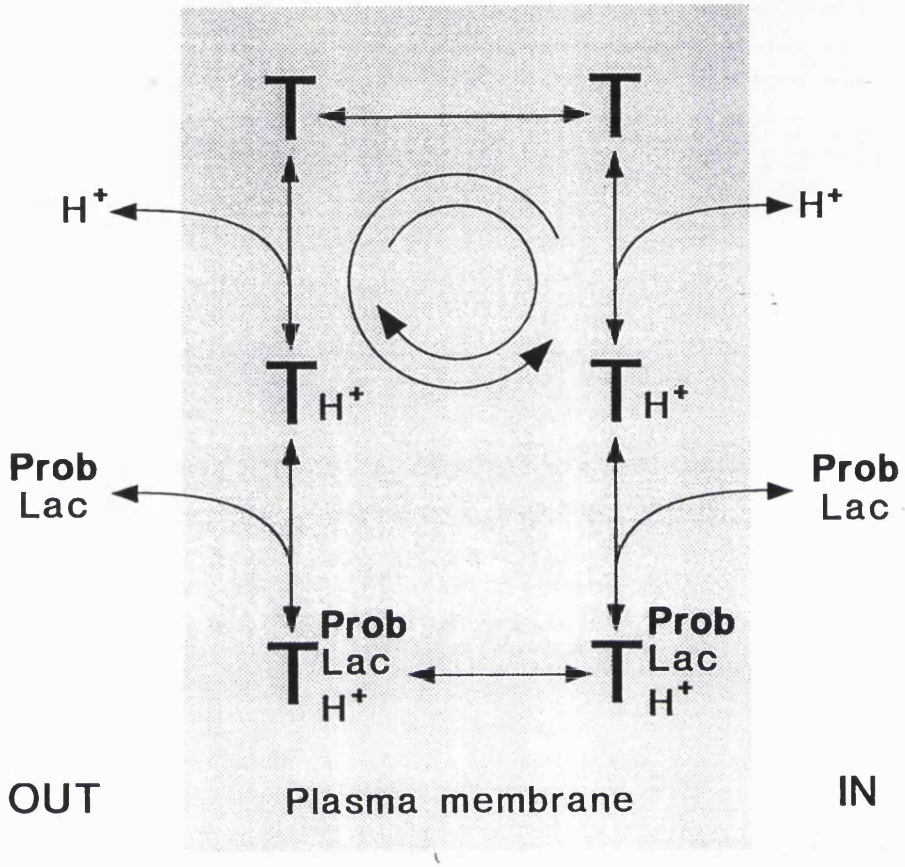


**FIG. 7.4.A** Model of heteroexchange illustrating the mechanism through which application of probenecid may increase extracellular lactate. According to this model: lactate binds to the internal site of the transporter, is translocated and released externally; probenecid binds to the external site and is translocated into the cell; release of probenecid occurs in exchange with another molecule of lactate which is then transported to the outside. This model is based on that described in Section 1.2.1.6 and Fig. 1.2.A.

## 7.4.2 High Extracellular $K^+$ and Initiation of Spreading Depression

### 7.4.2.1 Effect of Probenecid on $K^+$-Evoked Changes in Extracellular Lactate

Intracerebral application of probenecid suppressed the increases in extracellular lactate associated with periods of repolarisation during $K^+$-induced SD. With the onset of the $K^+$-stimulus extracellular lactate decreased, remaining at this reduced level until after the challenge when it returned to pre-$K^+$-stimulus levels. When a spike of depolarisation occurred (with 5 mM probenecid), there was no corresponding increase in lactate of the type observed after depolarisation during the control $K^+$ stimulus. The marked increase in lactate, consistently observed with repolarisation after the control stimulus was also absent in the presence of probenecid.

In contrast to ischaemia, 5 mM probenecid was sufficient to completely blocked the increases in lactate associated with SD. This is probably because the amount of lactate produced during SD is less in comparison to ischaemia.

The fact that, with probenecid, extracellular lactate decreased during the application of high $K^+$ medium could reflect a reduced lactate production during the sustained depolarisation produced by $K^+$, subsequent to inhibition of glycolysis by increased intracellular levels of $Na^+$ (as discussed in Section 7.2.2). On the other hand, the decrease in lactate could reflect an alteration in the heteroexchange mechanism by $K^+$. Heteroexchange may be altered due to a disruption of the $H^+$ gradient in the persistently depolarised cells surrounding the microdialysis probe. This is supported by the finding that during high $K^+$ application in the absence of probenecid, if a transient depolarisation occurred later in the challenge, extracellular lactate initially decreased with the onset of the stimulus (Fig. 6.4.B). It could be speculated that if no peaks of further depolarisation had occurred during the stimulus without probenecid (although this was never observed) the pattern of changes in lactate could have been similar to those seen with probenecid, i.e. a sustained low lactate level throughout the challenge. Therefore, in the presence of probenecid, changes in extracellular lactate may reflect alteration of lactate efflux and/or that of heteroexchange.

### 7.4.2.2 Effect of Probenecid on $K^+$-Evoked DC Potential Changes and Initiation of Spreading Depression

The finding that perfusion of probenecid altered the $K^+$-induced changes in the DC potential was unexpected. The sustained negative shift in the DC potential did not increase

with the $K^+$ concentration as seen in challenges without probenecid, suggesting that probenecid partially inhibited the depolarisation of the cells surrounding the microdialysis probe. Probenecid (5 and 20 mM) also markedly inhibited SD elicitation.

As both elicitation and propagation of SD require activation of the NMDA receptor ionophore complex (Lauritzen and Hansen, 1992; Sheardown, 1993), probenecid may inhibit SD by reducing NMDA receptor activation. Inhibition of NMDA receptors could result from extracellular acidosis associated with the probenecid-induced increase in extracellular lactate. Excitatory currents associated with activation of NMDA receptors are very sensitive to changes in $pH_o$; decreases in $pH_o$ reduced the magnitude of such currents in cultured neurons by a non-competitive action of $H^+$ on an extracellular site of the complex (Tang et al., 1990; Vyklicky et al., 1990; Traynelis and Cull-Candy, 1991). However, the probenecid-induced increase in extracellular lactate in this study was not associated with a significant reduction in dialysate pH, suggesting that increases in extracellular $H^+$ may have been buffered. Another plausible mechanism may be increased extracellular kynurenic acid. Kynurenic acid, the only known endogenous antagonist of glutamate receptors (Swartz et al., 1990), has affinity for the agonist recognition site of the NMDA-receptor channel complex, and is several times more potent at the glycine allosteric site (Birch et al., 1988; Kessler et al., 1989). Administered systemically kynurenic acid protects against ischaemia (Germano et al., 1987; Andine et al., 1988) and experimental brain injury (Hicks et al., 1994). Probenecid increased the concentrations of kynurenic acid in brain tissue, ECF and CSF by blocking its excretion (Moroni et al., 1988; Swartz et al., 1990; Miller et al., 1992; Nozaki and Beal, 1992; Russi et al., 1992; Vecsei et al., 1992a). Either alone or in combination with L-kynurenine (the precursor of L-kynurenic acid), probenecid protected against hypoxia-ischaemia, NMDA neurotoxicity and NMDA induced seizures (Nozaki and Beal, 1992; Vecsei et al., 1992b; Kravzov et al., 1993).

Probenecid also increases the concentration of cyclic nucleotides in the ECF and CSF (Sebens and Korf, 1975; Luo et al., 1994). As SD depends on the activation of NMDA receptor channel complexes which increases brain tissue cyclic guanosine 5'-monophosphate (cGMP) possibly through synthesis of nitric oxide (Garthwaite et al., 1988; Garthwaite, 1991), inhibition of SD by probenecid may be linked to an indirect action on second messenger systems. The fact that SD is immediately followed by a refractory period lasting several minutes when further depolarisation cannot be elicited

(Bures et al., 1974) during which the local brain tissue content of cGMP is markedly increased (Gault et al., 1994), supports this hypothesis.

Probenecid alters the brain clearance of the acidic monoamine metabolites homovanillic acid and 5-hydroxyindoleacetic acid (Sarna et al., 1983; Cumming et al., 1992). As the striatum is the brain structure with the highest density of dopaminergic terminals, and the dopamine receptor agonist quinpirole decreased the velocity of SD propagation in the retina (de Azeredo and Ribeiro, 1992), an interaction of probenecid with dopamine systems could contribute to the inhibition of SD. However, as the probenecid-induced increase in extracellular homovanillic acid was not associated with increased extracellular dopamine levels (Cumming et al., 1992), and microdialysis probenecid application produced SD inhibition in the rat cortex (Urenjak, J. and Obrenovitch, T.P., personal communication), it is unlikely that dopamine plays an important role in the inhibition of SD observed in this study. In contrast, to the marked inhibition of $K^+$-induced SD, probenecid had little effect on local depolarisation produced by co-application with NMDA (Urenjak et al., 1996). This could suggest that inhibition of SD elicitation by probenecid may not be linked to blockade of NMDA-receptor activation.

The effects of probenecid on lactate and SD may not be linked. There is little difference in effect between 5 and 20 mM probenecid on extracellular lactate, lactate only increased slightly when the probenecid concentration was increased from 5 to 20 mM. However, the effect between these two probenecid concentrations on SD was more significant. Probenecid is a general inhibitor and therefore produced changes in other anions (besides lactate) which may affect SD.

### 7.4.3 Effect of Probenecid on Extracellular Lactate During Terminal Complete Ischaemia (Cardiac Arrest)

Under normal conditions, terminal complete ischaemia produced a rapid, transient increase in extracellular lactate, which started to decrease after anoxic depolarisation. This is expected from a carrier-mediated system driven by $H^+$, since transport of lactate out of the cell should cease once the $H^+$ gradient is abolished. Despite the decrease after anoxic depolarisation, however, lactate did not return to the pre-ischaemic level, indicating a slow but persistent leakage from the cells surrounding the microdialysis probe. It is possible that these changes in dialysate lactate following anoxic depolarisation

may be exacerbated by a decrease in microdialysis recovery (Nicholson and Phillips, 1981; Scheller and Kolb, 1991) resulting from the shrinkage of the extracellular space known to be associated with this event (Kraig and Nicholson, 1978; Hansen and Olsen, 1980; Hansen and Zeuthen, 1981).

Ischaemia-induced increase in extracellular lactate observed in the presence of 5 mM probenecid was greatly reduced, as was its rate of increase, and it was abolished with 20 mM probenecid. With both concentrations of probenecid, lactate decreased rapidly after cardiac arrest to a level significantly less than that before ischaemia. Application of the lower dose of probenecid (5 mM) was not high enough to block lactate efflux totally after complete ischaemia probably because intracellular lactate reaches high levels under these conditions. Complete inhibition of lactate efflux by 20 mM probenecid provides evidence that the removal of intracellularly accumulated lactate during terminal ischaemia is via a carrier-mediated process, and emphasises the importance of this transport system in cellular lactate removal when anaerobic glycolysis becomes a major source of energy.

### 7.4.4 Transient Forebrain Ischaemia

#### 7.4.4.1 Effect of Probenecid on Ischaemia-Induced Changes in Extracellular Lactate

As observed after complete terminal ischaemia, the lower dose of probenecid partly blocked lactate efflux, and 20 mM of probenecid was necessary to completely block the efflux of intracellular lactate associated with the onset of transient forebrain ischaemia. With reperfusion, extracellular lactate increased, but did not reach the levels obtained in the absence of probenecid. The recovery of lactate during reperfusion was slow since probenecid blocked the re-uptake of lactate into the cells, this probably being the major route for the removal of extracellular lactate (Zimmer and Lang, 1975; Kuhr et al., 1988; see Section 7.2.2). Additional lactate formed due to impaired mitochondrial metabolism which may contribute to the marked increase in extracellular lactate after ischaemia, was absent with probenecid, since this drug would block its efflux.

When cardiac arrest was preceded by a period of forebrain ischaemia, there was a small increase in lactate with cardiac arrest in the presence of 20 mM probenecid. This was unexpected as, in the other experiments, cardiac arrest with 20 mM of this drug, was not associated with an increase in lactate. As recovery of extracellular lactate after ischaemia was slow in the presence of the drug, the intracellular lactate concentration may have been higher before cardiac arrest, than under normal conditions. Subsequently, with

cardiac arrest, a small efflux of lactate may have occurred as there was a higher level of cellular lactate to compete for the binding sites of the transporter.

#### 7.4.4.2 Effect of Probenecid on Ischaemia-Induced Changes in Electrophysiological Recordings

Although systemic administration of high doses of probenecid was reported to produce convulsions (McKinney et al., 1951; Akiyama et al., 1981), 20 mM probenecid perfused through the microdialysis probe did not produce significant changes in the amplitude of local EEG in the striatum. This suggests that the extracellular concentration of probenecid in the tissue surrounding the probe was presumably much lower than that of the perfusion medium, firstly because diffusion of the drug was restricted by the dialysis membrane (Scheller and Kolb, 1991), and secondly because probenecid probably diffused rapidly away from the site of application as it is a lipid-soluble compound (Roos et al., 1980) and a substrate of organic anion transports (Kuhr et al., 1988; Yulwiler et al., 1982; Miller et al., 1992). In contrast with the EEG, probenecid application evoked a negative shift of the DC potential, this was observed in all experiments in which the DC potential was recorded. The effect on the DC potential may result from probenecid being a competitive (i.e. transportable) inhibitor of organic anion exchanges, of which some are presumably coupled to the movement of ions such as $Na^+$, $K^+$, $H^+$, etc. Applied at high concentrations to the extracellular space, probenecid may be actively transported intracellularly, altering transmembrane ionic gradients and, therefore, the polarisation of the cellular membrane. This hypothesis is supported by the fact that 20 mM probenecid produced a rapid negativation of the DC potential (i.e. immediately after switching from ACSF to probenecid-medium, when the intracellular/extracellular gradient of probenecid was maximum), followed by partial normalisation while probenecid was still being applied (i.e. as the transmembrane probenecid gradient was progressively reduced (Fig. 6.5.L).

Although probenecid did not delay the occurrence of anoxic depolarisation, the drug significantly reduced the amplitude of the negative shift in the DC potential. This effect may be a consequence of the "depolarising" effect of probenecid, since perfusion of 20 mM of the drug through the microdialysis probe produced an initial negative shift of around 5 mV. However, most of this effect had regressed when ischaemia was induced (see above), and probenecid markedly inhibited $K^+$-induced depolarisation in the rat striatum (see Section 7.4.2.2), suggesting that this drug may have a direct effect on the amplitude of anoxic depolarisation.

# CHAPTER 8 GENERAL SUMMARY AND FUTURE DIRECTIONS

Experimental data strongly suggest that disruption of acid-base homeostasis is a common and major factor responsible for brain tissue damage resulting from inadequate oxygen supply to the brain. This investigation, by focusing on the extracellular activities of the variables involved in the regulation of brain tissue acid-base homeostasis, has contributed to a better understanding of the mechanisms underlying brain tissue acidification during both global ischaemia and spreading depression. The combination of two complementary methods within the same brain region of animal models (i.e. ion-selective microelectrodes and microdialysis) has largely contributed to the originality of the data.

Ischaemia markedly alters acid-base homeostasis by stimulation of anaerobic glycolysis with conversion of endogenous glucose (and glycogen) to lactic acid, and impairment of the ion exchanges contributing to intracellular pH regulation subsequent to deterioration of cerebral energy state. Spreading depression, which occurs repeatedly in the ischaemic penumbra, produces a transient disruption in ionic gradients leading to failure of residual acid-base homeostasis and subsequent acidification of brain tissue.

Direct measurement of extracellular $H^+$ in this study showed that the transmembrane mechanisms contributing to intracellular acid-base regulation are activated early. These mechanisms, which include $Na^+/H^+$ exchange presumably supplemented by $HCO_3^-/Cl^-$ exchanges, are driven by the $Na^+$ gradient maintained by the $Na^+/K^+$-ATPase. The rise in $[H^+]_e$ was accompanied by a decrease in $[CO_3^{2-}]_e$, indicating that progressive reduction of the $H^+$ buffering capacity of the ECF is an early event in ischaemia. A similar pattern of changes in $[H^+]_e$ and $[CO_3^{2-}]_e$ was observed during SD.

This study also showed that extracellular lactate increased markedly with the onset of ischaemia, although it is produced intracellularly by anaerobic glycolysis. This implies that intracellular lactate is rapidly removed to the ECF. Lactate transport across the plasma membrane into the ECF occurs mostly via a carrier mediated transport system and is, therefore, dependent upon transmembrane energy gradients. This is supported by the finding that in the presence of probenecid increases in extracellular lactate before anoxic depolarisation and during SD were no longer detectable. It is likely that lactate is cotransported with $H^+$ as in other tissues and therefore contributes to residual intracellular acid-base regulation early during ischaemia.

Disruption of transmembrane ionic gradients with depolarisation implies collapse of a number of plasmalemnal transport/exchange systems which are driven by these gradients. Anoxic depolarisation was associated with a sudden drop in $[H^+]_e$ and a rise in $[CO_3^{2-}]_e$. These findings suggest it is likely that this transient extracellular alkalosis may result from a rapid redistribution of $H^+$ and/or $CO_3^{2-}/HCO_3^-$ between the intra- and extracellular compartments, subsequent to the opening of ionic channels and/or increased membrane permeability. Analysis of the relationship between the magnitude of these shifts and the level of extracellular acidosis at the time they occurred indirectly supported this hypothesis. These findings imply collapse of active ion exchange mechanisms contributing to residual intracellular acid-base regulation in ischaemia with anoxic depolarisation. The alkalotic shift in $[H^+]_e$ also implies than an acid shift of $[H^+]_i$ occurs simultaneously with each transient alkalotic shift of $[H^+]_e$, and that intracellular biochemical processes are suddenly exposed to a more severe acidosis that will be sustained until energy becomes available again to restore ionic gradients. Anoxic depolarisation and SD markedly reduced lactate efflux suggesting that lactate removal from intracellular compartments is impaired when energy supplies to the brain can no longer maintain membrane integrity and function. These changes, and the observation that probenecid inhibited lactate efflux before anoxic depolarisation and during SD, confirmed that the removal of intracellular lactate during ischaemia and SD mainly occurs via a transporter, dependent on ionic gradients. Therefore, collapse of intracellular acid-base regulation subsequent to "trapping" of intracellular lactate and increased cellular membrane permeability to $H^+$ and pH-changing anions is likely to aggravate the deleterious effects of ischaemia.

This study also revealed that various cells of the central nervous system may have a different acid-base homeostasis, at least with regard to membrane permeability and exchange mechanisms for $HCO_3^-/CO_3^{2-}$, since there were two distinct patterns of $[CO_3^{2-}]_e$ changes associated with ischaemia. It has been suggested that glial cells and neurons behave differently in response during ischaemia, with glial cells buffering changes in $pH_e$ by releasing $HCO_3^-/CO_3^{2-}$ at the expense of their own homeostasis. Regulation of $pH_e$ may help sustain neuronal pH homeostasis since $pH_i$ regulation may only occur as long as $pH_e$ is maintained close to normal values.

Probenecid was used to inhibit lactate transport across the cellular membrane. However, application of probenecid dose-dependently increased extracellular lactate. This effect was opposite to that expected to occur subsequent to inhibition of lactate transport

across the cellular membrane and BBB, because lactate is produced intracellularly and its clearance across the BBB is small. The increase in extracellular lactate may essentially reflect a heteroexchange mechanism, whereby probenecid enters the cells in exchange for lactate, since probenecid is a competitive (i.e. transportable) inhibitor of organic acid transport.

Unexpectedly, direct application of probenecid into the rat striatum inhibited $K^+$-induced SD, and reduced the amplitude of anoxic depolarisation. As both elicitation and propagation of SD require activation of the NMDA-receptor ionophore complex, probenecid may inhibit SD by reducing NMDA-receptor activation, although recent data challenge this hypothesis (Urenjak et al., 1996). These findings may help identify novel strategies to control the elicitation of SD, now recognised as the most likely cause of migraine aura (Lauritzen, 1994) and to be deleterious to neuronal function and survival during focal ischaemia and head trauma (Somjen et al., 1990; Mayevsky et al., 1995).

In conclusion, this investigation has demonstrated that the transmembrane mechanisms contributing to intracellular pH regulation are markedly activated during ischaemia, and remain functional as long as anoxic depolarisation does not occur. Residual acid-base homeostasis is however abolished by anoxic depolarisation, because the driving forces of these mechanisms (i.e. ionic gradients) collapse subsequent to the sudden increase in plasma membrane ionic permeability. As SD implies transient collapse of ionic gradients, recurrent failure of residual acid-base homeostasis may also occur in the penumbra of focal ischaemia and contribute to increasing the volume of infarction (Obrenovitch, 1995). These findings strengthen the concept that anoxic depolarisation and spreading depression are critical events in the pathophysiology of cerebral ischaemia and, therefore, relevant targets for neuroprotective strategies against stroke.

This study has also provided directions for future work which may further elucidate mechanisms involved in acid-base regulation. Possible differences between glial and neuronal acid-base regulation deserve to be ascertained and characterised. The contribution of the different exchange/transport mechanisms known to be involved in acid-base regulation and specific to certain cell types, could be investigated by using specific inhibitors. The role of glial in acid-base regulation during ischaemia may be elucidated by inhibition of carbonic anhydrase with acetazolamide. This enzyme, predominantly located in glial cells and involved in the equilibrium of the $HCO_3^-/H_2CO_3$ buffer system, ensures rapid buffering of sudden changes in pH. Since glia are suspected to have a

higher rate of anaerobic glycolysis and produce more lactate than neurons, it would be relevant to examine the changes in lactate associated with ischaemia and SD using microdialysis and selective inactivation of glial cell metabolism with fluorocitrate (Paulsen et al., 1987).

With the insights into acid-base regulation gained in this study, it would be interesting to assess the validity of treatments based on reducing acidosis to protect brain tissue against transient ischaemic insults. Thrometamine (THAM), a weak alkalinising agent capable of penetrating the BBB, was found to provide some protection against experimental brain concussion (Rosner and Becker, 1984) and ischaemia (Kuyama et al., 1994). The results from such a study would be of primary importance in the protection of the brain of patients with cerebral aneurysm in whom pre-operative temporary artery occlusion may be of benefit. Histological assessment of selective injury to neurons (Ginsberg et al., 1985) and infarction would provide additional insight.

Supplementary research stemming from this investigation should contribute to improving the management of neural injuries resulting from transient inadequate oxygen supply or head trauma, and provide novel insights into the acid-base regulatory mechanisms in mammalian brain.

## REFERENCES

Ahmad, H.R. and Loescheke, H.H. (1983) Evidence for a carrier mediated exchange diffusion of $HCO_3^-$ against $Cl^-$ at the interphase of the central nervous system. In: *Central Neurone Environment* (Schläfke, M.F., Koepchen, H.P. and See, W.R. eds.) Berlin, FRG: Springer. pp 13-21.

Akiyama, T., Sato, M. and Otsuki, S. (1981) Probenecid-induced convulsion and cerebrospinal cyclic nucleotides in the kindling cat preparations. *Brain Nerve (Tokyo)* **33** : 1107-1113.

Ammann, D., Lanter, F., Steiner, R.A., Schulthess, P., Shijo, Y. and Simon, W. (1981) Neutral carrier based on $H^+$ ion-selective microelectrodes for extracellular and intracellular studies. *Anal. Chem.* **53** : 2267-2269.

Andiné, P., Jacobson, I. and Hagberg, H. (1988) Calcium uptake evoked by electrical stimulation is enhanced postischemically and precedes delayed neuronal death in CA1 of rat hippocampus: involvement of *N*-methyl-D-aspartate receptors. *J. Cereb. Blood Flow Metab.* **8** : 799-807.

Aronson, P.S. (1985) Kinetic properties of the plasma membrane $Na^+$-$H^+$ exchanger. *Ann. Rev. Physiol.* **47** : 545-560.

Assaf, H.M., Ricci, A.J., Whittingham, T.S., LaManna, J.C., Ratcheson, R.A. and Lust, W.D. (1990) Lactate compartmentation in hippocampal slices: Evidence for a transporter. *Metab. Brain Dis.* **5** : 143-154.

Astion, M.L. and Orkand, R.K. (1988) Electrogenic $Na^+/HCO_3^-$ cotransport in neuroglia. *Glia* **1** : 355-357.

Astion, M.L., Coles, J.A. and Orkand, R.K. (1987) Effects of bicarbonate on glial cell membrane potential in *Necturus* optic nerve. *Neurosci. Lett.* **76** : 47-52.

Astion, M.L., Chivatal, A., Coles, J.A. and Orkand, R.K. (1989) Intracellular pH regulation in glial cells of *Necturus* optic nerve. *Acta Physiol. Scand.* **136** (suppl. 582) : 64.

Astrup, J., Siesjö, B.K. and Symon, L. (1980) Thresholds of cerebral ischemia - The ischemic penumbra. *Stroke* **12** : 723-725.

Auer, R.N., Wieloch, T., Olsson, Y. and Siesjö, B.K. (1984) The distribution of hypoglycemic brain damage. *Acta Neuropathol.* **64** : 177-191.

Bachelard, H., Cox, D.W., Feeney, J. and Morris, R.G. (1985) $^{31}P$ Nuclear-magnetic resonance studies on superfused cerebral tissues. *Biochem. Soc. Trans.* **13** : 835-839.

Bachelard, H., Morris, P. and Taylor, A. (1994) Metabolism of [U-$^{13}C$] glutamate to glutamine and lactate in cortical slices: An NMR study. *J. Neurochem.* **63** (suppl. 1) : S47B.

Bass, N.H., Hess, H.H., Pope, A. and Thalheimer, C. (1971) Quantitative cytoarchitectonic disruption of neurons, glia, and DNA in rat cerebral cortex. *J. Comp. Neurol.* **143** : 481-490.

Benveniste, H. and Hüttemeier, P.C. (1990) Microdialysis - Theory and Application. *Prog. Neurobiol.* **35** : 195-215.

Benveniste, H., Hansen, A.J. and Ottosen, N.S. (1989) Determination of brain interstitial concentrations by microdialysis. *J. Neurochem.* **52** : 1741-1750.

Ben-Yoseph, O., Badar-Goffer, R.S., Morris, P.G. and Bachelard H.S. (1993) Glycerol 3-phosphate and lactate as indicators of the cerebral cytoplasmic redox state in severe and mild hypoxia respectively: a $^{13}C$- and $^{31}P$-NMR study. *Biochem. J.* **291** : 915-919.

Ben-Yoseph, O., Camp, D.M., Robinson, T.E. and Ross, B.D. (1995) Dynamic measurements of cerebral pentose phosphate pathway activity *in vivo* using [1,6-$^{13}C_2$6,6-$^{2}H_2$] glucose and microdialysis. *J. Neurochem.* **64** : 1336-1342.

Bernard, C. (1878) Leçons sur les Phenomènes de la Vie. Paris: J.-B. Baillieue et fils. Quoted by Nicholson, C. (1980).

Birch, P.J., Grossman, C.J. and Hayes, A.G. (1988) Kynurenic acid antagonises responses to NMDA via an action at the strychnine-insensitive glycine receptor. *Eur. J. Pharmacol.* **154** : 85-87.

Birken, D.L. and Oldendorf, W.H. (1989) *N*-acetyl-L-aspartic acid: A literature review of a compound prominent in $^{1}H$-NMR spectroscopic studies of brain. *Neurosci. Biobehav. Rev.* **13** : 23-31.

Bito, L., Davson, H., Levin, E., Murray, M. and Snider, N. (1966) The concentrations of free amino acids and other electrolytes in cerebrospinal fluid, *in vivo* dialysate of brain, and blood plasma of the dog. *J. Neurochem.* **13** : 1057-1067.

Blomqvist, P., Mabe, H., Ingvar, M. and Siesjö, B.K. (1984) Models for studying long-term recovery following forebrain ischemia in the rat. 1. Circulatory and functional effects of 4-vessel occlusion. *Acta Neurol. Scand.* **69** : 376-384.

Bock, A.C., Scheller, D., Tegtmeier, F., Dengler, K., Zacharias, E. and Höller, M. (1989) Postischemic recovery of electrophysiological function and extracellular pH during normo- and aglycemic reperfusion. *J. Cereb. Blood Flow Metab.* **9**(suppl. 1) : S642.

Bock, A.C., Tegtmeier, F., Hansen, A.J. and Höller, M. (1993) Lactate and postischemic recovery of energy metabolism and electrical activity in the isolated perfused rat brain. *J. Neurosurg. Anesth.* **5** : 94-103.

Bolander, H.G., Persson, L., Hillered, L., D'Argy, R., Ponten, U. and Olsson, Y. (1989) Regional cerebral blood flow and histopathological changes after middle cerebral artery occlusion. *Stroke* **20** : 930-937.

Boris-Möller, F., Drakenberg, T., Elmolén, K., Forsén, S. and Siesjö, B.K. (1988) Evidence against major compartmentalization of $H^+$ in ischemic rat brain tissue. *Neurosci. Lett.* **85** : 113-118.

Bormann, J., Hamill, O.P. and Sakmann, B. (1987) Mechanism of anion permeation through channels gated by glycine and aminobutyric acid in mouse cultured spinal neurons. *J. Physiol.* **385** : 243-286.

Boron, W. (1985) Intracellular pH-regulating mechanism of the squid axon: Relationship between external $Na^+$ and $HCO_3^-$-dependencies. *J. Gen. Physiol.* **85** : 325-345.

Boron, W. and Knakal, R. (1989) Intracellular pH-regulating mechanism of the squid axon: interaction between DNDS and extracellular $Na^+$ and $HCO_3^-$. *J. Gen. Physiol.* **93** : 123-150.

Boron, W.F., McCormick, W.C. and Roos, A. (1979) pH regulation in barnacle muscle fibers: dependence on intracellular and extracellular pH. *Am. J. Physiol.* **237**(3) : C185-C193.

Branston, N.M., Symon, L., Crockard, H.A. and Pasztor, E. (1974) Relationship between the cortical evoded potential and local cortical blood flow following acute middle cerebral artery occlusion in the baboon. *Exp. Neurol.* **45** : 195-208.

Brooks, K.J. and Bachelard, H.S. (1992) The regulation of intracellular pH studied by $^{31}P$- and $^{1}H$-NMR spectroscopy in superfused guinea-pig cerebral cortex slices. *Neurochem. Int.* **21** : 375-379.

Bures, J. and Buresová, O. (1960) Activation of latent foci of spreading cortical depression in rats. *J. Neurophysiol.* **23** : 225-236.

Bures, J., Buresová, O. and Krivanek, J. (1974) The Mechanisms and Applications of Leao's Spreading Depression of Electroencephalographic Activity. Academic Press. New York.

Busa, W.B. and Nuccitelli, R. (1984) Metabolic regulation via intracellular pH. *Am. J. Physiol.* **246** : R409-R438.

Cammack, J., Ghasemzadeh, B. and Adams, R.N. (1991) The pharmacological profile of glutamate-evoked ascorbic acid efflux measured by *in vivo* electrochemistry. *Brain Res.* **565** : 17-22.

Caspers, H., Speckmann, E.-J. and Lehmenkühler, A. (1984) Electrogenesis of slow potential of the brain. In: *Self-Regulation of the Brain and Behavior* (Elbert, T., Rockstroh, B., Lutzenberger, W. and Birbaumer, N., eds.) Springer, Berlin. pp 26-41.

Carvalho, A.P. (1982) Calcium in the nerve cell. In: *Handbook of Neurochemistry. Vol. 1: Chemical and Cellular Architecture* (Lajtha, A. ed.) Plenum Press, New York. pp 69-116.

Chesler, M. (1986) Regulation of intracellular pH in reticulospinal neurons of the lamprey, *Petromyzon marinus*. *J. Physiol. (Lond.)* **381** : 241-261.

Chesler, M. (1990) The regulation and modulation of pH in the nervous system. *Prog. Neurobiol.* **34** : 401-427.

Chesler, M. and Nicholson, C. (1985) Regulation of intracellular pH in vertebrate central neurons. *Brain Res.* **325** : 313-316.

Chesler, M. and Kraig, R.P. (1989) Intracellular pH transients of mammalian astrocytes. *J. Neurosci.* **9** : 2011-2019.

Chesler, M. and Kaila, K. (1992) Modulation of pH by neuronal activity. *Trends Neurosci.* **15** : 396-402.

Chesler, M., Chen, J.C. and Kraig, R.P. (1994) Determination of extracellular bicarbonate and carbon dioxide concentrations in brain slices using carbonate and pH-selective microelectrodes. *J. Neurosci. Meth.* **53** : 129-136.

Choi, D.W. (1988) Calcium-mediated neurotoxicity: Relationship to specific channel types and role in ischaemic damage. *Trends Neurosci.* **11** : 465-469.

Chopp, M., Finak, S., Walton, D.R., Smith, M.B. and Welch, K.M.A. (1987) Intracellular acidosis during and after cerebral ischemia: *In vivo* nuclear magnetic resonance study of hyperglycemia in cats. *Stroke* **18** : 919-923.

Cohen, M.M (1974) Animal models of cerebral infarction. In: *Models of Human Neurological Diseases* (Klawans, H.L. ed.) Amsterdam, Excerpta Medica. pp 205-211.

Conger, K.A., Halsey, J.H., Luo, K.-L., Tan, M.-J., Pohost, G.M. and Hetherington, H.P. (1995) Concomitant EEG, lactate, and phosphorus changes by $^{1}H$ and $^{31}P$ NMR spectroscopy during repeated brief cerebral ischemia. *J. Cereb. Blood Flow Metab.* **15** : 26-32.

Cox, D.W., Morris, P.G. and Bachelard, H.S. (1988) Kinetic analysis of the cerebral creatine kinase reaction under hypoxic and hypoglycaemic conditions *in vitro*. A $^{31}P$-NMR study. *Biochem. J.* **255**(2) : 523-257.

Cremer, J.E. and Heath, D.F. (1974) The estimation of rates of utilization of glucose and ketone bodies in the brain of the suckling rat using compartmental analysis of isotopic data. *Biochem. J.* **142** : 527-544.

Cremer, J.E., Cunningham, V.J., Pardridge, W.M., Braun, L.D. and Oldendorf, W.H. (1979) Kinetics of blood-brain barrier transport of pyruvate, lactate and glucose in suckling, weanling and adult rats. *J. Neurochem.* **33** : 439-445.

Csiba, L., Paschen, W. and Mies, G. (1985) Regional changes in tissue pH and glucose content during cortical spreading depression in rat brain. *Brain Res.* **336** : 167-170.

Cumming, P., Brown, E., Damsma, G. and Fibiger, H. (1992) Formation and clearance of interstitial metabolites of dopamine and serotonin in the rat striatum: an *in vivo* microdialysis study. *J. Neurochem.* **59** : 1905-1914.

De Azeredo, F.A. and Ribeiro, M.F. (1992) A simple biological way to screen dopaminergic agonists. *Metab. Brain Dis.* **7** : 211-221.

De Bruijne, A.W., Vreeburg, H. and van Steveninck, J. (1983) Kinetic analysis of L-lactate transport in human erythrocytes via the monocarboxylate-specific carrier system. *Biochim. Biophys. Acta* **732** : 562-568.

De Bruijne, A.W., Vreeburg, H. and van Steveninck, J. (1985) Alternative-substrate inhibition of L-lactate transport via the monocarboxylate-specific carrier system in human erythrocytes. *Biochim. Biophys. Acta* **812** : 841-844.

Deitmer, J.W. (1991) Electrogenic sodium-dependent bicarbonate secretion by glial cells of the leech central nervous system. *J. Gen. Physiol.* **98** : 637-655.

Deitmer, J.W. and Schlue, W.-R. (1987) The regulation of intracellular pH by identified glial and neurons in the central nervous system of the leech. *J. Physiol. (Lond.)* **388** : 261-283.

Deitmer, J.W. and Schlue W.-R. (1989) An inwardly directed electrogenic sodium-bicarbonate co-transport in leech glial cells. *J. Physiol. (Lond.)* **411** : 179-194.

Deitmer, J.W. and Szatkowski, M. (1990) Membrane potential dependence of intracellular pH regulation by identical glial cells in the leech central nervous system. *J. Physiol. (Lond.)* **421** : 617-631.

Deuticke, B. (1989) Monocarboxylate transport in red blood cells: kinetics and chemical modification. *Methods Enzymol.* **173** : 300-329.

Dienel, G.A., Cruz, N.F. and Adachi, K. (1995) Rapid efflux of lactate from rat cerebral cortex during spreading cortical depression: metabolite trafficking within brain. *J. Cereb. Blood Flow Metab.* **15** (suppl. 1) : S156.

Dobson G.P., Yamamoto E. and Hochachka P.W. (1986) Phosphofructokinase control in muscle: Nature and reversal of pH-dependent ATP inhibition. *Am. J. Physiol.* **250** : R71-R76.

Donoghue, J.P. and Wise, S.P. (1982) The motor cortex of the rat: Cytoarchitecture and microstimulation mapping. *J. Comp. Neurol.* **212** : 76-88.

Dringen, R. and Hamprecht, B. (1993) Inhibition by 2-deoxyglucose and 1,5-gluconolactone of glycogen mobilization in astroglia-rich primary cultures. *J. Neurochem.* **60** : 1498-1504.

Dringen, R., Gebhardt, R. and Hamprecht, B. (1993) Glycogen in astrocytes: Possible function as lactate supply for neighbouring cells. *Brain Res.* **623** : 208-214.

Dubinsky, W.P. and Racker, E. (1978) The mechanism of lactate transport in human erythrocytes. *J. Membrane Biol.* **44** : 25-36.

Duchen, M.R. (1990) Effects of metabolic inhibition on the membrane properties of isolated mouse primary sensory neurones. *J. Physiol. (Lond.)* **424** : 387-409.

Duchen, M.R., Valdeolmillos, M., O'Neill, S.C. and Eisner, D.A. (1990) Effects of metabolic blockade on the regulation of intracellular calcium in dissociated mouse sensory neurones. *J. Physiol (Lond.)* **424** : 411-426.

Duckrow, R.B., LaManna, J.S. and Rosenthal, M. (1981) Disparate recovery of resting and stimulated oxidative metabolism following transient ischemia. *Stroke* **12** : 677-686.

Duffy, T.E., Nelson, S.R. and Lowry, O.H. (1972) Cerebral carbohydrate metabolism during acute hypoxia and recovery. *J. Neurochem.* **19** : 959-977.

During, M.J., Fried, I., Leone, P., Katz, A. and Spencer, D.D. (1994) Direct measurement of extracellular lactate in the human hippocampus during spontaneous seizures. *J. Neurochem.* **62** : 2356-2361.

Ekholm, A., Katsura, K. and Siesjö, B.K. (1991) Tissue lactate content and tissue $P_{CO_2}$ in complete brain ischemia: Implications for compartmentation of $H^+$. *Neurol. Res.* **13** : 74-76.

Ekholm, A., Asplund, B. and Siesjö, B.K. (1992) Perturbation of cellular energy in complete ischemia: Relationship to dissipative ion fluxes. *Exp. Brain Res.* **90** : 47-53.

Ekholm, A., Katsura, K., Kristián, T., Lui, M., Folbergrová, J. and Siesjö, B.K. (1993) Coupling of cellular energy state and ion homeostasis during recovery following brain ischemia. *Brain Res.* **604** : 185-191.

Endres, W., Bellanyi, K., Serve, G. and Grafe, P. (1986) Excitatory amino acids and intracellular pH in motorneurons of the isolated frog spinal cord. *Neurosci. Lett.* **72** : 54-58.

Erecinska, M. and Silver, I.A. (1989) ATP and Brain Function. *J. Cereb. Blood Flow Metab.* **9** : 2-19.

Erecinska, M. and Silver, I.A. (1994) Ions and energy in mammalian brain. *Prog. Neurobiol.* **43** : 37-71.

Erecinska, M., Nelson, D., Dagani, F., Deas, J. and Silver, I.A. (1993) Relations between intracellular ions and energy metabolism under acidotic conditions: A study with nigericin in synaptosomes, neurons, and C6 glioma cells. *J. Neurochem.* **61** : 1356-1368.

Fencl, V. (1986) Acid-base balance in cerebral fluids. In: *Handbook of Physiology. Vol. II The Respiratory System. Control of Breathing* Am. Physiol. Soc: Bethesda. pp 115-140.

Flecknell, P.A. (1987) Laboratory Animal Anaesthesia. Academic Press Ltd. London.

Folbergrová, J., Lowry, O.H. and Passonneau, J.V. (1970) Changes in metabolites of the energy reserves in individual layers of the mouse cerebral cortex and subjacent white matter during ischemia and anaesthesia. *J. Neurochem.* **17** : 1155-1162.

Folbergrová, J., MacMillan, V. and Siesjö, B.K. (1972) The effect of moderate and marked hypercapnia upon the energy state and upon the cytoplasmic NADH/$NAD^+$ ratio of the brain. *J. Neurochem.* **19** : 2497-2505.

Folbergrová, J., Ljunggren, B. and Siesjö, B.K. (1974) Influence of complete ischemia on glycolytic metabolites, citric acid cycle intermediates, and associated amino acids in the rat cerebral cortex. *Brain Res.* **80** : 265-279.

Fox, P., Raichle, M.E., Mintum, D.C. and Derce, C. (1988) Non-oxidative glucose consumption during focal physiological neural activity. *Science* **241** : 462-464.

Frelin, C., Vigne, P., Ladoux, A. and Lazdunski, M. (1988) The regulation of the intracellular pH in cells from vertebrates. *Eur. J. Biochem.* **174** : 3-14.

Furlow, T.W. Jr. (1982) Cerebral ischemia produced by four-vessel occlusion in the rat: A quantitative evaluation of cerebral blood flow. *Stroke* 13(6) : 852-855.

Furlow, T.W. Jr. (1983) Cerebral blood flow in the four-vessel occlusion rat model. *Stroke* 14(5) : 832-834.

Gaddum, J.H. (1961) Push-pull cannulae. *J. Physiol. (Lond.)* **155** : 1P.

Garthwaite, J. (1991) Glutamate, nitric oxide and cell-cell signalling in the nervous system. *Trends Neurosci.* **14** : 60-67.

Garthwaite, J., Charles, S.L. and Chess-Williams, R. (1988) Endothelium-derived relaxing factor release on activation of NMDA receptors suggests role as intercellular messenger in the brain. *Nature* **336** : 385-388.

Gault, L.M., Lin, C-.W., LaManna, J. and Lust, W.D. (1994) Changes in energy metabolites, cGMP and intracellular pH during cortical spreading depression. *Brain Res.* **641** : 176-180.

Germano, I.M., Pritts, L.H., Meldrum, B.S., Bartowski, H.M. and Simon, R.P. (1987) Kynurenate inhibition of excitation decreases stroke size and deficits. *Ann. Neurol.* **22** : 730-734.

Gidö, G., Katsura, K., Kristián, T. and Siesjö, B.K. (1993) Influence of plasma glucose concentration on rat brain extracellular calcium transients during spreading depression. *J. Cereb. Blood Flow Metab.* **13** : 179-182.

Giffard, R.G., Monyer, H. and Choi, D.W. (1990a) Selective vulnerability of cultured cortical glia to injury by extracellular acidosis. *Brain Res.* **530** : 138-141.

Giffard, R.G., Monyer, H., Christine, C.W. and Choi, D.W. (1990b) Acidosis reduces NMDA receptor activation, glutamate neurotoxicity and oxygen-glucose deprivation neuronal injury in cortical cultures. *Brain Res.* **506** : 339-342.

Gill, R., Andiné, P., Hillered, L., Persson, L. and Hagberg, H. (1992) The effect of MK-801 on cortical spreading depression in the penumbral zone following focal ischaemia in the rat. *J. Cereb. Blood Flow Metab.* **12** : 371-379.

Ginsberg, M.D., Graham, D.I. and Busto, R. (1985) Regional glucose utilization and blood flow following graded forebrain ischemia in the rat: Correlation with neuropathology. *Ann. Neurol.* **18** : 470-481.

Gjedde, A., Hansen, A.J. and Quistorff, B. (1981) Blood-brain glucose transfer in spreading depression. *J. Neurochem.* **37** : 807-812.

Gleitz, J., Beile, A., Khan, S., Wilffert, B. and Tegtmeier, F. (1993) Anaerobic glycolysis and postanoxic recovery of respiration of rat cortical synaptosomes are reduced by synaptosomal sodium load. *Brain Res.* **611** : 286-294.

Goldberg, W.J., Kadingo, R.M. and Barrett, J.N. (1986) Effects of ischemia-like conditions on cultured neurons: protection by low $Na^+$, low $Ca^+$ solutions. *J. Neurosci.* **6** : 3144-3151.

Goldman, S.A., Pulsinelli, W.A., Clarke, W.Y., Kraig, R.P. and Plum F. (1989) The effects of extracellular acidosis on neurons and glia *in vitro*. *J. Cereb. Blood Flow Metab.* **9** : 471-477.

Gotoh, M., Davies, S.E.C. and Obrenovitch, T.P. (1997) Brain tissue acidosis: Effects on the extracellular concentration of *N*-acetylaspartate. *J. Neurochem.* **69** : 655-661.

Grichtchenko, I.I. and Chesler, M. (1994) Depolarization-induced acid secretion in gliotic hippocampal slices. *Neuroscience* **62**(4) : 1057-1070.

Griffiths, R., Dunlop, J., Gorman, A., Senior, J. and Grieve, A. (1994) L-*trans*-pyrrolidine-2,4-dicarboxylate and *cis*-1-aminocyclobutane-1,3-dicarboxylate behave as transportable, competitive inhibitors of the high-affinity glutamate transporters. *Biochem. Pharmacol.* **47** : 267-274.

Grinstein, S. and Rothstein, R. (1986) Mechanisms of regulation of $Na^+/H^+$ exchanger. *J. Membr. Biol.* **90** : 1-12.

Grinstein, S., Clarke, C. and Rothstein, A. (1983) Activation of $Na^+/H^+$ exchange in lymphocytes by osmotically induced volume changes and by cytoplasmatic acidification. *J. Gen. Physiol.* **82** : 619-638.

Grinstein, S., Furuya, W., Goetz, J.D. and Cohen, S. (1985) $Na^+/H^+$ exchange and the regulation of intracellular pH in lymphocytes and neutrophils. *J. Cereb. Blood Flow Metab.* **5** (suppl. 1) : S223-S224.

Grünewald, R.A. (1993) Ascorbic acid in the brain. *Brain Res. Rev.* **18** : 123-133.

Hakim, A.M. and Shoubridge, E.A. (1989) Cerebral acidosis in focal ischemia. *Cerebrovasc. Brain Metab. Rev.* 1 : 115-132.

Halestrap, A.P. (1975) The mitochondrial pyruvate carrier: kinetics and specificity for substrates and inhibitors. *Biochem. J.* **148** : 85-96.

Halestrap, A.P. (1976) Transport of lactate and pyruvate into human erythrocytes. *Biochem. J.* **156** : 181-183.

Halestrap, A.P., Poole, R.C. and Cranmer, S.L. (1990) Mechanisms and regulation of lactate, pyruvate and ketone body transport across the plasma membrane of mammalian cells and their metabolic consequences. *Biochem. Soc. Trans.* **18** : 1132-1135.

Halliwell, B. and Gutteridge, J.M.C. (1985) Oxygen radicals and the nervous system. *Trends Neurosci.* **8** : 22-26.

Hansen, A.J. (1977) Extracellular potassium concentration in juvenile and adult rat brain cortex during anoxia. *Acta Physiol. Scand.* **99** : 412-420.

Hansen, A.J. (1985) Effect of anoxia on ion distribution in the brain. *Physiol. Rev.* **65** : 101-148.

Hansen, A.J. and Nedergaard, M. (1988) Brain ion homeostasis in cerebral ischemia. *Neurochem. Pathol.* **9** : 195-209.

Hansen, A.J. and Nordström, C.H. (1979) Brain extracellular potassium and energy metabolism during ischemia in juvenile rats after exposure to hypoxia for 24 h. *J. Neurochem.* **32** : 315-320.

Hansen, A.J. and Olsen, C.E. (1980) Brain extracellular space during spreading depression and ischemia. *Acta Physiol. Scand.* **108** : 335-365.

Hansen, A.J. and Quistorff, B. (1993) Glucose metabolism in experimental spreading depression. In: *Migraine: Basic Mechanisms and Treatment* (Lehmenkühler, A., Grotemeyer, K.-H. and Tegtmeier, F. eds.) Urbanics & Schwartzenberg, Germany. pp 367-377.

Hansen, A.J. and Zeuthen, T. (1981) Extracellular ion concentrations during spreading depression and ischaemia in the rat brain cortex. *Acta Physiol. Scand.* **113** : 437-445.

Hansen, A.J., Lund-Andersen, H. and Crone, C. (1977) $K^+$ permeability of the blood brain barrier, investigated by aid of a $K^+$ sensitive microelectrode. *Acta Physiol. Scand.* **101** : 438-445.

Harris RJ (1985) Extracellular ion activity changes in cerebral ischaemia. Ph.D. thesis. Univeristy of London.

Harris, R.J. and Symon, L. (1981) A double ion-sensitive microelectrode for extracellular cerebral cortical measurements. *J. Physiol. (Lond.)* **312** : 3P.

Harris, R.J. and Symon, L. (1984) Extracellular pH, potassium, and calcium activities in progressive ischemia of rat cortex. *J. Cereb. Blood Flow Metab.* **4** : 178-186.

Haselgrove, J.C., Bashford, C.L., Barlow, C.H., Quistorff, B., Chance, B. and Mayevsky, A. (1990) Time resolved 3-dimensional recording of redox ratio during spreading depression in gerbil brain. *Brain Res.* **506** : 109-114.

Hassel, B. and Sonnewald, U. (1995) Glial formation of pyruvate and lactate from TCA cycle intermediates: Implications for the inactivation of transmitter amino acids? *J. Neurochem.* **65** : 2227-2234.

Herman, H.B. and Rechnitz, G.A. (1975) Preparation and properties of a carbonate ion-selective membrane electrode. *Anal. Chim. Acta* **76** : 155-164.

Herreras, O. and Somjen, G.G. (1993) Propagation of spreading depression among dendrites and somata of the same cell population. *Brain Res.* **610** : 276-282.

Hertz, L., Drejer, J. and Schousboe, A. (1988) Energy metabolism in glutamatergic neurons, GABAergic neurons and astrocytes in primary cultures. *Neurochem. Res.* **13** : 605-610.

Hetherington, H.P., Tan, M.J., Luo, K.L., Pohost, G.M., Halsey, J.H. Conger, K.A. (1994) Evaluation of lactate production and clearance kinetics by $^{1}H$ NMR in a model of brief repetitive cerebral ischemia. *J. Cereb. Blood Flow Metab.* **14** : 591-596.

Heuser, D., Astrup, J., Lassen, N.A. and Betz, E. (1975) Brain carbonic acid acidosis after actetazolamide. *Acta Physiol. Scand.* **93** : 385-90.

Hicks, R.R., Smith, D.H., Gennarelli, T.A. and McIntosh, T. (1994) Kynurenate is neuroprotective following experimental brain injury in the rat. *Brain Res.* **655** : 91-96.

Higashida, H., Mitarai, G. and Watanabe, S. (1974) A comparative study of membrane potential changes in neurons and neuroglial cells during spreading depression in the rabbit. *Brain Res.* **65** : 411-425.

Hille, B. (1991) Ionic Channels of Excitable Membranes. Sinauer Associates, Sunderland, MA.

Hillered, L., Muchiri, P.M., Nordenbrand, K. and Ernster, L. (1983) $Mn^{2+}$ prevents the $Ca^{2+}$-induced inhibition of ATP synthesis in brain mitochondria. *FEBS Lett.* **154** : 247-250.

Hillered, L., Smith, M.-L. and Siesjö, B.K. (1985) Lactic acidosis and recovery of mitochondrial function following forebrain ischemia in the rat *J. Cereb. Blood Flow Metab.* **5** : 259-266.

Hochachka, P.W. and Mommsen, T.P. (1983) Protons and anaerobiosis. *Science* **219** : 1391-1397.

Hoffmann, E.K. and Simonsen, L.O. (1989) Membrane mechanisms in volume and pH regulation in vertebrate cells. *Physiol. Rev.* **69** : 315-382.

Hossmann, K.A. (1985) Post-ischemic resuscitation of the brain: selective vulnerability versus global resistance. *Prog. Brain Res.* **63** : 3-17.

Iijima, T., Meis, G. and Hossmann, K-A. (1992) Repeated negative DC deflections in rat cortex following middle cerebral artery occlusion are abolished by MK-801: Effect on volume of ischemic injury. *J. Cereb. Blood Flow Metab.* **12** : 727-733.

Isaacson, J.S. and Nicoll, R.A. (1993) The uptake inhibitor L-*trans*-PDC enhances responses to glutamate but fails to alter the kinetics of excitatory synaptic currents in the hippocampus. *J. Neurophysiol.* **20**(5) : 2187-2191.

Jean, T., Frelin, C., Vigne, P., Barbry, P. and Lazdunski, M. (1985) Biochemical properties of the $Na^+/H^+$ exchange system in rat brain synaptosomes. *J. Biol. Chem.* **260**(17) : 9678-9684.

Jean, T., Frelin, C., Vigne, P. and Lazdunski, M. (1986) The $Na^+/H^+$ exchange system in glial cell lines. Properties and activation by an hyperosmotic shock. *Eur. J. Biochem.* **160** : 211-219.

Kaila, K. and Viopio, J. (1987) Postsynaptic fall in intracellular pH induced by GABA-activated bicarbonate conductance. *Nature* **330** : 163-165.

Kaila, K., Pasternack, M., Saarikoski, I. and Voipio, V. (1989) Influence of GABA-gated bicarbonate conductance on potential, current and intracellular chloride in crayfish muscle fibres. *J. Physiol. (Lond.)* **416** : 161-181.

Kajino, K., Matsumura, Y. and Fujimoto, M. (1982) Determination of dissociation exponent of $CO_2$ used in Henderson-Hasselbalch equation by means of bicarbonate-selective microelectrode. *Nippon Seirigaku Zasshi*. **44**(12) : 663-673.

Kalimo, H., Rehncrona, S., Söderfeldt, B., Olsson, Y. and Siesjö, B.K. (1981) Brain lactic acidosis and ischemic cell damage: 2 Histopathology. *J. Cereb. Blood Flow Metab.* **1** : 313-327.

Katsura, K., Ekholm, A., Asplund, B. and Siesjö, B.K. (1991) Extracellular pH in the brain during ischemia: relationship to the severity of lactic acidosis. *J. Cereb. Blood Flow Metab.* **11** : 597-599.

Katsura, K., Ekholm, A. and Siesjö, B.K. (1992) Tissue $PCO_2$ in brain ischemia related to lactate content in normo- and hypercapnic rats. *J. Cereb. Blood Flow Metab.* **12** : 270-280.

Katsura, K., Kristián, T., Nair, R. and Siesjö, B.K. (1994a) Regulation of intra- and extracellular pH in the rat brain in acute hypercapnia: a re-appraisal. *Brain Res.* **651** : 47-56.

Katsura, K., Kristián, T., Smith, M.-L. and Siesjö, B.K. (1994b) Acidosis induced by hypercapnia exaggerates ischemic brain damage. *J. Cereb. Blood Flow Metab.* **14** : 243-250.

Kauppinen, R.A. and Nicholls, D.G. (1986) Failure to maintain glycolysis in anoxic nerve terminals. *J. Neurochem.* **47** : 1864-1869.

Kauppinen, R.A. and Williams, S.R. (1990) Cerebral energy metabolism and intracellular pH during severe hypoxia and recovery: a study using $^1H$, $^{31}P$, and $^1H[^{13}C]$ nuclear magnetic resonance spectroscopy in the guinea-pig cerebral cortex *in vitro*. *J. Neurosci. Res.* **26** : 356-369.

Kauppinen, R.A., McMahon, H. and Nicholls, D.G. (1988) $Ca^{2+}$-dependent and $Ca^{2+}$-independent glutamate release, energy status and cytosolic free $Ca^{2+}$ concentration in isolated nerve terminals following metabolic inhibition: Possible relevance to hypoglycaemia and anoxia. *Neuroscience* **27** : 175-182.

Kehr, J. (1993) A survey on quantitative microdialysis: theoretical models and practical implications. *J. Neurosci. Meth.* **48** : 251-261.

Kempski, O., Staub, F., Jansen, M., Schödel, F. and Baethmann, A. (1988) Glial swelling during extracellular acidosis *in vitro*. *Stroke* **19** : 385-392.

Kessler, M., Terramani, T., Lynch, G. and Baudry, M. (1989) A glycine site associated with *N*-methyl-D-aspartic acid receptors: characterization and identification of a new class of antagonists. *J. Neurochem.* **52** : 1319-1328.

Kettenmann, H. and Schlue, W.-R. (1988) Intracellular pH regulation in cultured mouse oligodendrocytes. *J. Physiol. (Lond.)* **406** : 147-162.

Khuri, R.N., Bogharian, K.K. and Agulian, S.K. (1974) Intracellular bicarbonate in single skeletal muscle fibers. *Pflügers Arch.* **349** : 285-294.

Khuri, R.N., Agulian, S.K. and Bogharian, K.K. (1976) Intracellular bicarbonate of skeletal muscle under different metabolic states. *Am. J. Physiol.* **230**(1) : 228-232.

Kimelberg, H.K. (1981) Active accumulation and exchange transport of chloride in astroglial cells in culture. *Biochim. Biophys. Acta.* **646** : 179-184.

Kimelberg, H.K. and Bourke, R.S. (1982) Anion transport in the nervous system. In: *Handbook of Neurochemistry. Vol. 1: Chemical and Cellular Architecture* (Lajtha, A. ed.) Plenum Press, New York. pp 31-67.

Kimelberg, H.K., Biddlecome, S. and Bourke, R.S. (1979) SITS-inhibitable $Cl^-$ transport and $Na^+$-dependent $H^+$ production in primary astroglial cultures. *Brain Res.* **173** : 111-124.

Kimelberg, H.K., Bourke, R.S., Stieg, P.E., Barron, K.D., Hirata, H., Pelton, E.W. and Nelson, L.R. (1982) Swelling of astroglia after injury to the central nervous system: Mechanisms and consequences. In: *Head Injury: Basic and Clinical Aspects* (Grossman, R.G. and Gilendberg, P.L. eds.) Raven, New York. pp 31-44.

Kimelberg, H.K., Anderson, E. and Kettenmann, H. (1990a) Swelling-induced changes in electrophysiological properties of cultured astrocytes and oligodendrocytes. II Whole cell currents. *Brain Res.* **529** : 262-268.

Kimelberg, H.K., Barron, K.D., Bourke, R.S., Nelson, L.R. and Cragoe, E.J. (1990b) Brain anti-cytoxic edema agents. *Prog. Clin. Biol. Res.* **361** : 363.

Kjallqvist, A., Nardini, M. and Siesjö, B.K. (1969) The regulation of extra- and intracellular acid-base parameters in the rat brain during hyper- and hypocapnia. *Acta Physiol. Scand.* **76** : 485-494.

Knull, H.R. and Khandelwal, R.L. (1982) Glycogen metabolizing enzymes in brain. *Neurochem. Res.* **7** : 1307-1317.

Kocher, M. (1990) Metabolic and hemodynamic activation of postischemic rat brain by cortical spreading depression. *J. Cereb. Blood Flow Metab.* **10** : 564-571.

Koizumi, J. (1974) Glycogen in the central nervous system. *Prog. Histochem.* **6** : 1-35.

Korf, J. and Van Praag, H. (1971) Amine metabolism in the human brain: further evaluation of the probenecid test. *Brain Res.* **35** : 221-230.

Kraig, R.P. and Nicholson, C. (1978) Extracellular ionic variations during spreading depression. *Neuroscience* **3** : 1045-1059.

Kraig, R.P. and Chesler, M. (1987) Glial acid-base behavior in brain ischemia. *J. Cereb. Blood Flow Metab.* **7** (suppl. 1) : S126.

Kraig, R.P. and Cooper, J.L. (1987) Bicarbonate and ammonia changes in brain during spreading depression. *Can. J. Physiol. Pharmacol.* **65** : 1099-1104.

Kraig, R.P. and Petito, C.K. (1989) Astroglial acidosis and swelling occur after (normoglycemic) global ischemia. *J. Cereb. Blood Flow Metab.* **9** (suppl. 1) : S58.

Kraig, R.P. and Chesler, M. (1990) Astrocytic acidosis in hyperglycemic and complete ischemia. *J. Cereb. Blood Flow Metab.* **10** : 104-114.

Kraig, R.P., Ferreira-Filho, C.R. and Nicholson, C. (1983) Alkaline and acid transients in cerebellar microenvironment. *J. Neurophysiol.* **49** : 831-850.

Kraig, R.P., Pulsinelli, W.A. and Plum, F. (1985) Hydrogen ion buffering during complete brain ischemia. *Brain Res.* **342** : 281-290.

Kraig, R.P., Pulsinelli, W.A. and Plum, F. (1986) Carbonic acid buffer changes during complete brain ischemia. *Am. J. Physiol.* **250** : R348-R357.

Kraig, R.P., Petito, C.K., Plum, F. and Pulsinelli, W.A. (1987) Hydrogen ions kill brain at concentrations reached in ischemia. *J. Cereb. Blood Flow Metab.* **7** : 379-386.

Kravzov, J., Santamaria, A., Rios, C., Flores, A. and Altagracia, M. (1993) Protective effect of probenecid on circling behaviour of rats with unilateral quinolinic acid induced striatal lesions. *Proc. West Pharmacol. Soc.* **36** : 255-257.

Krebs, H., Woods, H. and Alberti, K. (1975) Hyperlactataemia and lactic acidosis. *Essays Med. Biochem.* **1** : 81-103.

Kristián, T., Katsura, K., Gidö, G. and Siesjö, B.K. (1994) The influence of pH on cellular calcium influx during ischemia. *Brain Res.* **641** : 295-302.

Kuhr, W.G. and Korf, J. (1988) Extracellular lactic acid as an indicator of brain metabolism: continuous on-line measurement in conscious, freely moving rats with intrastriatal dialysis. *J. Cereb. Blood Flow Metab.* **8** : 130-137.

Kuhr, W.G., van den Berg, C.J. and Korf, J. (1988) *In vivo* identification and quantitative evaluation of carrier-mediated transport of lactate at the cellular level in the striatum of conscious, freely moving rats. *J. Cereb. Blood Flow Metab.* **8** : 848-856.

Kuyama, H., Kitaoka, T., Fujita, K. and Nagoa, S. (1994) The effect of alkalizing agents on experimental focal cerebral ischemia. *Acta Neurochir. Suppl. Wein* **60** : 325-328.

Lacombe, P., Sercombe, R., Correze, J.L., Springhetti, V. and Seylaz, J. (1992) Spreading depression induces prolonged reduction of cortical blood flow reactivity in the rat. *Exp. Neurol.* **117** : 278-286.

LaManna, J.C., Harrington, J.F., Vendel, L.M., Abi-Saleh, K., Lust, W.D. and Harik, S.I. (1993) Regional blood-brain lactate influx. *Brain Res.* **614** : 164-170.

LaManna, J.C., Griffith, J.K., Cordisco, B.R., Bell, H.E., Lin, C.-W., Pundik, S. and Lust, W.D. (1995) Rapid recovery of rat brain intracellular pH after cardiac arrest and resuscitation. *Brain Res.* **687** : 175-181.

Larrabee, M.G. (1992) Extracellular intermediates of glucose metabolism: fluxes of endogenous lactate and alanine through extracellular pools in embryonic sympathetic ganglia. *J. Neurochem.* **59** : 1041-1052.

Larrabee, M.G. (1995) Lactate metabolism and its effects on glucose metabolism in an excised neural tissue. *J. Neurochem.* **64** : 1734-1741.

Lauritzen, M. (1987) Cerebral blood flow in migraine and cortical spreading depression. *Acta Neurol. Scand.* **76** : 9-40.

Lauritzen, M. (1994) Pathophysiology of the migraine aura: The spreading depression theory. *Brain* **117** : 199-210.

Lauritzen, M. and Hansen, A.J. (1992) The effect of glutamate receptor blockade on anoxic depolarisation and cortical spreading depression. *J. Cereb. Blood Flow Metab.* **12** : 223-229.

Lauritzen, M., Jorgensen, M.B., Diemer, N.H., Gjedde, A. and Hansen, A.J. (1982) Persistent oligemia of rat cerebral cortex in the wake of spreading depression. *Ann. Neurol.* **12** : 469-474.

Lauritzen, M., Hansen, A.J., Kronborg, D. and Wieloch, T. (1990) Cortical spreading depression is associated with arachidonic acid accumulation and preservation of energy charge. *J. Cereb. Blood Flow Metab.* **10** : 115-122.

Leào, A.A.P. (1944) Further observations on spreading depression of activity in the cerebral cortex. *J. Neurophysiol.* **7** : 359-390.

Lehninger, A.L. (1982) Principles of Biochemistry. Worth Publishers Inc. New York, USA.

Ljunggren, B., Norberg, K. and Siesjö, B.K. (1974a) Influence of tissue acidosis upon restitution of brain energy metabolism following total ischemia. *Brain Res.* **77** : 173-186.

Ljunggren, B., Ratcheson, R.A. and Siesjö, B.K. (1974b) Cerebral metabolic state following complete compression ischemia. *Brain Res.* **73** : 291-307.

Ljunggren, B., Schutz, H. and Siesjö, B.K. (1974c) Changes in energy state and acid-base parameters of the rat brain during compression ischemia. *Brain Res.* **73** : 277-289.

Lomneth, R., Medrano, S. and Gruenstein, E.I. (1990) The role of transmembrane pH gradients in the lactic acid induced swelling of astrocytes. *Brain Res.* **523** : 69-77.

Lowry, O.H., Passonneau J.V., Hasselberger, F.K. and Schultz, D.W. (1964) Effect of ischemia on known substrates and cofactors of the glycolytic pathway in brain. *J. Biol. Chem.* **239** : 18-30.

Lund-Andersen, H. (1979) Transport of glucose from blood to brain. *Physiol. Rev.* **59** : 305-352.

Luo, D., Leung, E. and Vincent, S.R. (1994) Nitric oxide-dependent efflux of cGMP in rat cerebellar cortex: an *in vivo* microdialysis study. *J. Neurosci.* **14** : 263-271.

Mabe, H., Blomqvist, P. and Siesjö, B.K. (1983) Intracellular pH in the brain following transient ischemia. *J. Cereb. Blood Flow Metab.* **3** : 109-114.

MacMillan, V. (1987) Effect of probenecid on cerebral and cisternal cerebrospinal fluid lactate content. *J. Cereb. Blood Flow Metab.* **7**: 118-123.

MacMillan, V. and Siesjö, B.K. (1973) The influence of hypocapnia upon intracellular pH and upon some carbohydrate substrates, amino acids and organic phosphates in the brain. *J. Neurochem.* **21** : 1283-1299.

Mann, G.E., Zlokovic, B.V. and Yudilevich, D.L. (1985) Evidence for a lactate transport system in the sarcolemmal membrane of the perfused rabbit heart: kinetics of unidirectional influx, carrier specificity and effects of glucagon. *Biochim. Biophys. Acta* **819** : 241-248.

Marsden, C.A., Brazell, M.P. and Maidment, N.T. (1984) An introduction to *in vivo* electrochemistry. In : *Measurement of Neurotransmitter Release In Vivo.* (Marsden, C.A. ed.) Wiley, New York. pp 127-153.

Marshall B.E. and Longnecker, D.E. (1996) General Anesthetics. In: *The Pharmacological Basis of Therapeutics* (Hardman, J.G., Limbird, L.E., Molinoff, P.B., Ruddon, R.W. Gilman, A.G. eds) McGraw-Hill. London. pp 307-330.

Marshall, W.H. (1959) Spreading cortical depression of Leào. *Physiol. Rev.* **39** : 239-279.

Matthews, J.N.S., Altman, D.G., Campbell, M.J. and Royston, P. (1990) Analysis of serial measurements in medical research. *Br. Med. J.* **300** : 230-235.

Mayevsky, A., Doron, A., Manor, T., Meilin, S., Salame, K. and Ouaknine, G.E. (1995) Repetitive cortical spreading depression cycle development in the human brain : A multiparametric monitoring approach. *J. Cereb. Blood Flow Metab.* **15** (suppl. 1) : S34.

McKinney, S.E., Peck, H.M., Bockey, J.M., Byham, B.B., Schucharadt, G.S. and Beyer, K.H. (1951) Benemid, p-(di-n-propyl-sulfamyl)-benzoic acid: toxicologic properties. *J. Pharmacol. Exp. Therap.* **102** : 208-241.

Meldrum, B.S. (1983) Metabolic factors during prolonged seizures and their relation to nerve cell death. *Advances in Neurology* **34** : 261-275.

Mellergård, P., Ou-yang, Y. and Siesjö, B.K. (1993) Intracellular pH regulation in cultured rat astrocytes in $CO_2/HCO_3^-$-containing media. *Exp. Brain Res.* **95** : 371-380.

Mellergård, P., Ou-yang, Y. and Siesjö, B.K. (1994b) The regulation of intracellular pH is strongly dependent on extracellular pH in cultured rat astrocytes and neurons. *Acta Neurochir. Supp. Wein.* **60** : 34-37.

Messeter, K. and Siesjö, B.K. (1971) The intracellular pH in the brain in acute and sustained hypercapnia. *Acta Physiol. Scand.* **83** : 210-219.

Mies, G. and Paschen, W. (1984) Regional changes of blood flow, glucose and ATP content determined from brain sections during a single passage of spreading depression in the rat brain cortex. *Exp. Neurol.* **84** : 249-258.

Miller, J.M., MacGarvey, U. and Beal, M.F. (1992) The effect of peripheral loading with kynurenine and probenecid on extracellular striatal kynurenic acid concentrations. *Neurosci. Lett.* **146** : 115-118.

Mitchell, R.A, Herbert, D.A. and Carman, C.T. (1965) Acid-base constants and temperature coefficients for cerebrospinal fluid. *J. Appl. Physiol.* **20**(1) : 27-30.

Moody, W.J. (1981) The ionic mechanism of intracellular pH regulation in crayfish neurones. *J. Physiol. (Lond.)* **316** : 293-308.

Moroni, F. and Pepeu, G. (1984) The cortical cup technique. In : *Measurement of Neurotransmitter Release In Vivo.* (Marsden, C.A. ed.) Wiley, New York. pp 63-81.

Moroni, F., Russi, P., Lombardi, G., Beni, M. and Carlà, V. (1988) Presence of kynurenic acid in the mammalian brain. *J. Neurochem.* **51** : 177-180.

Mutch, W.A.C. and Hansen, A.J. (1984) Extracellular pH changes during spreading depression and cerebral ischaemia: mechanisms of brain pH regulation. *J. Cereb. Blood Flow Metab.* **4** : 17-27.

Myers, R.E. and Yamaguchi, S. (1977) Nervous system effects of cardiac arrest in monkeys. *Arch. Neurol.* **34** : 65-74.

Nakada, T. (1991) Brain maturation and acid-base balance: taurine/N-acetyl-aspartate replacement hypothesis. In: *Microcirculatory Disorders in the Heart and Brain* (Niimi, H., Hori, M. and Naritomi, H. eds.) Harwood Academic Publishers, Philadelphia, PA. pp 175-188.

Nakada, T., Hida, K. and Kwee, I.L. (1991) pH-lactate dissociation during anoxic insult: taurine effect. *NeuroRep.* **2** : 325-328.

Nakada, T., Hida, K. and Kwee, I.L. (1992) Brain pH and lactic acidosis: quantitative analysis of taurine effect. *Neurosci. Res.* **15** : 115-123.

Naschen, D.A. and Drapeau, P. (1988) The regulation of cytosolic pH in isolated presynaptic nerve terminals from rat brain. *J. Gen. Physiol.* **91** : 289-303.

Nedergaard, M. and Astrup, J. (1986) Infarct rim: effect of hyperglycemia on direct current potential and [$^{14}$C]2-deoxyglucose phosphorylation. *J. Cereb. Blood Flow Metab.* **6** : 607-615.

Nedergaard, M. and Hansen, A.J. (1988) Spreading depression is not associated with neuronal injury in the normal brain. *Brain Res.* **449** : 395-398.

Nedergaard, M., Goldman, S.A. and Pulsinelli, W.A. (1989) Lactic-acid-induced intracellular acidification in primary cultures of mammalian brain. *J. Cereb. Blood Flow Metab.* **9**(1) : S384.

Nedergaard, M., Kraig, R.P., Tanabe, J. and Pulsinelli, W.A. (1991) Dynamics of intracellular and extracellular pH in the evolving infarct. *Am. J. Physiol.* **260** : R581-R588.

Nemoto, E.M. and Frinak, S. (1981) Brain tissue pH after global ischemia and barbiturate loading in rat. *Stroke* **12** : 77-82.

Newman, E.A. and Astion, M.L. (1991) Localization and stoichiometry of electrogenic sodium bicarbonate cotransport in retinal glial cells. *Glia* **4** : 424-428.

Newman, G.C., Hospod, F.E. and Schissel, S.L. (1991) Ischemic brain slice glucose utilization: effects of slice thickness, acidosis and $K^+$. *J. Cereb. Blood Flow Metab.* **11** : 398-406.

Nicholson, C. (1980) Dynamics of the Brain Cell Microenvironment. *Neurosci. Res. Prog. Bull.* **18**(2) : 183-187.

Nicholson, C. and Kraig, R.P. (1975) Chloride and potassium changes measured during spreading depression in catfish cerebellum. *Brain Res.* **96** : 384-389.

Nicholson, C. and Kraig, R.P. (1981) The behaviour of extracellular ions during spreading depression. In: *The Application of Ion-Selective Microelectrodes* (Zeuthen, T. ed.) Amsterdam: Elsevier. pp 217-238.

Nicholson, C. and Phillips, J.M. (1981) Ion diffusion modified by tortuosity and volume fraction in extracellular microenvironment of rat cerebellum. *J. Physiol. (Lond.)* **321** : 225-257.

Nicholson, C. and Rice, M. (1986) The migration of substances in the neuronal microenvironment. *Ann. N.Y. Acad. Sci.* **481** : 55-71.

Nilsson, P., Hillered, L., Ponten, U. and Ungerstedt, U. (1990) Changes in cortical extracellular levels of energy-related metabolites and amino acids following concussive brain injury in rats. *J. Cereb. Blood Flow Metab.* **10** : 631-637.

Norenberg, M.D., Mozes, L.W., Gregorios, J.B. and Norenberg, L.-O.B. (1987) Effects of lactic acid on astrocytes in primary culture. *J. Neuropathol. Exp. Neurol.* **46** : 154-166.

Nozaki, K. and Beal, M.F. (1992) Neuroprotective effects of L-kynurenine on hypoxia-ischemia and NMDA lesions in neonatal rats. *J. Cereb. Blood Flow Metab.* **12** : 400-407.

Obrenovitch T.P. (1995) The ischaemic penumbra: Twenty years on. *Cerebrovas. Brain Metab. Rev.* **7** : 297-323.

Obrenovitch, T.P. and Richards, D.A. (1995) Extracellular neurotransmitter changes in cerebral ischaemia. *Cerebrovasc. Brain Metab. Rev.* **7** : 1-54.

Obrenovitch, T.P., Garofalo, O., Harris, R.J., Bordi, L., Ohno, M., Momma, F., Bachelard, H.S. and Symon, L. (1988) Brain tissue concentration of ATP, phosphocreatine, lactate and tissue pH in relation to reduced cerebral blood flow following experimental acute middle cerebral artery occlusion. *J. Cereb. Blood Flow Metab.* **8** : 866-874.

Obrenovitch, T.P., Scheller, D., Matsumoto, T., Tegtmeier, F., Höller, M. and Symon, L. (1990a) A rapid redistribution of hydrogen ions is associated with depolarization and repolarization subsequent to cerebral ischaemia/reperfusion. *J. Neurophysiol.* **64** : 1125-1133.

Obrenovitch, T.P., Sarna, G.S. and Symon, L. (1990b) Ionic homeostasis and neurotransmitter changes in ischaemia. In: *Pharmacology of Cerebral Ischemia* (Krieglstein, J. and Oberpichler, H. eds.) Wiss. Verlag., Stuttgart. pp 97-112.

Obrenovitch, T.P., Sarna, G.S., Millan, M.H., Lok, S.-Y., Kawauchi, M., Ueda, Y. and Symon, L. (1990c) Intracerebral dialysis with on-line enzyme fluorimetric detection: a novel method to investigate the changes in the extracellular concentration of glutamic acid. In: *Pharmacology of Cerebral Ischemia* (Krieglstein, J. and Oberpichler, H. eds.) Wiss, Verlag, Stuttgart. pp 23-31.

Obrenovitch, T.P., Richards, D.A., Sarna, G.S. and Symon, L. (1993) Combined intracerebral microdialysis and electrophysiological recording: methodology and applications. *J. Neurosci. Methods* **47** : 139-145.

Obrenovitch, T.P., Zilka, E. and Urenjak, J. (1995) Intracerebral microdialysis: Electrophysiological evidence of a critical pitfall. *J. Neurochem.* **64** : 1884-1887.

Oldendorf, W.H. (1972) Blood brain barrier permeability to lactate. *Eur. Neurol.* **6** : 49-55.

Oldendorf, W.H., Braun, L. and Cornford, E. (1979) pH dependence of blood-brain barrier permeability to lactate and nicotine. *Stroke* **10**(5) : 577-581.

Olsnes, S., Tønnessen, T., Ludt, J. and Sandvig, K. (1987) Effect of intracellular pH on the rate of chloride uptake and efflux in different mammalian cell lines. *Biochem.* **26** : 2778-2785.

Ou-yang, Y., Mellergård, P. and Siesjö, B.K. (1993) Regulation of intracellular pH in single rat cortical neurons *in vitro*: a microspectrofluorometric study. *J. Cereb. Blood Flow Metab.* **13** : 827-840.

Ou-yang, Y., Kristián, K., Mellergård, P. and Siesjö, B.K. (1994) The influence of pH on glutamate- and depolarization-induced increases of intracellular calcium concentration in cortical neurons in primary culture. *Brain Res.* **646**(1) : 65-72.

Pardridge, W.M. and Olendorf, W.H. (1977) Transport of metabolic substrates through the blood-brain barrier. *J. Neurochem.* **28** : 5-12.

Parsons, L.H. and Justice, J.B. Jr. (1992) Extracellular concentration and *in vivo* recovery of dopamine in the nucleus accumbens using microdialysis. *J. Neurochem.* **58** : 212-218.

Paschen, W., Djuricic, B., Mies, G., Schmidt-Kastner, R. and Linn, F. (1987) Lactate and pH in the brain: association and dissociation in different pathophysiological states. *J. Neurochem.* **48** : 154-159.

Passonneau, J.V. and Lowry, O.H. (1962) Phosphofructokinase and the Pasteur effect. *Biochem. Biophys. Res. Commun.* **7** : 10-15.

Paulsen, R.E., Contestabile, A., Villani, L. and Fonnum. F. (1987) An *in vivo* model for studying function of brain tissue temporarily devoid of glial cell metabolism: the use of fluorocitrate. *J. Neurochem.* **48** : 1377-1385.

Pauwels, P.J., Opperdoes, F.R. and Trouet, A. (1985) Effects of antimycin, glucose deprivation, and serum on cultures of neurons, astrocytes, and neuroblastoma cells. *J. Neurochem.* **44** : 143-148.

Paxinos, G. and Watson, C. (1986) The Rat Brain in Stereotaxic Coordinates. 2nd Edition, Academic Press, London.

Pearce, J.M.S. (1985) Is migraine explained by Leáo's spreading depression?. *Lancet* **ii** : 763-766.

Pfeiffer, B., Elmer, K., Roggendorf, W. and Hamprecht, B. (1990) Immunohistochemical demonstration of glycogen phosphorylase in rat brain slices. *Histochem.* **94** : 73-80.

Phillips, J.M. and Nicholson, C. (1979) Anion diffusion in spreading depression investigated with ion sensitive microelectrodes. *Brain Res.* **173** : 561-571.

Pirtillä, T.-R.M. and Kauppinen, R.A. (1992) Recovery of intracellular pH in cortical brain slices following anoxia studied by nuclear magnetic resonance spectroscopy: role of lactate removal, extracellular sodium and sodium/hydrogen exchange. *Neuroscience* **47** : 155-164.

Plum, F. (1983) What causes infarction in ischemic brain? The Robert Wartenberg Lecture. *Neurology* **33** : 222-233.

Poole, R.C. and Halestrap, A.P. (1993) Transport of lactate and other monocarboxylates across mammalian plasma membranes. *Am. J. Physiol.* **264** : C761-C782.

Pulsinelli, W.A. and Brierley, J.B. (1979) A new model of bilateral hemispheric ischemia in the unanesthetized rat. *Stroke* **10** : 267-272.

Pulsinelli, W.A. and Buchan, A.M. (1988) The four-vessel occlusion rat model: method for complete occlusion of vertebral arteries and control of collateral circulation. *Stroke* **19** : 913-914.

Pulsinelli, W.A., Waldman, S., Rawlinson, D. and Plum, F. (1982) Moderate hyperglycemia augments ischemic brain damage: a neuropathological study in the rat. *Neurology* **32** : 1239-1246.

Pulsinelli, W.A., Levy, D.E. and Duffy, T.E. (1983) Cerebral blood flow in the four-vessel occlusion rat model. *Stroke* **14** : 832-833.

Pulsinelli, W.A., Kraig, R.P. and Plum, F. (1985) Hyperglycemia, cerebral acidosis, and ischemic brain damage. In: *Cerebrovascular Diseases* (Plum, F. and Pulsinelli, W.A. eds.) New York, Raven Press. pp 201-205.

Quistorff, B., Gjedde, A. and Hansen, A.J. (1979) Spatial analysis of the freeze trapped brain provides for temporal resolution of an event. Metabolic-electrical and blood flow changes during spreading depression. *Acta Scand. Physiol.* **105** : 42A.

Rehncrona, S., Rosén, I. and Siesjö, B.K. (1981) Brain lactic acidosis and ischemic cell damage: 1. Biochemistry and neurophysiology. *J. Cereb. Blood Flow Metab.* **1** : 297-311.

Rehncrona, S., Hauge, H.N. and Siesjö, B.K. (1989) Enhancement of iron-catalyzed free radical formation by acidosis in brain homogenates: differences in effect by lactic acid and $CO_2$. *J. Cereb. Blood Flow Metab.* **9** : 65-70.

Rice, M.E. and Nicholson, C. (1988) Behavior of extracellular $K^+$ and pH in skate (*Raja erinacea*) cerebellum. *Brain Res.* **461** : 328-334.

Robinson, R.A. and Stokes, R.H. (1965) Electrolyte solutions. Butterworth and Co. Ltd., London.

Roos, A. and Boron, W.F. (1981) Intracellular pH. *Physiol. Rev.* **61** : 296-434.

Roos, B.-E., Wickström, G., Hartvig, P. and Nilsson, J.L.G. (1980) Quantification of CSF concentrations and biological activity of probenecid metabolites. *Eur. J. Clin. Pharmacol.* **17** : 223-226.

Rose, I.A. and Rose, Z.B. (1969) Glycolysis: regulation and mechanisms of the enzymes. In: *Comprehensive Biochemistry: Carbohydrate Metabolism* (Florkin, M. and Stotz, E.H. eds.) Elsevier, Amsterdam. Vol. 17, pp 93-161.

Rosner, M.J. and Becker, D.P. (1984) Experimental brain injury: successful therapy with the weak base thrometamine. With an overview of CNS acidosis. *J. Neurosurg.* **60** : 961-971.

Rothman, S.M. and Olney, J.W. (1987) Excitotoxicity and the NMDA receptor. *Trends Neurosci.* **10** : 299-302.

Rouslin, W. (1991) Effects of acidosis and ATP depletion on cardiac muscle electron transfer complex. *J. Molec. Cell Cardiol.* **23** : 1127-1135.

Russi, P., Alesiani, M., Lombardi, G., Davolio, P., Pellicciari, R. and Moroni, F. (1992) Nicotinylalanine increases the formation of kynurenic acid in the brain and antagonises convulsions. *J. Neurochem.* **59** : 2076-2080.

Saito, R., Kawase, T., Toya, S., Koga, K. and Miura, I. (1992) Reversibility of energy metabolism and intracellular pH after cerebral ischemia evaluated by $^{31}$P-MRS. *Neurol. Res.* **14**(5) : 411-416.

Saito, R., Graf, R., Rosner, G., Hubel, K., Taguchi, T. and Heiss, W.-D. (1993) Anesthesia affects potassium evoked spreading depression in cats. *J. Cereb. Blood Flow Metab. Suppl.* **13** : 86.

Salford, L.G. and Siesjö, B.K. (1974) The influence of arterial hypoxia and unilateral carotid artery occlusion upon regional blood flow and metabolism in the rat brain. *Acta Physiol. Scand.* **92** : 130-141.

Salford, L.G., Plum, F. and Siesjö, B.K. (1973) Graded hypoxia-oligemia in rat brain. I. Biochemical alterations and their implications. *Arch. Neurol.* **29** : 227-233.

Sánchez-Armass, S., Martínez-Zacuilán, R. and Martínez, G.M. (1994) Regulation of pH in rat brain synaptosomes. I. Role of sodium, bicarbonate, and potassium. *J. Neurophysiol.* **71** : 2236-2249.

Sarna, G.S., Hutson, P.H., Tricklebank, M.D. and Curzon, G. (1983) Determination of brain 5-hydroxytryptamine turnover in freely moving rats using repeated sampling of cerebrospinal fluid. *J. Neurochem.* **40** : 383-388.

Scheller, D. and Kolb, J. (1991) The internal reference technique in microdialysis: a practical approach to monitoring dialysis efficiency and to calculating tissue concentration from dialysate samples. *J. Neurosci. Meth.* **40** : 31-38.

Scheller, D., Kolb, J. and Tegtmeier, F. (1992) Lactate and pH change in close correlation in the extracellular space of the rat brain during cortical spreading depression. *Neurosci. Lett.* **135** : 83-86.

Schneider, U., Poole, R.C., Halestrap, A.P. and Grafe, P. (1993). Lactate-proton cotransport and its contribution to interstitial acidification during hypoxia in isolated rat spinal roots. *Neuroscience* **53** : 1153-1162.

Schurr, A., West, C.A. and Rigor, B.M. (1988) Lactate-supported synaptic function in the rat hippocampal slice preparation. *Science* **240** : 1326-1328.

Sebens, J.B. and Korf, J. (1975) Cyclic AMP in cerebrospinal fluid: accumulation following probenecid and biogenic amines. *Exp. Neurol.* **46** : 333-344.

Shankar, R. and Quastel, J.H. (1972) Effects of tetrodotoxin and anaesthetics on brain metabolism and transport during anoxia. *Biochem. J.* **126** : 851-867.

Sheardown, M.J. (1993) The triggering of spreading depression in the chicken retina: a pharmacological study. *Brain Res.* **607** : 189-194.

Shields, C.B., Ratcliffe, D.J., Beasley, D.J. and Fry, D.E. (1980) The influence of acidosis upon canine brain mitochondria. *Surg. Forum.* **31** : 483-484.

Siemkowicz, E. and Hansen, A.J. (1978) Clinical restitution following cerebral ischemia in hypo-, normo-, and hyperglycemic rats. *Acta Neurol. Scand.* **58** : 1-8.

Siemkowicz, E. and Hansen, A.J. (1981) Brain extracellular ion composition and EEG activity following 10 minutes ischemia in normo- and hyperglycemic rats. *Stroke* **12** : 236-240.

Siesjö, B.K. (1978) Brain Energy Metabolism. Wiley, Chichester, N.Y.

Siesjö, B.K. (1981) Cell damage in the brain: A speculative synthesis. *J. Cereb. Blood Flow Metab.* **1** : 155-185.

Siesjö, B.K. (1984) Cerebral circulation and metabolism (review article). *J. Neurosurg.* **60** : 883-908.

Siesjö, B.K. (1985) Acid-base homeostasis in the brain: physiology, chemistry and neurochemical pathology. *Prog. Brain Res.* **63** : 121-154.

Siesjö, B.K. (1988a) Hypoglycemia, brain metabolism and brain damage. *Diabetes Metab. Rev.* **4** : 113-144.

Siesjö, B.K. (1988b) Acidosis and ischemic brain damage. *Neurochem. Pathol.* **9** : 31-88.

Siesjö, B.K. (1988c) Historical overview: Calcium, ischemia, and death of brain cells. *Ann. N.Y. Acad. Sci.* **522** : 638-661.

Siesjö, B.K. (1992) Pathophysiology and treatment of focal cerebral ischemia. Part 1: Pathophysiology. *J. Neurosurg.* **77** : 169-184.

Siesjö, B.K. and Messeter, K. (1971) Factors determining intracellular pH. In: *Ion Homeostasis of the Brain* (Siesjö, B.K. and Sorensen, S.C. eds.) Munksgaard. Copenhagen. pp 244-262.

Siesjö, B. K. and Bengtsson, F. (1989) Calcium fluxes, calcium antagonists and calcium-related pathology in brain ischemia, hypoglycemia and spreading depression: a unifying hypothesis. *J. Cereb. Blood Flow Metab.* **9** : 127-140.

Siesjö, B.K., Folbergrová, J. and MacMillan, V. (1972) The effect of hypercapnia upon intracellular pH in the brain, evaluated by the bicarbonate-carbonic acid method and from the creatine phosphokinase equilibrium. *J. Neurochem.* **19** : 2483-2495.

Siesjö, B.K., von Hanwehr, R., Nergelius, G., Nevander, G. and Ingvar, M. (1985a) Extra- and intracellular pH in the brain during seizures and in the recovery period following the arrest of seizure activity. *J. Cereb. Blood Flow Metabol.* **5** : 47-57.

Siesjö, B.K., Bendek, G., Koide, T., Westerberg, E. and Wieloch, T. (1985b) Influence of acidosis on lipid peroxidation in brain tissue *in vitro*. *J. Cereb. Blood Flow Metab.* **5** : 253-258.

Siesjö, B.K., Agardh, C.-D. and Bengtsson, F. (1989) Free radicals and brain damage. Cerebrovasc. *Brain Metab. Rev.* **1** : 165-211.

Siesjö, B.K., Ekholm, A., Katsura, K. and Theander, S. (1990) Acid-base changes during complete brain ischemia. *Stroke* **21** : 194-199.

Siesjö, B.K., Katsura, K., Mellergård, P., Ekholm, A., Lundgren, J. and Smith, M.-L. (1993) Acidosis-related brain damage. *Prog. Brain Res.* **96** : 23-48.

Siesjö, B.K., Katsura, K.I., Kristián, T., Li, P.-A. and Siesjö, P. (1996a) Molecular mechanisms of acidosis-mediated damage. *Acta Neurochir. Suppl.* **66** : 8-14.

Siesjö, B.K., Katsura, K. and Kristián, T. (1996b) Acidosis-related damage. *Advances in Neurology* **71** : 209-236.

Silver, I.A. and Erecinska, M. (1992) Ion homeostasis in rat brain *in vivo*: Intra- and extracellular [$Ca^{2+}$] and [$H^+$] in the hippocampus during recovery from short-term, transient ischemia. *J. Cereb. Blood Flow Metab.* **12** : 759-772.

Smith, M.-L., Auer, R.N. and Siesjö, B.K. (1984) The density and distribution of ischemic brain injury in the rat following 2-10 min of forebrain ischemia. *Acta Neuropathol.* **64** : 319-332.

Smith, M.-L., von Hanwehr, R. and Siesjö, B.K. (1986) Changes in extra- and intracellular pH during and following ischemia in hyperglycaemic and in moderately hypoglycaemic rats. *J. Cereb. Blood Flow Metab.* **6** : 574-583.

Soleimani, M. and Aronson, P. (1989) Ionic mechanisms of $Na^+$-$HCO_3^-$ cotransport in rabbit renal basolateral membrane vesicles. *J. Biol. Chem.* **264** : 18302-18308.

Somjen, G.G., Aitken, P.G., Balestrino, M., Herreras, O. and Kawasaki, K. (1990) Spreading depression-like depolarisation and selective vulnerability of neurons: a brief review. *Stroke* **21**(suppl. III) : 179-183.

Somjen, G.G., Aitken, P.G., Czéh, G.L., Herreras, O., Jing, J. and Young, J.N. (1992) Mechanisms of spreading depression: a review of recent findings and a hypothesis. *Can. J. Physiol. Pharmacol.* **70** : S248-S254.

Sonnewald, U., Westergaard, N., Petersen, S.B., Insgård, G. and Schousboe, A. (1993) Metabolism of [U-$^{13}$C] glutamate in astrocytes studied by $^{13}$C NMR spectroscopy: Incorporation of more label into lactate than into glutamine demonstrates the importance of the tricarboxylic acid cycle. *J. Neurochem.* **61** : 1179-1182.

Spencer, T.L. and Lehninger, A.L. (1976) L-lactate transport in Ehrlich ascites-tumour cells. *Biochem. J.* **154** : 405-414.

Spira, M.E., Yarom, Y. and Zeldes, D (1984) Neuronal interations mediated by neuronally evoked changes in the extracellular potassium concentration. *J. Exp. Biol.* **112** : 179-197.

Spuler, A., Endres, W. and Grafe, P. (1987) Metabolic origin of activity-related pH changes in mammalian peripheral and central unmyelinated fibre tracts. *Pflügers Arch.* **408** : R69.

Sramka, M., Brozek, G., Bures, J. and Nádvornik, P. (1977/78) Functional ablation by spreading depression: Possible use in human stereotactic surgery. *Appl. Neurophysiol.* **40** : 48-61.

Stewart, P.A. (1981) How to Understand Acid-Base. Edward Arnold. New York.

Sturman, J.A., Rassin, D.K. and Gaull, G.E. (1977) Taurine in developing rat brain: maternal-fetal transfer of [$^{35}$S]taurine and its fate in the neonate. *J. Neurochem.* **28** : 31-39.

Sugaya, E., Takato, M. and Noda, Y. (1975) Neuronal and glial activity during spreading depression in cerebral cortex of cat. *J. Neurophysiol.* **38** : 822-841.

Sutherland, G., Peeling, J., Lesiuk, H. and Saunders, J. (1990) Experimental cerebral ischemia studied using nuclear magnetic resonance imaging and spectroscopy. *Can. Assoc. Radiol. J.* **41**(1): 24-31.

Swartz, K.J., During, M.J., Freese, A. and Beal, M.F. (1990) Cerebral synthesis and release of kynurenic acid: an endogenous antagonist of excitatory amino acid receptors. *J. Neurosci.* **10**(9) : 2965-2973.

Szerb, J.C. (1991) Glutamate release and spreading depression in the fascia dentata in response to microdialysis with high $K^+$: role of glia. *Brain Res.* **542** : 259-265.

Takagaki, G. (1968) Control of aerobic glycolysis and pyruvate kinase activity in cerebral cortex slices. *J. Neurochem.* **15** : 903-916.

Tanaka, K., Dora, E., Greenberg, J.H. and Reivich, M. (1986) Cerebral glucose metabolism during the recovery period after ischemia - its relationship to NADH fluorescence, blood flow, ECoG and histology. *Stroke* **17** : 994-1004.

Tang, C.-M., Dichter, M. and Morad, M. (1990) Modulation of the *N*-methyl-D-aspartate channel by extracellular $H^+$. *Proc. Natl. Acad. Sci.* **87** : 6445-6449.

Taylor, D.L., Davies, S.E.C., Obrenovitch, T.P., Urenjak, J., Richards, D.A., Clark, J.B. and Symon, L. (1994a) Extracellular N-Acetylaspartate in the rat brain: *in vivo* determination of basal levels and changes evoked by high $K^+$. *J. Neurochem.* **62** : 2349-2355.

Taylor, D.L., Richards, D.A., Obrenovitch, T.P. and Symon, L. (1994b) Time course of changes in extracellular lactate evoked by transient $K^+$-induced depolarisation in the rat striatum. *J. Neurochem.* **62** : 2368-2374.

Taylor, D.L., Davies, S.E.C., Obrenovitch, T.P., Doheny, M.H., Patsalos, P.N., Clark, J.B. and Symon, L. (1995) Investigation into the role of N-acetylaspartate in cerebral osmoregulation. *J. Neurochem.* **65** : 275-281.

Taylor, D.L., Obrenovitch, T.P. and Symon, L. (1996) Changes in extracellular acid-base homeostasis in cerebral ischaemia. *Neurochem. Res.* **21** : 1013-1021.

Tegtmeier, F. (1993) Differences between spreading depression and ischemia. In: *Migraine: Basic Mechanisms and Treatment* (Lehmenkühler, A., Grotenmeyer, K.-H. and Tegtmeier, F. eds.) Urban and Schwarzenberg. Germany. pp 511-532.

Thomas, R.C. (1977) The role of bicarbonate, chloride and sodium ions in the regulation of intracellular pH of snail neurons. *J. Physiol. (Lond)* **255** : 715-735.

Thomas, R.C. (1978) Comparison of the mechanisms controlling intracellular pH and sodium in snail neurones. *Res. Physiol.* **33** : 63-73.

Thomas, R.C. (1984) Experimental displacement of intracellular pH and the mechanisms of its subsequent recovery. *J. Physiol.* **354** : 3-22.

Thomas, R.C. and Meech, R.W. (1982) Hydrogen ion currents and intracellular pH in depolarized voltage-clamped snail neurones. *Nature* **299** : 826-827.

Thorn, W. and Heitmann, R. (1954) pH der Gehirnride vom Kaninchen in situ während perakuter, totaler Ischämie, reiner Anoxie und in der Erholung. *Pflügers Arch. ges Physiol.* **258** : 501-510. Quoted from Kraig et al., 1987.

Tolkovsky, A. and Richards, C. (1987) $Na^+/H^+$ exchange is the major mechanism of pH regulation in cultured sympathetic neurons: measurements in single cell bodies and neurites using a fluorescent pH indicator. *Neuroscience* **22** : 1093-1102.

Tombaugh, G.C. and Sapolsky, R.M. (1990) Mild acidosis protects hippocampal neurons from injury induced by oxygen and glucose deprivation. *Brain Res.* **506** : 343-345.

Tombaugh, G. C. and Sapolsky, R. M. (1993) Evolving concepts about the role of acidosis in ischemic neuropathology. *J. Neurochem.* **61** : 793-803.

Traynelis, S.F. and Cull-Candy, S.G. (1990) Proton inhibition of *N*-methyl-D-aspartate receptors in cerebellar neurons. *Nature* **345** : 347-350.

Traynelis, S.F. and Cull-Candy, S.G. (1991) Pharmacological properties and $H^+$ sensitivity of excitatory amino acid receptor channels in rat cerebellar granule neurones. *J. Physiol. (Lond.)* **433** : 727-762.

Trivedi, B. and Danforth, W.H. (1966) Effect of pH on the kinetics of frog muscle phosphofructokinase. *J. Biol. Chem.* **241** : 4110-4114.

Tsacopoulos, M. and Lehmenkühler, A. (1977) A double-barrelled Pt-microelectrode for simultaneous measurement of $Po_2$ and bioelectrical activity in excitable tissues. *Experienta.* **33** : 1337.

Tsien, R.Y. and Rink, T.J. (1980) Neutral carrier ion-selective microelectrode for measurements of intracellular free calcium. *Biochim. Biophys. Acta* **599** : 623-638.

Tyson, G.W., Teasdale, G.M., Graham, D.I. and McCulloch, J. (1984) Focal cerebral ischemia in the rat: topography of hemodynamic and histopathological changes. *Ann. Neurol.* **15** : 559-567.

Ungerstedt, U., Herrera-Marchintz, M., Jungnelius, U., Ståhle, L., Tossman, U. and Zetterström, T. (1982) Dopamine synaptic mechanisms reflected in studies combining behaviourial recordings and brain dialysis. In: *Advances in Dopamine Research* (Kotisaka M., ed.) Pergamon Press, New York. pp 219-231.

Urenjak, J., Obrenovitch, T.P. and Zilkha, E. (1996) Effect of probenecid on depolarizations evoked by *N*-methyl-D-aspartate (NMDA) in the rat striatum. *Arch. Pharmacol.* **354** : 1-7.

Van der Poel, F.W., Van Praag, H.M. and Korf, J. (1977) Evidence for a probenecid-sensitive transport system of acid monoamine metabolites from the spinal subarachnoid space. *Psychopharmacol.* **52** : 35-40.

Van Nimmen, D., Weyne, J., Demeester, G. and Leusen, I. (1986) Local cerebral glucose utilization during intracerebral pH changes. *J. Cereb. Blood Flow Metab.* **6** : 584-589.

Vecsei, L., Miller, J., MacGarvey, U. and Beal, M.F. (1992a) Effects of kynurenine and probenecid on plasma and brain tissue concentrations of kynurenic acid. *Neurodegeneration* **1** : 17-26.

Vecsei, L., Miller, J., MacGarvey, U. and Beal, M.F. (1992b) Kynurenine and probenecid inhibit pentylenetetrazol- and NMDLA-induced seizures and increase kynurenic acid concentrations in the brain. *Brain Res. Bull.* **28** : 233-238.

Vicario, C., Arizmendi, C., Malloch, G., Clark, J.B. and Medina, J.M. (1991) Lactate utilization by isolated cells from early neonatal rat brain. *J. Neurochem.* 57 : 1700-1707.

von Hanwehr, R., Smith, M.-L. and Siesjö, B.K. (1986) Extra- and intracellular pH during near-complete forebrain ischemia in the rat. *J. Neurochem.* **46** : 331-339.

Vyklicky, L., Vlachova, V. and Krusek, J. (1990) The effect of external pH changes on responses to excitatory amino acids in mouse hippocampal neurones. *J. Physiol.* **430** : 497-517.

Vyskocil, F., Kriz, N. and Bures, J. (1972) Potassium-selective microelectrodes used for measuring the extracellular brain potassium during spreading depression and anoxic depolarisation in rats. *Brain Res.* **39** : 255-259.

Wahl, F., Obrenovitch, T.P., Hardy, A.M., Plotkine, M., Boulu, R. and Symon, L. (1994) Extracellular glutamate during focal ischaemia in rats: Time course and calcium-dependency. *J. Neurochem.* **63** : 1003-1011.

Walz, W. (1992) Role of Na/K/Cl cotransport in astrocytes. *Can. J. Physiol. Pharmacol. Suppl.* **70** : S260-S262.

Walz, W. and Mukerji, S. (1988a) Lactate production and release in cultured astrocytes. *Neurosci. Lett.* **86** : 296-300.

Walz, W. and Mukerji, S. (1988b) Lactate release from cultured astrocytes and neurons: A comparison. *Glia* **1** : 366-370.

Walz, W. and Mukerji, S. (1988c) KCl movements during potassium-induced cytotoxic swelling of cultured astrocytes. *Exp. Neurol.* **99** : 17-29.

Walz, W. and Mukerji, S. (1990) Simulation of aspects of ischemia in cell culture: Changes in lactate compartmentation. *Glia* **3** : 522-528.

Watanabe, H. and Passonneau, J.V. (1973) Factors affecting the turnover of cerebral glycogen and limit dextrin *in vivo*. *J. Neurochem.* **20** : 1543-1554.

Weitasch, K. and Kraig, R.P. (1991) Carbonic acid buffer species measured in real time with an intracellular microelectrode array. *Am. J. Physiol.* **261** : R760-R765.

Welsh, F.A., Ginsberg, M.D., Rieder, W. and Budd, W.W. (1980) Deleterious effect of glucose pretreatment on recovery from diffuse cerebral ischemia in the cat. II. Regional metabolite levels. *Stroke* **11** : 355-363.

Wise, W.M. (1973) Bicarbonate Ion-Sensitive Electrode. U.S. Patent 3,723,281.

Wuttke, W. and Walz, W. (1990) Sodium- and bicarbonate-independent regulation of intracellular pH in cultured mouse astrocytes. *Neurosci. Lett.* **117** : 105-110.

Xie, Y., Dengler, K., Zacharias, E., Wilffert, B. and Tegtmeier, F. (1994) Effects of the sodium channel blocker tetrodotoxin (TTX) on cellular ion homeostasis in rat brain subjected to complete ischemia. *Brain Res.* **652** : 216-224.

Yuwiler, A., Bennett, B.L. and Geller, E. (1982) Is there a probenecid sensitive transport system for monoamine catabolites at the level of the brain capillary plexus? *Neurochem. Res.* **7** : 1277-1285.

Zetterström, T., Vernet, L., Ungerstedt, U., Tossman, U., Jonzon, B. and Fredholm, B.B. (1982) Purine levels in the intact rat brain, studies with implanted perfused hollow fibre. *Neurosci. Lett.* **29** : 111-115.

Zeuthen, T. (1981) The application of ion selective microelectrodes. Elsevier, Amsterdam.

Zimmer, R. and Lang, R. (1975) Rates of lactic acid permeation and utilization in the isolated dog brain. *Am. J. Physiol.* **229** : 432-437.

# PUBLISHED WORK

*Journal of Neurochemistry*
Raven Press, Ltd., New York


# Time Course of Changes in Extracellular Lactate Evoked by Transient $K^+$-Induced Depolarisation in the Rat Striatum

D. L. Taylor, D. A. Richards, T. P. Obrenovitch, and L. Symon

*Gough-Cooper Department of Neurological Surgery, Institute of Neurology, London, England*

**Abstract:** The purpose of this study was to establish whether excessive lactate production associated with local application of $K^+$ is reflected at the extracellular level *during* or *after* the $K^+$ challenge. Changes in extracellular lactate were continuously monitored by microdialysis coupled to on-line fluorimetric analysis. $K^+$-induced changes in dialysate lactate were closely related to those of the direct current potential. High $K^+$ evoked a large and sustained negative shift of direct current potential onto which were superimposed a variable number of transient peaks of further depolarisation. The initial negative shift in direct current potential was associated with a decrease in dialysate lactate, but after each transient depolarisation, the positive shift in direct current potential indicating cell repolarisation was associated with a marked increase in extracellular lactate. When repetitive transient depolarisations occurred during a stimulus, only a small increase after each depolarisation was observed. However, recordings consistently revealed a marked and rapid increase in extracellular lactate after the $K^+$ stimulus. These data indicate that extracellular lactate mostly increased during periods of repolarisation. This suggests strongly that lactic acid transport out of brain cells may be impaired when their transmembrane ionic gradients are disrupted. **Key Words:** Lactate—Microdialysis—Extracellular fluid—High potassium stimulus—Spreading depression.
*J. Neurochem.* **62,** 2368–2374 (1994).

The term spreading depression (SD) describes propagating waves of cellular depolarisation generally initiated in the brain of laboratory animals by local application of a high concentration of $K^+$ (Bures et al., 1974). This phenomenon has triggered much interest because it produces disruptions of cellular ionic homeostasis that are similar to those associated with anoxic/ischaemic depolarisation (Kraig and Nicholson, 1978; Tegtmeier, 1993). Spreading depression may also be the animal correlate of classical migraine (Lauritzen, 1987*a*; Young and Van Vliet, 1991).

As energy demand increases markedly during SD (Rosenthal and Somjen, 1973; Shinohara et al., 1979; Mies and Paschen, 1984), anaerobic glycolysis is stimulated and lactic acid accumulates (Mutch and Hansen, 1984; Lauritzen et al., 1990). Scheller and colleagues (1992) showed that the SD-induced excess of intracellular lactate was transferred rapidly to the extracellular fluid (ECF), but whether this occurs *during* or *after* the wave of SD remained uncertain as high $K^+$ was only applied to the cortical surface for 2 min. Lactate transport across the cellular membrane may be linked to transmembrane ionic gradients as it was effective only when energy supplies could maintain membrane integrity and function (Kuhr et al., 1988). If such a dependence exists, then intra-/extracellular transport of lactate should be impaired during SD, when ionic gradients are markedly perturbed.

The purpose of this study was to establish whether excessive lactate production associated with local application of $K^+$ is reflected at the extracellular level during or after the $K^+$ challenge. High $K^+$ was applied for 20 min so that any lactate changes that might occur during the challenge could be recorded. Changes in extracellular lactate were continuously monitored by microdialysis coupled to on-line fluorimetric analysis to improve time resolution (Kuhr and Korf, 1988). Simultaneous recording of the direct current (DC) potential at the same tissue site allowed correlation of ionic and ECF lactate changes (Obrenovitch et al., 1993).

## MATERIALS AND METHODS

### Animal preparation and intracerebral microdialysis

Experiments were performed on 12 male Sprague–Dawley rats (mean ± SEM weight, 330 ± 6 g; Bantin and Kingman, Grimston, U.K.) with food and water freely available. All animal procedures used were in strict accordance with the Home Office guidelines and specifically licenced under the Animals (Scientific Procedures) Act, 1986. After pre-

Received August 31, 1993; revised manuscript received October 29, 1993; accepted November 1, 1993.

Address correspondence and reprint requests to Dr. T. P. Obrenovitch at Gough-Cooper Department of Neurological Surgery, Institute of Neurology, Queen Square, London WC1N 3BG, U.K.

The present address of Dr. D. A. Richards is Department of Pharmacology, School of Pharmacy, Brunswick Square, London WC1N 1AX, U.K.

*Abbreviations used:* ACSF, artificial cerebrospinal fluid; DC, direct current; ECF, extracellular fluid; $[lact]_d$, dialysate lactate concentration; SD, spreading depression.

medication with atropine sulphate (15–30 μg/kg i.m.), anaesthesia was induced and maintained with halothane (2% and 0.8–1.5%, respectively) in $N_2O/O_2$ (1:1). A femoral artery was catheterised for continuous recording of the mean arterial blood pressure and determination of arterial blood gases, pH, and glucose. Body temperature was maintained at 37.5–38.0°C throughout the experiment by using a homeothermic pad. Microdialysis concentric cannulae (4 mm length, 0.25 mm diameter, AN69 Hospal Medical, New Brunswick, NJ, U.S.A.; Obrenovitch et al., 1993) were implanted in the dorsolateral striatum (coordinates: 0.8 mm anterior to bregma, 3 mm lateral and 7 mm deep from the dural surface; Paxinos and Watson, 1986) and perfused with artificial CSF (ASCF; composition in mmol/L: NaCl 125, KCl 2.5, $MgCl_2$ 1.18, $CaCl_2$ 1.26) at 0.5 μl/min with a syringe pump (CMA/Microdialysis, Stockholm, Sweden).

### Biochemical measurements

Lactate concentration in the dialysate was determined by on-line fluorimetric detection of NADH resulting from the reaction of lactate and $NAD^+$ catalysed by lactate dehydrogenase (LDH) (Kuhr and Korf, 1988; Obrenovitch et al., 1990). The reagent contained 5.4 U/ml LDH (L-lactate:NAD oxidoreductase, EC 1.1.1.27, isolated from rabbit muscle; 500 U/mg specific activity), 45.25 mmol/L $NAD^+$, 0.29% (vol/vol) hydrazine in Tris buffer (100 mmol/L, pH 8.7). A peristaltic pump (Minipulse 3, Gilson France, Villiers Le Bel, France; 20 μl/min flow rate) mixed the enzymatic reagent with the brain dialysate as it emerged from the implanted microdialysis probe. After flowing through polyethylene tubing (530 mm length, 0.4 mm inner diameter, Portex Ltd., Hythe, U.K.) to allow the enzymatic reaction to occur, NADH was detected fluorimetrically (Perkin-Elmer LC-240, Beaconsfield, U.K.), using a 4-μl flow cell, with excitation and emission wavelengths of 340 and 450 nm, respectively. We have verified in preliminary experiments that modifying the $K^+$ concentration of the perfusing medium did not alter the flow enzymatic analysis of lactate. Calibration was achieved using standard solutions of lactate (0, 0.5, 1.0, and 2.0 mmol/L). As recovery of endogenous compounds in vivo cannot be compared with that in vitro (Scheller and Kolb, 1991; Parsons and Justice, 1992; Kehr, 1993), results were not corrected for recovery and are given as dialysate concentration. As lactate can become a major energy source in brain tissue under certain circumstances (Schurr et al., 1988; Bock et al., 1989), which probably includes repolarisation (see Discussion), using the internal reference technique of Scheller and Kolb (1991) with L-[$^{14}$C]-lactate to calculate extracellular concentration would have been inappropriate as this method requires the radiolabelled tracer to be inert.

### Experimental protocol

After a 180-min stabilisation/control period, the perfusing fluid was switched from ACSF to an isoosmotic medium containing high $K^+$ (composition in mmol/L: KCl 100, NaCl 27.5, $CaCl_2$ 1.26, $MgCl_2$ 1.18) for 20 min, before a recovery period of 40 min (normal ACSF). A second $K^+$ challenge of the same duration was produced with a further recovery period of 40 min. Experiments were concluded by killing the animal by rapid intravenous injection of 1-ml bolus of air or, in some cases, by 5% halothane and anoxia. All parameters continued to be monitored for 30 min after death.

### Recording of extracellular DC potential

DC potential recording was performed with a small chlorided silver wire incorporated within the microdialysis probe (Obrenovitch et al., 1993). A silver/silver chloride reference electrode was placed directly onto the skull, using a drop of electrode gel (Neptic, Sandev Ltd., Harlow, U.K.). The Ag/AgCl reference was made of a pellet of Ag-AgCl (type E225; 0.8 mm outer diameter; Clark Electromedical Instruments, Reading, U.K.) placed in a glass tube (1.5 mm inner diameter) closed at one end with porous glass and filled with physiological saline. The potential between the wire within the probe and the reference was first amplified with a high impedance input preamplifier (Neurolog System, Digitimer Ltd., Welwyn Garden City, U.K.). The antenna effect of the tubing between the syringes and the microdialysis probe was eliminated by grounding the metal needle of the syringes with wires incorporating 0.01-μF capacitors. A dedicated application program allowed all parameters to be continuously acquired, displayed, and stored. DC potential and dialysate lactate were digitised and converted to absolute values from prior calibration.

All values in Results are mean ± SEM. Statistical analysis was by Student's unpaired or paired *t* test.

## RESULTS

Mean arterial blood pressure, blood gases, pH, and glucose concentration were within the following ranges: $P_{CO_2}$, 63 ± 2 mm Hg; $P_{O_2}$, 154 ± 6 mm Hg; pH, 7.30 ± 0.01; glucose, 7.8 ± 0.3 mmol/L (n = 12).

The dialysate concentrations of lactate ($[lact]_d$) remained relatively stable throughout the 60-min control period (0.56 ± 0.06 mmol/L). High $K^+$ evoked a large and sustained negative shift of DC potential (mean amplitude, 15.4 ± 0.8 mV) onto which were superimposed transient peaks of further depolarisation. The number of these peaks varied between experiments and between the two challenges of the same experiment (between 1 and 6), but the amplitudes of the shifts were similar (mean amplitude, 9.9 ± 0.94 mV). When normal ACSF was perfused, the DC potential returned to a level comparable with that of the control period (mean amplitude of change, 16.5 ± 0.97 mV). $K^+$-induced changes in $[lact]_d$ were closely related to those of the DC potential, with different patterns of activity depending on the number of depolarisations and the time at which these occurred during the challenge.

The large sustained negative shift in DC potential was associated with a small decrease in $[lact]_d$ (Fig. 1). However, when a transient depolarisation occurred shortly after the shift in DC potential, this decrease in $[lact]_d$ was masked by a transient increase (Fig. 2). Whenever a single transient depolarisation peak occurred at the end of the high $K^+$ stimulus, an exaggerated increase of $[lact]_d$ was observed as DC potential was returning to its control level.

Multiple depolarisations during a $K^+$ stimulus produced a sustained increase in $[lact]_d$ starting with the initial decrease in DC potential (Fig. 3). In these cases, small $[lact]_d$ increases were detected after each tran-

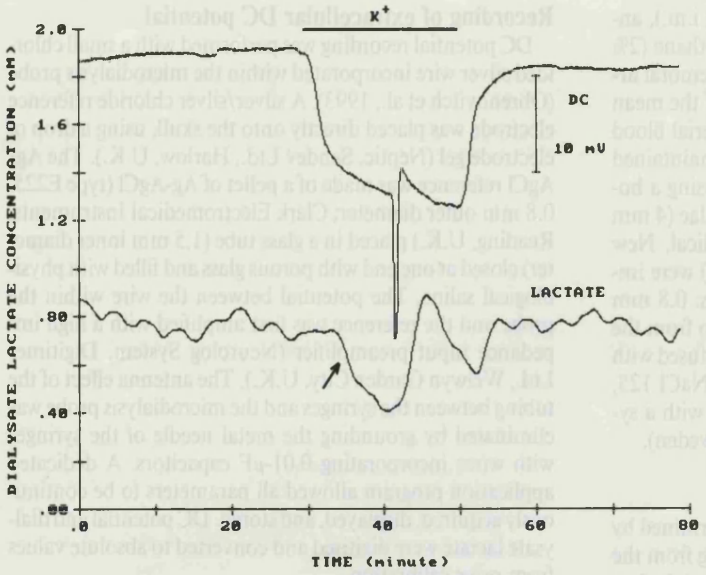


**FIG. 1.** Representative changes in $[lact]_d$ and DC potential during a 20-min $K^+$ stimulus, where the decrease in $[lact]_d$ associated with the initial negative shift in DC potential was clearly visible (arrow). The horizontal line at the top of the figure ($K^+$) indicates the periods of high $K^+$ stimulation.

sient depolarisation. During recovery, as repolarisation occurred, a large increase in $[lact]_d$ was consistently observed, lasting for 15 min, before returning to near baseline level. The magnitude of the $[lact]_d$ increase during DC potential recovery after the first challenge was always higher than that of the second (1.1 ± 0.2, 1.0 ± 0.15 mmol/L, respectively; $p < 0.005$, paired $t$ test). The rate of increase in $[lact]_d$ after the $K^+$ challenge was much faster than its rate of decrease (0.2 ± 0.03, 0.07 ± 0.01 mmol/min, respectively; $p < 0.001$, paired $t$ test).

Each of these different patterns had several common characteristics. (1) Regardless of the number of transient depolarisations, there was an increase in $[lact]_d$ after each repolarisation and with the end of the $K^+$ stimulus (see arrows in Fig. 2). (2) Between the two $K^+$ challenges and before cardiac arrest, $[lact]_d$ was higher than the original control level (0.68 ± 0.08 and 0.69 ± 0.09 mmol/L, respectively, $p = 0.05$). And (3), with cardiac arrest, there was an immediate and rapid increase in $[lact]_d$ at 0.39 ± 0.04 mmol/min, to 1.9 ± 0.2 mmol/L, where it stabilised and only decreased slightly during the 30-min recording post-mortem.

Mean changes of $[lact]_d$ for the 12 experiments are summarised in Fig. 4. There was a slight difference between the pre-$K^+$ stimuli levels of the first and second challenges (B) but not between the 20-min $K^+$ stimuli (K). A marked $[lact]_d$ increase was observed after each high $K^+$ challenge, the magnitude of which was higher after the first challenge than the second as already mentioned.

## DISCUSSION

Lactic acid production is stimulated whenever oxygen demand exceeds its supply. The distribution of lactic acid between the intra- and extracellular space

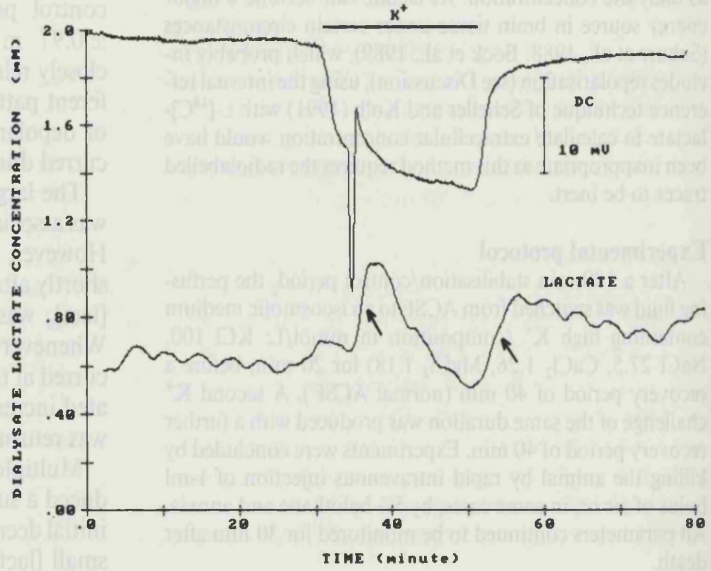


**FIG. 2.** Representative changes in $[lact]_d$ and DC potential during a 20-min $K^+$ stimulus, where a single depolarisation occurred. An increase in $[lact]_d$ was observed after the transient depolarisation. $[lact]_d$ then decreased slowly to a level below that of the control before a second increase in $[lact]_d$ corresponding to repolarisation after the high $K^+$ stimulus. Arrows indicate the two increases in $[lact]_d$ after each repolarisation. The horizontal line at the top of the figure ($K^+$) indicates the periods of high $K^+$ stimulation.

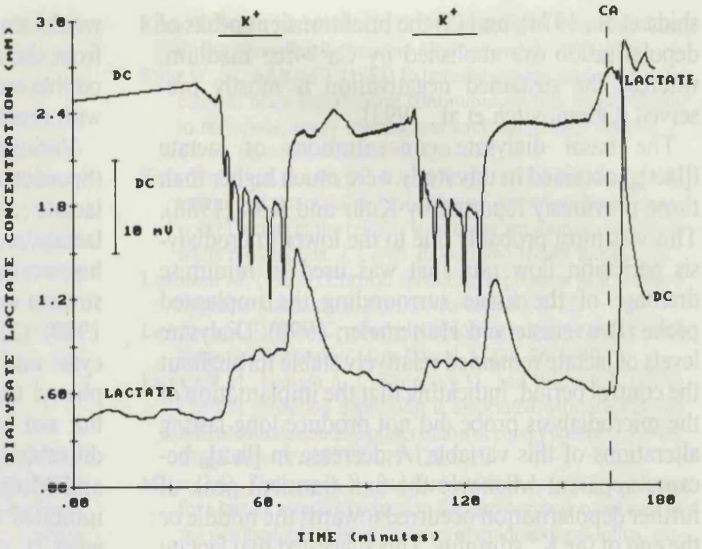


**FIG. 3.** Representative changes in $[lact]_d$ and DC potential during two successive 20-min $K^+$ stimuli that were associated with multiple depolarisations. $[lact]_d$ increased with the initial negative shift in DC potential, with small $[lact]_d$ increases detected after each transient depolarisation. After the $K^+$ stimulus a large increase in $[lact]_d$ was observed that slowly decreased to a level higher than that of the control. The magnitude of the $[lact]_d$ increase after the first stimulus was larger than after the second. With cardiac arrest (induced with 5% halothane and anoxia), $[lact]_d$ increased immediately, reaching a peak at which it stabilised, and only decreased slightly thereafter. The horizontal lines at the top of the figure ($K^+$) indicate periods of high $K^+$ stimulation. CA = cardiac arrest.

under these circumstances warrants examination because it may play an important part in the overall mechanisms leading to brain tissue damage. The deleterious effects of stroke and head trauma, which combine lactacidosis and altered membrane function, may be aggravated by a collapse of intracellular acid–base regulation subsequent to "trapping" of intracellular lactate and increased cellular membrane permeability to $H^+$ and $HCO_3^-$ (Obrenovitch et al., 1990; Taylor et al., 1991). Furthermore, marked increases in ECF lactate, to which extracellular acidosis is associated (Symon et al., 1993), may modify the sensitivity of ligand-operated ionic channels such as the *N*-methyl-D-aspartate receptor ionophore complex (Giffard et al., 1990; Traynelis and Cull-Candy, 1990).

Lactate exchanges across the plasma membrane are generally considered to occur by passive diffusion of undissociated lactic acid (Nedergaard et al., 1989), or via a lactate transporter that may be coupled to energy-dependent $Na^+/K^+$ transmembrane gradients (Kuhr and Korf, 1988). The latter implies that transmembrane lactate transport may be altered during $K^+$-induced depolarisation when ionic gradients are severely disrupted. To test this hypothesis, we looked at the effect of 20-min high $K^+$ on extracellular lactate, using on-line measurement of $[lact]_d$.

Recording of the DC potential with a microelectrode placed within the microdialysis probe is equivalent to that obtained with a conventional glass capillary (Obrenovitch et al., 1993). Data accumulated with this method of DC potential recording suggest that the $K^+$-induced sustained negative shift reflects sustained depolarisation of the cell populations that are immediately next to the surface of the dialysis membrane (Caspers et al., 1984). The peaks of further negativation may result from the depolarisation of cells either further away from the probe or that are more resistant to high $K^+$–induced depolarisation. The following information suggests that the transient peaks may be mostly of neuronal origin: (1) Changes in the DC potential reflect alterations in the membrane potential of both glial cells and neurons (Higa-

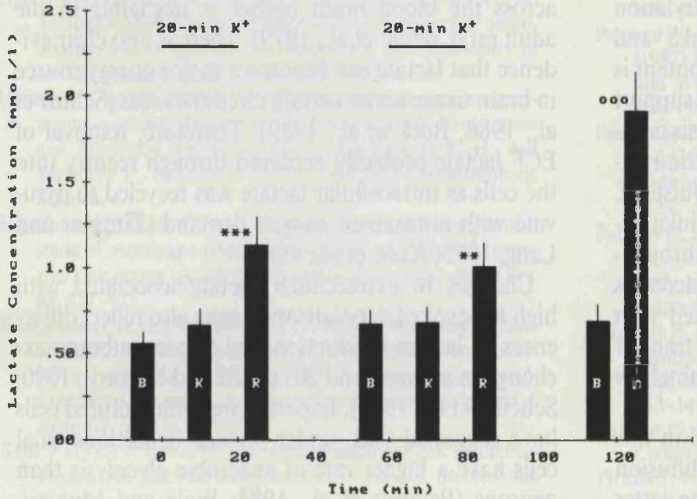


**FIG. 4.** Average changes in $[lact]_d$. Values are mean ± SEM, n = 12. B, average concentration during 5 min preceding a stimulus and cardiac arrest; K, mean $[lact]_d$ during the 20-min stimulus, was calculated from three values taken at 5, 12, and 19 min during the challenge; R, level reached after perfusate was switched back to normal ACSF. There was no difference between B and K for either of the two stimuli, but there was a significant difference between K and R for each challenge ($^{**}p < 0.01$; $^{***}p < 0.001$, paired *t* test). The increase after the first $K^+$ stimulus was higher than that observed after the second. The increase during the postmortem period was significantly higher than the preceding resting level ($^{ooo}p < 0.001$, paired *t* test). The horizontal lines at the top of the figure ($K^+$) indicate periods of high $K^+$ stimulation.

shida et al., 1974), and (2) the brief transient peaks of depolarisation are abolished by $Ca^{2+}$-free medium, whereas the sustained negativation is mostly preserved (Obrenovitch et al., 1993).

The basal dialysate concentrations of lactate ($[lact]_d$) obtained in this study were much higher than those previously reported by Kuhr and Korf (1988). This was most probably due to the lower microdialysis perfusion flow rate that was used to minimise drainage of the tissue surrounding the implanted probe (Benveniste and Hüttemeier, 1990). Dialysate levels of lactate remained relatively stable throughout the control period, indicating that the implantation of the microdialysis probe did not produce long-lasting alterations of this variable. A decrease in $[lact]_d$ became apparent whenever the first transient peak of further depolarisation occurred towards the middle or the end of the $K^+$ stimulus. This suggested that lactate transport out of some cells was altered very early after application of high $K^+$. Within each SD, the positive shift in DC potential indicating cell repolarisation was associated with an increase in $[lact]_d$. This phenomenon was observed irrespective of whether the SD was isolated or part of a repetitive pattern. That $[lact]_d$ changes associated with isolated SD appeared better resolved than those associated with repeated SD (Figs. 1 and 2) may reflect a slow removal of lactate from the extracellular space. Another consistent feature was a marked and rapid increase in ECF lactate after the $K^+$ stimulus. Taken together, these data strongly suggest that extracellular lactate levels mostly increased during periods of repolarisation.

Activation of anaerobic metabolism is known to occur early with SD and exposure to high $K^+$ (Mutch and Hansen, 1984), probably initiated by the collapse of the cation gradients coupled to membrane depolarisation (Bures et al., 1974) and according to the following cascade of events: (1) High extracellular $K^+$ and intracellular $Na^+$ activate $Na^+,K^+$-ATPase (Walz, 1992) leading to a decline in ATP with increased ADP and AMP levels. (2) These changes, in turn, stimulate glycolysis via phosphofructokinase activation, and enhanced mitochondrial oxidative phosphorylation with higher oxygen consumption (Erecińska and Silver, 1989). (3) When the cellular oxygen content is reduced below the critical level necessary to support oxidative phosphorylation, anaerobic glycolysis is enhanced and intracellular lactic acid production increased (Assaf et al., 1990; Hansen and Quistorff, 1993). It is very likely, therefore, that intracellular accumulation of lactic acid occurred early and throughout the $K^+$ stimuli in these experiments. As increases of extracellular lactate were mainly associated with periods of repolarisation, this implies that the transfer of lactate across the plasma membrane was somehow impaired during depolarisation.

The changes in extracellular lactate found in this study cannot be explained by simple passive diffusion of lactate across the plasma membrane. The latter would imply a sustained increase of $[lact]_d$ starting from the onset of the $K^+$ stimulus, and it is not compatible with the marked $[lact]_d$ increases associated with repolarisation.

Various data have suggested that, as in other tissues (Spencer and Lehninger, 1976; Mann et al., 1985), lactate can be released from neurons and glial cells by lactate/proton cotransport. (1) Lactate release from hippocampal slices during a number of metabolic stresses was saturable and stereospecific (Assaf et al., 1990). (2) Lactate release from both cultured astrocytes and neurons was inhibited by DL-*p*-hydroxyphenyl lactate (a lactate/proton exchange inhibitor) but not by the $HCO_3^-/Cl^-$ exchange inhibitor 4,4′-diisothiocyanostilbene-2,2′-disulphonic acid (Walz and Mukerji, 1988). (3) Lactate efflux to ECF was inhibited by probenecid (Pardridge et al., 1975; Yuwiler et al., 1982; Kuhr et al., 1988). However, the energy dependency of lactate transport from brain remains unclear. On one hand, lactate exchanges between brain slices and the outer medium were neither dependent on ATP (Assaf et al., 1990; Kauppinen and Williams, 1990) nor on $Na^+$ (Pirtillä and Kauppinen, 1992). In contrast, increases in ECF lactate during complete ischaemia and after electroconvulsive shock were delayed in comparison with those of tissue lactate (Kuhr and Korf, 1988), suggesting that lactate removal from intracellular compartments may involve a transporter coupled to energy-dependent $Na^+/K^+$ transmembrane gradients. The latter hypothesis is strongly supported by the $K^+$ effects observed in the present study. That lactate appeared very rapidly in the ECF after cardiac arrest, but stabilized as terminal anoxic depolarisation occurred, is in line with this hypothesis.

The rate of extracellular lactate removal after the $K^+$ stimulus was significantly slower than its initial release. It is unlikely that clearance via the vascular system was a significant contributor to removal of extracellular lactate, despite the transient hyperaemia subsequent to SD and high $K^+$ stimuli (Lauritzen, 1987*b*), because monocarboxylic acid transport across the blood–brain barrier is negligible in the adult rat (Cremer et al., 1979). There is also clear evidence that lactate can become a major energy source in brain tissue under certain circumstances (Schurr et al., 1988; Bock et al., 1989). Therefore, removal of ECF lactate probably occurred through reentry into the cells as intracellular lactate was recycled to pyruvate with normalised oxygen demand (Zimmer and Lang, 1975; Kuhr et al., 1988).

Changes in extracellular lactate associated with high $K^+$-evoked depolarisation may also reflect differences in lactate production and transmembrane exchange in neurons and glia (Walz and Mukerji, 1990; Scheller et al., 1992). Experiments with cultured cells have suggested that, under normal conditions, glial cells have a higher rate of anaerobic glycolysis than neurons (Pauwels et al., 1985; Walz and Mukerji,

1990). In contrast, astrocytes and neurons have apparently identical transport mechanisms for lactate (Walz and Mukerji, 1988). It would be relevant to examine this question further using microdialysis and selective inactivation of glial cell metabolism with fluorocitrate (Paulsen et al., 1987; Paulsen and Fonnum, 1989).

In conclusion, microdialysis data strongly suggest that lactate removal from intracellular compartments may involve a transporter coupled to energy-dependent $Na^+/K^+$ transmembrane gradients. This hypothesis deserves further investigation because of its relevance to neuroprotection.

**Acknowledgment:** We acknowledge the skilful technical assistance of Mr. A. Hardy. This work was supported by the Brain Research Trust (Institute of Neurology, London) and funds provided by the Joint Research Advisory Committee (The National Hospitals, Queen Square, London).

## REFERENCES

Assaf H. M., Ricci A. J., Whittingham T. S., LaManna J. C., Ratcheson R. A., and Lust W. D. (1990) Lactate compartmentation in hippocampal slices: evidence for a transporter. *Metab. Brain Dis.* **5**, 143–154.

Benveniste H. and Hüttemeir P. C. (1990) Microdialysis: theory and application. *Prog. Neurobiol.* **35**, 195–215.

Bock A. C., Scheller D., Tegtmeier F., Hansen A. J., Dengler K., Zacharias E., and Höller M. (1989) Postischemic recovery of electrophysiological function and extracellular pH during normo- and aglycemic reperfusion. *J. Cereb. Blood Flow Metab.* **9** (Suppl. 1), S642.

Bures J., Buroseva O., and Krivanek J. (1974) *The Mechanism and Applications of Leao's Spreading Depression of Electroencephalographic Activity.* Academic Press, New York.

Caspers H., Speckmann E.-J., and Lehmenkühler A. (1984) Electrogenesis of slow potential of the brain, in *Self-Regulation of the Brain and Behavior* (Elbert T., Rockstroh B., Lutzenberger W., and Birbaumer N., eds), pp. 26–41. Springer, Berlin.

Cremer J. E., Cunningham V. J., Pardridge W. M., Braun L. D., and Oldendorf W. H. (1979) Kinetics of blood–brain barrier transport of pyruvate, lactate, and glucose in suckling, weanling, and adult rats. *J. Neurochem.* **33**, 439–445.

Erecińska M. and Silver I. A. (1989) ATP and brain function. *J. Cereb. Blood Flow Metab.* **9**, 2–19.

Giffard R. G., Monyer H., Christine C. W., and Choi D. W. (1990) Acidosis reduces NMDA receptor activation, glutamate neurotoxicity, and oxygen-glucose deprivation neuronal injury in cortical cultures. *Brain Res.* **506**, 339–342.

Hansen A. J. and Quistorff B. (1993) Glucose metabolism in experimental spreading depression, in *Migraine: Basic Mechanisms and Treatment* (Lehmenkühler A., Grotemeyer K.-H., and Tegtmeier F., eds), pp. 367–377. Urban and Schwartzenberg, Munich.

Higashida H., Mitarai G., and Watanabe S. (1974) A comparative study of membrane potential changes in neurons and neuroglial cells during spreading depression in the rabbit. *Brain Res.* **65**, 411–425.

Kauppinen R. A. and Williams S. R. (1990) Cerebral energy metabolism and intracellular pH during severe hypoxia and recovery: a study using $^1H$, $^{31}P$, and $^1H[^{13}C]$ nuclear magnetic resonance spectroscopy in the guinea-pig cerebral cortex *in vitro*. *J. Neurosci. Res.* **26**, 356–369.

Kehr J. (1993) A survey on quantitative microdialysis: theoretical models and practical implications. *J. Neurosci. Methods* **48**, 251–261.

Kraig R. P. and Nicholson C. (1978) Extracellular ionic variations during spreading depression. *Neuroscience* **3**, 1045–1059.

Kuhr W. G. and Korf J. (1988) Extracellular lactic acid as an indicator of brain metabolism: continuous on-line measurement in conscious, freely moving rats with intrastriatal dialysis. *J. Cereb. Blood Flow Metab.* **8**, 130–137.

Kuhr W. G., van den Berg C. J., and Korf J. (1988) In vivo identification and quantitative evaluation of carrier-mediated transport of lactate at the cellular level in the striatum of conscious, freely moving rats. *J. Cereb. Blood Flow Metab.* **8**, 848–856.

Lauritzen M. (1987*a*) Cortical spreading depression as a putative migraine mechanism. *Trends Neurosci.* **10**, 8–12.

Lauritzen M. (1987*b*) Cerebral blood flow in migraine and cortical spreading depression. *Acta Neurol. Scand.* **76**, 9–40.

Lauritzen M., Hansen A. J., Kronborg D., and Wieloch T. (1990) Cortical spreading depression is associated with arachidonic acid accumulation and preservation of energy charge. *J. Cereb. Blood Flow Metab.* **10**, 115–122.

Mann G. E., Zlokovic B. V., and Yudilevich D. L. (1985) Evidence for a lactate transport system in the sarcolemmal membrane of the perfused rabbit heart: kinetics of unidirectional influx, carrier specificity and effects of glucagon. *Biochim. Biophys. Acta* **819**, 241–248.

Mies G. and Paschen W. (1984) Regional changes of blood flow, glucose and ATP content determined from brain sections during a single passage of spreading depression in the rat brain cortex. *Exp. Neurol.* **84**, 249–258.

Mutch W. A. C. and Hansen A. J. (1984) Extracellular pH changes during spreading depression and cerebral ischaemia: mechanisms of brain pH regulation. *J. Cereb. Blood Flow Metab.* **4**, 17–27.

Nedergaard M., Goldman S. A., and Pulsinelli W. A. (1989) Lactic-acid-induced intracellular acidification in primary cultures of mammalian brain. *J. Cereb. Blood Flow Metab.* **9** (Suppl. 1), S384.

Obrenovitch T. P., Sarna G. S., Millan M. H., Lok S.-Y., Kawauchi M., Ueda Y., and Symon L. (1990) Intracerebral dialysis with on-line enzyme fluorimetric detection: a novel method to investigate the changes in the extracellular concentration of glutamic acid, in *Pharmacology of Cerebral Ischaemia,* (Krieglstein J. and Oberpichler H., eds), pp. 23–31. Wiss, Verlag, Stuttgart.

Obrenovitch T. P., Richards D. A., Sarna G. S., and Symon L. (1993) Combined intracerebral microdialysis and electrophysiological recording: methodology and applications. *J. Neurosci. Methods* **47**, 139–145.

Pardridge W. M., Conner J. D., and Crawford I. L. (1975) Permeability changes in the blood–brain barrier: causes and consequences. *CRC Crit. Rev. Toxicol.* **3**, 159–199.

Parsons L. H. and Justice J. B. Jr. (1992) Extracellular concentration and in vivo recovery of dopamine in the nucleus accumbens using microdialysis. *J. Neurochem.* **58**, 212–218.

Paschen W., Djuricic B., Mies G., Schmidt-Kastner R., and Linn F. (1987) Lactate and pH in the brain: association and dissociation in different pathophysiological states. *J. Neurochem.* **48**, 154–159.

Paulsen R. E. and Fonnum F. (1989) Role of glial cells for the basal and $Ca^{2+}$-dependent $K^+$-evoked release of transmitter amino acids investigated by microdialysis. *J. Neurochem.* **52**, 1823–1829.

Paulsen R. E., Contestabile A., Villani L., and Fonnum F. (1987) An in vivo model for studying function of brain tissue temporarily devoid of glial cell metabolism: the use of fluorocitrate. *J. Neurochem.* **48**, 1377–1385.

Pauwels P. J., Opperdoes F. R., and Trouet A. (1985) Effects of antimycin, glucose deprivation, and serum on cultures of neurons, astrocytes, and neuroblastoma cells. *J. Neurochem.* **44**, 143–148.

Paxinos G. and Watson C. (1986) *The Rat Brain in Stereotaxic Coordinates.* Academic Press, London.

Pirttilä T.-R. M. and Kauppinen R. A. (1992) Recovery of intracellular pH in cortical brain slices following anoxia studied by

nuclear magnetic resonance spectroscopy: role of lactate removal, extracellular sodium and sodium/hydrogen exchange. *Neuroscience* **47,** 115–164.

Roos A. and Boron W. F. (1981) Intracellular pH. *Physiol. Rev.* **61,** 296–434.

Rosenthal M. and Somjen G. (1973) Spreading depression, sustained potential shifts, and metabolic activity of cerebral cortex of cats. *J. Neurophysiol.* **36,** 739–749.

Scheller D. and Kolb J. (1991) The internal reference technique in microdialysis: a practical approach to monitoring dialysis efficiency and to calculating tissue concentration from dialysate samples. *J. Neurosci. Methods* **40,** 31–38.

Scheller D., Kolb J., and Tegtmeier F. (1992) Lactate and pH change in close correlation in the extracellular space of the rat brain during cortical spreading depression. *Neurosci. Lett.* **135,** 83–86.

Schurr A., West C. A., and Rigor B. M. (1988) Lactate-supported synaptic function in the rat hippocampal slice preparation. *Science* **240,** 1326–1328.

Shinohara M., Dollinger B., Brown F., Rapoport S., and Sokoloff L. (1979) Cerebral glucose utilization: local changes during and after recovery from spreading cortical depression. *Science* **203,** 188–190.

Spencer T. L. and Lehninger A. L. (1976) L-Lactate transport in Ehrlich ascites-tumour cells. *Biochem. J.* **154,** 405–414.

Symon L., Taylor D. L., and Obrenovitch T. P. (1993) Aspects of acid-base homeostasis in ischemia, in *Cerebral Ischemia and Basic Mechanisms* (Hartmann A., Yatsu F., and Kuschinsky W., eds), (in press). Springer-Verlag, Berlin.

Taylor D. L., Obrenovitch T. P., Ueda Y., and Symon L. (1991) Direct evidence for a rapid redistribution of bicarbonate ions during anoxic depolarisation. *J. Cereb. Blood Flow Metab.* **11** (Suppl. 2), S519.

Tegtmeier F. (1993) Differences between cortical spreading depression and ischemia, in *Migraine: Basic Mechanisms and Treatment* (Lehmenkühler A., Grotemeyer K.-H., and Tegtmeier F., eds), pp. 511–532. Urban and Schwartzenberg, Munich.

Traynelis S. F. and Cull-Candy S. G. (1990) Proton inhibition of *N*-methyl-D-aspartate receptors in cerebellar neurons. *Nature* **345,** 347–350.

Walz W. (1992) Role of Na/K/Cl cotransport in astrocytes. *Can. J. Physiol. Pharmacol.* **70** (Suppl.), S260–S262.

Walz W. and Mukerji S. (1988) Lactate release from cultured astrocytes and neurons: a comparison. *Glia* **1,** 366–370.

Walz W. and Mukerji S. (1990) Simulation of aspects of ischemia in cell culture: changes in lactate compartmentation. *Glia* **3,** 522–528.

Young D. B. and Van Vliet B. N. (1991) Migraine with aura: a vicious cycle perpetuated by potassium-induced vasoconstriction. *Headache* **32,** 24–34.

Yuwiler A., Bennett B. L., and Geller E. (1982) Is there a probenecid sensitive transport system for monoamine catabolites at the level of the brain capillary plexus? *Neurochem. Res.* **7,** 1277–1285.

Zimmer R. and Lang R. (1975) Rates of lactic acid permeation and utilization in the isolated dog brain. *Am. J. Physiol.* **229,** 432–437.

Neurochemical Research, Vol. 21, No. 9, 1996, pp. 1013–1021

# Changes in Extracellular Acid-Base Homeostasis in Cerebral Ischemia*

Deanna L. Taylor,[1] Tihomir P. Obrenovitch,[1,2] and Lindsay Symon[1]

(Accepted December 5, 1995)

The purpose of this study was to examine the changes in extracellular $CO_3^{2-}$ and lactate concentration produced by ischemia, especially in relation to the occurrence of anoxic depolarization, and how some of these changes are altered by the inhibition of organic acid transport systems with probenecid. These data demonstrate that (i) the transmembrane mechanisms contributing to intracellular acid-base regulation ($Na^+/H^+$ and $HCO_3^-/Cl^-$ exchanges, and lactate/$H^+$ cotransport) are markedly activated during ischemia; (ii) the efficacy of these mechanisms is abolished as the cellular membrane permeability to ions, including $H^+$ and pH-changing anions, suddenly increases with anoxic depolarization; and (iii) efflux of intracellular lactate during ischemia, and its reuptake with reperfusion, mainly occur via a transporter. These findings imply that residual cellular acid-base homeostasis persists as long as cell depolarization does not occur, and strengthen the concept that anoxic depolarization is a critical event for cell survival during ischemia.

KEY WORDS: Cerebral ischemia; extracellular acidosis; lactate; acid-base regulation; microdialysis; probenecid.

## INTRODUCTION

Brain tissue is extremely sensitive to inadequate blood supply, and even brief ischemic episodes can lead to irreversible neurological deficits. Experimental studies of cerebral ischemia have identified four dominant processes which, alone or combined, underlie ischemia-induced neuronal damage: intracellular $Ca^{2+}$ overload (1), free radical-related damage which may primarily target vascular tissue (2), glutamate-receptor mediated neurotoxicity (3), and acidosis (4). Acidosis promotes ischemic brain tissue damage (5), by itself, and by potentiating other deleterious processes such as lipid peroxidation (6), although extracellular acidosis protects cultured neurons against *N*-methyl-D-aspartate (NMDA)-receptor mediated injury (7).

One major element of intracellular acid-base regulation is the plasmalemnal $Na^+/H^+$ exchanger, possibly supplemented by $HCO_3^-/Cl^-$ exchanges (8). These exchanges are driven by the $Na^+$ gradient maintained across the cellular membrane by the $Na^+/K^+$-ATPase and, therefore, are dependent on ATP availability. Bicarbonate buffering ($CO_2/HCO_3^-$) and production/metabolism of lactic acid also contribute to intracellular acid-base regulation (9).

Although intracellular acidosis has been extensively investigated (9) and new insights have recently been provided by nuclear magnetic resonance spectroscopy (10–12), extracellular (i.e., the neuronal microenvironment) acid-base changes are also important. Our previous work has focused on changes in extracellular [$H^+$], tissue partial pressure of carbon dioxide, and total tissue concentration of lactic acid in anoxia and ischemia (13–16). From this several relevant features emerged: (i) lactic

[1] Gough-Cooper Department of Neurological Surgery, Institute of Neurology, London, United Kingdom.
[2] Address reprint requests to: Dr. T. P. Obrenovitch, Department of Neurochemistry, Institute of Neurology, Queen Square, London WC1N 3BG, United Kingdom.
* Special issue dedicated to Dr. Herman Bachelard.



0364-3190/96/0900-1013$09.50/0 

acid accumulation resulting from anaerobic metabolism is closely associated with brain tissue acidification (15); (ii) increased levels of carbon dioxide contribute to acidosis of the extracellular space (13,14); and (iii) a rapid intra-/extracellular redistribution of $H^+$ is associated with anoxic depolarization (i.e. sudden increase in the ionic permeability of the plasma membrane), suggesting that transmembrane acid-base regulation mechanisms persist, to some degree, as long as this event does not occur, but collapse subsequent to it (16).

The present study focuses on changes in extracellular $CO_3^{2-}$ and lactate concentrations in relation to the occurrence of anoxic depolarization, and how some of these changes are altered by pharmacological inhibition of organic acid transport systems.

The capacity of the extracellular fluid to buffer $H^+$ is largely dependent on $HCO_3^-$ and $CO_3^{2-}$. Although the extracellular concentration of $HCO_3^-$ is around 200 fold larger than that of $CO_3^{2-}$ (9,17), $CO_3^{2-}$ is an important component of the bicarbonate/carbonic acid buffer system (a), and in equilibrium with $HCO_3^-$. Furthermore, as opposed to $HCO_3^-$, $CO_3^{2-}$ concentrations can be accurately recorded in vivo with ion-selective electrodes (17).

$$CO_2 + H_2O <\!\!-\!\!> H_2CO_3 <\!\!-\!\!> \underset{+\ H^+}{HCO_3^-} <\!\!-\!\!> CO_3^{2-} + H^+ \quad \text{(a)}$$

## EXPERIMENTAL PROCEDURE

Extracellular recording of $CO_3^{2-}$ or lactate levels was combined with that of the extracellular direct current (DC) potential and electroencephalogram (EEG). These electrophysiological variables provided information on the severity of ischemia, and the DC potential was used for the detection of anoxic depolarization (18). Ischemia-induced changes in extracellular lactate were examined using microdialysis probes perfused with either control artificial cerebrospinal fluid (ACSF), or 20 mM probenecid in ACSF to inhibit lactic acid transport (19).

*Animal Preparation.* Experiments were performed on male Wistar rats (Bantin and Kingman, Grimston, U.K.) (weight, 320 ± 12 g; mean ± SEM) with food and water freely available. All animal procedures used were in accordance with the Home Office guidelines and specifically licensed under the Animals (Scientific Procedures) Act, 1986. After premedication with atropine sulphate (15–30 $\mu g \cdot Kg^{-1}$ i.m.) anaesthesia was induced and maintained with halothane (2% and 1.0–1.5%, respectively) in $O_2$:$N_2O$ (1:1). A femoral artery was catheterised for monitoring of the mean arterial blood pressure and determinations of arterial blood gases, pH and glycaemia, and a vein for drug administration. After tracheotomy, the animal was relaxed with tubocurarine (1 $mg \cdot Kg^{-1}$ i.v., repeated every hour) and ventilated with appropriate parameters to maintain normocapnia. Rats were prepared for transient forebrain ischemia produced by 4-vessel occlusion (20), with both common carotid arteries encircled with inflatable vascular occluders (Type OC2A, In Vivo Metric, Healdsburg, CA, U.S.A.) to allow remote induction of ischemia. Once surgical procedures were completed the concentration of halothane in the breathing mixture was reduced to 0.8–1.2%. Body temperature was maintained at 37.5–38°C throughout.

*Ion-selective Measurements of Extracellular $CO_3^{2-}$ Concentration.* Microelectrodes (10–15 µm tip diameter) were constructed from double-barrelled borosilicate capillaries. The tip of the active barrel was rendered hydrophobic with a 10% solution of N,N-dimethyltrimethylsilyamine (Aldrich Chemical Company, Gillingham, Dorset, U.K.) and filled with ion-exchange resin selective for $CO_3^{2-}$ (IE310, WPI, Stevenage, Herts, U.K.) followed by an internal reference solution (490 mM KCl; 10 mM $KHCO_3$; 10 mM potassium citrate; pH 4.82). The reference barrel contained 150 mM KCl. The electrodes were left to equilibrate overnight in 150 mM NaCl.

*In Vitro Assessment.* Electrodes were placed in 10 mM $NaHCO_3$ (37 °C) bubbled with air (i.e. $pCO_2$ 2–4 mmHg). After stabilization of the ion-selective microelectrode output and solution pH, bubbling was switched to 10% $CO_2$ in $N_2$ (i.e. $pCO_2$ around 76 mmHg). This change in $pCO_2$ produced a large decrease in the concentration of $CO_3^{2-}$ (21). Bubbling was then turned back to air, which increased the $CO_3^{2-}$ concentration steadily as the solution acidity returned to its initial level. ISM output was recorded, and plotted against changes in $CO_3^{2-}$ concentration calculated from the solution $pCO_2$ and pH. These latter variables were determined with miniature electrodes (WPI, Stevenage, Herts, U.K.) and verified with a blood gas analyzer (AVL Medical Instruments Ltd., Staffs, U.K.). Microelectrode responses to changes in $CO_3^{2-}$ concentration were linear over the range tested, and the response time adequate for the recording of sudden changes occurring in vivo. Experiments with potential interfering ions showed that the selectivity of microelectrodes $CO_3^{2-}$ was also appropriate.

Ion-selective microelectrodes were implanted into the frontal cortex (coordinates: 3 mm posterior to bregma, 1.5 mm lateral, and 1 mm deep from the cortical surface) (22). The exposed cortical surface was prevented from drying out by covering it with warm paraffin oil.

*Microdialysis.* Microdialysis probes (4 mm length, 0.25 mm diameter) (Cuprophan GFE 9, Gambro Ltd., Sidcup, U.K.) incorporating a recording electrode in the inlet tube (Fig. 1, left panel) (23) were implanted in the dorsolateral striatum (coordinates: 0.8 mm anterior to the bregma, 3 mm lateral, 7 mm deep from the dural surface) (22). Unless otherwise stated, they were perfused with control ACSF (composition in mM NaCl 125, KCl 2.5, $MgCl_2$ 1.18, $CaCl_2$ 1.26; unbuffered but with pH adjusted to 7.3) at 0.5 $\mu l \cdot min^{-1}$ with a syringe pump (CMA/100; CMA/Microdialysis, Stockholm, Sweden). A liquid switch (CMA/110; CMA/Microdialysis) enabled switching from normal ACSF to probenecid-ACSF (see experimental protocol).

*Flow Enzyme-Fluorescence Assay of Dialysate Lactate Levels.* Lactate concentration was determined by on-line fluorometric detection of NADH resulting from the reaction of lactate and $NAD^+$ catalysed by lactate dehydrogenase (LDH) (Fig. 1, right panel) (24,25). The enzymatic reagent contained 5.4 $U \cdot ml^{-1}$ LDH (EC 1.1.1.27, 500 $U \cdot mg^{-1}$ specific activity; Boehringer Mannhein UK Ltd., East Sussex, U.K.), 45.25 mM $NAD^+$ and 0.29 % v/v hydrazine in Tris buffer (100 mM; pH 8.7). A peristaltic pump (Minipulse 3, Gilson France, Villiers Le Bel, France; 20 $\mu l \cdot min^{-1}$ flow rate) mixed the reagent with the brain dialysate as it emerged from the implanted microdialysis probe. After flowing through polyethylene tubing (530 mm length, 0.4 mm i.d., Portex Ltd., Hythe, U.K.) to allow the enzymatic reaction to occur (3.3 min reaction time), NADH was detected fluorometrically (Merck-Hitachi F-1050, Merck-BDH, Leicestershire, U.K.), using a 4 µl flow cell, with excitation and emission wavelengths of 340 and 450 nm, respectively. Calibration was achieved using standard solutions of lactate (0, 0.5, 1.0, and 2.0 mM; L-Lactic acid, Fluka Chemicals Ltd.,

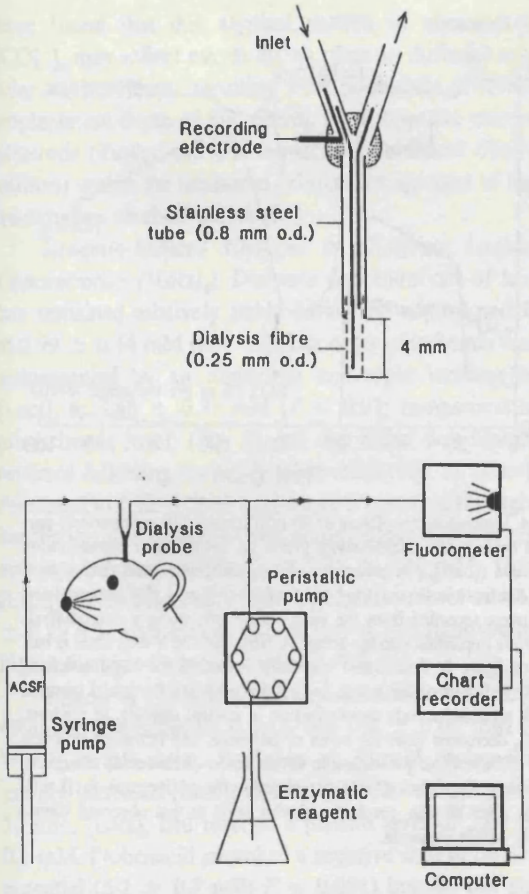


Fig. 1. Diagrams of the two essential elements which made possible the dual recording of changes in extracellular lactate concentration and DC potential at the same tissue site: microdialysis probes incorporating a chlorided silver electrode in the inlet tubing (left panel); and on-line enzyme-fluorescence assay of lactate in the dialysate emerging from the implanted microdialysis probe (Top). ACSF, artificial cerebrospinal fluid.

Dorset, U.K.). Results were not corrected for recovery and are given as dialysate concentrations (26,27).

*Electrophysiological Measurements.* The DC potential and EEG were derived from the potential between the electrode built into the microdialysis probe or the reference barrel of the ISM (depending on the method used), and a Ag/AgCl reference electrode placed on the conjunctiva or directly under the scalp. The signal recorded with the microdialysis electrode is equivalent to that obtained with a glass capillary electrode whose tip is positioned next to the outer surface of the dialysis membrane (23). The potential between the recording electrode and the reference was first amplified with a high impedance input preamplifier (NL102G, Neurolog System, Digitimer Ltd., Welwyn Garden City, U.K.). The AC component in the 1–30 Hz window, amplified 6,000–8,000 times, provided EEG, and the DC component, the DC potential.

*Experimental Protocol.* A delay of at least 2 h was allowed after implantation of the recording device. After a 60-min control period, transient ischemia was produced for 20 min by occlusion of the carotid arteries, and this was followed by 80 min of reperfusion.

The purpose of the first series of experiments was to study the changes in extracellular $CO_3^{2-}$ levels. Measurements were performed in the cerebral cortex because most previous investigations of ischemia-induced ionic changes have been performed in this structure (28,29).

The second series examined changes in extracellular lactate levels during transient ischemia, and how these changes might be altered by inhibition of organic acid transport with probenecid. These experiments were performed in the dorsolateral striatum because our previous studies on changes in extracellular lactate with $K^+$-induced depolarization had been performed in this region (30). In control experiments, normal ACSF was perfused throughout. In the others, 20 mM probenecid was perfused through the microdialysis probe for 50 min before ischemia, and then continuously throughout the experiment.

*Data Acquisition and Statistical Analysis.* A dedicated application program allowed all parameters to be continuously acquired, displayed and stored. Linear spectra of consecutive EEG data sections (4 sec) were computed using the fast Fourier transformation. For each 4 second epoch, the average amplitude of the EEG linear spectrum within the 6–21 Hz frequency window was computed and displayed as an index of electrical activity. The DC potential and ion-selective microelectrode output values were also digitised and converted to absolute values from prior calibration. Lactate data were stored and converted to molar concentrations, from post-experimental calibration.

All values in Results are mean ± SEM. Statistical analysis was by Student's unpaired or paired *t*-test.

## RESULTS

*Systemic Parameters and Ischemia-Induced Changes in EEG and DC Potential.* In all series, averages of arterial blood gases, pH, concentration of bicarbonate, and glycaemia were within the normal range throughout the experiment. Occlusion of the carotid arteries consistently reduced the EEG amplitude to noise level (Figs. 3 and 4), except in a few cases where significant activity persisted during the ischemic episode, despite a rapid and pronounced anoxic depolarization (see for example Fig. 2). Anoxic depolarization was marked and occurred within a few minutes in all experiments. The average amplitude of anoxic depolarization was 21.6 ± 2.5 mV (n = 6) when measured in the cerebral cortex with glass capillaries. It was not significantly different when measured in the striatum with a microdialysis electrode perfused with normal ACSF (18.1 ± 1.1 mV; n = 11), but was reduced to 12.4 ± 1.75 mV (n = 10; $P < 0.01$) by 20 mM probenecid in ACSF. Reperfusion was accompanied by a rapid positive shift in the DC potential indicating repolarization (Fig. 2, 3 and 4), but EEG recovery was much slower, and still incomplete after 80 min of reperfusion. At this point, EEG was 62.1 ± 9.9% (n = 6) of its original control value in the cortex (i.e. experiments with ion-selective measurements of $CO_3^{2-}$), but only 26.6 ± 4.2%

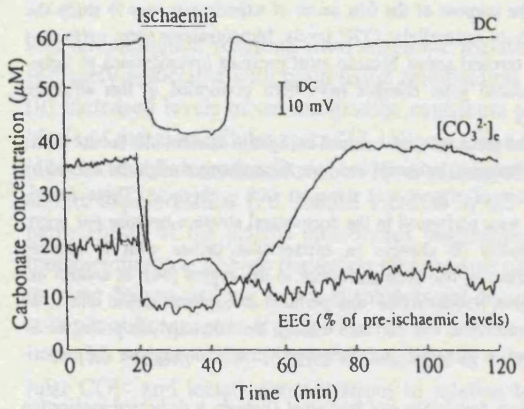


Fig. 2. Representative changes in extracellular carbonate concentration ($[CO_3^{2-}]_e$), DC potential and EEG during 20 min of forebrain ischemia (top horizontal line) and reperfusion. All parameters were recorded from the same tissue site, using a combined glass capillary electrode implanted 1 mm deep into the cerebral cortex. The EEG is presented in percent of the average amplitude computed over the last 20 min of control period (dotted horizontal line). The $[CO_3^{2-}]_e$ trace shows 3 relevant features: (i) immediate decrease of $[CO_3^{2-}]_e$ from the onset of ischemia; (ii) transient increase, synchronous with anoxic depolarization, and superimposed upon the steady decrease in $[CO_3^{2-}]_e$; and (iii) a further drop in $[CO_3^{2-}]_e$, closely associated with repolarization, preceding its progressive normalization during reperfusion.

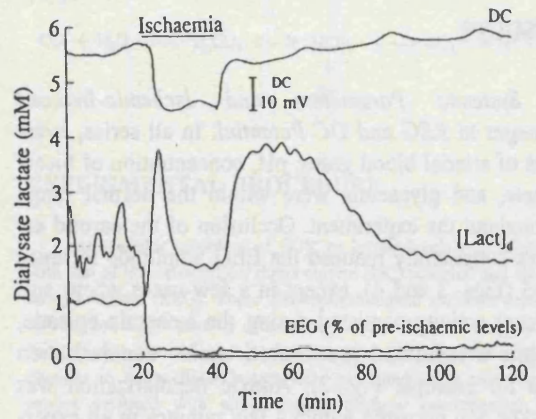


Fig. 3. Representative changes in extracellular concentration of lactate ($[Lact]_d$), DC potential and EEG during 20 min of forebrain ischemia (top horizontal line) and reperfusion. All parameters were recorded from the same tissue site, using a microdialysis *electrode* implanted into the striatum. The EEG is presented in percent of the average amplitude computed over the last 20 min of control period (dotted horizontal line). Ischemia immediately provoked a rapid and marked increase in extracellular lactate, but this change was reversed subsequent to anoxic depolarization. Reperfusion produced a second, sustained increase in $[Lact]_d$, followed by a gradual decrease to near basal levels.

(n = 11) and 32.4 ± 3.2% (n = 10) in the striatum (i.e. microdialysis experiments with normal ACSF and 20 mM probenecid in ACSF, respectively; $P < 0.01$, comparison to EEG recovery in the $CO_3^{2-}$ series).

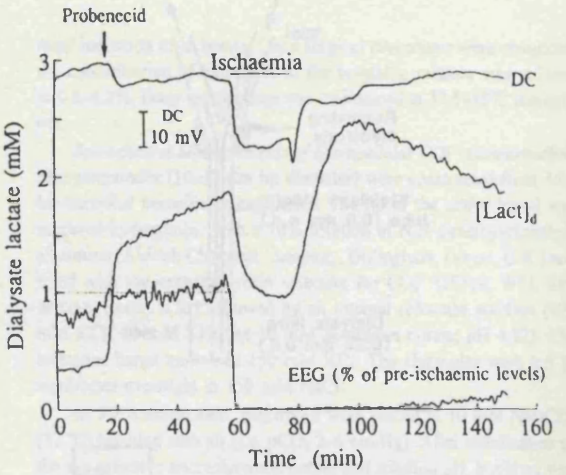


Fig. 4. Representative effects of 20 mM probenecid continuously perfused through the microdialysis probe on extracellular concentration of lactate ($[Lact]_d$), in otherwise normal conditions, and during transient forebrain ischemia (top horizontal line). $[Lact]_d$, DC potential and EEG were recorded from the same tissue site, using a microdialysis *electrode* implanted into the striatum. Note that the Y-axis scale is half that of figure 3. Probenecid markedly increased the basal levels of lactate (left part of the trace), but totally inhibited the initial increase which preceded anoxic depolarization in control animals. In contrast, $[Lact]_d$ decreased from the onset of ischemia, and remained at a low level (relatively to pre-ischemic levels under probenecid) thoughout the insult. Reperfusion was associated with an increase in $[Lact]_d$ which, after 80 min, reached a similar level to that observed immediately before ischemia.

*Ischemia-Induced Changes in Extracellular Carbonate ($[CO_3^{2-}]_e$).* Cortical $[CO_3^{2-}]_e$ remained stable during the control period at 50.1 ± 5.8 μM (n = 6) (Fig. 2). With the onset of ischemia, there was an immediate decrease in $[CO_3^{2-}]_e$, to 37.1 ± 5.2 μM (a decrease of 16.3 ± 3.7 μM; $P < 0.01$) immediately before anoxic depolarization (Fig. 2). A sudden transient increase in $[CO_3^{2-}]_e$ (amplitude = 12.0 ± 3.3 μM), superimposed upon its steady decrease, was closely associated with the fast negative shift in the DC potential indicating anoxic depolarization (21.6 ± 2.5 mV) (Fig. 2). Then, $[CO_3^{2-}]_e$ decreased to 22.2 ± 3.0 μM, and remained at this level for the remainder of the ischemic period. With reperfusion, a further drop in $[CO_3^{2-}]_e$ of 5.0 ± 1.5 μM preceded gradual normalization. After 80 min of reperfusion, $CO_3^{2-}$ had reached a concentration similar to that observed before ischemia (57.0 ± 6.5 μM).

It is noteworthy that, in a few experiments (n = 3) which were excluded from this study, the characteristic transient increase in $[CO_3^{2-}]_e$ associated with anoxic depolarization was not present. In these cases, a slight rise in $[CO_3^{2-}]_e$ preceded its steady decrease shortly after the onset of ischemia (data not shown). Subsequent studies

have found that this atypical pattern of changes in $[CO_3^{2-}]_e$ may reflect events taking place in different cellular environments, resulting from a slightly different implantation depth of the recording ion-selective microelectrode (Taylor and Obrenovitch, unpublished observations) within the laminated cellular arrangement of the mammalian cerebral cortex (31).

*Ischemia-Induced Changes in Dialysate Lactate Concentration ($[Lact]_d$).* Dialysate concentrations of lactate remained relatively stable during the control period at 0.99 ± 0.14 mM (n = 11). The onset of ischemia was accompanied by an immediate and rapid increase in $[Lact]_d$ to 3.46 ± 0.38 mM ($P < 0.01$; comparison to pre-ischemic level) (Fig. 3), but this effect was rapidly reversed following anoxic depolarization (Fig. 3). $[Lact]_d$ decreased to 1.92 ± 0.23 mM where it remained throughout the insult. Reperfusion was accompanied by a marked and rapid increase in $[Lact]_d$ to 3.84 ± 0.38 mM. Then $[Lact]_d$ decreased steadily reaching a plateau level of 1.62 ± 0.29 mM after 80 min of reperfusion, still significantly higher than pre-ischemic levels ($P < 0.01$).

*Effects of Probenecid on Ischemia-Induced $[Lact]_d$ Changes.* Pre-ischemic $[Lact]_d$ was 0.6 ± 0.09 mM (n = 10) in this series. Perfusion of 20 mM probenecid rapidly increased $[Lact]_d$ to 1.91 ± 0.09 mM and, after 50 min, $[Lact]_d$ had reached a plateau level of 2.08 ± 0.1 mM. Probenecid provoked a negative shift of the DC potential (5.2 ± 0.7 mV; $P < 0.001$) but did not significantly alter the EEG. Under these conditions, the initial increase in $[Lact]_d$ with the onset of ischemia that was seen in the control was absent (Fig. 4). In contrast, there was a rapid decrease in $[Lact]_d$ to 1.13 ± 0.07 mM ($P < 0.001$; comparison to pre-ischemic levels). This low level persisted throughout the insult until reperfusion, when $[Lact]_d$ increased to a level higher than that before ischemia (2.47 ± 0.08 mM, $P < 0.001$). Then, $[lact]_d$ steadily decreased and after 80 min had returned to pre-ischemic levels (1.95 ± 0.11 mM).

## DISCUSSION

*Ischemia-Induced Changes in EEG and DC Potential.* EEG amplitude decreased to noise level within 30 sec of carotid artery occlusion, and marked anoxic depolarization occurred consistently within 2–3 min of ischemia, confirming that 4-vessel occlusion produces near-complete forebrain ischemia in male Wistar rats (20,32). The 'residual' EEG observed in a few experiments (e.g. Fig. 2) probably reflected electrical activity from posterior regions, remote from the recording site and spared from the ischemic insult, as it persisted even when marked and sustained anoxic depolarization was demonstrated.

Repolarization occurred shortly after reperfusion, and was rapid in all experiments, contrasting with EEG recovery which was gradual, and incomplete after 80 min of recirculation. EEG recovery after ischemia was greater in the cortex than in the striatum. One explanation for the poor recovery in the striatum could be a deleterious interaction of microdialysis since, in otherwise normal conditions, both glucose phosphorylation and local cerebral blood flow were disturbed in the first hours after probe insertion (33). However, other experiments in which EEG was recorded from the cortex with microdialysis electrodes showed a time course for EEG recovery (data not shown) similar to that obtained with glass capillary electrodes, suggesting that the striatum may be more vulnerable than the cortex in this model of ischemia, at least with regards to early functional recovery (34,35).

Although systemic administration of high doses of probenecid was reported to produce convulsions (36), 20 mM probenecid perfused through the microdialysis probe did not produce significant changes in the amplitude of local EEG in the striatum. This suggests that the extracellular concentration of probenecid in the tissue surrounding the probe was presumably much lower than that of the perfusion medium, firstly because diffusion of the drug was restricted by the dialysis membrane (26), and secondly because probenecid probably rapidly diffused away from the site of application as it is a lipid-soluble compound (37) and a substrate of organic anion transports (19,38). In contrast to its lack of effect on the EEG, probenecid application evoked a significant negative shift of the DC potential. This latter effect may result from probenecid being a competitive (i.e. transportable) inhibitor of organic anion exchanges, of which some are presumably coupled to the movement of ions such as $Na^+$, $K^+$, or $H^+$. Applied at high concentrations to the extracellular space, probenecid may be actively transported intracellularly, altering transmembrane ionic gradients and, therefore, the polarization of the cellular membrane. This hypothesis is supported by the fact that 20 mM probenecid produced a rapid negativation of the DC potential (i.e. immediately after switching from ACSF to probenecid-medium, when the intra-/extracellular gradient of probenecid was maximum), followed by partial normalization while probenecid was still being applied (i.e. as the transmembrane probenecid gradient was progressively reduced) (Fig. 4).

*Changes in Extracellular Carbonate ($[CO_3^{2-}]_e$) Induced by Transient Cerebral Ischemia.* Extracellular levels of $CO_3^{2-}$ decreased immediately after carotid artery

occlusion, indicating that progressive reduction of the $H^+$ buffering capacity of the extracellular fluid is an early event in ischemia, closely associated with the rising extracellular concentration of $H^+$ (16,39). These initial changes in extracellular $H^+$ and $CO_3^{2-}$ may be partly due to increased brain tissue concentration of $CO_2$ (9,40) since this gas diffuses freely through all brain tissue compartments, but they may also reflect a marked activation of $Na^+/H^+$ and $HCO_3^-/Cl^-$ exchanges. Increased intracellular $[H^+]$ is known to stimulate the $Na^+/H^+$ antiport (i.e. extrusion of $H^+$ in exchange for $Na^+$) (41,42) and $HCO_3^-/Cl^-$ exchange (i.e. influx of $HCO_3^-$ against its own electrochemical gradients with $Cl^-$ leaving the cell) (8). The efficacy of these exchanges requires both maintenance of the overall impermeability of plasma membranes to ions, and functional $Na^+/K^+$-ATPase pump. Therefore, the early, progressive reduction in $[CO_3^{2-}]_e$ supports the hypothesis that transmembrane ionic exchanges contributing to intracellular $[H^+]$ regulation are functional and activated in the initial stage of an ischemic insult, with intracellular $[H^+]$ being kept close to normal levels (43) to the detriment of extracellular $[H^+]$ (16).

Anoxic depolarization is due to a marked, sudden increase in the permeability of the cellular membrane to ions and, consequently, the extracellular ionic composition approaches that of the intracellular compartment subsequent to efflux of $K^+$ and influxes of $Na^+$, $Cl^-$ and $Ca^{2+}$ (16,28). Disruption of transmembrane ionic gradients implies the collapse of a number of plasmalemnal transport/exchange systems which are driven by these gradients, including those contributing to cellular acid-base homeostasis. Direct measurement of $[CO_3^{2-}]_e$ consistently revealed a sudden transient increase, superimposed upon the steady $[CO_3^{2-}]_e$ decrease, and intimately related to cell membrane depolarization (Fig. 2), suggesting a sudden efflux of $CO_3^{2-}$ and other pH-changing anions (i.e. $OH^-$, $HCO_3^-$). This rapid change is very similar to the alkalotic shift in extracellular $[H^+]$ associated with membrane depolarization (16,39). These findings support the theory that there is a rapid redistribution of both $H^+$ and pH-changing anions between the intra- and extracellular compartments due to increased membrane permeability to ions and, therefore, a collapse of active ion exchange mechanisms contributing to residual intracellular acid-base regulation in ischemia (16).

Recirculation was accompanied by a further decrease in $[CO_3^{2-}]_e$ associated with membrane repolarization (Fig. 2). Transient increases in $[H^+]_e$ have also been observed with repolarization (16,44). These events, both of which indicate a transient worsening of extracellular acidosis with repolarization, may reflect restoration of normal membrane ionic permeability and active recovery of intracellular $[H^+]$ regulation subsequent to that of the inward $Na^+$ gradient, resulting in very effective extrusion of $H^+$ and/or influx of pH-changing anions. Another contributing factor may be increased production of $H^+$ resulting from enhanced ATP hydrolysis due to the ionic pumps actively restoring the transmembrane ionic gradients.

*Changes in Extracellular Lactate Induced by Transient Cerebral Ischemia.* Although lactic acid accumulates intracellularly subsequent to stimulation of anaerobic metabolism (9,12,15,40), extracellular levels of lactate increased rapidly after carotid artery occlusion (Fig. 3), indicating that removal of lactate from the intra- to extracellular space is effective early in ischemia (26,45), and that this mechanism contributes to the rapid acidification of the extracellular space when oxygen supply becomes deficient.

Lactate exchanges across the plasma membrane are generally considered to occur by passive diffusion of undissociated lactic acid (46), or via a lactate transporter (24). Although lactate exchanges between brain slices and the outer medium were neither dependent on ATP (47,48) nor on extracellular $Na^+$ (49), observations in vivo suggest that lactate removal from intracellular compartments may involve a transporter that is either directly or indirectly coupled to energy-dependent transmembrane gradients (30,37). For example, lactate appeared very rapidly in the extracellular fluid when complete ischemia was provoked by cardiac arrest, but extracellular lactate decreased following terminal anoxic depolarization (30) despite lactate formation possibly being sustained for several minutes after this event (50). In addition, lactate efflux from cultured neurons and glia was impaired by an inhibitor of lactate/$H^+$ transport (DL-p-hydroxyphenyl lactate) (51) suggesting that, as in other tissues (52), a lactate/$H^+$ cotransporter dependent on transmembrane gradients is active in the brain (53,54). The effectiveness of such a mechanism in nervous tissue is also supported by the finding that lactate/$H^+$ transport, and not $Na^+/H^+$ or $HCO_3^-/Cl^-$ exchange, was the dominant process responsible for interstitial acidification in hypoxic, isolated peripheral nerves (55).

Efflux of lactate via a transporter dependent on functional plasma membrane implies inactivation of this efflux with anoxic depolarization, since this latter event reflects the collapse of transmembrane ionic gradients. The sudden switch from increase to decrease in extracellular lactate which occurred with anoxic depolarization (Fig. 3) is consistent with this hypothesis. This rapid change in the time course of changes in dialysate lactate

cannot be exclusively attributed to glucose shortage (see ref. 50, and below). The decrease in extracellular lactate observed at this point presumably reflected cessation of lactate efflux, superimposed to persistent microdialysis drainage of the region under study (56).

The drop in extracellular lactate associated with anoxic depolarization could also partly reflect a reduction in the rate of lactate production, subsequent to glucose shortage *and* inhibition of anaerobic glycolysis by the influx of $Na^+$ and efflux of $K^+$ occurring with anoxic depolarization. Pyruvate kinase, a regulatory step in glycolysis, is activated by $K^+$ and inhibited by $Na^+$ (57), and inhibition of anerobic metabolism by $Na^+$ loading (58) was recently confirmed in synaptosomes (59). It is also possible that the decrease in dialysate lactate following anoxic depolarization may be exacerbated by a decrease in microdialysis recovery (26,60) resulting from the shrinkage of the extracellular space known to be associated with this ischemic event (61).

The rapid increase in extracellular concentration of lactate with recirculation, synchronous with repolarization (Fig. 4), supports the hypothesis that lactate formation, and/or its transport out of brain cells, may be inhibited by anoxic depolarization. The sustained increase in $[Lact]_d$ during reperfusion also confirmed that normalization of brain tissue acid-base is progressive, and much slower than the recovery of transmembrane gradients of $Na^+$, $K^+$ and $Ca^{2+}$ (29). The return of extracellular lactate to pre-ischemic levels, reached after about 1 hr of reperfusion, is unlikely to have resulted from clearance via the vascular system because monocarboxylic acid transport across the blood-brain barrier is negligible in the adult rat (19,62), and only a small fraction of lactate produced during hypoxia was found in cerebral venous blood (63). As there is clear evidence that lactate can become a major energy source for brain tissue under certain circumstances (64,65), clearance of extracellular lactate probably occurred through re-entry into the cells, and recycling to pyruvate with normalized oxygen supply (19,63).

*Effect of Probenecid on Basal Extracellular Lactate and Ischemia-Induced Changes.* Probenecid perfused through the microdialysis probe markedly increased the basal extracellular concentration of lactate (Fig. 4), confirming the previous observations of Kuhr and co-workers (19). This effect is opposite to that expected to occur subsequent to inhibition of lactate transport across the cellular membrane and blood-brain barrier, because lactate is produced intracellularly and its clearance across the blood-brain barrier is small (62). Rather, these increased dialysate lactate levels may reflect a heteroexchange mechanism (i.e. probenecid enters the cells surrounding the dialysis fibre in exchange for lactate), since probenecid is a competitive (i.e. transportable) inhibitor of organic acid transport systems. Heteroexchange of transportable substrates was shown with other carriers, especially that for glutamate across plasma membranes (66,67).

In the presence of probenecid, the increase in extracellular lactate before anoxic depolarization was no longer detectable, confirming that the removal of intracellular lactate during ischemia mainly occurs via a transporter. This is also supported by the finding that, with probenecid, extracellular levels of lactate during reperfusion did not reach those obtained in the absence of the drug (Figs. 3 and 4; Note the difference in Y-axis scale). The slower, secondary normalization of lactate under probenecid presumably reflected blockade of lactate re-uptake into the cells, supporting the concept that this is the main route for removal of extracellular lactate during recirculation.

Probenecid significantly reduced the amplitude of the negative shift in the DC potential indicating depolarization. This effect may be a consequence of the 'depolarizing' effect of probenecid, since perfusion of 20 mM of the drug through the microdialysis probe produced an initial negative shift of around 5 mV. However, most of this effect had regressed when ischemia was induced, and previous studies demonstrated that probenecid markedly inhibits $K^+$-induced depolarization in the rat striatum (68), suggesting that this drug may have a direct effect on the amplitude of anoxic depolarization.

In conclusion, these studies demonstrate that the transmembrane mechanisms contributing to intracellular pH regulation are markedly activated during ischemia, and remain functional as long as anoxic depolarization does not occur. These mechanisms include $Na^+/H^+$ exchange, presumably supplemented by $HCO_3^-/Cl^-$ exchanges, and removal of intracellular lactate (with $H^+$) via a transporter. Residual acid-base homeostasis is however abolished by anoxic depolarization, because the driving forces of these mechanisms (i.e. ionic gradients) collapse subsequent to the sudden increase in plasma membrane ionic permeability. As spreading depression implies transient collapse of ionic gradients (69), recurrent failure of residual acid-base homeostasis may also occur in the penumbra of focal ischemia and contribute to increasing the volume of infarction (70). These findings strengthen the concept that anoxic depolarization and spreading depression are critical events in the pathophysiology of cerebral ischemia and, therefore, relevant targets for neuroprotective strategies against stroke.

## ACKNOWLEDGMENTS

The authors are grateful to Mr C. Bashford and A. Hardy for their skilful technical assistance. They also wish to thank Dr. D. A. Richards (Department of Pharmacology, School of Pharmacy, London) for his critical comments. This work was supported by the Brain Research Trust (Institute of Neurology, London), The Thompson Fund, and the Joint Research Advisory Committee (The National Hospitals, Queen Square, London).

## REFERENCES

1. Siesjö, B. K., and Bengtsson, F. 1989. Calcium fluxes, calcium antagonists and calcium-related pathology in brain ischemia, hypoglycemia and spreading depression: a unifying hypothesis. J. Cereb. Blood Flow Metab. 9:127–140.
2. Siesjö, B. K., Lundgren, J., and Pahlmark, K. 1990. The role of free radicals in ischemic brain damage: a hypothesis. Pages 319–323, *in* Krieglstein, J., and Oberpichler, J. (eds.), Pharmacology of Cerebral Ischemia 1990, Wiss. Verlag., Stuttgart.
3. Obrenovitch, T. P., and Richards, D. A. 1995. Extracellular neurotransmitter changes in cerebral ischemia. Cerebrovasc. Brain Metab. Rev. 7:1–54.
4. Siesjö, B. K. 1988. Acidosis and ischemic brain damage. Neurochem. Pathol. 9:31–88.
5. Siesjö, B. K., Katsura, K., Mellergård, P., Ekholm, A., Lundgren, J., and Smith, M.-L. 1993. Acidosis-related brain damage. Prog. Brain Res. 96:23–48.
6. Siesjö, B. K., Bendek, G., Koide, T., Westerberg, E., and Wieloch, T. 1985. Influence of acidosis on lipid peroxidations in brain tissues in vitro. J. Cereb. Blood Flow Metab. 5:253–258.
7. Tombaugh, G. C., and Sapolsky, R. M. 1993. Evolving concepts about the role of acidosis in ischemic neuropathology. J. Neurochem. 61:793–803.
8. Chesler, M. 1990. The regulation and modulation of pH in the nervous system. Prog. Neurobiol. 34:401–427.
9. Siesjö, B. K. 1985. Acid-base homeostasis in the brain: physiology, chemistry, and neurochemical pathology. Pages 121–154, *in* Kogure, K., Hossmann, K.-A., Siesjö, B. K., and Welsch, F. A. (eds.), Progress in Brain Research vol. 63, Elsevier, Amsterdam.
10. Brooks, K. J., and Bachelard, H. S. 1992. The regulation of intracellular pH studied by 31P- and 1H-NMR spectroscopy in superfused guinea-pig cerebral cortex slices. Neurochem. Int. 21:375–379.
11. Ben-Yoseph, O., Badar-Goffer, R. S., Morris, P. G., and Bachelard H. S. 1993. Glycerol 3-phosphate and lactate as indicators of the cerebral cytoplasmic redox state in severe and mild hypoxia respectively: a 13C- and 31P-NMR study. Biochem. J. 291:915–919.
12. Conger, K. A., Halsey, J. H., Luo, K.-L., Tan, M.-J., Pohost, G. M., and Hetherington, H. P. 1995. Concomitant EEG, lactate, and phosphorus changes by $^{1}H$ and $^{31}P$ NMR spectroscopy during repeated brief cerebral ischemia. J. Cereb. Blood Flow Metab. 15: 26–32.
13. Ohno, M., Obrenovitch, T. P., Hartell, N., Barrett, S., Bachelard, H. S., and Symon, L. 1989 Simultaneous recording of tissue $pCO_2$, interstitial pH and potassium activity in the rat cerebral cortex during anoxia and the subsequent recovery period. J. Neurol. Res. 11:153–159.
14. Matsumoto, T., Obrenovitch, T. P., Parkinson, N. A., and Symon, L. 1990. Cortical activity, ionic homeostasis, and acidosis during rat brain repetitive ischemia. Stroke 21:1192–1198.
15. Obrenovitch, T. P., Garofalo, O., Harris, R. J., Bordi, L., Ohno, M., Momma, F., Bachelard, H. S., and Symon, L. 1988. Brain tissue concentration of ATP, phosphocreatine, lactate and tissue pH in relation to reduced cerebral blood flow following experimental acute middle cerebral artery occlusion. J. Cereb. Blood Flow Metab. 8:866–874.
16. Obrenovitch, T. P., Scheller, D., Matsumoto, T., Tegtmeier, F., Höller, M., and Symon, L. 1990. A rapid redistribution of hydrogen ions is associated with depolarization and repolarization subsequent to cerebral ischemia/reperfusion. J. Neurophysiol. 64: 1125–1133.
17. Chesler, M., Chen, J. C., and Kraig, R. P. 1994. Determination of extracellular bicarbonate and carbon dioxide concentrations in brain slices using carbonate and pH-selective microelectrodes. J. Neurosci. Meth. 53:129–136.
18. Sugaya, E., Takato, M., and Noda, Y. 1975. Neuronal and glial activity during spreading depression in cerebral cortex of cat. J. Neurophysiol. 38:822–841.
19. Kuhr, W. G., van den Berg, C. J., and Korf, J. 1988. In vivo identification and quantitative evaluation of carrier-mediated transport of lactate at the cellular level in the striatum of conscious, freely moving rats. J. Cereb. Blood Flow Metab. 8:848–856.
20. Pulsinelli, W. A., and Buchan, A. M. 1988. The four-vessel occlusion rat model: method for complete occlusion of vertebral arteries and control of collateral circulation. Stroke 19:913–914.
21. Stewart, P. A. 1981. How to understand acid-base: A quantitative acid-base primer for biology and medicine. Edward Arnold, London.
22. Paxinos, G., and Watson, C. 1986. The Rat Brain in Stereotaxic Coordinates. Academic Press, London.
23. Obrenovitch, T. P., Richards, D. A., Sarna, G. S., and Symon, L. 1993. Combined intracerebral microdialysis and electrophysiological recording: Methodology and applications. J. Neurosci. Meth. 47:139–145.
24. Kuhr, W. G., and Korf, J. 1988. Extracellular lactic acid as an indicator of brain metabolism: continuous on-line measurement in conscious, freely moving rats with intrastriatal dialysis. J. Cereb. Blood Flow Metab. 8:130–137.
25. Obrenovitch, T. P., Sarna, G. S., Millan, M. H., Lok, S.-Y., Kawauchi, M., Ueda, Y., and Symon, L. 1990. Intracerebral dialysis with on-line enzyme fluorometric detection: A novel method to investigate the changes in the extracellular concentration of glutamic acid. Pages 23-31, *in* Krieglstein, J., and Oberpichler, H. (eds.), Pharmacology of Cerebral Ischemia 1990, Wiss. Verlag., Stuttgart.
26. Scheller, D., and Kolb, J. 1991. The internal reference technique in microdialysis: a practical approach to monitoring dialysis efficiency and to calculating tissue concentration from dialysate samples. J. Neurosci. Meth. 40:31–38.
27. Kehr, J. 1993. A survey on quantitative microdialysis: theoretical models and practical implications. J. Neurosci. Meth. 48:251–261.
28. Hansen, A. J., and Nedergaard, M. 1988. Brain ion homeostasis in cerebral ischemia. Neurochem. Pathol. 9:195–209.
29. Obrenovitch, T. P., Sarna, G. S., and Symon, L. 1990. Ionic homeostasis and neurotransmitter changes in ischemia. Pages 97–112, *in* Krieglstein, J., and Oberpichler, H. (eds.), Pharmacology of Cerebral Ischemia 1990, Wiss. Verlag., Stuttgart.
30. Taylor, D. L., Richards, D. A., Obrenovitch, T. P., and Symon, L. 1994. Time course of changes in extracellular lactate evoked by transient $K^+$-induced depolarization in the rat striatum. J. Neurochem. 62:2368–2374.
31. Donoghue, J. P., and Wise, S. P. 1982. The motor cortex of the rat: Cytoarchitecture and microstimulation mapping. J. Comp. Neurol. 212:76–88.
32. Blomqvist, P., Mabe, H., Ingvar, M., and Siesjö, B. K. 1984. Models for studying long-term recovery following forebrain ischemia in the rat. 1. Circulatory and functional effects of 4-vessel occlusion. Acta Neurol. Scand. 69:376–384.
33. Benveniste, H., Drejer, J., Schousboe, A., and Diemer, N. H. 1987. Regional cerebral glucose phosphorylation and blood flow after

insertion of a microdialysis fiber through the dorsal hippocampus in the rat. J. Neurochem. 49:729–734.
34. Smith, M.-L., Auer, R. N., and Siesjö, B. K. 1984. The density and distribution of ischemic brain injury in the rat following 2–10 min of forebrain ischemia. Acta Neuropathol. 64:319–332.
35. Ginsberg, M. D., Graham, D. I., and Busto, R. 1985. Regional glucose utilization and blood flow following graded forebrain ischemia in the rat: correlation with neuropathology. Ann. Neurol. 18:470–481.
36. Akiyama, T., Sato, M., and Otsuki, S. 1981. Probenecid-induced convulsion and cerebrospinal cyclic nucleotides in the kindling cat preparations. Brain Nerve (Tokyo) 33:1107–1113.
37. Roos, B.-E., Wickström, G., Hartvig, P., and Nilsson, J. L. G. 1980. Quantitation of CSF concentrations and biological activity of probenecid metabolites. Eur. J. Clin. Pharmacol. 17:223–226.
38. Miller, J. M., MacGarvey, U., and Beal, M. F. 1992. The effect of peripheral loading with kynurenine and probenecid on extracellular striatal kynurenic acid concentrations. Neurosci. Lett. 146: 115–118.
39. Mutch, W. A. C., and Hansen, A. J. 1984. Extracellular pH changes during spreading depression and cerebral ischemia: mechanisms of brain pH regulation. J. Cereb. Blood Flow Metab. 4: 17–27.
40. Smith, M. L., von Hanwehr, R., and Siesjö, B. K. 1986. Changes in extra- and intracellular pH during and following ischemia in hyperglycaemic and in moderately hypoglycaemic rats. J. Cereb. Blood Flow Metab. 6:574–583.
41. Aronson, P. S. 1985. Kinetic properties of the plasma membrane $Na^+$-$H^+$ exchanger. Annu. Rev. Physiol. 47:545–560.
42. Grinstein, S., and Rosthein, A. 1986. Mechanisms of regulation of the $Na^+/H^+$ exchanger. J. Membr. Biol. 90:1–12.
43. Ekholm, A., Asplund, B., and Siesjö, B. K. 1992. Perturbation of cellular energy in complete ischemia: relationship to dissipative ion fluxes. Exp. Brain Res. 90:47–53.
44. Nemoto, E. M., and Frinak, S. 1981. Brain tissue pH after global ischemia and barbiturate loading in rat. Stroke 12:77–82.
45. Symon, L., Taylor, D. L., and Obrenovitch, T. P. 1994. Aspects of acid-base homeostasis in ischemia. Pages 51–57, *in* Cerebral Ischemia and Basic Mechanisms, Hartmann, A., Yatsu, F., and Kuschinsky, W. (eds.), Springer-Verlag, Berlin.
46. Nedergaard, M., Goldman, S. A., and Pulsinelli, W. A. 1989. Lactic acid-induced intracellular acidification in primary cultures of mammalian brain. J. Cereb. Blood Flow Metab. 9(Suppl. 1):S384.
47. Kauppinen, R. A., and Williams, S. R. 1990. Cerebral energy metabolism and intracellular pH during severe hypoxia and recovery: a study using $^1H$, $^{31}P$, and $^1H[^{13}C]$ nuclear magnetic resonance spectroscopy in the guinea-pig cerebral cortex in vitro. J. Neurosci. Res. 26:356–369.
48. Assaf, H. M., Ricci, A. J., Whittingham, T. S., LaManna, J. C., Ratcheson, R. A., and Lust, W. D. 1990. Lactate compartmentation of hippocampal slices: evidence for a transporter. Metab. Brain Dis. 5:143–154.
49. Pirtillä, T.-R. M., and Kauppinen, R. A. 1992. Recovery of intracellular pH in cortical brain slices following anoxia studied by nuclear magnetic resonance spectroscopy: role of lactate removal, extracellular sodium and sodium/hydrogen exchange. Neuroscience 47:155–164.
50. Lowry, O. H., Passoneau J. V., Hasselberger, F. K., and Schultz, D. W. 1964. Effect of ischemia on known substrates and cofactors of the glycolytic pathway in brain. J. Biol. Chem. 239:18–30.
51. Walz, W., and Mukerji, S. 1988. Lactate release from cultured astrocytes and neurons: A comparison. Glia 1:366–370.
52. Halestrap, A. P., Poole, R. C., and Cranmer, S. L. 1990. Mechanisms and regulation of lactate, pyruvate and ketone body transport across the plasma membrane of mammalian cells and their metabolic consequences. Biochem. Soc. Trans. 18:1132–1135.
53. Lomneth, R., Medrano, S., and Gruenstein, E. I. 1990. The role of transmembrane pH gradients in the lactic acid induced swelling of astrocytes. Brain Res. 523:69–77.
54. Walz, W., and Mukerji, S. 1990. Simulation of aspects of ischemia in cell culture: Changes in lactate compartmentation. Glia 3:522–528.
55. Schneider, U., Strupp, M., Jund, R., and Grafe, P. 1993. Lactate-proton cotransport and its activation by hypoxia in the mammalian peripheral nervous system. Pflügers Arch. 420:R25.
56. Benveniste, H., and Hüttemeier, P. C. 1990. Microdialysis—Theory and application. Prog. Neurobiol. 35:195–215.
57. Rose, I. A., and Rose, Z. B. 1969. Glycolysis: Regulation and mechanisms of the enzymes. Pages 93–161, *in* Florkin, M., and Stotz, E. H. (eds.), Comprehensive Biochemistry, Carbohydrate Metabolism, vol. 17, Elsevier, Amsterdam.
58. Shankar, R., and Quastel, J. H. 1972. Effects of tetrodotoxin and anaesthetics on brain metabolism and transport during anoxia. Biochem. J. 126:851–867.
59. Gleitz, J., Beile, A., Khan, S., Wilffert, B., and Tegtmeier, F. 1993. Anaerobic glycolysis and postanoxic recovery of respiration of rat cortical synaptosomes are reduced by synaptosomal sodium load. Brain Res. 611:286–294.
60. Nicholson, C., and Phillips, J. M. 1981. Ion diffusion modified by tortuosity and volume fraction in extracellular microenvironment of rat cerebellum. J. Physiol. (Lond.) 321:225–257.
61. Hansen, A. J., and Olsen, C. E. 1980. Brain extracellular space during spreading depression and ischemia. Acta Physiol. Scand. 108:335–365.
62. Cremer, J. E., Cunningham, V. J., Pardridge, W. M., Braun, L. D., and Oldendorf, W. H. 1979. Kinetics of blood-brain barrier transport of pyruvate, lactate and glucose in suckling, weanling and adult rats. J. Neurochem. 33:439–445.
63. Zimmer, R., and Lang, R. 1975. Rates of lactic acid permeation and utilization in the isolated dog brain. Am. J. Physiol. 229:432–437.
64. Schurr, A., West, C. A., and Rigor, B. M. 1988. Lactate-supported synaptic function in the rat hippocampal slice preparation. Science 240:1326–1328.
65. Bock, A. C., Scheller, D., Tegtmeier, F., Dengler, K., Zacharias, E., and Höller, M. 1989. Postischemic recovery of electrophysiological function and extracellular pH during normo- and aglycemic reperfusion. J. Cereb. Blood Flow Metab. 9(Suppl. 1):S642.
66. Cammack, J., Ghasemzadeh, B., and Adams, R. N. 1991. The pharmacological profile of glutamate-evoked ascorbic acid efflux measured by in vivo electrochemistry. Brain Res. 565:17–22.
67. Griffiths, R., Dunlop, J., Gorman, A., Senior, J., and Grieve, A. 1994. L-*trans*-pyrrolidine-2,4-dicarboxylate and *cis*-1-aminocyclobutane-1,3-dicarboxylate behave as transportable, competitive inhibitors of the high-affinity glutamate transporters. Biochem. Pharmacol. 47:267–274.
68. Taylor, D. L., Obrenovitch, T. P., Gotoh, M., and Symon, L. 1994. Inhibition of spreading depression by probenecid. Page 291, *in* New Advances in Headache Research: 4, Rose, F. C. (ed.), Smith-Gordon Ltd, London.
69. Hansen, A. J., and Zeuthen, T. 1981. Extracellular ion concentrations during spreading depression and ischemia in the rat brain cortex. Acta Physiol. Scand. 113:437–445.
70. Obrenovitch, T. P. 1995. The ischemic penumbra: Twenty years on. Cerebrovasc. Brain Metab. Rev. 7:297–323.

**Brain Research 1997**
*in press*

# Effects of probenecid on the elicitation of spreading depression in the rat striatum.

Taylor, DL., Urenjak, J., Zilkha, E. and Obrenovitch, TP.

Spreading depression (SD) is a wave of cellular depolarization which contributes to neuronal damage in experimental focal ischaemia, and may also underlie the migraine aura. The purpose of this study was to examine the effects of probenecid, and inhibitor of organic anion transport, on $K^+$-evoked SD in vivo. Microdialysis electrodes were implanted in the rat striatum, and recurrent SD elicited by perfusion of artificial cerebrospinal fluid containing 160 mM $K^+$ for 20 min. Probenecid was administered either directly though the microdialysis probe, starting 50 min before the application of high $K^+$, or intravenously.

SD was markedly reduced by perfusion of 5 mM probenecid through the microdialysis probe. In contrast, a high intravenous dose of probenecid (250 mg/kg) only slightly inhibited SD elicitation 90 min after treatment, despite clear changes in the amplitude and spectrum of the electroencephalogram, as early as 10 min after drug administration, confirming that probenecid readily penetrated the central nervous system. As SD is inhibited by hypercapnia, we have examined the possibility that probenecid may inhibit SD through extracellular acidification subsequent to blockade of lactate transport. Perfusion of 1-20 mM probenecid increased dose-dependently the dialysate levels of lactate, but without extracellular acidosis since the dialysate pH was not significantly reduced. How probenecid inhibits SD deserves further investigation because it may help to identify novel strategies to suppress this phenomenon, now recognized deleterious to neuronal function and survival.